Polyisocyanide Polymersomes

een wetenschappelijke proeve op het gebied van de
Natuurwetenschappen, Wiskunde en Informatica

Proefschrift

ter verkrijging van de graad van doctor
aan de Radboud Universiteit Nijmegen
op gezag van de Rector Magnificus prof. dr. C.W.P.M. Blom,
volgens besluit van het College van Decanen
in het openbaar te verdedigen op dinsdag 1 februari 2005
des namiddags om 1.30 uur precies

door

Dennis Manuel Vriezema

geboren op 11 augustus 1975
te Arnhem

Promotor:

Prof. dr. R.J.M. Nolte

Copromotor:

Dr. A.E. Rowan

Manuscriptcommissie:

Prof. dr. ir. J.C.M. van Hest
Dr. D.B. Amabilino (Institut de Ciència de Materials de Barcelona)
Dr. J.J.L.M. Cornelissen

Printing: PrintPartners Ipskamp, Enschede

ISBN: 90-9018980-7

voor papa, mama, Danielle en Paula

Paranimfen:

Irene Reynhout
Pieter de Witte

Table of Contents

Chapter 1 Functional Polymer Architectures

1.1	Introduction	1
1.2	Polymer Based Supramolecular Micro- and Nanoreactors	3
1.3	Polyisocyanides	21
1.4	Outline of the Thesis	31
1.5	References and Notes	32

Chapter 2 Synthesis and Characterization of Thiophene-Containing Polyisocyanides Derived from Alanine

2.1	Introduction	37
2.2	Thiophene-Containing Polyisocyanides Derived from Alanine	41
2.3	Thiophene-Containing Polyisocyanides Derived from Alanyl-Alanine	54
2.4	Conclusions	59
2.5	Experimental Section	60
2.6	References and Notes	67

Chapter 3 Aggregation Behavior of Thiophene-Containing Rigid-Rod Diblock Copolymers Based on Styrene and Isocyanide

3.1	Introduction	69
3.2	Synthesis and Characterization	71
3.3	Aggregation Behavior	77
3.4	Conclusions	100
3.5	Experimental Section	101
3.6	References and Notes	104

Chapter 4 Membrane Cross-linking of Thiophene-Containing Diblock Copolymer Vesicles

4.1	Introduction	107
4.2	Results and Discussion	111
4.3	Conclusions	123
4.4	Experimental Section	124
4.5	References and Notes	125

Chapter 5 Nanoreactors Based on Enzyme-Containing Diblock Copolymer Vesicles

5.1 Introduction 127
5.2 Results and Discussion 130
5.3 Conclusions 145
5.4 Experimental Section 145
5.5 References and Notes 148

Chapter 6 Aggregation Studies of Thiophene-Containing Octadecene-*Block*-Polyisocyanide Copolymers

6.1 Introduction 151
6.2 Synthesis and Characterization 152
6.3 Aggregation Behavior 159
6.4 Conclusions 165
6.5 Experimental Section 166
6.6 References and Notes 168

Chapter 7 Towards Electron Conducting Polyisocyanide Nanowires

7.1 Introduction 169
7.2 Polyisocyanides with Hexabenzocoronene Side Groups 176
7.3 Polyisocyanides with Tetrathiafulvalene Side Groups 178
7.4 Conclusions 180
7.5 Experimental Section 180
7.6 References and Notes 183

Summary 185

Samenvatting 188

Dankwoord 191

Curriculum Vitae 194

List of Publications 195

Chapter 1

Functional Polymer Architectures

1.1 Introduction

Polymers are a very important class of compounds and they are part of every day life. It is somewhat surprising that less than a century ago it was common belief that polymers could not exist. Staudinger was the first to postulate the concept of polymers as being long chain molecules, built up from smaller units which are linked together via covalent bonds.[1] The scientific society at that time (1920) refused to accept this idea and he was ridiculed in public by articles in newspapers in which Staudinger was compared to an explorer that found an elephant in Africa of hundreds of meters long. After painstaking scientific experiments on the synthesis of oligomers, he clearly showed that their properties converged towards those of the polymer. In 1953 Staudinger received the Nobel Prize for his important contributions to the field of polymers.

In nature polymers are also very important and vital to many biological systems, such as cellulose, which is a simple polyglucose, but is the most abundant component of plant cells. Nucleic acids (DNA and RNA) and proteins are by far the most important functional biopolymers we can think of. Their structures are very well defined. DNA and RNA are composed of long strands of sugar units which contain base pairs, and are linked by phosphate groups.[2] Proteins and enzymes are constructed from polypeptide chains that are built up from 20 different amino acids. Depending on the sequence of the amino acids the protein can contain two periodic structures, the α-helix and the β-sheet. These structural motifs are stabilized by hydrogen bonds between the amide groups in the main chain.

Nature uses a limited number of monomeric building blocks, but synthetic chemists have innumerous different monomers at their disposal to prepare polymers with, in principle,

every desirable property. This is reflected in the use of polymers in our daily life, where they can be found in many aspects of life from construction materials, cars, computers, clothing, to pharmaceuticals and food.

Polymers exist in a wide variety of compositions, molecular weights, dispersities, functionalities, shapes, etc. Nowadays, they can be tailor-made from a large choice of monomers, allowing the fine-tuning of their properties. This makes them attractive compounds for numerous applications.[3-5] Amphiphilic character block copolymers, constructed from at least two blocks with different properties, tend to aggregate in solvents selective for one of the constituent blocks, thus resembling traditional surfactants. Analogous to surfactants a range of morphologies can be observed when dispersions of amphiphilic copolymers are prepared, i.e. micellar,[6] bilayer,[7] chiral,[8] and other architectures[9] (Figure 1). The driving force for self-assembly is generally considered to be microphase separation of the insoluble blocks.[6]

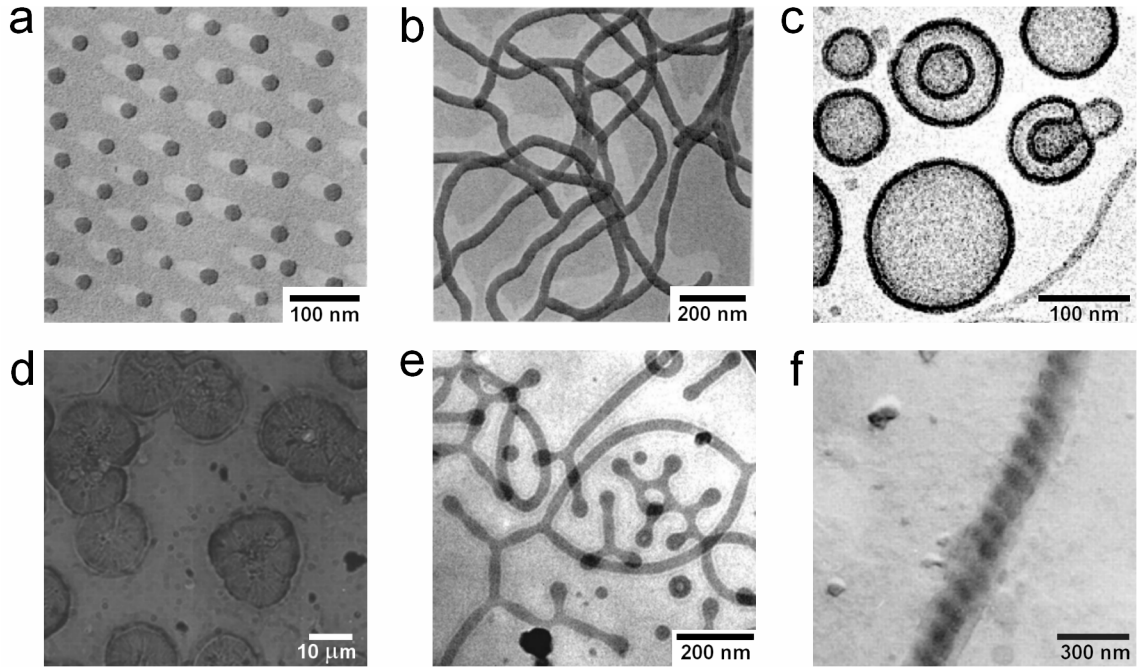

Figure 1. *Electron micrographs of various types of morphologies formed by aggregated block copolymers. a) Micelles and b) micellar rods from polystyrene*-b-*poly(acrylic acid),*[6] *c) vesicles from poly(ethylene oxide)*-b-*polyethylethylene,*[7] *d) lamellae from polystyrene*-b-*poly(phenylquinoline),*[10] *e) branched wormlike micelles from poly(ethylene oxide)*-b-*polybutadiene,*[9] *and f) left-hand helices from polystyrene*-b-*poly(L-isocyanoalanyl-L-alanine).*[8]

1.2 Polymer Based Supramolecular Micro- and Nanoreactors

1.2.1 Introduction

The majority of synthetic reactions are carried out in solution, in which the reactants are free to move. When brought into close proximity of each other, for instance in a cavity or on a surface, the probability of reactants undergoing a reaction increases due to their high local concentration. Enzymes owe their high activity and selectivity partly to the fact that their cavities can bind substrates and can change shape in order to accommodate these guest molecules. Enzyme cavities also play an important role in orientating the substrate in the right spatial manner to facilitate its conversion, using various supramolecular interactions like hydrogen bonding, $\pi - \pi$ stacking, and electrostatic interactions. The structure of the enzyme cavity has a direct effect on the selectivity of the reaction. Large molecules are not able to enter the cavity. The conversion of stereoisomers is unequal due to a difference in fit inside the cavity, resulting in a difference in kinetics as a result of a variation in stabilizing the transition state. In this way enzymes play a fundamental role in catalyzing the chemistry of life.

Various groups have worked on preparing enzyme mimics, i.e. synthetic systems with cavities that possess the possibility to host reactants, starting from simple low molecular weight compounds. More recently, complex supramolecular systems and polymers have been applied.[11] In this section we will focus on polymers as building blocks for micro- and nanoreactors, forming cavities within which substrates can react. The application of polymers as micro- or nanoreactors, either as single macromolecules possessing hollow interiors, or as self-assembled structures having one or more cavities, is a new, emerging field.

1.2.2 Polymersomes as nanoreactors

Vesicles are closed, hollow aggregates with a spherical shape, constructed from self-assembled amphiphilic molecules that form a membrane structure. They can be prepared from a wide variety of amphiphilic molecules, viz. phospholipids, which are the main components of the cell membrane.[12] Bangham,[13] Kunitake,[14] and Ringsdorf,[15] have pioneered the synthesis and construction of these supramolecular structures and have studied their properties. Vesicles, also called liposomes, can be used to encapsulate a variety of compounds

for different purposes. In the cosmetics industry liposomes are filled with, for instance, vitamins and are added to creams.[16] Encapsulation of enzymes inside vesicles allows liposome reactors to be constructed, whilst offering protection from proteases and denaturation. For this purpose mostly phospholipid based liposomes have been used. A comprehensive review discussing enzyme-containing vesicles has been published by Walde and Ichikawa.[17]

Vesicles can also be prepared from macromolecular amphiphiles, i.e. block copolymers, which are referred to as polymersomes. Since the first reports,[18, 19] a large number of examples describing the formation of polymersomes has been published.[20-23] The structure of vesicle-forming block copolymers can vary from simple coil-coil diblock copolymers, rod-coil diblock copolymers to coil-coil and rod-coil multiblock copolymers with and without additional cross-linkable groups (Scheme 1).

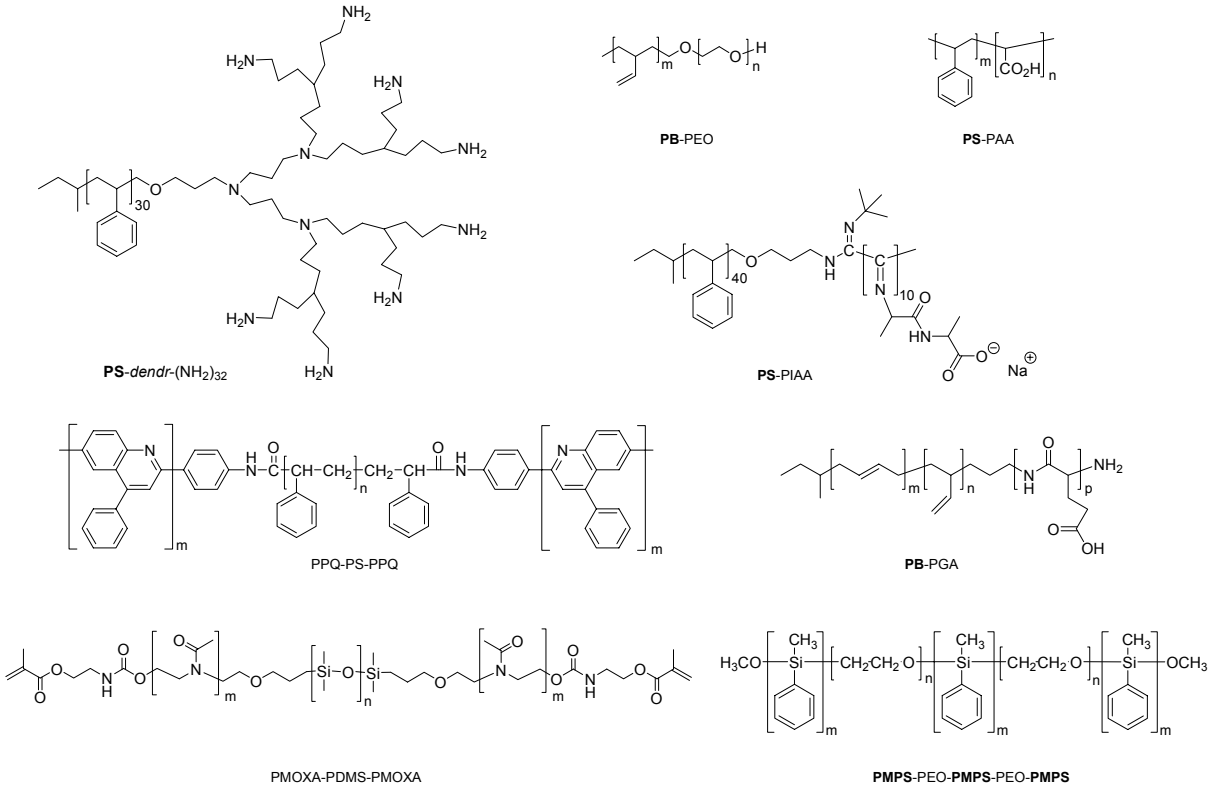

Scheme 1. *Structure formulas of various polymersome-forming block copolymers.*

The advantage of polymersomes over liposomes is their increased stability and the rigidity of their membrane system, which contribute to their increased lifetime. The vast amount of available monomers and the ability to vary the ratio of the two blocks, make it possible to tune the properties of the resulting vesicles, e.g. vesicle size, polarity, stability,

toxicity, etc. In general, however, the permeability of the membranes of block copolymer vesicles is reduced since their thicknesses are higher and their membranes have less fluidic character compared to liposomes.[21]

In the group of Discher much effort has been put into establishing the physicochemical properties of polymersomes based on poly(ethylene oxide)-*b*-polybutadiene (PEO-PBD) and poly(ethylene oxide)-*b*-polyethylethylene (PEO-PEE).[7, 24-26] As a first step towards *in vivo* applications, encapsulation experiments were performed with the proteins myoglobin, hemoglobin, and albumin (Figure 2).

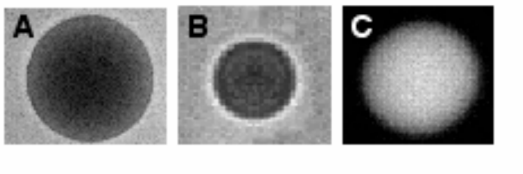

Figure 2. *Encapsulation of proteins using block copolymers made of PEO-PEE.[27] a) A polymersome containing myoglobin (diameter is 15 μm), b) a polymersome containing hemoglobin (diameter is 5 μm), c) a polymersome containing fluorescein-labeled BSA (diameter is 15 μm).*

The encapsulation of these proteins was rather straightforward, viz. adding the solid block copolymer to an aqueous solution of the desired solute and waiting for 24 h. The encapsulation efficiencies for the different proteins, however, varied.[27] The polymersomes appeared to be stable in blood plasma and were observed to be inert to white blood cells and cultured cells. *In vivo* studies performed with these polymersomes in rats showed that their *in vivo* circulation times were about two times longer than "PEGylated" stealth liposomes (20-30 h in rats).[28] These circulation times turned out to be primarily dependent on the PEO block length, rather than on the hydrophobic core-forming block. These experiments clearly show that these PEO-based diblock copolymers have great potential as drug delivery vehicles.

For the controlled release of encapsulated solutes, much effort is being focused on the development of stimuli-responsive vesicles, that is, capsules that are disrupted by changes in their environment. Such a system, based on polymersomes, was prepared by encapsulating the enzyme glucose oxidase (GOx) within polymersomes of poly(ethylene glycol)-*b*-poly(propylene sulfide)-*b*-poly(ethylene glycol) (PEG-PPS-PEG) (Figure 3).[29]

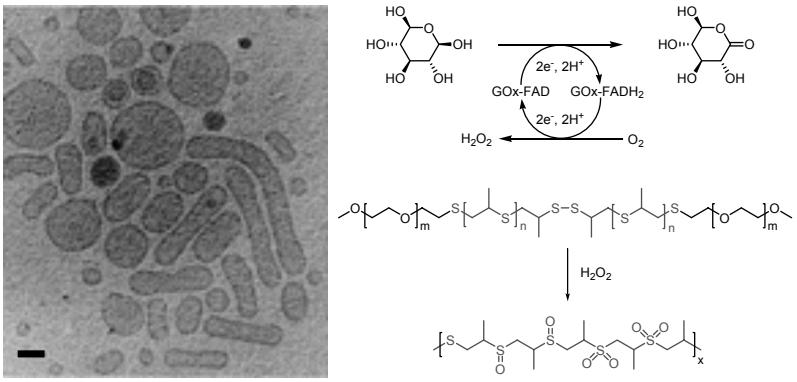

Figure 3. *Glucose-responsive capsules based on oxidation-sensitive PEG-PPS-PEG polymersomes encapsulating GOx.[29] Left: Cryo-TEM micrograph of the capsules, right: Reaction scheme showing the oxidation of glucose which leads to the formation of H_2O_2 and consequently the oxidation of the thioethers. A possible repeating unit of PPS after oxidation by H_2O_2 is shown.*

The thioethers in the hydrophobic middle block are converted to more hydrophilic sulfoxides and sulfones upon exposure to an oxidative environment, in that way increasing the hydrophilicity and solubility of the macromolecular amphiphile. GOx converts glucose to gluconolactone and in the presence of oxygen, hydrogen peroxide is formed. It was shown that destabilization of the GOx-encapsulating polymersomes occurred upon the oxidative action of the formed hydrogen peroxide when glucose was extravesicularly added. This approach to develop stimulus-responsive vehicles for drug delivery seems feasible, but also appears to be rather limited and complex, since the presence of GOx and glucose are required for every application. Another stimulus-responsive polymersome was developed based on polybutadiene-*b*-poly(γ-L-glutamic acid).[30] The size of the polymersome molecules could be reversibly altered by changing both the pH and ion strength. Bellomo *et al.* also recently published on pH-sensitive polymersomes, which are based on diblock copolypeptides.[31] Najafi *et al.* have prepared di- and triblock copolymers containing anhydride groups from fumaric/sebacic acid and PEG.[32] The diblock copolymers formed micelles, while the triblock copolymers yielded polymersomes. It was observed that the hydrolytic degradation of the triblock copolymers was slower than that of the diblock copolymers.

The group of Meier has developed a nanoreactor by incorporating the OmpF channel protein in the membrane and β-lactamase enzymes inside the water pool of polymersomes from the amphiphilic ABA triblock copolymer poly(2-methyloxazoline)-*b*-poly(dimethylsiloxane)-*b*-poly(2-methyloxazoline) (PMOXA-PDMS-PMOXA) (Figure 4).[33]

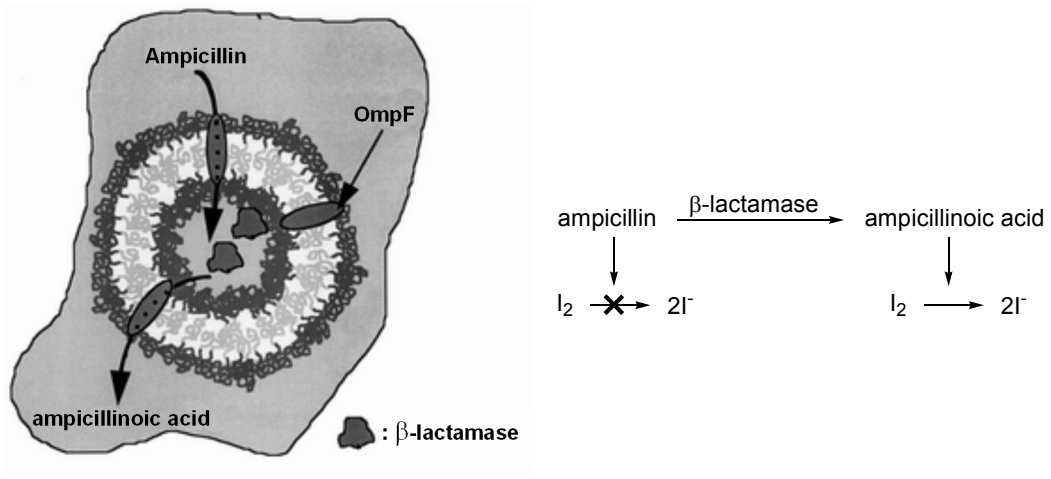

Figure 4. *Polymersome nanoreactor developed by the group of Meier.[33] Left: The nanoreactor is composed of a PMOXA-PDMS-PMOXA vesicle encapsulating β-lactamase enzymes in its inner aqueous compartment and incorporating OmpF channel proteins in its membrane. Right: Oxidation of ampicillin to ampicillinoic acid carried out in the nanoreactor.*

The triblock copolymer carried methacrylate groups at both ends, thus allowing cross-linking of the block copolymers inside the membrane upon irradiation of the polymersomes with UV light, resulting in very stable aggregates. Transport of reagents through the membrane was achieved by the nonspecific OmpF channel protein encapsulated in the membrane, which allows passive diffusion of small solutes up to a molecular weight of 400 $g.mol^{-1}$. The activity of the encapsulated enzyme β-lactamase was determined by external addition of the substrate ampicillin to a nanoreactor dispersion in the presence of a starch-iodine solution. The ampicillin is hydrolyzed by β-lactamase to ampicillinoic acid and only the latter is able to reduce iodine to iodide, resulting in decolorization of the starch-iodine solution, hence allowing the enzyme activity to be monitored spectrometrically (Figure 4).

The same experiment carried out with polymersomes having no membrane channels did not show any enzyme activity during the course of the experiment, indicating that no substrate could diffuse through the membrane. Interestingly, the channel protein showed no decrease in permeability after cross-linking of the membrane.

The OmpF channel protein closes upon increasing the transmembrane potential above a critical value of 100 mV. Since molecules above 400 $g.mol^{-1}$ are unable to pass the membrane, poly(styrene sulfonate) having sodium counterions was used to increase the potential. The sodium ions will equally distribute between the in- and outside of the polymersome while the poly(styrene sulfonate) remains outside, in this way establishing a

potential, known as a Donnan potential. By this approach the conversion of ampicillin could be stopped, while dilution of the dispersion or addition of NaCl opened the channels again, resulting in complete regeneration of the nanoreactor activity.[34]

The growth of calcium phosphate crystals within polymersomes of the same PMOXA-PDMS-PMOXA triblock copolymer has also been studied.[35] For these experiments ion carrying ionophores instead of the OmpF channel protein described in the above studies were incorporated in the polymersome membranes to facilitate the transport of calcium ions. The polymersomes were prepared in the presence of phosphate buffer and the free phosphate ions were removed by dialysis. This was followed by the addition of a $CaCl_2$ solution. Fractions were taken from the sample and they were mixed with three different ionophores. The polymersomes were studied by electron microscopy and after 1 h the growth of calcium phosphate crystals on the inner membrane could be observed. After 24 h a considerable amount of space inside the polymersomes was filled with calcium phosphate crystals. In contrast, polymersomes that were not mixed with ionophores did not show crystal formation.

The versatility of PMOXA-PDMS-PMOXA polymersomes was further demonstrated by the injection of λ phage DNA by λ phages *via* a bacterial channel-forming protein incorporated in the polymersome membrane.[36] The bacterial channel-forming protein served as a receptor for the λ phage and triggered the ejection of the phage DNA. It is noteworthy that the bacterial channel-forming protein and λ phage functioned well within the unnatural environment of the polymersomes. This showed that complex biological processes can be simulated by using polymeric materials, opening the way toward hybrid cells.

An interesting example of the application of capsules filled with a reactive compound was presented by White *et al*.[37] They developed a polymer with self-healing capacity by incorporating microcapsules containing dicylcopentadiene monomers and a polymerization catalyst within an epoxy matrix. When the matrix was placed under stress cracks were formed, which ruptured the microcapsules, thereby releasing the monomers into the crack through capillary forces. Polymerization was initiated by contact with the embedded catalyst, resulting in bonding of the crack faces. Fracture experiments yielded 75 % recovery in toughness compared to the virgin material.

A different approach towards the preparation of catalytically active polymersomes is the use of “giant” amphiphiles, in which proteins or enzymes act as the polar head group of the amphiphile and a synthetic polymer as the apolar tail. Boerakker *et al.* have developed such a bio-hybrid amphiphile by reconstituting apo-horseradish peroxidase with its cofactor,

ferriprotoporphyrin IX, carrying a polystyrene tail (Figure 5 a and b).[38] In water the enzyme-polymer hybrid formed vesicular aggregates with diameters of 80 – 400 nm (Figure 5 c).

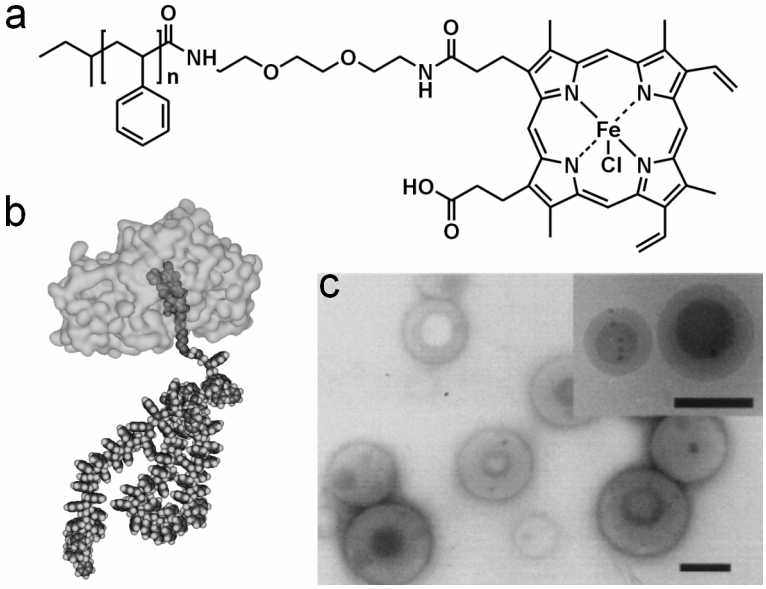

Figure 5. *Vesicles formed in water by a bio-hybrid amphiphile of horseradish peroxidase-polystyrene.[38] a) Structure formula of the modified cofactor, b) computer-generated model of the bio-hybrid, and c) transmission electron micrograph of the formed vesicles. Scale bars represent 200 nm.*

Catalytic activity measurements showed that the horseradish peroxidase-polystyrene aggregates were still active. This approach is promising, since other ferriprotoporphyrin IX-containing enzymes could also be used to construct giant amphiphiles. The resulting different hybrids can be combined within one aggregate to give a catalytic system that is capable of performing cascade reactions.

1.2.3 Polymer micelles as nanoreactors

A regularly seen morphology for block copolymers is that of a micelle, in which the polar block is on the outside and the apolar block on the inside or vice versa, depending on whether the solvent is polar or apolar. Micelles, which can be spherical, rod-like or display a hexagonal phase, have a compartment that is capable of accommodating solutes.

The use of micelle-forming amphiphilic block copolymers in the stabilization of metal nanoparticles has been intensively studied, especially by the groups of Antonietti, Möller, and Cohen.[3, 39-41] Not only does the presence of the polymeric shell around the metal particles aid

in the prevention of agglomeration and precipitation, it also improves their processability. The block copolymer micelles can indeed be regarded as nanoreactors, because metal nanoparticles are synthesized inside their interior. Homopolymers have also been frequently employed for the stabilization of metal colloids, mainly poly(*N*-vinyl-2-pyrrolidone) (PVP). Although the resulting homopolymer-metal particle hybrids are not micelles, they are discussed in this paragraph, because their dimensions and behavior are comparable to the micellar systems presented here. The nanosize dimensions of the metal particles give rise to a number of intriguing electronic, magnetic, optical, and catalytic properties, which is the result of size quantization effects and the high number of surface atoms compared to the number of atoms in the bulk of the particle.[5, 39] The steps involved in the formation of such metal particles are depicted in Figure 6.

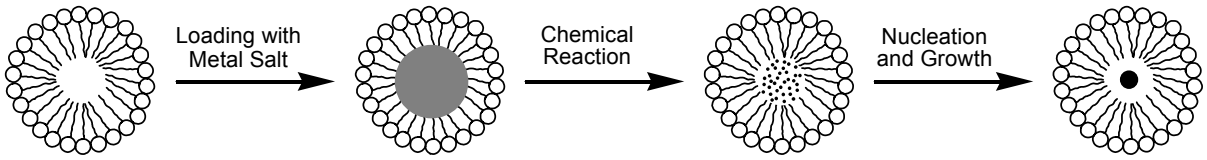

Figure 6. *Steps involved in the preparation of a metal nanoparticle inside a micellar nanoreactor.*

In Figure 6 only one approach using metal salts for the formation of polymer-metal hybrids is given, but other approaches have been developed as well. It is also possible to first complex the metal ions to the monomers, then polymerize the monomers and finally, induce aggregation of the resulting metal-polymer hybrids. In order to obtain stable hybrid materials of polymers and inorganic material there has to be sufficient adhesion between the polymer chains and the metal particles. For that purpose homopolymers and block copolymers have been synthesized with functional blocks, i.e. acidic, basic, or neutral coordinating blocks. The formation of the metal colloids inside the loaded micelles occurs by performing a chemical reaction, typically a reduction. For this purpose H_2, $NaBH_4$, $LiAlH_4$, $LiBEt_3H$ and hydrazine are commonly applied to prepare nanoparticles of Ag, Au, Co, Cu, Ni, Pb, Pd, Pt, Rh, and Zn.[3, 40] The formed metal particles subsequently aggregate to yield larger particles by nucleation and growth processes. Depending on the degree of supersaturation with the metal particle-forming salt, the interfacial tension of the block copolymer/metal particle interface, and the diffusivity of the metal ions, one or more metal nanoclusters are formed within a micelle.[3] In Figure 7 the effect of supersaturation with the salt $Pd(OAc)_2$ inside diblock

copolymer micelles of polystyrene-b-poly(4-vinylpyridine) (PS-P4VP) is shown.[42] When the solubilized $Pd(OAc)_2$ was rapidly reduced (high supersaturation), numerous small metal particles were formed within the micellar core, also referred to as the "raspberry" morphology. Slow reduction (low supersaturation), however, led to on average one large particle per micelle, which is called the "cherry" morphology.[42]

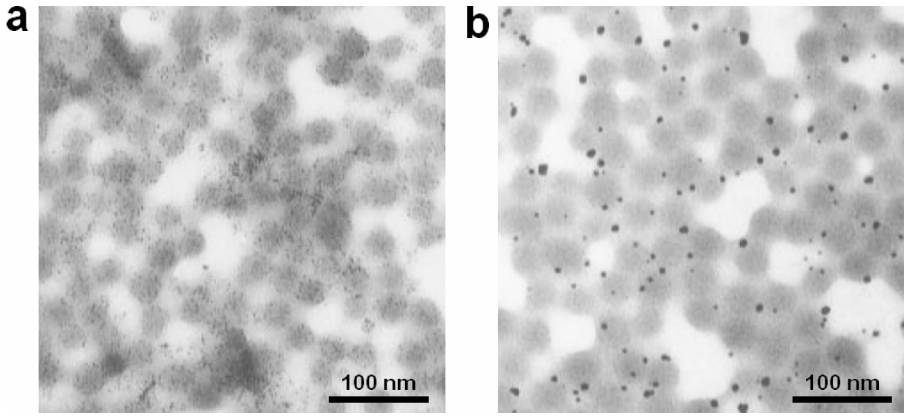

Figure 7. *Formation of metal nanoparticles inside block copolymer micelles.[42] a) Many Pd colloids are formed inside micelles during fast reduction (raspberry morphology). b) On average one large Pd colloid per micelle is formed during slow reduction (cherry morphology).*

Not only metal colloids, but also metal oxides,[5, 43] e.g. Fe_2O_3, TiO_2, and ZnO, and metal sulfides,[5, 44] e.g. CdS, CoS, CuS, FeS, PbS, and ZnS, can be formed within micellar nanoreactors. The latter nanoparticles are mostly formed by addition of H_2S to the metal precursors inside the nanoreactors, while the former nanoparticles are prepared by oxidation reactions. The optical properties of the metal sulfide semiconducting nanocrystals are very size-dependent and size control can be obtained by varying the size of the polymer aggregates. In smaller domains nanoparticles of lower dimensions are formed, which have absorption edges at smaller wavelengths due to the size quantization effect. Reducing the dimensions of semiconductor nanoparticles, furthermore, results in photogenerated electrons that have higher energies, which can be utilized in photovoltaic devices, and increased optical absorption coefficients. The latter is useful in applications where UV protection is an issue. Micellar fibers of block copolymers of carbosilane dendrimers and polyisocyanopeptides have been applied to prepare silver arrays by clustering Ag^+ ions inside these fibers.[45] Further details are given in section 1.3.3.

The polymer micelle-metal hybrid itself can also be considered to be a nanoreactor, since the catalytically active metal colloid is buried inside the micelle core and the reactants have to pass the micellar shell in order to reach the interior. These hybrid particles combine the advantages of homogeneous and heterogeneous catalysis, since they can be dissolved in organic solvents, due to their polymeric shell, while catalyst recovery is straightforward by performing ultrafiltration or precipitation in poor solvents for the polymer.

So far, the polymer micelle-metal hybrids have mainly been applied in the hydrogenation of olefins and acetylenes, where advances have been made in chemo-, stereo-, and regioselective hydrogenations of various substrates.[39, 46] A nice example of chemoselective hydrogenation was presented by Yu *et al*. who used Pt nanoparticles stabilized by PVP to reduce the carbonyl group in cinnamaldehyde to cinnamic alcohol, while leaving the double bond intact.[47] Ethyl pyruvate was reduced enantioselectively to (*R*)-ethyl lactate in 95-98 % enantiomeric excess by Pt colloids stabilized by PVP with cinchonidine as chiral modifier.[48] Colloidal dispersions of PVP-stabilized Au/Pd bimetallic clusters, prepared by successive reduction, were employed by Harada *et al.* for partial selective reduction of cycloocta-1,3-diene to cyclooctene.[49]

Polymer-stabilized metal colloids have also been used in oxidation reactions. The catalytic oxidation of ethylene to ethylene oxide by colloidal Ag catalysts, which were protected by PVP or sodium polyacrylate, was studied by Toshima and coworkers.[50, 51] Both systems had higher catalytic activities than commercial Ag powder, while the sodium polyacrylate-stabilized Ag particles gave the best results due to a higher thermal stability.

Another field of catalysis in which polymer-metal hybrid nanoreactors have been explored is C-C coupling reactions. The first example of methanol carbonylation, which is one of the most important industrial processes, was presented by Wang *et al.* who applied PVP-stabilized Rh colloids.[52] The catalysts were used under harsh conditions of 140°C and 54 bar, but could still be recycled 6 times, resulting in an overall turnover number of 19,700/atom Rh. Pd colloids stabilized by either PS-P4VP or PVP have proven to be useful in Heck reactions (Scheme 2).[42, 53]

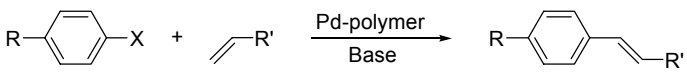

Scheme 2. *Heck reaction catalyzed by Pd-polymer hybrids.*[42, 53]

The polymer-stabilized Pd nanoparticles displayed activities comparable to those of low molecular weight Pd complexes traditionally used in Heck reactions, while having much higher stabilities; turnover numbers (moles of substrate/mole of Pd) as high as 100,000 have been reported.[53] The higher stability of the polymer-metal hybrid is also reflected in the high temperature (140°C) at which these reactions were carried out.

El-Sayed and coworkers have used the Suzuki coupling as a test reaction to investigate the effect of the polymeric stabilizers on both the catalytic activity and stability of Pd colloids (Scheme 3).[54]

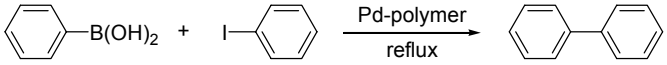

Scheme 3. *Suzuki coupling reaction catalyzed by polymer-stabilized Pd nanoreactors.*[54]

They prepared polymer encapsulated Pd nanoparticles with the help of three different polymers: a PAMAM dendrimer, polystyrene-*b*-poly(sodium acrylate) and PVP. All three nanoreactor systems were efficient catalysts for the Suzuki reaction between aryl boronic acids and aryl halides. It was found that a strong interaction between the metal particle and the polymer resulted in a loss of catalytic activity. Lee *et al.* investigated the same type of reaction in water using aggregates of rod-coil triblock copolymers as micellar nanoreactors.[55] At ambient temperatures the Suzuki cross-coupling reaction of aryl halides and aryl boronic acids was performed in the absence of organic solvents, resulting in a potentially environmentally friendly reaction process.

Micelle-forming polymers have been employed to encapsulate enzymes. Micelle-like aggregates built up from diblock copolymers of (*N*-acetylimino)ethylene and (*N*-pentanoylimino)ethylene were capable of encapsulating horseradish peroxidase, lipase OF, and lipase P. Interestingly, the hydrolytic activities of the lipases in aqueous solutions increased by ca. 30% compared to the free enzyme.[56] Even in water-saturated organic solvents the enzymes showed enhanced activities. Harada and Kataoka have published several papers on supramolecular assemblies of micelle-forming poly(ethylene glycol)-poly(aspartic acid) block copolymers and chicken egg white lysozyme.[57, 58] The polyion complex (PIC) micelles could be reversibly formed and dissociated by changes in the ionic strength, simply by varying the NaCl concentration (Figure 8).[59]

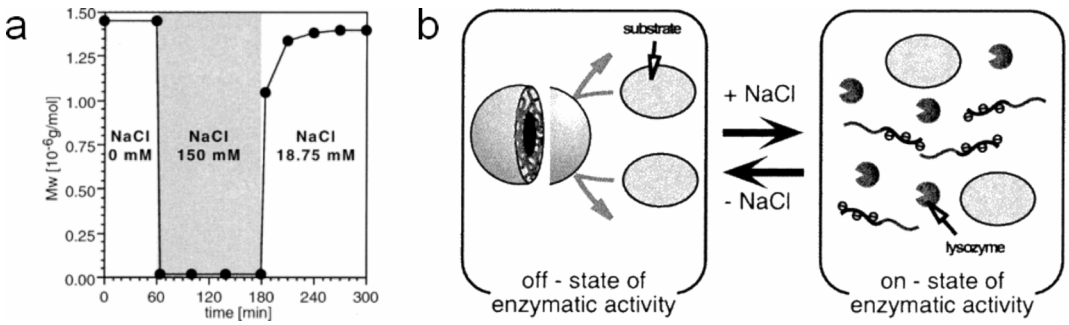

Figure 8. *On-off control of enzymatic activity of PIC micelles with entrapped lysozyme enzymes. a) Reversible formation and dissociation of PIC micelles through a change in NaCl concentration. b) Schematic model of on-off control of enzymatic activity through reversible formation of PIC micelles.*[59]

Lysozyme entrapped within the core of the micelles showed no enzymatic activity, but upon an increase in the ionic strength the micelles dissociated, thus releasing the enzymes and enzymatic activity was detected. A reduction of the ionic strength resulted in complete inhibition of the enzymatic activity. The dissociation of the PIC micelles to obtain enzyme activity is not a nanoreactor behavior, but Harada and Kataoka also performed experiments using the substrate *p*-nitrophenyl-penta-*N*-acetyl-β-chitopentaoside, and they observed conversion within the core of the micelles.[60] The apparent enzymatic activity of the entrapped enzymes was higher than that of the free enzymes, which was attributed to accumulation of substrate in the corona of the micelles. Applying a pulsed electric field to the polymer-enzyme hybrids above a critical potential reduced the enzymatic activity to that of the free enzyme, presumably due to a minute change in the local microenvironment in the core of the micelles.[61] The enzymatic activity was fully restored when the electric field was shut-off.

As described above, giant amphiphiles of polymers and enzymes can be prepared by reconstituting apo-enzymes with its cofactor carrying a polymer tail.[38] Velonia *et al.* have constructed another type of bio-hybrid amphiphile by specific attachment of a polystyrene block to a reduced disulfide bridge of CAL B, exposed on the outer surface of the enzyme.[62] TEM studies of aqueous dispersions of PS-CAL B giant amphiphiles revealed the presence of micrometer long fibers (Figure 9).

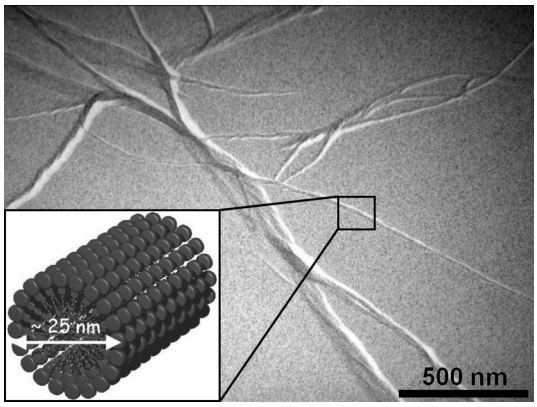

Figure 9. *TEM image of the micellar aggregates present in aqueous dispersions of PS-CAL B hybrids.*

Closer examination of these fibers showed that they were built up from bundles of rods, which had dimensions corresponding to a rod-like micellar architecture. Catalysis experiments on these enzyme-polymer hybrids revealed that the enzymes retained activity, though notably reduced when compared to the native enzyme. Although this is not a nanoreactor, this approach of making catalytically active giant amphiphiles is a promising strategy in the preparation of ensembles of different enzymes and has potential for the construction of multi-component nanoreactors in which substrates are converted in several cascade-like steps into the desired product(s).

Micelles in which emulsion polymerizations are carried out can also be considered as nanoreactors. Apart from low molecular weight surfactants,[63] micelle forming block copolymers have been applied for this purpose. Jang and Ha have used poly(oxyethylene)-*b*-poly(oxypropylene)-*b*-poly(oxyethylene) in order to make hollow polystyrene nanospheres.[64] Mini-emulsion polymerization has also proven to be a valuable tool for the fabrication of polymeric capsules.[65] Mini-emulsions are stable emulsions consisting of droplets of 50 – 500 nm in diameter created by shearing a mixture of oil, water, surfactant, and a highly hydrophobic compound. The hydrophobic compound prevents Ostwald ripening while the surfactant stabilizes the droplets against collisions.[66] This process allows the preparation of latex particles having cavities with control of particle size, cavity volume fraction, and structure.[67] The differences in the hydrophilicity of the oil and the polymer proved to be the driving force for capsule formation. Although mini-emulsion polymerizations do not involve the formation of micelles it is an interesting technique to prepare hollow polymeric capsules with broad applicability.

1.2.4 Unimolecular nanoreactors

The dynamic nature of polymeric micelles makes them sensitive to environmental conditions. To overcome this, covalent systems such as dendrimers, hyperbranched polymers and star polymers have recently been employed and they have found application as stabilizers in the formation of nanoparticles, recoverable metal catalysts, and nanoreactors. These unimolecular compounds are, to some extent, comparable with micelles since they possess an inner compartment capable of accommodating guest molecules, the main difference being that they are not dynamic assemblies. Although the above mentioned types of polymers are not self-assembled structures, we will discuss them briefly in this chapter, because of their similarity to polymer micelles.

A dendrimer is a single molecule with a central core from which in a regular fashion branches emerge radially. The overall shape of dendrimers and the existence of cavities inside these compounds are topics of controversy. Most dendrimers are flexible structures, but they adopt a globular shape at a certain generation, which results in an increase in their rigidity.[68] The use of dendrimers in catalysis is well documented in the literature and is described in a number of reviews.[68-74] Covalently attached catalytic sites in dendrimers can be present at the periphery, at intermediate places or can constitute the center of the dendrimer. In the last case the catalytic site is protected by the dendritic branches, resulting in an enzyme mimic. In general, three types of dendrimer nanoreactors can be distinguished: *i*) dendrimers with a catalytically active core,[70, 71] *ii*) free-energy driven dendrimer nanoreactors, which are not directly involved in the reaction,[73] and *iii*) dendrimers that stabilize a catalytically active metal nanoparticle (Figure 10).[69]

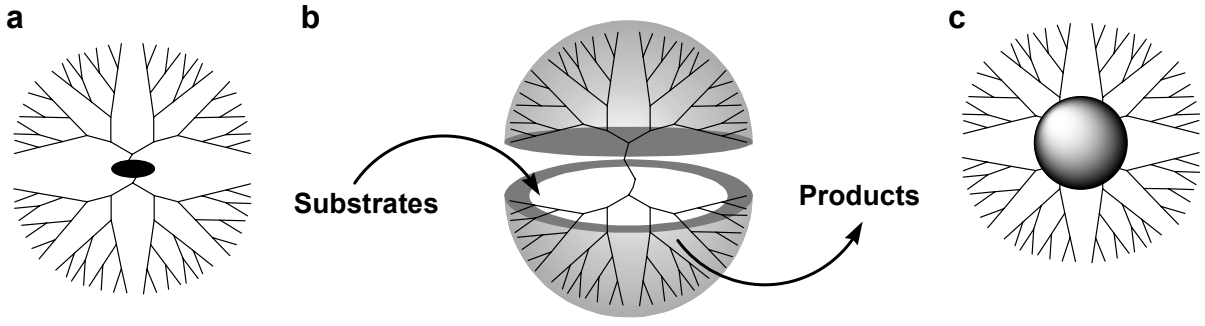

Figure 10. *Three different types of catalytically active dendrimers: a) dendrimer with a catalytically active core, b) free-energy driven dendrimer nanoreactor, and c) catalytically active metal nanoparticle stabilized inside a dendrimer.*

The results obtained with these types of dendrimer nanoreactors in catalysis vary greatly, but in general the dendrimers have an added value, i.e. by stabilizing the catalytically active center, by increasing the stereo- and regioselectivity of the reaction, and by allowing easy recovery of the catalyst, e.g. by filtration or precipitation.[70]

Hyperbranched and star polymers are cheaper alternatives of dendrimers, because these three-dimensional macromolecular structures can be prepared more easily using conventional polymerization methods.[75-77] In a similar fashion to block copolymer micelles it has recently been demonstrated by several groups that these hyperbranched and star polymers are capable of encapsulating catalytically active metal complexes and nanoparticles within their cores.[77-80]

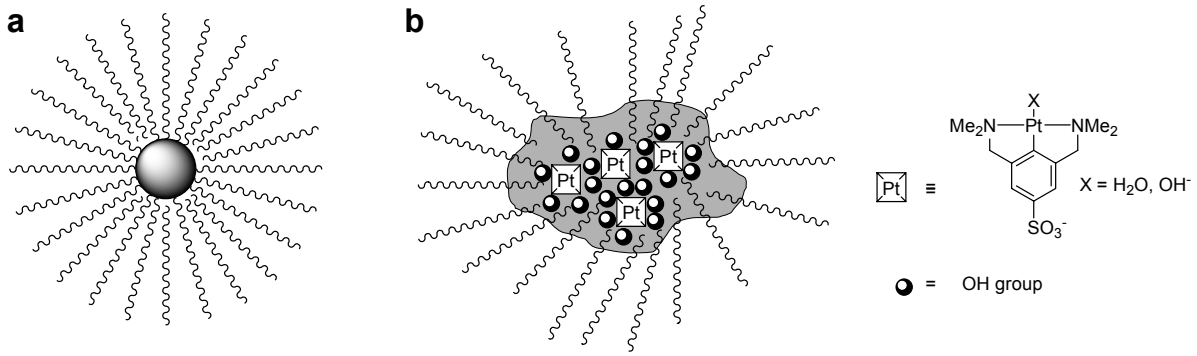

Figure 11. *Catalysis inside star and hyperbranched polymers, a) star polymer encapsulating a catalytically active nanoparticle,[77] b) hyperbranched polyglycerol nanocapsule with catalytically active pincer Pt complexes.[79]*

These nanoreactors were applied in a wide variety of catalytic processes, e.g. the hydrogenation of cyclohexene,[78] a double Michael addition,[79] a Heck reaction,[77] and the oxidation of alcohols to ketones,[80] thus showing that these macromolecular structures are very versatile and can be used in a broad scope of reactions. Like block copolymer micelles the recovery of polymer-metal hybrids from the reaction mixture is easy using dialysis or precipitation, while they have the advantage of an enhanced stability due to their less dynamic nature.

1.2.5 Other supramolecular polymeric systems as nanoreactors

Numerous papers have been published dealing with systems that are potential nanoreactors. We will discuss below some systems that have a good chance of being

transformed into a working nanoreactor. In this section also polymeric nanoreactors will be discussed that cannot be classified under the subjects of the previous paragraphs.

Chernyshov *et al.* have used a chelating diblock copolymer, polystyrene-*b*-poly(*m*-vinyl-triphenylphosphine) (PS-*b*-PPH), to prepare polymeric $PdCl_2$ complexes.[81] They found that this hybrid system self-assembled to yield finite structures upon dispersion in THF; no gels were formed. Depending on the ratio phosphine/Pd, different morphologies were obtained, i.e. disk-like micelles, uni- and multilamellar vesicles, and "perforated hulls". Although not described by the authors, these aggregates might be useful catalysts in Heck reactions or other processes that require Pd, with the advantage that the aggregates can be easily recovered by filtration or precipitation.

A variety of other systems have also been developed for the construction of nanoreactors. Jungmann *et al.* have prepared hollow amphiphilic poly(organosiloxane) nanospheres by sequential condensation of silanes and have used them as nanoreactors for the synthesis of Ag, Au, and Pd nanoparticles (Figure 12).[82]

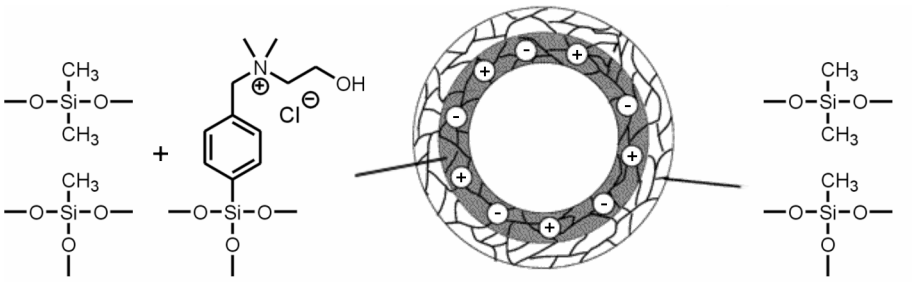

Figure 12. *Schematic picture of the hollow amphiphilic nanoreactor that was used by Jungmann* et al. *for the synthesis of metal colloids.[82] The grey part consists of dimethylsiloxane, methylsiloxane, and a quaternary ammonium salt, the outer shell is built up from dimethylsiloxane and methylsiloxane only.*

After loading the hollow poly(organosiloxane) nanospheres with salts of the noble metals, reduction was performed with $LiBEt_3H$, resulting in the formation of 2-5 nm size metal colloids.

Polymer-containing hollow spheres can also be prepared in a self-assembling approach, viz. by assembling polymers around spherical colloids.[83] This method, referred to as layer-by-layer (LbL) technique, allows the formation of nano-capsules with a well-defined constitution by coating the colloidal templates with alternating layers of polyanions and polycations.[84] The templates can be removed by changing the pH or by using solvents

selective for the templates.[85] These hollow particles have recently been applied as nanoreactors for a variety of reactions.[86] Adopting a ship-in-a-bottle approach, hollow polymeric capsules were loaded with different monomers and consecutively polymerized. The capsule wall proved permeable for the monomers whereas the polymers were trapped inside. In this way the physicochemical properties of the capsule interior could be varied over a broad range (ion strength, pH, viscosity, etc.). In a similar manner the cationic dye 1,1'-diethyl-2,2'-cyanine (DEC) was crystallized inside polymeric capsules that contained poly(styrene sulfonate) (PSS).[87] The PSS was introduced inside the capsules by the ship-in-a-bottle approach (Figure 13).

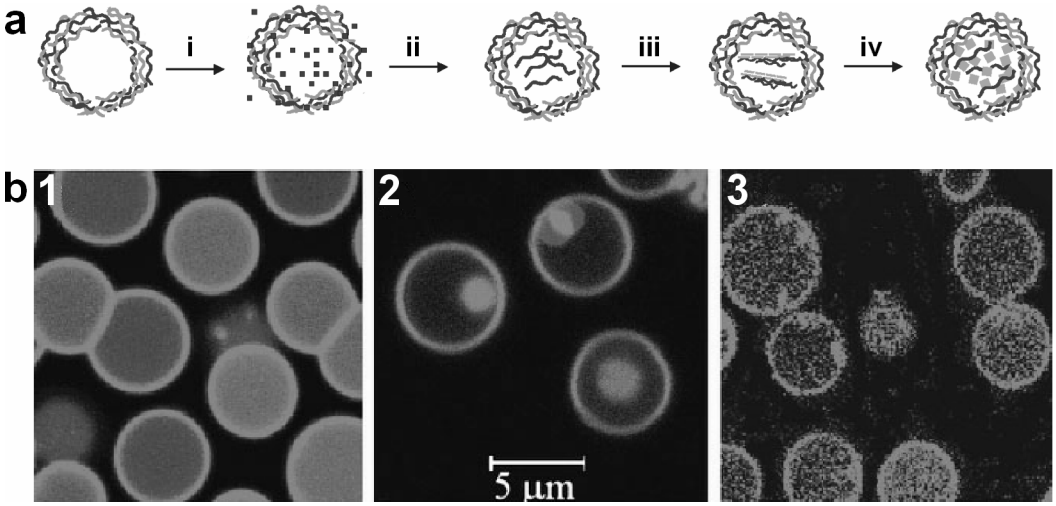

Figure 13. *a) Steps involving the crystallization of DEC inside polymeric capsules, i) loading of the shell with styrene sulfonate, ii) polymerization of styrene sulfonate inside the capsule, iii) polymer-induced formation of DEC-PSS aggregates, iv) precipitation of DEC crystals and the release of free PSS within the polymer shell, b) confocal laser scanning micrographs of 1) capsules containing styrene sulfonate (visualized using rhodamine 6G), 2) fluorescence arising from DEC-PSS aggregates formed inside the capsules, 3) destruction of the DEC-PSS aggregates by laser light.*[87]

The formed fluorescent DEC-PSS aggregates were highly photosensitive and light irradiation resulted in destruction of the aggregates and redistribution of PSS inside the capsules. Addition of tetraphenylborate ions resulted in precipitation of fluorescent DEC-BPh_4 nanocrystals and release of PSS inside the polymer shells.

The versatility of the LbL technique was further demonstrated by coating human erythrocytes with alternating layers of polyanions and polycations.[88] A protein destruction

treatment was carried out to decompose the cytoplasmic proteins of the erythrocytes, which were removed by centrifugation or filtration. The resulting shells were used for the controlled precipitation or crystallization of organic and inorganic materials. In another biomimetic approach $CaCO_3$ was synthesized exclusively inside micron-sized polyelectrolyte capsules.[89] Urea hydrolysis, catalyzed by urease, led to the fermentative formation of CO_3^{2-} ions and the precipitation of $CaCO_3$ which completely filled the capsule interior. The LbL approach was also adopted by Ghan *et al.* to polymerize phenols within polyelectrolyte microcapsules.[90] After formation, horseradish peroxidase (HRP) could be loaded inside the hollow shells by adjusting the pH of the solution to 4.0, resulting in an increase in the shell wall permeability which was large enough to allow HRP to diffuse inside. An increase of pH to 8.5 closed the capsule walls again, entrapping the HRP enzymes. Polymerization of 4-(2-aminoethyl)phenol hydrochloride catalyzed by HRP-containing capsules in the presence of H_2O_2 gave easily detectable fluorescent polymers. The capsule walls turned out to be selective: the monomer and H_2O_2 were able to diffuse in and out, whereas the polymer remained inside the capsule. These experiments show that the hollow capsules prepared by the LbL technique create many new possibilities for the synthesis of composite materials under biologically friendly conditions.

For the development of blood substitutes polymers have been applied to encapsulate hemoglobin, and some of these systems are already in clinical trials (Figure 14).[91]

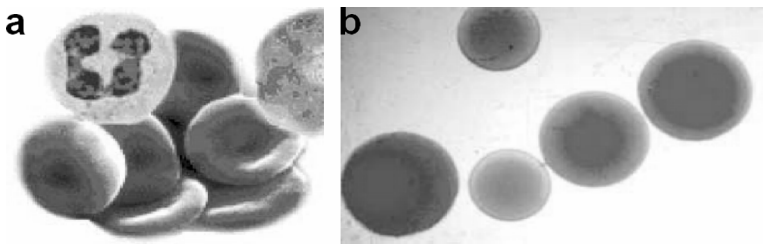

Figure 14. *Optical micrographs of a) red blood cells (7 μm in diameter), and b) artificial red blood cells containing hemoglobin and enzymes.*[91]

Although the first attempts of making artificial blood cells date back to the 1950's, only in the 1990's serious attention was given to these systems in connection with studies aimed at avoiding the risks of HIV infection. The use of biodegradable polylactide allows one to encapsulate the whole content of red blood cells, and the amount of hemoglobin that can be captured matches that of red blood cells. Additional enzymes can be encapsulated in these systems while the products of reactions taking place inside the nanocapsules can diffuse out

and, therefore, do not accumulate. Furthermore, reducing agents from the plasma can also diffuse into the nanocapsules where they reduce methemoglobin to oxygen-carrying hemoglobin. Animals have been infused with these nanocapsules to the extent of one-third of their total blood volume. Higher circulation life-times were obtained with ultrathin membrane nanocapsules containing hemoglobin and enzymes based on poly(ethylene glycol)-polylactide (PEG-PLA).[92] The PEG-PLA nanocapsules were optimized by using polymerized hemoglobin, higher molecular weight PLA, higher concentrations of PEG-PLA and cross-linking of the PEG-PLA nanocapsules.

1.3 Polyisocyanides

1.3.1 Introduction

Polyisocyanides are prepared from isocyanide monomers, resulting in a polymer that has a backbone consisting of only carbon atoms. A special feature of these polymers is that every carbon atom in the backbone bears a substituent (Scheme 4).

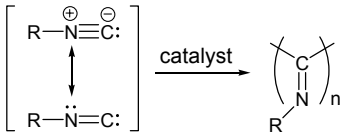

Scheme 4. *Polymerization of isocyanide molecules.*

As a result, steric hindrance and therefore restricted rotation around the carbon-carbon single bonds in the polymer backbone are present. Polymers of *t*-butyl isocyanide could be separated on a chiral column into two fractions with opposite values of optical rotation, from which it was concluded that helical polymers were formed, having an excess of left- and right-handed poly(*t*-butyl isocyanide) helices.[93] The helical arrangement of polyisocyanides is the result of the restricted rotation around the single bonds connecting the carbon atoms of the polymer backbone. The helical structure of a polyisocyanide is a so called four-over-one helix, denoted as 4_1 (Figure 15). Another effect of the hindered rotation is an increased rigidity of the polymer backbone. It has been recently found that the rigidity of polyisocyanides can be further increased by preparing polymers from monomers that contain side groups capable of forming intramolecular hydrogen bonds.[94]

Figure 15. *Left: modeled structure of the 4_1 helical conformation of a polyisocyanide, middle: schematic drawing of the right-handed helix, right: top view of the helix.*

From optically pure amino acids polyisocyanopeptides were synthesized, which had a higher persistence length than DNA (76 nm vs. 53 nm).[95] The advantage of using amino acids is the availability of a large variety of different optically pure amino acids, the vast knowledge about peptide chemistry available in the literature and the relatively easy way amino acids can be converted into peptides and into isocyanides via the corresponding formamides (Scheme 5).

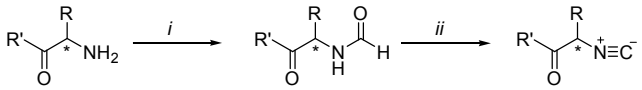

Scheme 5. *Preparation of an isocyanide from an amino acid or a peptide via the intermediate formamide; i) HCO_2Et, HCO_2Na; ii)* N-*methylmorpholine, diphosgene.*

The first catalysts found to polymerize isocyanides were acids. Millich used acid-coated glass plates for the preparation of polyisocyanides.[96] Nolte *et al.* studied the use of nickel(II) salts as potential catalysts for the polymerization of isocyanides and discovered that $NiCl_2.6H_2O$ and $Ni(Acac)_2$ (HAcac = acetylacetone) are very efficient catalysts.[97] Based on kinetic measurements and experiments with optically active isocyanides a mechanism for the Ni(II) catalyzed polymerization was proposed.[98] When a Ni(II) salt is added to a solution of isocyanide monomers, a square planar complex is formed (Scheme 6). The polymerization is initiated by attack of a nucleophilic species on one of the coordinated isocyanides. Amines and alcohols are good nucleophiles for this purpose. It was shown by spectroscopic studies that the nucleophile first coordinates to the Ni center and then forms a carbene complex. This carbene ligand attacks a neighboring coordinated isocyanide, thus forming the first C-C bond of the polymer, immediately followed by the complexation of an isocyanide from solution to fill up the created vacancy. When achiral isocyanides are used the chances of attacking the left or the right neighbor are equal, but a preferred direction of attack can be achieved when either a chiral initiator or a chiral isocyanide is used.[93, 99]

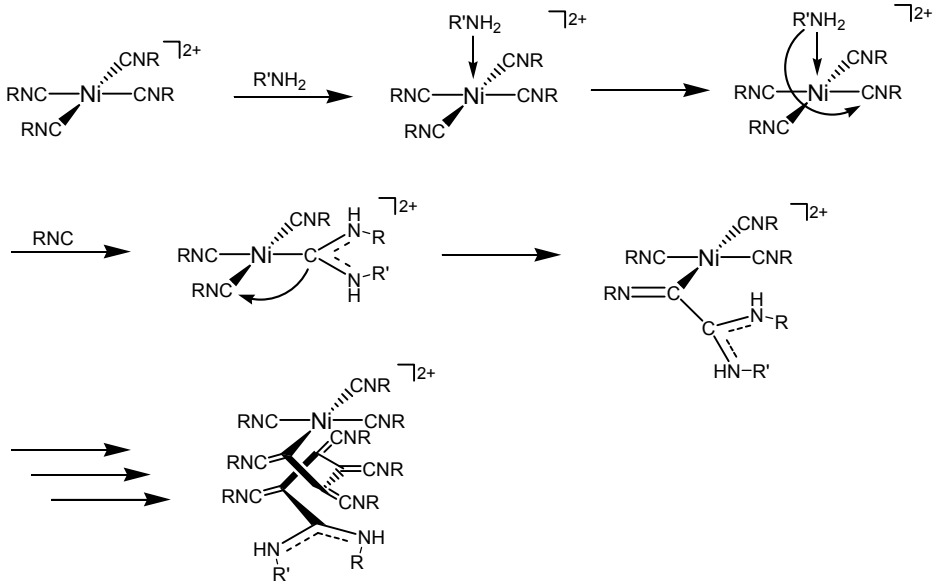

Scheme 6. *Proposed 'merry-go-round' mechanism for the polymerization of isocyanides by a* Ni^{2+} *catalyst.*

According to theoretical calculations on octamers of polyisocyanides with aliphatic side chains performed by Clericuzio *et al.* the helical arrangement of a polyisocyanide is a local energy minimum and not the absolute minimum, which is the so-called *syndio* structure (Figure 16).[100]

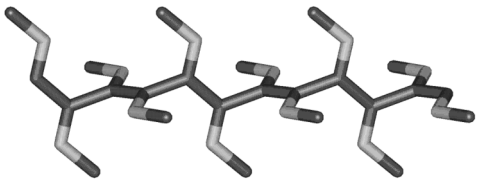

Figure 16. *The* syndio *structure of a 12 units long polyisocyanide is the thermodynamically most favorable structure, according to calculations by Clericuzio* et al.*[100]*

The results of the calculations were compared with CD, UV-Vis and NMR spectroscopic data of polyisocyanides reported in the literature and it was found that several features did not support the predominance of the 4_1 helix. For aliphatic polyisocyanides absorption at long wavelengths was constantly observed and was ascribed to conjugation of imine chromophores. In the geometry of the *syndio* structure such a conjugation is present, which can account for the absorption at higher wavelength. Calculations of the CD spectra of polyisocyanides in both the 4_1 helical conformation and in the *syndio* conformation showed that the experimental data for aliphatic polyisocyanides are closer to the values calculated for

the *syndio* conformation. It needs to be noted that the obtained results are for polymers in a thermodynamically stable state, whereas most polyisocyanides are formed under kinetic control. If the helix inversion barrier is low, however, unfolding of the polymer into the *syndio* structure can readily occur. Calculations carried out by Kollmar and Hoffmann indicated that steric hindrance prevents the possibility for polyisocyanides to adopt a planar all-trans structure.[101] They concluded that the principle minimum for the conformation of polyisocyanides is close to that of a 4_1 helix, which is in contrast to the findings of Clericuzio *et al*. From the results of calculations carried out by Hezemans *et al.* it was concluded that a compact helical conformation with a backbone torsional angle of 78.6-degrees and 3.76 units per turn was the energetically most favourable state of oligomers of *t*-butyl isocyanide.[102] These results are comparable to the work of Kollmar and Hoffmann and indicate that the size of the side groups determines the energy minimum of the polyisocyanide.

1.3.2 Polyisocyanides containing functional side groups

In the literature applications are described that make use of the helicity of polyisocyanides, e.g. as chiral stationary phases in HPLC columns allowing the separation of racemates. Poly[(+)-*sec*-butyl isocyanide] and poly[(–)-*sec*-butyl isocyanide], both prepared from the corresponding optically pure isocyanide, were used as stationary phases to separate poly(*t*-butyl isocyanide) into the left- and right-handed polymers,[97] while polyisocyanides carrying sugar moieties as side groups were able to separate 10 different low molecular weight racemates.[103]

Additional functionality, next to the helicity, can be given to polyisocyanides by introducing functional side groups. Many examples can be found in the literature where the rigid helical backbone of polyisocyanides has been used to attach functional groups, thus functioning as scaffolds. It is possible to prepare polyisocyanides from a wide variety of isocyanides having attached functional side groups,[93, 98, 104] e.g. dyes,[105, 106] side groups with double and triple bonds,[107] aromatic rings,[108-111] crown ether rings,[112] stable radical groups,[113] and redox active groups (Scheme 7).[114]

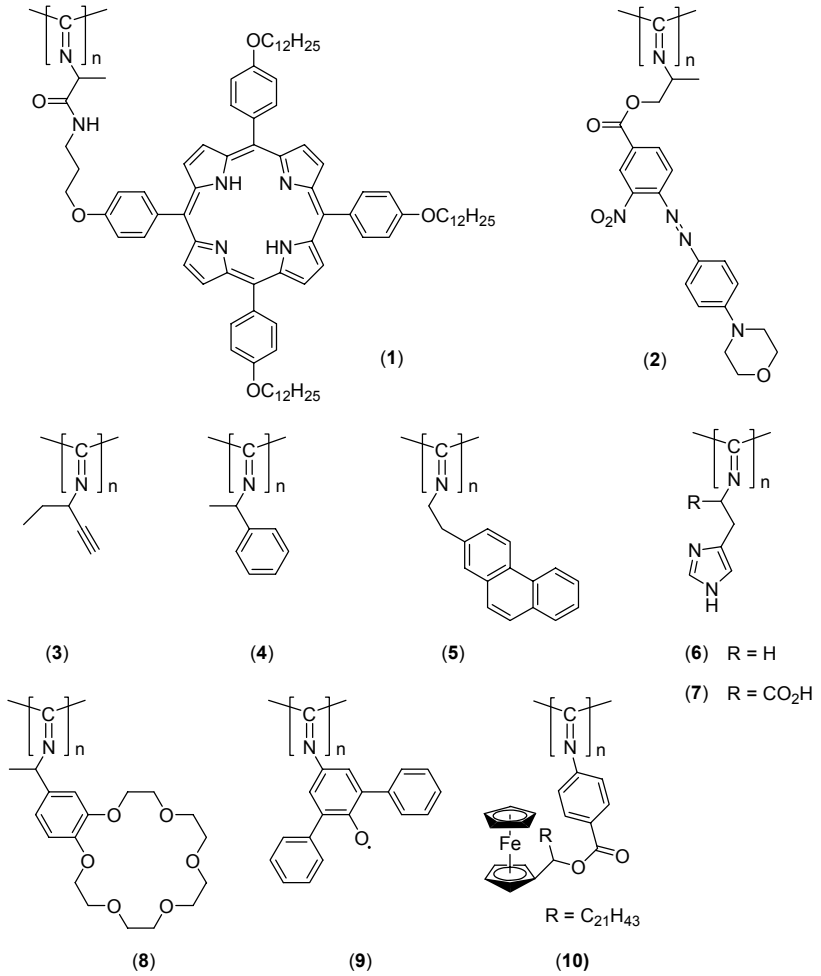

Scheme 7. *Overview of polyisocyanides containing functional side groups.*

The functional side groups present in these polyisocyanides can lead to special properties, for instance the non-linear optics of compound (**2**) have been studied and it was found that the polymers possess very high β-values.[106] The binding interactions with bilirubin (Figure 17), which is the end product of heme catabolism in humans and most animals, were studied with polymers (**6**) and (**7**).[111]

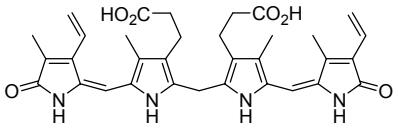

Figure 17. *Chemical structure of Bilirubin.*

The pK_a values of the imidazole groups of compounds (**6**) and (**7**) are 5.2 and 9.4 respectively. Bilirubin at a pH of 7.3 was added to both polyisocyanides and complex formation was found to occur only with the former polymer. Spectroscopic and other studies

indicated that approximately one bilirubin molecule was bound per helical turn of polyisocyanide (**6**). At pH 7.3 bilirubin is a dianion, polymer (**6**) neutral and polymer (**7**) protonated, from which it was concluded that binding of bilirubin involves hydrogen bonding interactions, rather then salt bridges to charged histidine residues of the polymers.

Membrane transport across human or animal cell walls is precisely regulated by specific mechanisms. The most common mode of ion transport through the membrane is by proteins that form a transmembrane ion channel, the archetype being Gramicidin A.[2] Various groups have been working on artificial systems to mimic the function of this protein.[115] Roks *et al.* have constructed an artificial ion channel by preparing a polyisocyanide with crown ether rings as side groups (**8**).[112] Due to the 4_1 helical architecture of the polyisocyanide four stacks of crown ether rings run parallel to the polymer backbone in this polymer, thus creating four channels. The ion transport through the crown ether channels was studied by incorporation of the polyisocyanides into the membrane of dihexadecyl phosphate (DHP) vesicles (Figure 18 a). The dye 4-(2-pyridylazo)resorcinol mono sodium salt (PAR), which forms colored complexes with cobalt(II) ions, was encapsulated inside these vesicles. A Co(II) salt was added to the vesicle dispersion and the increase in UV-Vis absorption was followed in time. In the presence of channels, ion transport was observed, while only a very small or no absorption was observed in the absence of channels (Figure 18 b).

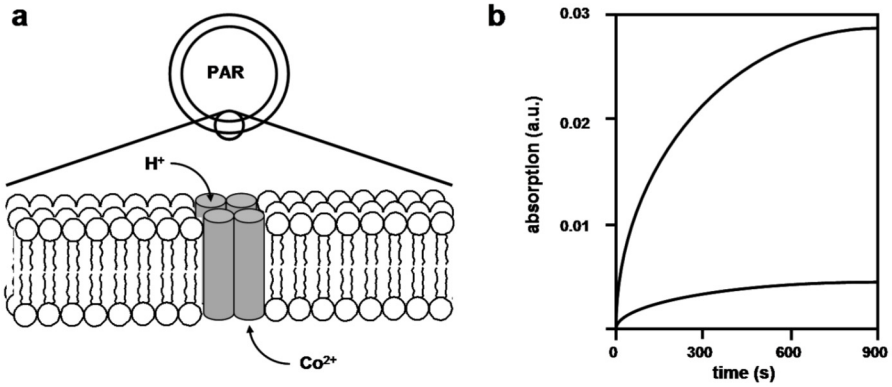

Figure 18. *a) Polyisocyanide **8** forms an artificial ion channel in a DHP vesicle. b) Plots of the change in absorbance of the Co(II)-PAR complex against time for vesicles with (upper curve) and without (lower curve) ion channel mimic.*

1.3.3 Block copolymers of polyisocyanides

Block copolymers of polyisocyanides have been prepared by different groups for various reasons. Takei *et al.* have prepared a series of diblock and triblock copolymers from two different aryl isocyanides, one containing an (L)-menthyl group and the other a porphyrin group, with the purpose of determining the helical sense of poly(aryl isocyanide)s by CD spectroscopy using the porphyrin as a spectator group.[116] With the synthesized diblock copolymers, uncertainty remained with respect to the helicity of the main chain, and therefore a triblock copolymer was designed where the porphyrin-containing isocyanide made up the middle block and the (L)-menthyl-containing isocyanide the two outer blocks. Comparison of the Cotton effect at 364 nm, arising from the porphyrin groups, for triblock copolymers with decreasing length of the porphyrin-containing block led to the conclusion that the polymers were right-handed helices.

The same group used successfully di- and trinuclear Pt complexes (Figure 19) as living polymerization catalysts in the preparation of di- and triblock copolymers of isocyanides.[117] Interesting applications can be foreseen for these block copolymers as charge transfer and light harvesting systems.

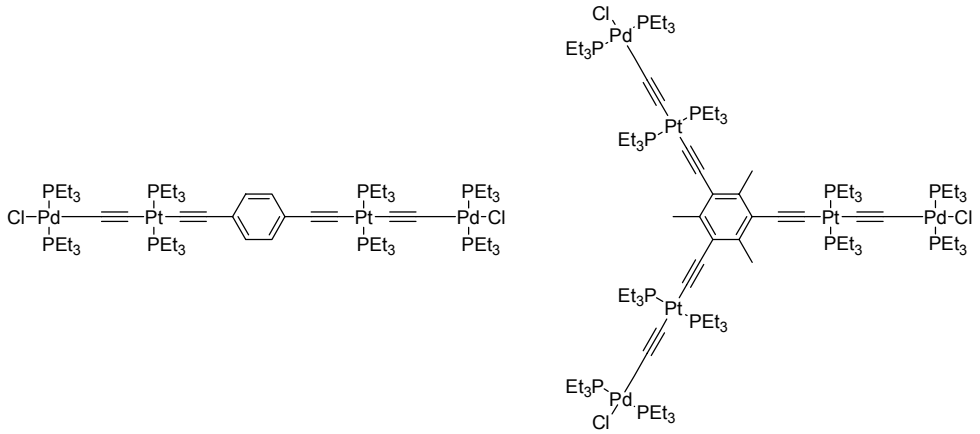

Figure 19. *Chemical structures of di- and trinuclear isocyanide polymerization catalysts.*

It is well known that block copolymers can display amphiphilic behavior and can undergo phase separation in selective solvents when these polymers are built up from blocks having different solubilities. Diblock copolymers consisting of two coiled blocks are known to self-assemble into other structures than diblock copolymers constructed of a coil and a rod block.[118] It has already been mentioned that polyisocyanopeptides are exceptionally rigid

polymers. It is highly interesting, therefore, to prepare polyisocyanide-based amphiphilic block copolymers and study their aggregation behavior. A useful method to synthesize a polyisocyanide diblock copolymer is to make use of a macromolecular initiator complex, viz. an amine functionalized polymer coordinated to a catalytic nickel(II) complex (Scheme 8).[8]

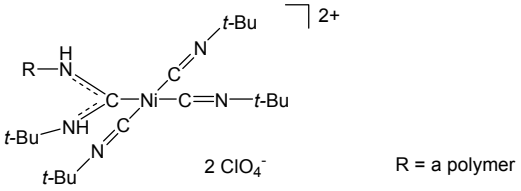

Scheme 8. *Chemical structure of the macromolecular initiator used to prepare block copolymers of isocyanides.*

When this complex is added to a solution of an isocyanide, the polymer with the amine function is built in as the first segment of the growing polyisocyanide chain, eventually after completion of the reaction, resulting in the formation of a block copolymer. This approach was used by Cornelissen *et al.* to make amphiphilic isocyanide diblock copolymers containing a polystyrene block[8] or a carbosilane dendrimer block[45] (Scheme 9).

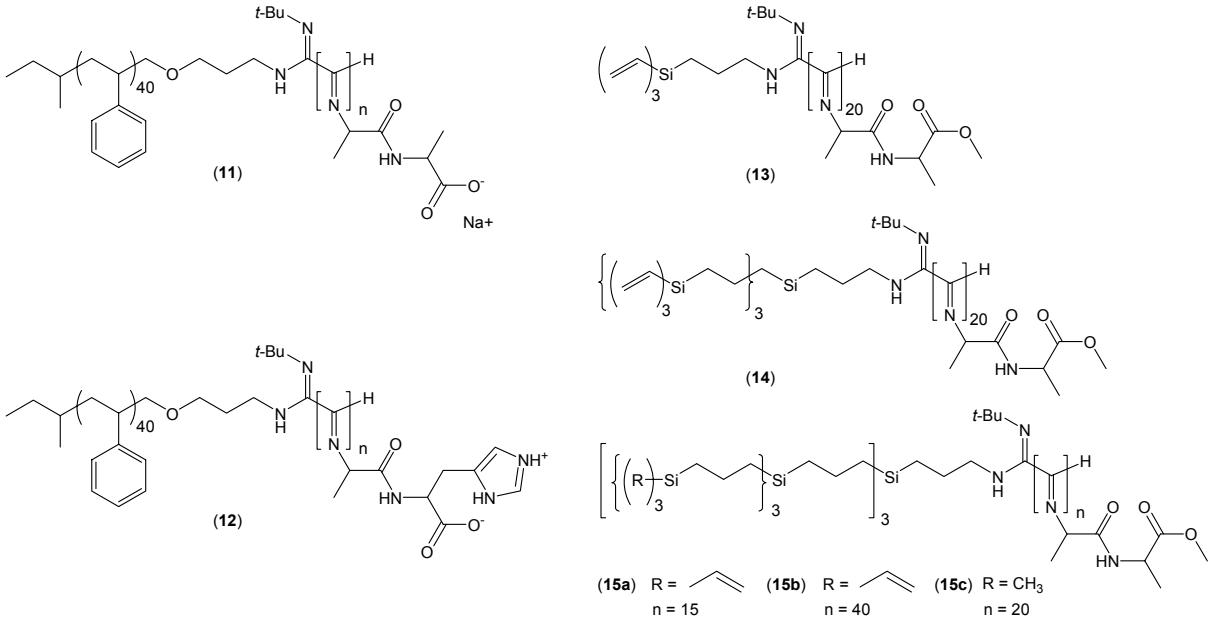

Scheme 9. *Chemical structures of amphiphilic polyisocyanide based diblock copolymers prepared via the macromolecular initiator route.*

Electron microscopy studies on aqueous dispersions prepared from molecules (**11**) and (**12**), having various head group sizes, showed that a range of morphologies could be obtained, i.e. micellar rods, vesicles, bilayer filaments, and superhelical aggregates (Figure 20 a-d). It was proposed, based on the dimensions of the aggregate, that the latter type of aggregate was built up from smaller bundles of diblock copolymers. The superhelicity was a direct effect of the chirality of the polymeric amphiphile, caused by the helical organization of the polyisocyanide backbone. Interestingly, for compounds (**11**) and (**12**) opposite helicities were found.

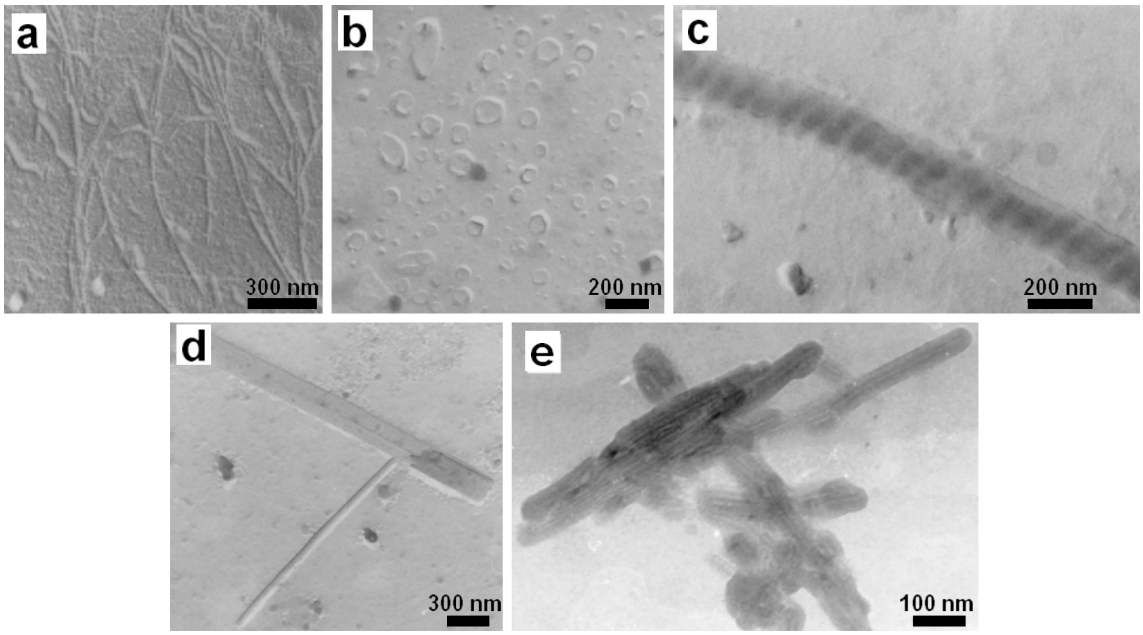

Figure 20. *TEM micrographs of aggregates obtained from amphiphilic polyisocyanide diblock copolymers. a) Micellar rods of (**11**, n = 20), b) vesicles of (**11**, n = 10), c) left-handed superhelix of (**11**, n = 10), d) bilayer of (**11**, n = 10), and e) nanoarrays of (**15a**).*

Induction of aggregate formation for polymers (**13**)-(**15**) was not as straightforward as for (**11**) and (**12**). Dynamic light scattering (DLS) studies in $CHCl_3$ at concentrations higher than 0.5 % (w/w) showed that two types of structures were present, but electron microscopy studies did not reveal the presence of well-defined aggregates. Saponification of the ester functions of (**15a**) made this compound soluble in water and as a result no aggregates were formed. In a third attempt aggregate formation could be induced by adding silver ions to dispersions of (**15**). CD spectroscopy revealed that the Ag^+ ions formed complexes with the peptide units of the polyisocyanides instead of with the allyl functions of the carbosilane

dendrimers, as initially expected. With the help of TEM the formation of nanoarrays of diblock copolymers and silver could be observed (Figure 20 e).

Deming and Novak have developed a method to prepare diblock copolymers of butadiene and methylbenzyl isocyanide by using only one type of metal complex, i.e. $[(\eta^3\text{-}C_3H_5)Ni(OC(O)CF_3)]_2$, to polymerize both blocks.[108] The microphase separation of this diblock copolymer in spin-cast thin films was studied by scanning electron microscopy (SEM) and revealed the presence of highly textured morphologies distinctly characteristic of microphase separation (Figure 21). In this example, the polyisocyanide component apparently exists as cylindrical domains dispersed in a continuous polybutadiene phase, which is a consequence of the rod-coil character of the diblock copolymer.

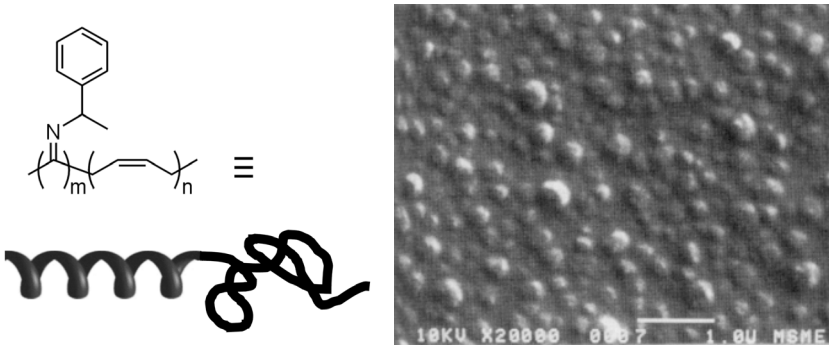

Figure 21. *Left: chemical and schematic structure of polybutadiene*-b-*poly(α-methylbenzyl isocyanide). Right: SEM micrograph of microphase separated domains formed by this diblock copolymer.*[108]

A series of homo-, di- and triblock copolymers of 2-naphtylethyl isocyanide, 9-anthrylethyl isocyanide and 2-phenantrylethyl isocyanide (Scheme 7, compound (**5**)) have been synthesized by Hong *et al.* to study the photophysical properties of these block copolymers.[119] It was stated that the absence of excimer emission in the fluorescence spectra of the homopolymers of the three isocyanides was indicative of the presence of a rigid polymeric backbone. In more flexible polymeric systems the formation of excimers is a serious complication. Fluorescence quenching in block copolymers containing a dimethylaniline donor block and a naphthalene acceptor or anthracene acceptor block took place through directional energy migration to the acceptor – quencher interface. Quenching occurred either by photoinduced electron transfer in the anthracene-dimethylaniline diblock copolymer or by exciplex formation in the naphthalene-dimethylaniline diblock copolymer

(Figure 22). Transient absorption spectra of these polymers revealed the formation of radical ion pairs, with a lifetime of 1.1 μs in the anthracene-dimethylaniline diblock copolymer.

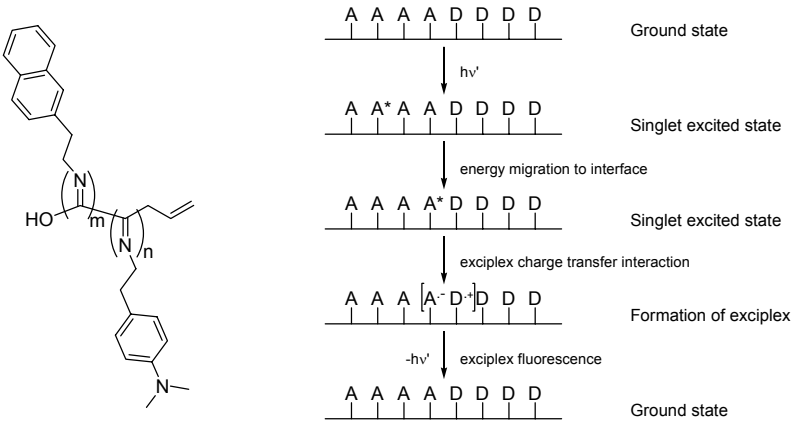

Figure 22. *Left: chemical structure of the naphthalene-dimethylaniline diblock copolymer studied by Hong* et al. *Right: mechanism for exciplex fluorescence in this diblock copolymer.*[119]

1.4 Outline of the Thesis

The self-organization of polymers and block copolymers has reached a high level of understanding and the precision and complexity by which the formed aggregates can be made, has increased considerably in the past years.[120] Our interest is mainly to construct vesicles from diblock copolymers (polymersomes) using polyisocyanides as the polar head group and another polymer as the apolar tail. The advantage of such block copolymers is the increased stability and shape persistence of the resulting aggregates, thereby simplifying the analysis of their structures using various microscopic techniques.

The studies described in Chapter 2 are carried out to develop the synthesis of a new type of isocyanide polymer with thiophene side groups and to characterize its properties. It is demonstrated that polyisocyanides having two alanine side groups have a better defined helical structure than the polyisocyanides with only one alanine side group as a result of a better defined hydrogen bonding network in the polymer backbone.

In Chapter 3 the synthesis of diblock copolymers of styrene and a thiophene-containing isocyanide is described as well as their aggregation behavior in different solvents under various conditions. This amphiphilic macromolecule forms vesicles in both organic and

aqueous mixtures. Fusion is observed when the diblock copolymer vesicles are kept for prolonged periods of time in the aqueous dispersion.

The polymerization of the thiophene groups within the vesicle membrane is described in Chapter 4. The addition of a chemical oxidative complex was found to be a better method to cross-link the vesicle membrane than electrochemical polymerization. Both spectroscopic and electrochemical techniques revealed the presence of polythiophenes in the membranes, while preliminary studies indicated that electron conductive pathways within the membranes are possible.

By encapsulating enzymes inside the diblock copolymer vesicles nano- and microreactors can be prepared. It is demonstrated in Chapter 5 that the polystyrene-*b*-polyisocyanide vesicles can be loaded with *Candida antarctica* lipase B, horseradish peroxidase, and glucose oxidase enzymes, resulting in capsules in which the enzymes remain active. The membrane of the capsules turned out to be permeable for small solutes, but impermeable for the enzymes. Varying the cross-linking time of the membranes enabled control over the pore size, hence the diffusion through the membranes.

Another type of diblock copolymer is discussed in Chapter 6. It consists of the same polyisocyanide head group as described in Chapter 3, but it has an octadecene instead of polystyrene tail. A change of morphology was observed in the resulting diblock copolymer dispersion when the head group size was increased systematically, as observed by electron microscopy. Diblock copolymers of a certain length form vesicles and fuse into larger vesicles in a similar way as described for the vesicles in Chapter 3.

Polyisocyanides carrying electroactive side groups, viz. hexabenzocoronene and tetrathiavulvalene, are described in Chapter 7. These polymers might be good candidates as components for the construction of conducting nanowires.

1.5 References and Notes

[1] Y. Furukawa, *Inventing polymer science : Staudinger, Carothers, and the emergence of macromolecular science*, University of Pennsylvania Press, Philadelphia, **1998**.
[2] L. Stryer, *Biochemistry*, W. H. Freeman, New York, **1988**.
[3] S. Förster, M. Antonietti, *Adv. Mater.* **1998**, *10*, 195.
[4] C. Park, J. Yoon, E. L. Thomas, *Polymer* **2003**, *44*, 6725.
[5] S. Förster, M. Konrad, *J. Mater. Chem.* **2003**, *13*, 2671.
[6] N. S. Cameron, M. K. Corbierre, A. Eisenberg, *Can. J. Chem.* **1999**, *77*, 1311.
[7] B. M. Discher, Y.-Y. Won, D. S. Ege, J. C.-M. Lee, F. S. Bates, D. E. Discher, D. A. Hammer, *Science* **1999**, *284*, 1143.
[8] J. J. L. M. Cornelissen, M. Fischer, N. A. J. M. Sommerdijk, R. J. M. Nolte, *Science* **1998**, *280*, 1427.
[9] S. Jain, F. S. Bates, *Science* **2003**, *300*, 460.

[10] S. A. Jenekhe, X. L. Chen, *Science* **1998**, *279*, 1903.
[11] W. B. Motherwell, M. J. Bingham, Y. Six, *Tetrahedron* **2001**, *57*, 4663.
[12] D. D. Lasic, *Liposomes: from physics to applications*, Elsevier, Amsterdam, **1993**.
[13] A. D. Bangham, *Chem. Phys. Lipids* **1993**, *64*, 275.
[14] T. Kunitake, *Angew. Chem. Int. Ed.* **1992**, *31*, 709.
[15] H. Ringsdorf, B. Schlarb, J. Venzmer, *Angew. Chem. Int. Ed. Engl.* **1988**, *27*, 113.
[16] G. Redziniak, *Pathol. Biol.* **2003**, *51*, 279.
[17] P. Walde, S. Ichikawa, *Biomol. Eng.* **2001**, *18*, 143.
[18] J. C. M. van Hest, D. A. P. Delnoye, M. W. P. L. Baars, M. H. P. van Genderen, E. W. Meijer, *Science* **1995**, *268*, 1592.
[19] L. Zhang, A. Eisenberg, *Science* **1995**, *268*, 1728.
[20] B. M. Discher, D. A. Hammer, F. S. Bates, D. E. Discher, *Curr. Opin. Colloid Interface Sci.* **2000**, *5*, 121.
[21] D. E. Discher, A. Eisenberg, *Science* **2002**, *297*, 967.
[22] M. Antonietti, S. Förster, *Adv. Mater.* **2003**, *15*, 1323.
[23] P. L. Soo, A. Eisenberg, *J. Polym. Sci., Part B: Polym. Phys.* **2003**, *42*, 923.
[24] H. Aranda-Espinoza, H. Bermudez, F. S. Bates, D. E. Discher, *Phys. Rev. Lett.* **2001**, *87*, 208301.
[25] H. Bermudez, A. K. Brannan, D. A. Hammer, F. S. Bates, D. E. Discher, *Macromolecules* **2002**, *35*, 8203.
[26] B. M. Discher, H. Bermudez, D. A. Hammer, D. E. Discher, Y.-Y. Won, F. S. Bates, *J. Phys. Chem. B* **2002**, *106*, 2848.
[27] J. C.-M. Lee, H. Bermudez, B. M. Discher, M. A. Sheehan, Y.-Y. Won, F. S. Bates, D. E. Discher, *Biotechnol. Bioeng.* **2001**, *73*, 135.
[28] P. J. Photos, L. Bacakova, B. M. Discher, F. S. Bates, D. E. Discher, *J. Controlled Release* **2003**, *90*, 323.
[29] A. Napoli, M. J. Boerakker, N. Tirelli, R. J. M. Nolte, N. A. J. M. Sommerdijk, J. A. Hubbell, *Langmuir* **2004**, *20*, 3487.
[30] F. Chécot, S. Lecommandoux, H.-A. Klok, Y. Gnanou, *Eur. Phys. J. E* **2003**, *10*, 25.
[31] E. G. Bellomo, M. D. Wyrsta, L. Pakstis, D. J. Pochan, T. J. Deming, *Nat. Mater.* **2004**, *3*, 244.
[32] F. Najafi, M. N. Sarbolouki, *Biomaterials* **2003**, *24*, 1175.
[33] C. Nardin, S. Thoeni, J. Widmer, M. Winterhalter, W. Meier, *Chem. Commun.* **2000**, 1433.
[34] C. Nardin, J. Widmer, M. Winterhalter, W. Meier, *Eur. Phys. J. E* **2001**, *4*, 403.
[35] M. Sauer, T. Haefele, A. Graff, C. Nardin, W. Meier, *Chem. Commun.* **2001**, 2452.
[36] A. Graff, M. Sauer, P. van Gelder, W. Meier, *Proc. Natl. Acad. Sci. U.S.A.* **2002**, *99*, 5064.
[37] S. R. White, N. R. Sottos, P. H. Geubelle, J. S. Moore, M. R. Kessler, S. R. Sriram, E. N. Brown, S. Viswanathan, *Nature* **2001**, *409*, 794.
[38] M. J. Boerakker, J. M. Hannink, P. H. H. Bomans, P. M. Frederik, R. J. M. Nolte, E. M. Meijer, N. A. J. M. Sommerdijk, *Angew. Chem. Int. Ed.* **2002**, *41*, 4239.
[39] A. B. R. Mayer, *Polym. Adv. Techn.* **2001**, *12*, 96.
[40] I. W. Hamley, *Nanotechnology* **2003**, *14*, R39.
[41] G. Kastle, H. G. Boyen, F. Weigl, G. Lengl, T. Herzog, P. Ziemann, S. Riethmuller, O. Mayer, C. Hartmann, J. P. Spatz, M. Möller, M. Ozawa, F. Banhart, M. G. Garnier, P. Oelhafen, *Adv. Funct. Mater.* **2003**, *13*, 853.
[42] S. Klingelhöfer, W. Heitz, A. Greiner, S. Oestreich, S. Förster, M. Antonietti, *J. Am. Chem. Soc.* **1997**, *119*, 10116.
[43] J. Spatz, S. Mössmer, M. Möller, M. Kocher, D. Neher, G. Wegner, *Adv. Mater.* **1998**, *10*, 473.
[44] M. Moffit, L. McMahon, V. Pessel, A. Eisenberg, *Chem. Mater.* **1995**, *7*, 1185.
[45] J. J. L. M. Cornelissen, R. van Heerbeek, P. C. J. Kamer, J. N. H. Reek, N. A. J. M. Sommerdijk, R. J. M. Nolte, *Adv. Mater.* **2002**, *14*, 489.
[46] A. Roucoux, J. Schulz, H. Patin, *Chem. Rev.* **2002**, *102*, 3757.
[47] W. Yu, H. Liu, Q. Tao, *Chem. Commun.* **1996**, 1773.
[48] X. Zuo, H. Liu, M. Liu, *Tetrahedron Lett.* **1998**, *39*, 1941.
[49] M. Harada, K. Asakura, N. Toshima, *J. Phys. Chem.* **1993**, *97*, 5103.
[50] Y. Shiraishi, N. Toshima, *J. Mol. Catal. A: Chem.* **1999**, *141*, 187.
[51] Y. Shiraishi, N. Toshima, *Colloids Surf., A* **2000**, *169*, 59.
[52] Q. Wang, H. Liu, M. Han, X. Li, D. Jiang, *J. Mol. Catal. A: Chem.* **1997**, *118*, 145.
[53] J. Le Bars, U. Specht, J. S. Bradley, D. G. Blackmond, *Langmuir* **1999**, *15*, 7621.
[54] Y. Li, M. A. El-Sayed, *J. Phys. Chem. B* **2001**, *105*, 8938.
[55] M. Lee, C.-J. Jang, J.-H. Ryu, *J. Am. Chem. Soc.* **2004**, *126*, 8082.
[56] K. Naka, Y. Kubo, A. Ohki, S. Maeda, *Polym. J.* **1994**, *26*, 243.

[57] A. Harada, K. Kataoka, *Macromolecules* **1998**, *31*, 288.
[58] A. Harada, K. Kataoka, *Langmuir* **1999**, *15*, 4208.
[59] A. Harada, K. Kataoka, *J. Am. Chem. Soc.* **1999**, *121*, 9241.
[60] A. Harada, K. Kataoka, *J. Controlled Release* **2001**, *72*, 85.
[61] A. Harada, K. Kataoka, *J. Am. Chem. Soc.* **2003**, *125*, 15306.
[62] K. Velonia, A. E. Rowan, R. J. M. Nolte, *J. Am. Chem. Soc.* **2002**, *124*, 4224.
[63] M. Häger, F. Currie, K. Holmberg, *Top. Curr. Chem.* **2003**, *227*, 53.
[64] J. Jang, H. Ha, *Langmuir* **2002**, *18*, 5613.
[65] K. Landfester, *Colloid Chemistry II, Vol. 227*, Springer Verlag, Berlin, **2003**.
[66] K. Landfester, R. Montenegro, U. Scherf, R. Güntner, U. Asawapirom, S. Patil, D. Neher, T. Kietzke, *Adv. Mater.* **2002**, *14*, 651.
[67] F. Tiarks, K. Landfester, M. Antonietti, *Langmuir* **2001**, *17*, 908.
[68] A. W. Bosman, H. M. Janssen, E. W. Meijer, *Chem. Rev.* **1999**, *99*, 1665.
[69] R. M. Crooks, M. Zhao, L. Sun, V. Chechik, L. K. Yeung, *Acc. Chem. Res.* **2001**, *34*, 181.
[70] R. Heerbeek, P. C. J. Kamer, P. W. N. M. van Leeuwen, J. N. H. Reek, *Chem. Rev.* **2002**, *102*, 3717.
[71] L. J. Twyman, A. S. H. King, I. K. Martin, *Chem. Soc. Rev.* **2002**, *31*, 69.
[72] J. M. J. Fréchet, *Macromol. Symp.* **2003**, *201*, 11.
[73] J. M. J. Fréchet, *J. Polym. Sci., Part A: Polym. Chem.* **2003**, *41*, 3713.
[74] A.-M. Caminade, C.-O. Turrin, P. Sutra, J.-P. Majoral, *Curr. Opin. Colloid Interface Sci.* **2003**, *8*, 282.
[75] A. Sunder, R. Hanselmann, H. Frey, R. Mülhaupt, *Macromolecules* **1999**, *32*, 4240.
[76] J. H. Youk, M.-K. Park, J. Locklin, R. Advincula, J. Yang, J. Mays, *Langmuir* **2002**, *18*, 2455.
[77] A. W. Bosman, R. Vestberg, A. Heumann, J. M. J. Fréchet, C. J. Hawker, *J. Am. Chem. Soc.* **2003**, *125*, 715.
[78] S. Mecking, R. Thomann, H. Frey, A. Sunder, *Macromolecules* **2000**, *33*, 3958.
[79] M. Q. Slagt, S.-E. Stiriba, R. J. M. Klein Gebbink, H. Kautz, H. Frey, G. van Koten, *Macromolecules* **2002**, *35*, 5734.
[80] T. Terashima, M. Kamigaito, K.-Y. Baek, T. Ando, M. Sawamoto, *J. Am. Chem. Soc.* **2003**, *125*, 5288.
[81] D. M. Chernyshov, L. M. Bronstein, H. Börner, B. Berton, M. Antonietti, *Chem. Mater.* **2000**, *12*, 114.
[82] N. Jungmann, M. Schmidt, M. Maskos, *Macromolecules* **2003**, *36*, 3974.
[83] E. Donath, G. B. Sukhorukov, F. Caruso, S. A. Davis, H. Möhwald, *Angew. Chem. Int. Ed.* **1998**, *37*, 2201.
[84] G. Decher, *Science* **1997**, *277*, 1232.
[85] F. Caruso, R. A. Caruso, H. Möhwald, *Science* **1998**, *282*, 1111.
[86] L. Dähne, S. Leporatti, E. Donath, H. Möhwald, *J. Am. Chem. Soc.* **2001**, *123*, 5431.
[87] C. S. Peyratout, H. Möhwald, L. Dähne, *Adv. Mater.* **2003**, *15*, 1722.
[88] E. Donath, S. Moya, B. Neu, G. B. Sukhorukov, R. Georgieva, A. Voigt, H. Baümler, H. Kiesewetter, H. Möhwald, *Chem. Eur. J.* **2002**, *8*, 5481.
[89] A. Antipov, D. Shchukin, Y. Fedutik, I. Zanaveskina, V. Klechkovskaya, G. B. Sukhorukov, H. Möhwald, *Macromol. Rapid Commun.* **2003**, *24*, 274.
[90] R. Ghan, T. Shutava, A. Patel, V. T. John, Y. Lvov, *Macromolecules* **2004**, *37*, 4519.
[91] T. M. S. Chang, *J. Intern. Med.* **2003**, *253*, 527.
[92] T. M. S. Chang, D. Powanda, W. P. Yu, *Artif. Cell. Blood Sub.* **2003**, *31*, 231.
[93] W. Drenth, R. J. M. Nolte, *Acc. Chem. Res.* **1979**, *12*, 30.
[94] J. J. L. M. Cornelissen, J. J. J. M. Donners, R. de Gelder, W. S. Graswinckel, G. A. Metselaar, A. E. Rowan, N. A. J. M. Sommerdijk, R. J. M. Nolte, *Science* **2001**, *293*, 676.
[95] P. Samorí, C. Ecker, I. Gössl, P. A. J. de Witte, J. J. L. M. Cornelissen, G. A. Metselaar, M. B. J. Otten, A. E. Rowan, R. J. M. Nolte, J. P. Rabe, *Macromolecules* **2002**, *35*, 5290.
[96] F. Millich, *Chem. Rev.* **1972**, *72*, 101.
[97] R. J. M. Nolte, A. J. M. van Beijnen, W. Drenth, *J. Am. Chem. Soc.* **1974**, *96*, 5932.
[98] R. J. M. Nolte, *Chem. Soc. Rev.* **1994**, *23*, 11.
[99] P. C. J. Kamer, R. J. M. Nolte, W. Drenth, *J. Am. Chem. Soc.* **1988**, *110*, 6818.
[100] M. Clericuzio, G. Alagona, C. Ghio, P. Salvadori, *J. Am. Chem. Soc.* **1997**, *119*, 1059.
[101] C. Kollmar, R. Hoffmann, *J. Am. Chem. Soc.* **1990**, *112*, 8230.
[102] C. J. M. Huige, A. M. F. Hezemans, R. J. M. Nolte, W. Drenth, *Recl. Trav. Chim. Pays-Bas* **1993**, *112*, 33.
[103] A. Tsuchida, T. Hasegawa, K. Kobayashi, C. Yamamoto, Y. Okamoto, *Bull. Chem. Soc. Jpn.* **2002**, *75*, 2681.
[104] J. J. L. M. Cornelissen, A. E. Rowan, R. J. M. Nolte, N. A. J. M. Sommerdijk, *Chem. Rev.* **2001**, *101*, 4039.

[105] P. A. J. de Witte, M. Castriciano, J. J. L. M. Cornelissen, L. M. Scolaro, R. J. M. Nolte, A. E. Rowan, *Chem. Eur. J.* **2003**, *9*, 1775.
[106] M. Kauranen, T. Verbiest, C. Boutton, M. N. Teerenstra, A. J. Schouten, R. J. M. Nolte, A. Persoons, *Science* **1995**, *270*, 966.
[107] A. J. M. van Beijnen, R. J. M. Nolte, A. J. Naaktgeboren, J. W. Zwikker, W. Drenth, *Macromolecules* **1983**, *16*, 1679.
[108] T. J. Deming, B. M. Novak, *Macromolecules* **1991**, *24*, 6043.
[109] B. Hong, M. A. Fox, *Macromolecules* **1994**, *27*, 5311.
[110] D. M. Vriezema, J. Hoogboom, K. Velonia, K. Takazawa, P. C. M. Christianen, J. C. Maan, A. E. Rowan, R. J. M. Nolte, *Angew. Chem. Int. Ed.* **2003**, *42*, 772.
[111] J. M. van der Eijk, R. J. M. Nolte, V. E. M. Richters, W. Drenth, *Biopolymers* **1980**, *19*, 445.
[112] U. F. Kragten, M. F. M. Roks, R. J. M. Nolte, *J. Chem. Soc., Chem. Commun.* **1985**, 1275.
[113] E. J. Vlietstra, R. J. M. Nolte, J. W. Zwikker, W. Drenth, E. W. Meijer, *Macromolecules* **1990**, *23*, 946.
[114] N. Hida, F. Takei, K. Onitsuka, K. Shiga, S. Asaoka, T. Iyoda, S. Takahashi, *Angew. Chem. Int. Ed.* **2003**, *42*, 4349.
[115] G. W. Gokel, W. M. Leevy, M. E. Weber, *Chem. Rev.* **2004**, *104*, 2723.
[116] F. Takei, H. Hayashi, K. Onitsuka, N. Kobayashi, S. Takahashi, *Angew. Chem. Int. Ed.* **2001**, *40*, 4092.
[117] N. Ohshiro, A. Shimizu, R. Okumura, F. Takei, K. Onitsuka, S. Takahashi, *Chem. Lett.* **2000**, 786.
[118] J. T. Chen, E. L. Thomas, C. K. Ober, G.-P. Mao, *Science* **1996**, *273*, 343.
[119] B. Hong, M. A. Fox, *Can. J. Chem.* **1995**, *73*, 2101.
[120] D. G. Bucknall, H. L. Anderson, *Science* **2003**, *302*, 1904.

Chapter 2

Synthesis and Characterization of Thiophene-Containing Polyisocyanides Derived from Alanine

2.1 Introduction

The precise arrangement of functional systems is of great importance for the operation of numerous devices. A micro-processor with its thousands of circuits will only work properly when every single one of them can be addressed exactly, whilst in a zipper all the teeth need to be aligned parallel in order to close it. In nature a variety of scaffolds are used to position and orientate functional units, such as chromophores and base pairs, into the required arrangement for efficient functioning. In the photosynthetic system of purple bacteria the light harvesting 2 (LH2) complex is a self-assembled system which is responsible for collecting sun light and the transport of energy.[1] These tasks are carried out by nine pairs of circularly arranged and accurately ordered chlorophyll groups in a highly efficient manner.[2] The base pairs in DNA strands are anchored to deoxyriboses. These deoxyriboses are linked by phosphate groups and form a rigid helical backbone that is essential to the way hydrogen bonds can be formed between the base pairs of two strands of DNA, resulting in a very rigid double stranded DNA chain.

Polyisocyanides are ideal scaffolds for the arrangement of functional groups, since they possess a well-defined and rigid backbone (Figure 1).[3, 4] Each carbon atom in the polymer main chain carries a substituent, resulting in appreciable steric hindrance and therefore restricted rotation around the carbon-carbon single bonds of the polyisocyanide backbone.

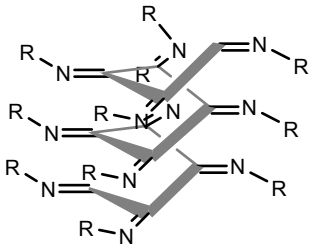

Figure 1. *Chemical structure of a polyisocyanide with a helical backbone (shown in grey).*

These polymers are synthesized by the catalyzed polymerization of isocyanides, which have already been studied since the 1960's. First by Millich *et al.* who used acid catalysts for the preparation of polyisocyanides,[5] while several other groups have investigated the possibility of using nickel ion complexes as catalysts.[6, 7] It has been shown both by Nolte and Takahashi that polyisocyanides can also be prepared with other transition metal ions as catalysts, such as Ti, Co, Cu, Pd, and Pt salts.[8-10] When nickel (II) is used as a catalyst, four isocyanides coordinate in a square planar fashion to the nickel ion and upon addition of a nucleophile, i.e. an alcohol or amine, the polymerization is initiated.[3] Millich proposed a 4_1 helical conformation, also depicted as $n/(n + 4)$, for the polyisocyanide backbone, which means that each turn, or pitch, of the helix consists of 4 isocyanide units.[5] Nolte *et al.* proved experimentally that polyisocyanides exist as helices by separating the left- and right-handed helical chains of poly(*t*-butyl isocyanide) with the help of column chromatography.[11] For the Ni(II) catalyzed polymerization of isocyanides a so-called "merry-go-round mechanism" has been proposed.[3] In this mechanism the isocyanides coordinated to the Ni ion are polymerized either clockwise or anticlockwise around the Ni(II) center, resulting in the formation of a helical polymer.

When enantiomerically pure isocyanides are polymerized or when chiral Ni(II) catalysts are used, an excess of either left- or right-handed helices is formed.[3] The resulting helices, depending on their side chain can slowly unfold after some time since the polymer is a kinetic product. Cornelissen *et al.* have shown that the rigidity and stability of polyisocyanides can be further increased if isocyanopeptides are used as monomers in the polymerization reaction.[12],[13] The helical structure of the resulting polymer is stabilized by a hydrogen bonding network between the amide groups of the peptide side-chains (Figure 2), leading to an architecture similar to that of β-helical proteins.[14]

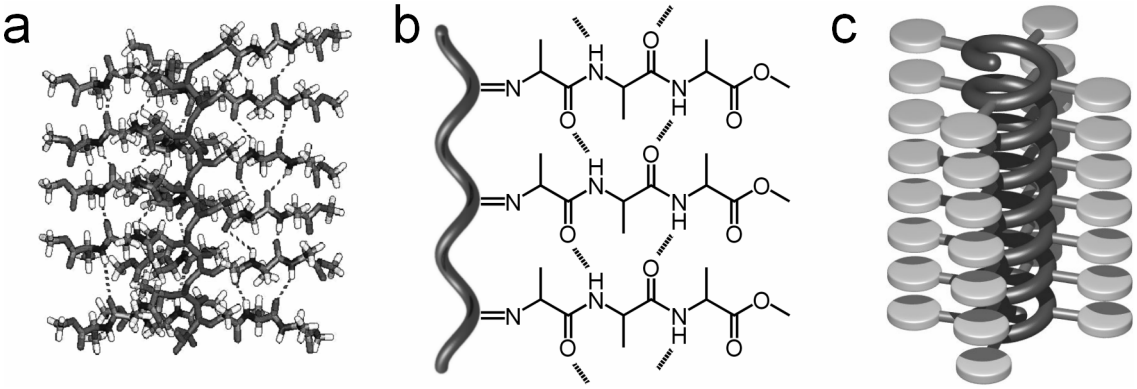

Figure 2. *Hydrogen bonding network that is formed between the amide groups of the peptides in the side chains of polyisocyanopeptides. a) Computer generated model of a polyisocyanide having three alanine side groups, b) schematic representation of the model shown in a), and c) drawing of a well-defined polyisocyanide chain with ordered functional side groups.*

The possibility of using polyisocyanides as scaffolds for the preparation of well-defined arrays of functional groups (Figure 2 c) was for the first time demonstrated by Roks *et al*.[15] They made models of ion-channel proteins by synthesizing polyisocyanides with aligned crown ether side groups, which formed four ion channels parallel to the polymer backbone. In a more recent study polyisocyanides with stacked porphyrin side groups have been prepared. In these stacked systems energy could be delocalized over more than 100 Å, resembling photosynthetic antenna systems.[16] It would be very interesting from both an academic and technological point of view to develop electronic wires based on polyisocyanides which can transport electrons. One possible approach is to start from a polyisocyanide with stacked thiophene side groups. Polymerization of these thiophene groups along the polyisocyanide backbone would give four single nanowires (Figure 3). Polythiophenes are very important from a technological point of view. They are thermally stable materials, which have been applied in polymer light emitting diodes (LEDs), sensors, electrical conductors, solar cells, and nonlinear optical devices and have even been used as electrodes.[17] Polythiophenes can be readily obtained from thiophenes by either chemical or electrochemical polymerization methods, resulting in fully conjugated polymers. The mechanism of conductivity in these polymers is based on the motion of charged defects within the conjugated network. The charge carriers, either positive or negative, are created by oxidizing or reducing the polymer, which is called doping.[18] The highest conductivity is obtained when the thiophene rings in the polymer are coplanar.[19]

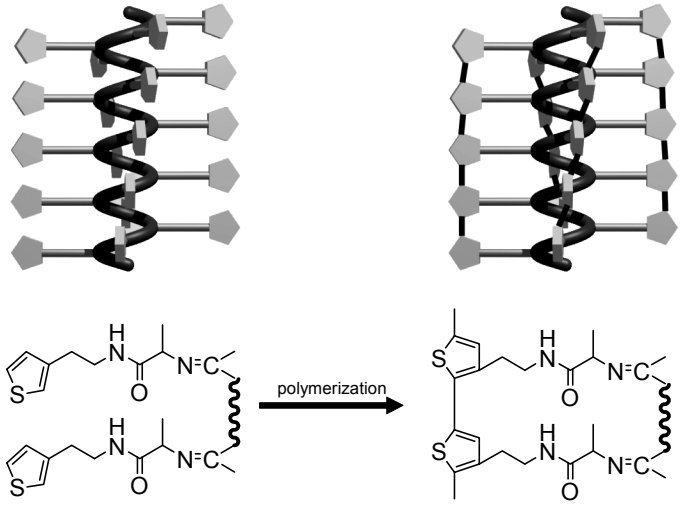

Figure 3. *Schematic representation of a polyisocyanide with polymerizable thiophene side groups.*

Attempts to order oligo- and polythiophenes have already been made by several research groups using different approaches. Hempenius *et al.* synthesized a triblock copolymer consisting of an oligothiophene block of 11 units with polystyrene blocks at both ends.[20] This polymer was found to self-assemble into spherical, micellar structures with an average diameter of 12 nm. Electrochemical doping of the thiophene block was hampered by the polystyrene shell. McCullough and coworkers prepared highly electron conductive "nanowires" by casting a diblock copolymer solution of styrene and 3-hexyl-thiophene in toluene (Figure 4). The polystyrene block improved the solubility and therefore the processing properties, but also contributed to the phase separating behavior of this compound.[21]

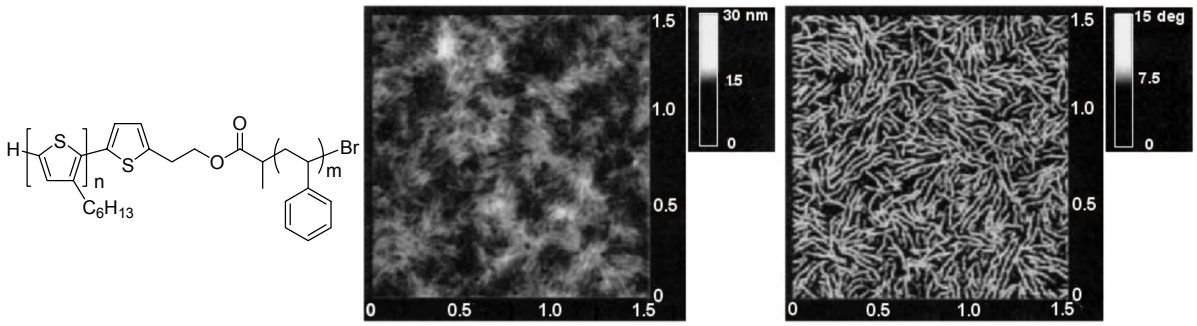

Figure 4. *AFM height (left) and phase (right) images of poly(3-hexyl-thiophene)*-b-*polystyrene diblock copolymers which self-assemble into electron conductive "nanowires".*[21]

In the group of Feringa hydrogen bond-forming urea moieties were used to orientate terthiophene functionalities. These compounds were found to form well-defined two-dimensional assemblies based upon hydrogen bonding, as was concluded from scanning tunneling microscopy (STM, see Figure 5).[22] Scanning tunneling spectroscopy studies performed on these molecules showed that they had interesting electronic properties, due to electron transfer between the stacked thiophenes.[23]

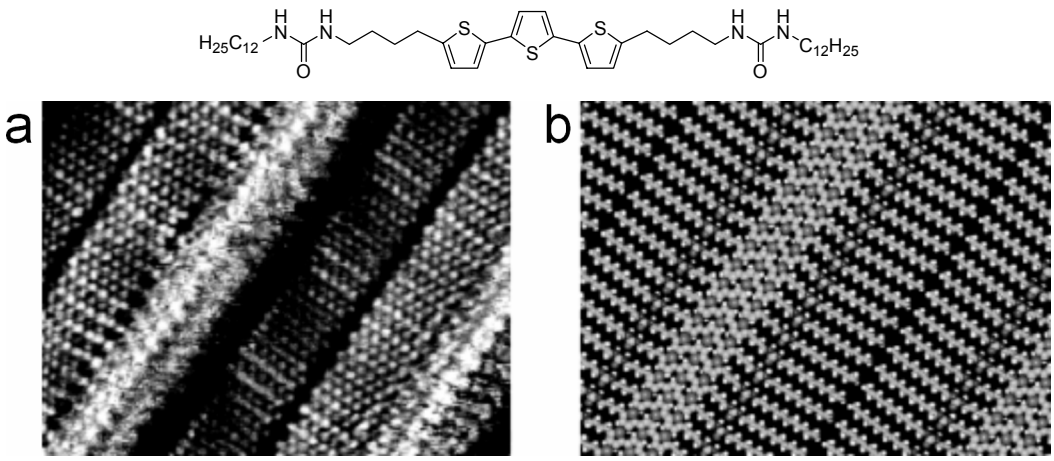

Figure 5. *Ordering of oligothiophenes on a surface.[23] a) STM micrograph of a monolayer of the bisurea-terthiophene molecule shown above, b) a molecular model of the image on the left.*

In this chapter, our attempts to order thiophene functions using the framework of the synthesis of polyisocyanides containing side chains with one or two alanine groups functionalized with a single thiophene ring, will be described and the physical properties of these compounds will be discussed.

2.2 Thiophene-Containing Polyisocyanides Derived from Alanine

2.2.1 Synthesis

Thiophene-3-acetonitrile was used as a starting material for the synthesis of the thiophene-containing polyisocyanides described in this section and in Paragraph 2.3. This compound was reduced using $LiAlH_4$ to give β-3-thienylethylamine. The most direct approach to couple this compound to an alanine-containing formamide is to react it with *N*-

formyl-L-alanine, using an activating agent, such as dicyclohexyl carbodiimide (DCC), to give *N*-formyl-L-alanine(2-thiophen-3-yl-ethyl)amide (FAT) (Scheme 1, route 1).

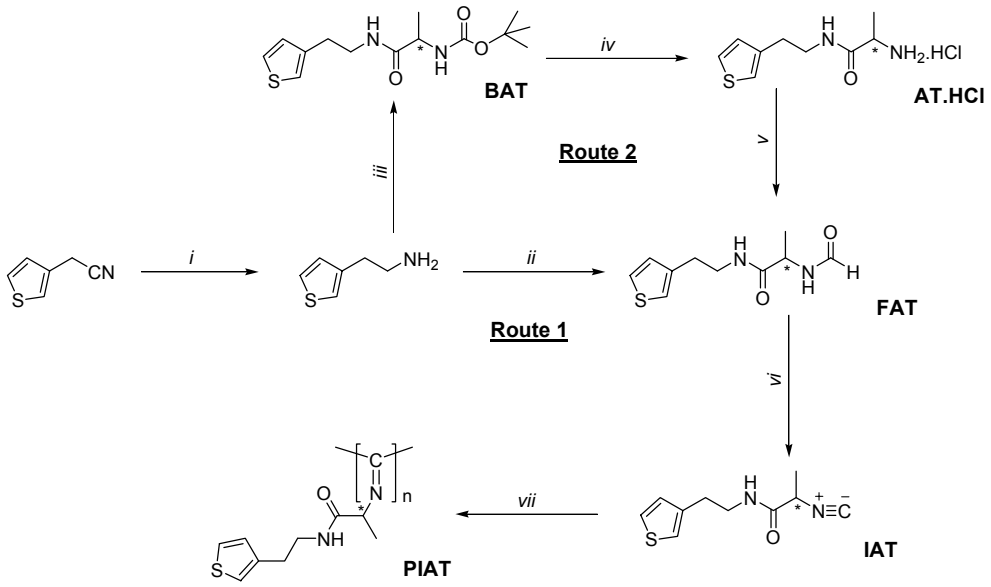

Scheme 1. *Synthesis of poly(L-isocyanoalanine(2-thiophen-3-yl-ethyl)amide) (PIAT) via two different routes; i) $LiAlH_4$, Et_2O; ii)* N-*for-L-Ala-OH, DCC, DMAP, CH_2Cl_2; iii), Boc-L-Ala-OH, DCC, DMAP, CH_2Cl_2; iv) HCl in EtOAc; v) HCO_2Et, HCO_2Na; vi)* N-*methylmorpholine, diphosgene, CH_2Cl_2; and vii) $Ni(ClO_4)_2$, EtOH, CH_2Cl_2.*

It is known, however, that *N*-acyl amino acids can undergo racemization when their acid group is activated.[24] An oxazolone can be formed, which is prone to epimerization (Scheme 2).

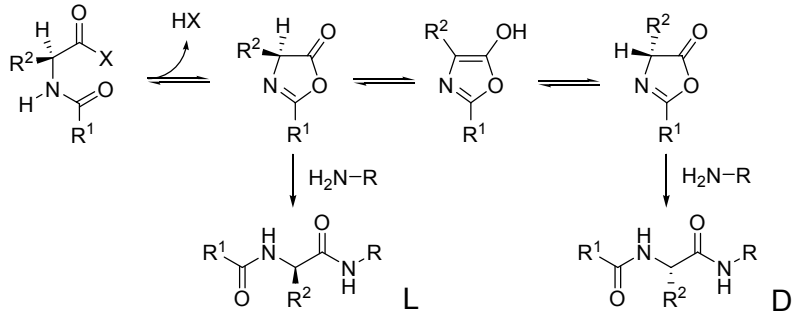

Scheme 2. *Mechanism for the occurrence of racemization in amino acids during activation.[24]*

In order to avoid this problem another route, which had a significantly reduced chance of racemization, was chosen. This route involved the coupling of Boc-protected L-alanine (Boc-L-Ala-OH) to β-3-thienylethylamine using DCC, followed by removal of the Boc-group under acidic conditions and formylation of the deprotected amine group of alanine (Scheme 1, route 2). Comparison of the optical rotation data of FAT prepared using the two different routes revealed that racemization did occur when using route 1. The optical rotation of FAT (route 1) was $[\alpha]_D^{20}$ = -40°.cm^2.g^{-1} (CH_2Cl_2, *c* 0.1), whilst it was $[\alpha]_D^{20}$ = -54°.cm^2.g^{-1} (CH_2Cl_2, *c* 1.0) for FAT (route 2). From HPLC analysis, using a chiral column, the amount of racemization was determined to be 22 % for route 1, whereas no racemization was found for route 2. The final step towards L-isocyanoalanine(2-thiophen-3-yl-ethyl)amide (IAT) was dehydration of the *N*-formyl group of FAT using diphosgene and *N*-methylmorpholine (NMM). This reaction proceeded in a yield of 87 %. The single crystal X-ray structure of IAT could be resolved. It clearly showed the preference of the isocyanide monomers to form a stacked arrangement in the solid state. In addition, the crystal structure revealed the presence of hydrogen bonding between the molecules with a distance of 4.8 Å between the amide groups (Figure 6).

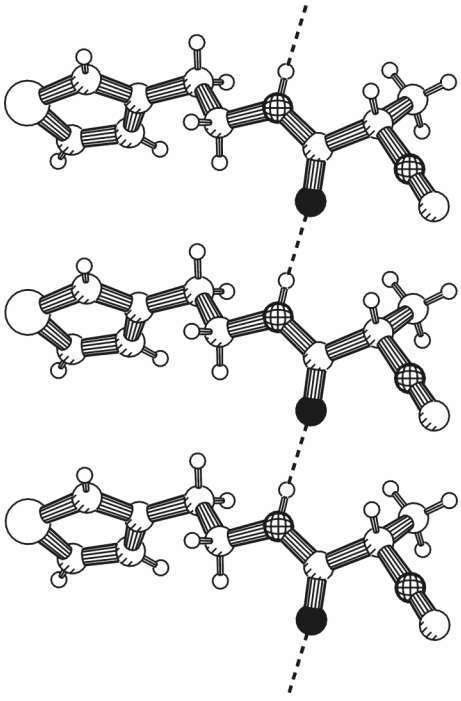

Figure 6. *PLUTON[25] representation of the single crystal X-ray structure of IAT prepared according to route 1, showing the hydrogen bonds between the amide groups. The most abundant conformation of the thiophene ring is given.*

The optical rotation of IAT prepared according to route 1 was observed to be lower than that of IAT prepared following route 2, resulting in values $[\alpha]_D^{20}$ of +11°.cm^2.g^{-1} (CH_2Cl_2, *c* 0.5) and +17°.cm^2.g^{-1} (CH_2Cl_2, *c* 1.0), respectively.

Polymers of IAT were prepared by a Ni(II) catalyzed polymerization reaction. Unfortunately, precipitation of the resulting polymer was frequently observed. In general the solubility of the prepared PIAT polymers was very low. The amount of precipitated polymer turned out to be higher when IAT prepared according to route 2 was used. This low solubility has a negative influence on the degree of polymerization, because a precipitated polymer chain will no longer be active in the polymerization process. Attempts were made, therefore, to optimize the polymerization conditions for IAT by varying the solvent, the catalyst and the ratio of monomer to catalyst. The temperature, an obvious parameter to vary, was kept unchanged, because it had been shown that polyisocyanopeptides uncoil at elevated temperatures, analogous to the denaturation of proteins.[12] As solvents CH_2Cl_2, toluene and 1,2,4-trichlorobenzene (TCB) were used, while $Ni(ClO_4)_2$ and (*t*-BuNC)$_4$Ni$(ClO_4)_2$ were tried as catalysts (Table 2). The molar ratio of monomer/catalyst was varied from 20 to 250. It has recently been reported by Cornelissen *et al.* that poly(L-2-isocyanoalanyl-D-alanine) (L,D-PIAA) can be rapidly formed in the presence of catalytic amounts of acid.[12] One attempt was made to polymerize IAT using trifluoroacetic acid (TFA) as a catalyst. Interestingly, after five days still no polymerization was found to take place, as judged by thin layer chromatography (TLC). Instead, partial reconversion of IAT into the formamide (FAT) was observed, probably due to the presence of traces of water in TFA. Metselaar has recently noted that FAA is the major product formed during the acid catalyzed polymerization of IAA when the isocyanide to acid ratio is lower than 16:1.[26]

For polymerization reactions of IAT (route 1) in CH_2Cl_2 using 1/250 equivalent of Ni (II) catalyst, precipitation of polymer was observed, whereas reactions carried out in TCB showed no precipitation under the same conditions. Precipitation could not be prevented for the polymerization of IAT (route 2) under any of the conditions studied. This is thought to be a result of the increased rigidity of the optically pure polymer compared to the racemized polymer (*vide infra*). It is known for other types of polymers that an increase in rigidity results in a decreased solubility.[27, 28] Another possibility is a difference in molecular weight between the optically pure polymer and the racemized polymer. The time needed for the polymerization reactions to go to completion, as measured by IR spectroscopy, ranged from 30 minutes to two days, depending on the conditions chosen. For the polymerization reactions carried out in TCB less time was needed for complete consumption of IAT than for the

polymerization reactions in CH_2Cl_2. The polymerization of IAT (route 2) proceeded much faster than that of IAT (route 1) under all studied conditions. This is likely the result of steric hindrance during the formation of the Ni(II) complex when both isocyanide enantiomers are involved (Figure 7).

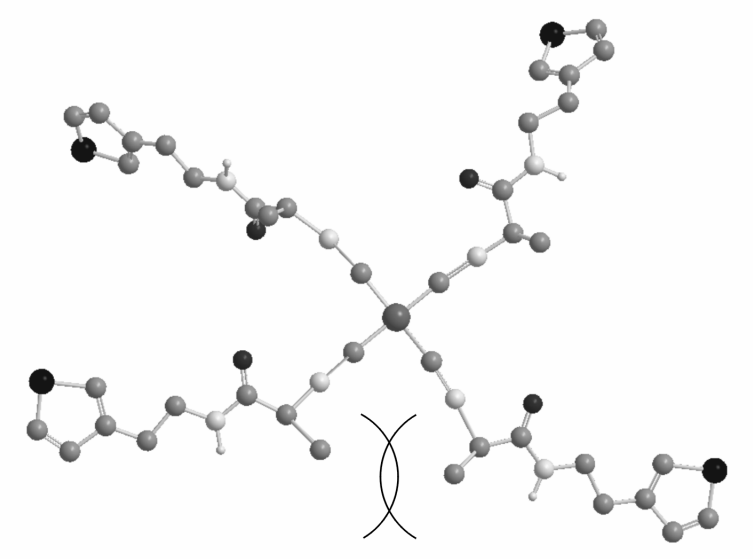

Figure 7. *Computer generated model showing the steric hindrance that can occur between the α-methyl groups of the alanine units when the IAT monomers coordinate to the nickel center.*

It was found by Cornelissen that polymerizations of isocyanides which take more than about 2 h will lead to polymers with no well-defined hydrogen bonding arrays.[29]

2.2.2 Characterization

IR spectroscopy is a very convenient technique to study isocyanides, since these compounds have a characteristic and strong vibration around 2150 cm^{-1}. Upon polymerization this vibration disappears and an imine vibration of the polyisocyanide backbone becomes visible around 1618 cm^{-1}. Comparison of the positions of the N-H stretch, C=O stretch and N-H bend vibrations in the IR spectra of IAT and PIAT revealed that the vibrations of the latter compound were shifted to lower wave numbers, as a result of a weakening of their bond strengths (Figure 8, Table 1), due to hydrogen bond formation between the amide groups in the polymer side chains.

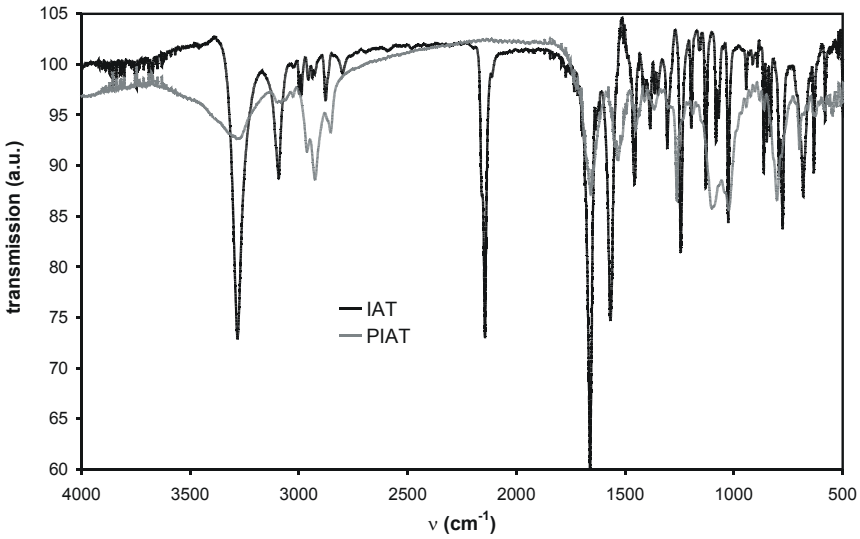

Figure 8. *IR spectra of IAT and PIAT, prepared via route 1.*

Table 1. ***IR data of IAT and PIAT prepared via routes 1 and 2***[a]

Compound	N-H stretch	CN stretch[b]	C=O stretch	N-H bend
IAT (route 1)	3282	2145	1661	1567
PIAT (route 1)	3278	1618	1654	1533
IAT (route 2)	3283	2145	1661	1567
PIAT (route 2)	3273	1617	1654	1531
L,L-IAA[c]	3279	2158, 2147	1669	1559
L,L-PIAA[c]	3276	1618	1657	1530
L-IAG[c]	3302	2158	1674	1564
L-PIAG[c]	3380, 3304	1619	1665	1530

[a] The vibrations are given in cm^{-1}. Measured as a solid in KBr. [b] For the monomers the C≡N stretch is given, while the C=N stretch is reported for the polymers. [c] Values found in the literature.[30]

As mentioned above, the single crystal X-ray structure of IAT revealed the presence of hydrogen bonding arrays between the amide groups of stacked molecules. Upon polymerization the hydrogen bonding becomes stronger. The IR properties of PIAT synthesized via the two described routes are rather similar, suggesting that the differences in hydrogen bonding strength in the polymer chains are small. The IR results obtained for PIAT

resemble more closely the values reported for L,L-PIAA than for poly(L-isocyanoalanyl-glycine methyl ester) (L-PIAG), which is more similar in chemical structure to PIAT than L,L-PIAA (Figure 9), because L-PIAG and PIAT both lack extra methyl groups that reduce the rotational freedom of the side groups.[30] For L,L-PIAA it was found that the hydrogen bonding arrays between the side chains are well-defined, thereby contributing to the stability and rigidity of the helical conformation of the polymer. It should be noted, however, that the amide group in PIAT is not a peptidic amide (Figure 9), implying that comparisons with PIAA and PIAG should be made with caution.

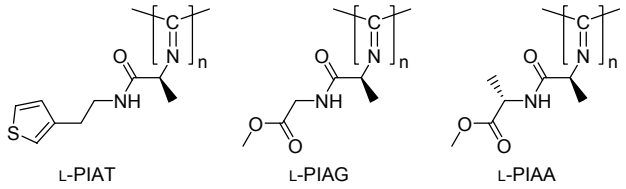

Figure 9. *Chemical structures of L-PIAT, L-PIAG, and L,L-PIAA.*

In order to obtain more insight in the structural organization of the PIAT polymers CD spectra were recorded (Figure 10). In the CD spectrum of a polyisocyanide a Cotton effect can often be observed in the range of 250 to 400 nm which is thought to originate from the n–π* transition of the helically arranged imine groups in the polymer backbone. Two characteristic types of spectra can be distinguished for polyisocyanopeptides using CD spectroscopy: *i*) a single strong Cotton effect around 310 nm, or *ii*) a couplet with a lower intensity.[31] For polyisocyanopeptides having hydrogen bonds between side chains directly on top of each other, i.e. $n/(n + 4)$ helices, the first type of spectrum is observed, as seen for L,L-PIAA. For L-PIAG the second type of spectrum is found, because it has less well-defined hydrogen bonding arrays. CD spectroscopy only gives indirect information about the strength of the hydrogen bonds between the side groups, since it is the imine bond that is monitored in the absence of other chromophores. Taking the results obtained for L,L-PIAA and L-PIAG as a lead,[30] it is tentatively postulated that a red shift of the Cotton effect occurs when the helix is better defined as a result of a higher degree of order in the hydrogen bonding network in the side chains.

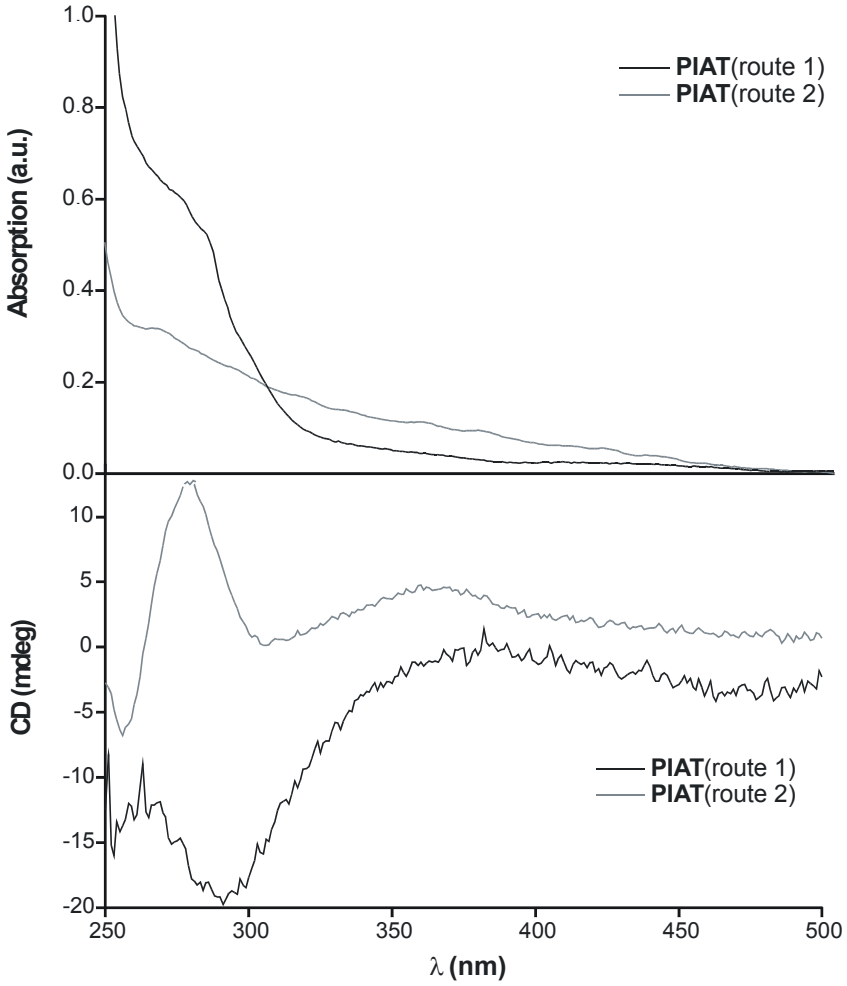

Figure 10. *UV-Vis (top) and CD spectra (bottom) in CH_2Cl_2 of PIAT polymerized via the two different routes.*

The CD spectra of PIAT do not show a single strong Cotton effect around 310 nm and the shape of the spectra resembles that of L-PIAG, which is comparable in structure to PIAT. The CD results (Figure 10), however, are in contradiction with the obtained IR results, where PIAT more closely resembles L,L-PIAA. The CD spectrum of PIAT (route 2) appears to be shifted towards longer wavelengths compared to PIAT (route 1), while the relative heights and the signs of the Cotton effects of these two compounds differ as well. The differences in the CD spectra of these two compounds can be directly correlated to the difference in structures of the two polymers. As a result of the incorporation of both enantiomers in the PIAT (route 1) a less-well defined structure and conformation is expected. Polymerization experiments performed with a mixture of L,D-IAA and L,L-IAA have indicated that both diastereomers can be readily incorporated into the growing polymer chain. The resulting polymers, however, are less rigid than the enantiomerically pure polymers, as was concluded from CD measurements.[32] The outcome of our experiments suggests that the polymer chains

of PIAT (route 1) contain both IAT enantiomers and, therefore, have a higher degree of disorder than those of PIAT (route 2). Van Beijnen *et al.* have shown that the relative intensities of the Cotton bands in a similar set of chiral, similar polyisocyanides, having the same helix sense, are a measure of the excess screw sense.[33] Unfortunately, due to availability of only a limited set of data no estimation of the excess of helix sense in the PIAT polymers could be made.

When the ratio of monomer to catalyst in the synthesis of PIAT (route 1) was increased from 20 to 250 a 4-fold increase of the Cotton effect was observed, probably as a result of an increased polymer chain length and, therefore, a better defined polymer backbone, which is in agreement with the optical rotation and GPC results described below.

The optical rotation of polyisocyanides originates from the helical arrangement of the backbone imine functions. In Table 2 the optical rotation data and the molecular weights at the maximum of the peak (M_p's) obtained by gel permeation chromatography (GPC) for PIAT are reported. In this table only the values of PIAT prepared via route 1 are given, since it was not possible to prepare polymers of sufficient solubility via route 2.

Table 2. ***Optical rotation and GPC data of PIAT prepared under various conditions***

Catalyst	Solvent	Ratio **IAT**/catalyst	Optical rotation[a]	M_p[b]
$Ni(ClO_4)_2$	CH_2Cl_2	50	-35	-
$Ni(ClO_4)_2$	CH_2Cl_2	250	-44	4,700
$Ni(ClO_4)_2$	TCB[c]	250	-68	14,200
$(t\text{-BuNC})_4Ni(ClO_4)_2$	CH_2Cl_2	20	-24	-
$(t\text{-BuNC})_4Ni(ClO_4)_2$	CH_2Cl_2	50	-38	4,500
$(t\text{-BuNC})_4Ni(ClO_4)_2$	CH_2Cl_2	250	-40	7,900
$(t\text{-BuNC})_4Ni(ClO_4)_2$	TCB[c]	50	-64	10,300
$(t\text{-BuNC})_4Ni(ClO_4)_2$	TCB[c]	250	-78	17,000

[a] $[\alpha]_D^{20}$ in °.cm^2.g^{-1}, measured in CH_2Cl_2 (*c* 1.0). [b] In g.mol^{-1}. Determined by GPC using polystyrene standards. [c] TCB is 1,2,4-trichlorobenzene.

The optical rotations of the polymers prepared in TCB are almost two times higher than those of the polymers prepared in CH_2Cl_2. A similar observation is made when the GPC results are compared; higher molecular weights are found for PIAT formed in TCB. The propagating polymer chains in TCB probably participate longer in the polymerization process

due to a better solubility of PIAT in this solvent and therefore longer polymer chains are formed. As soon as a polymer strand precipitates it will no longer be active in the polymerization process.[34]

Van Beijnen *et al.* have studied the possibility to determine the helix sense of polyisocyanides from optical rotation and CD data. It was shown that left-handed (*M*) isocyanide polymers give rise to a (+)-contribution of the optical rotation at 578 nm, whereas right-handed (*P*) polymers give rise to a (–)-contribution.[35] Based on CD calculations it was found that a Z-shaped (negative) couplet in the wavelength region of the n–π* transitions of the imine bonds in poly(*t*-butyl isocyanide) originates from a right-handed helical conformation, whereas an S-shaped (positive) couplet corresponds to a left-handed helix.[33] For L-PIAG a right-handed helical conformation was determined.[31] Since this polymer and PIAT have similar CD spectra and the same negative optical rotation, it is postulated that PIAT also has a right-handed helix.

The variations in optical rotation of the polymers prepared with different Ni(II) catalysts are small, while the molecular weights for PIAT prepared using $(t\text{-BuNC})_4Ni(ClO_4)_2$ are slightly higher, when compared to the other catalysts, which can be partly explained by the occasional incorporation of a *t*-BuNC molecule, thereby building in more monomers than calculated. Another possibility is a difference in catalyst efficiency between $Ni(ClO_4)_2$ and $(t\text{-BuNC})_4Ni(ClO_4)_2$. The used GPC columns were calibrated with polystyrene samples. Since the hydrodynamic properties of polystyrene and polyisocyanides are very different, the determined molecular weights for PIAT can only be used as relative molecular weights. A clear increase in the molecular weight could be observed when the ratio monomer/catalyst was increased (Table 2), however, no correlation was observed. The polymeric compounds prepared using low ratios of monomer to catalyst had retention times which were very close to those of low molecular weight compounds and, therefore, are probably oligomers. In the chromatograms of these oligomers it was not possible to determine the end of the oligomer peak, due to interference with the solvent peak. As a result no reliable estimations of the number average (M_n) and weight average molecular weight (M_w) of these samples could be made (Figure 11). It was therefore decided to use M_p.

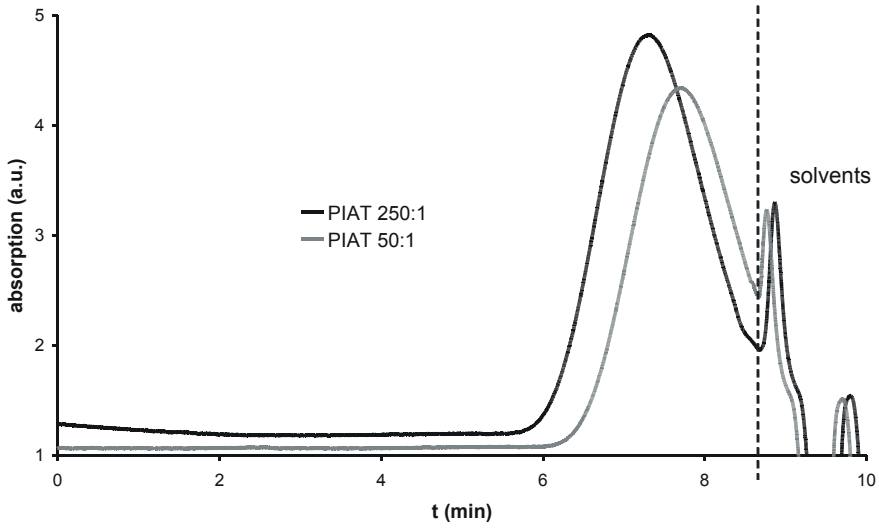

Figure 11. *GPC chromatograms of PIAT synthesized in TCB using $Ni(ClO_4)_2$ as a catalyst. The grey trace represents PIAT synthesized with a monomer/catalyst ratio of 50:1 and the black trace PIAT synthesized with a monomer/catalyst ratio of 250:1. The peaks after 8.5 minutes are caused by water and the eluent THF.*

Remarkably, fluorescence spectroscopy studies showed that racemized PIAT must contain fluorophores. When a solution of this macromolecule was excited at 280 nm, two emission peaks appeared, one at 312 nm and another at 482 nm, while excitation at 395 nm resulted in only one strong emission peak at 482 nm (Figure 12). In the absorption spectra of the different batches of PIAT only a very weak absorption could be observed at wavelengths higher than 300 nm (Figure 10). The excitation spectrum of racemized PIAT, recorded by using an emission wavelength of 480 nm, was distinctly different from the absorption spectrum. It had a large excitation peak at 395 nm, whereas the absorption spectrum does not have a distinct peak at this wavelength. When both FAT and IAT were excited at 280 nm, a peak with a very low intensity appeared at 308 nm, thus excluding the possibility that the emission at 312 nm originates from the amide groups. Therefore, the peak at 312 nm in the spectrum of PIAT must come from the imine groups in the polymers. The observed emission peak at 482 nm cannot be ascribed to the presence of the thiophene groups, because it is known that monothiophenes do not fluoresce, in contrast to oligo- and polythiophenes which are highly fluorescent. It is possible that partial polymerization of the thiophenes had occurred. The observed emission, however, is most likely originating from conjugated imine groups.

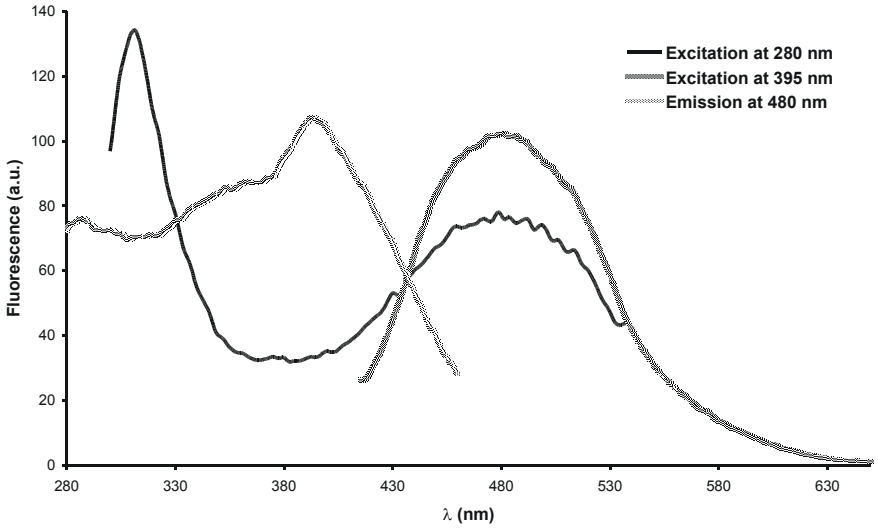

Figure 12. *Fluorescence excitation and emission spectra of racemized PIAT in CH_2Cl_2.*

Due to the presence of both enantiomers during polymerization racemized PIAT will have a more ill-defined backbone. This might lead to a partial uncoiling of the polymer backbone. The observed fluorescence might also be the result of defects, which are incorporated during the polymerization process. Clericuzio *et al.* have calculated that the syndio structure is the lowest energy state for simple polyisocyanides (Figure 13).[36]

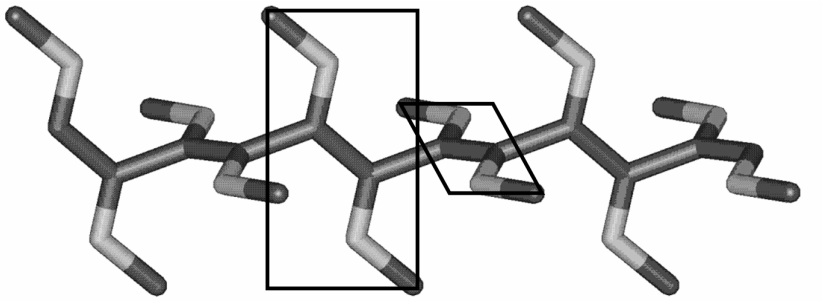

Figure 13. *The* syndio *conformation of a 12 units long polyisocyanide. This conformation was calculated by Clericuzio* et al. *to be the thermodynamically most favorable structure and has conjugated imine pairs.*

In the syndio conformation conjugation of the imine bonds is possible, which would explain the absorption and emission bands at higher wavelengths. Since the uncoiling will not be identical for all polyisocyanide molecules the number of conjugated imine bonds can vary in each chain and even in a single chain sets of several isolated groups of conjugated imine bonds can be present. This was observed by exciting the polymer at different wavelengths,

resulting in a shift of the second emission peak to wavelengths as high as 520 nm (at an excitation wavelength of 440 nm). The color of the prepared polymers varied from slightly orange to orange/brown, which is another indication for the existence of conjugated imine bonds or defects in the polymer chains. The latter is known to occur when isocyanides are polymerized with Ni catalysts.[31] The fluorescence intensity of the optically pure PIAT was barely detectable, indicating the influence of the presence of enantiomers during polymerization.

It was possible, using atomic force microscopy (AFM) to directly visualize the differences in chain lengths between batches of polymers with different molecular weights. Two batches of PIAT were synthesized using TCB as solvent, the first batch with 1/50 equivalent of (t-BuNC)$_4$Ni(ClO$_4$)$_2$ as catalyst and the second batch with 1/250 equivalent of this catalyst. In Figure 14 the resulting images of the tapping mode AFM measurements are shown.

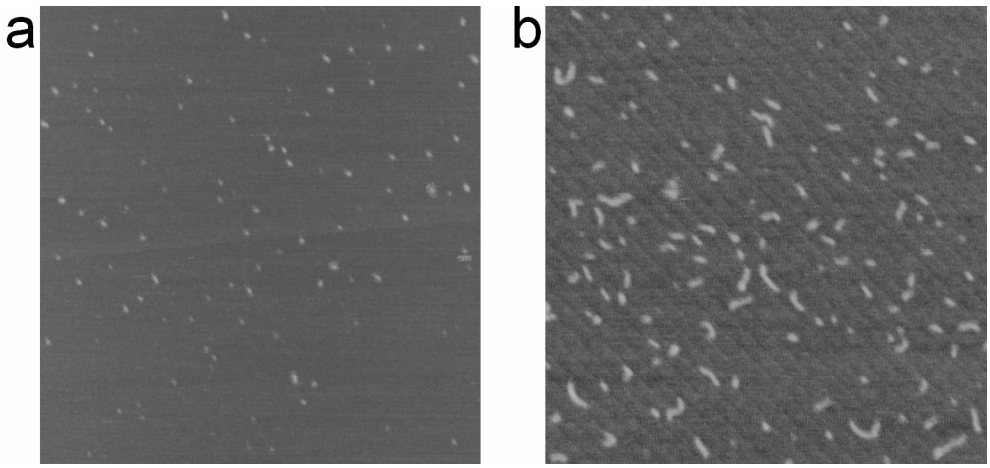

Figure 14. *AFM height images of PIAT synthesized in TCB with a) 1/50 equivalent of (t-BuNC)$_4$Ni(ClO$_4$)$_2$, and b) 1/250 equivalent of this catalyst. The width of both images corresponds to 1 μm. The substrate used was mica.*

For PIAT synthesized with 1/50 equivalent of (t-BuNC)$_4$Ni(ClO$_4$)$_2$ only small circular objects were observed with an average diameter of 7 nm, while rod-like structures, with an average length of 28 nm, were seen when 1/250 equivalent of catalyst was used. For L,L-PIAA and L-PIGA a helical pitch of 4.6 Å was measured by powder X-ray diffraction.[37] This value was used to estimate the average number of isocyanide units per polymer chain for the PIAT polymers studied by AFM. Every isocyanide unit in the polymer chain, therefore, corresponds to a length of 1.2 Å. The average length of the polymer chains as determined

from the AFM images was divided by this number. For the shorter polymer an average of ~61 isocyanide units per polymer chain was calculated, while for the longer polymer a value of ~243 isocyanide monomers per chain was determined. These numbers match the numbers of equivalents of catalyst per monomer that were used in the polymerization reactions. If these results are used to calculate the number average molecular weight (M_n), values of M_n = 13×10^3 g.mol^{-1} and 53×10^3 g.mol^{-1} are obtained respectively. By definition the M_n is always lower than M_p, or equal to this number when the polydispersity is 1. This means that the M_p values determined by GPC are too low which is probably a consequence of the difference in the persistence length between polystyrene and a polyisocyanopeptide.[13] It was observed that a large degree of tailing occurred when polyisocyanides were analyzed by GPC.[38]

2.3 Thiophene-Containing Polyisocyanides Derived from Alanyl-Alanine

2.3.1 Synthesis

In the previous paragraph the synthesis and characterization of a thiophene-containing polyisocyanide derived from alanine were described. In this polymer the hydrogen bonding networks are based on single amide functions and not on multiple peptidic amides. From CD measurements it was concluded that the helix of PIAT was not very well defined. It is known that polyisocyanides having two alanine groups in their side chains do have ordered arrays of hydrogen bonds along the polymer backbone.[12] The logical next step to improve the order in the polymer chains was to prepare a polyisocyanide in which the thiophene ring is connected to a dialanine group. The resulting polymer will have an additional amide group for hydrogen bond formation, thereby further rigidifying the polymer backbone. In Scheme 3 the synthesis of such a polymer is given. BAT, which was used as a building block in the preparation of PIAT, was also utilized in the synthesis of poly(2-isocyanoalanyl-alanine(2-thiophen-3-yl-ethyl)amide) (PIAAT). This compound was first deprotected with HCl and then coupled using DCC to either L- or D-Boc-Ala-OH, resulting in Boc-(L or D)-alanyl-L-alanine(2-thiophen-3-yl-ethyl)amide ((L or D),L-BAAT). In a way analogous to the synthesis of FAT, BAAT was converted into the concomitant formamide by dissolving the former compound in HCl-saturated ethyl acetate, resulting in the loss of the Boc-group, followed by formylation with ethyl formate and sodium formate to give *N*-formyl-alanyl-alanine(2-thiophen-3-yl-ethyl)amide (FAAT).

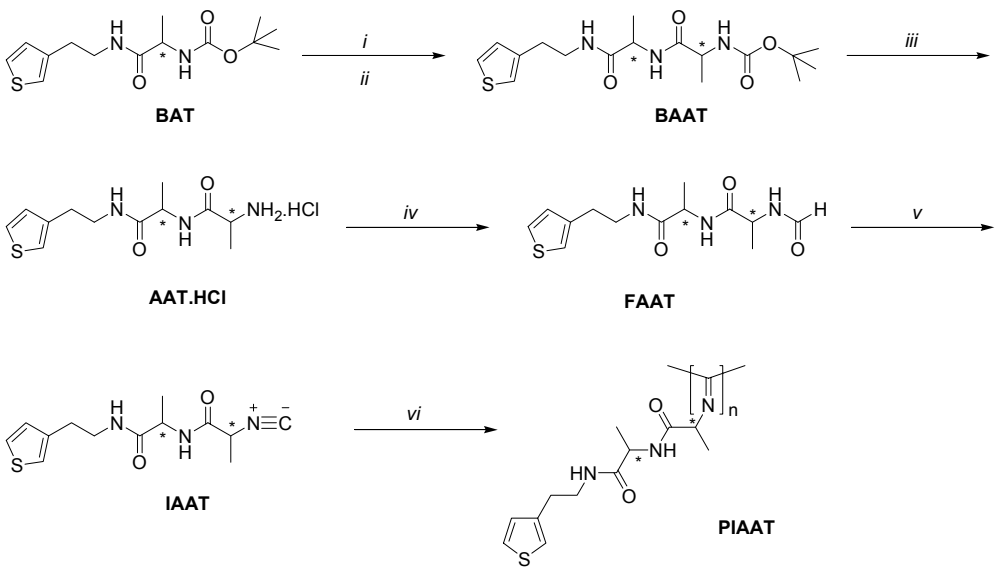

Scheme 3. *Synthesis of poly(2-isocyanoalanyl-alanine(2-thiophen-3-yl-ethyl)amide) (PIAAT), i) HCl in EtOAc; ii) Boc-Ala-OH, DCC, HOBT, DMAP, CH_2Cl_2; iii) HCl in EtOAc; iv), HCO_2Et, HCO_2Na; v)* N-*methylmorpholine, diphosgene, CH_2Cl_2; and vi) $Ni(ClO_4)_2$, EtOH, CH_2Cl_2.*

The desired isocyanide was subsequently obtained by dehydration of the formamide group with diphosgene, giving 2-isocyanoalanyl-alanine(2-thiophen-3-yl-ethyl)amide) (IAAT) as a white crystalline material. Polymerization of IAAT was performed by using $Ni(ClO_4)_2$ as a catalyst. Interestingly, the solubility of the PIAAT polymers in chlorinated solvents was considerably higher than that of PIAT (route 2). As in the case of PIAT, attempts were made to polymerize D,L-IAAT using TFA, but this was successful only once in a test reaction using a small quantity of monomer. The resulting CD spectrum was comparable to the CD spectrum for D,L-PIAAT prepared using $Ni(ClO_4)_2$ as a catalyst. When larger amounts of D,L-IAAT were used, the polymerization reaction did not proceed and the isocyanide was partly reconverted into the formamide.

2.3.2 Characterization

The polymer samples were studied with the help of IR spectroscopy (Figure 15). The data for the IAAT monomers and PIAAT polymers are summarized in Table 3.

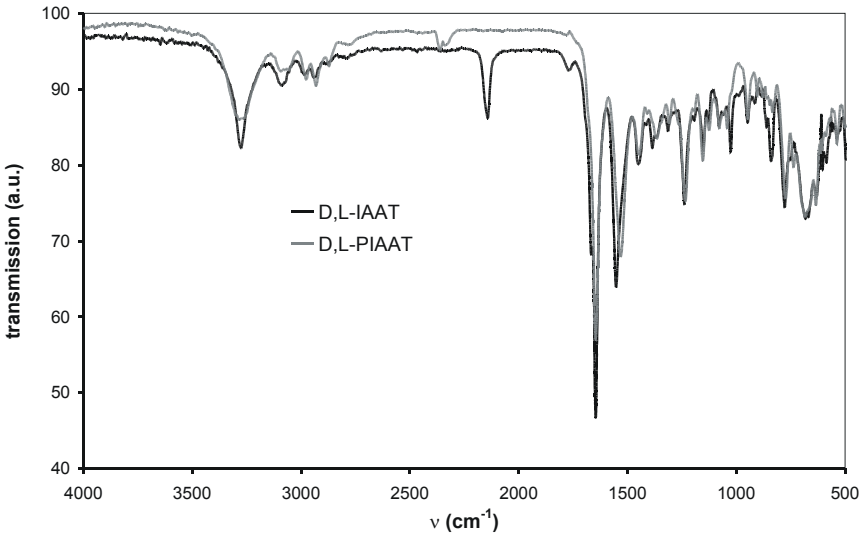

Figure 15. *IR spectra of D,L-IAAT and D,L-PIAAT.*

Table 3. ***IR data for IAAT and PIAAT***[a]

Compound	N-H stretch	CN stretch[b]	C=O stretch	N-H bend
D,L-IAAT	3275	2142	1666, 1646	1552
D,L-PIAAT	3310, 3284	[c]	1742, 1645	1540, 1520
L,L-IAAT	3310, 3288	2142	1652	1551, 1532
L,L-PIAAT	3305, 3284	[c]	1647	1531
L,L-IAA[d]	3279	2158, 2147	1669	1559
L,L-PIAA[d]	3276	1618	1657	1530
L,D-IAA[d]	3304	2156, 2144	1668	1560
L,D-PIAA[d]	3280	1618	1659	1530

[a] Values are in cm^{-1}. Measured as a solid by ATR-FTIR. [b] For the monomers the C≡N stretching vibration is given, while for the polymers the C=N stretching vibration is shown. [c] No signal for the C=N vibration could be distinguished. [d] Values found in the literature.[30]

Lower wavenumbers for the amide signals are observed after polymerization, indicating a decrease in bond strength. Differences in IR results are noted between the IAAT diastereomers, as well as between the PIAAT polymers. Interestingly, for L,L-PIAAT only one vibration was observed for the C=O stretch and N-H bend vibrations, suggesting that the amide groups are identical, while these vibrations for D,L-PIAAT were split up into two

signals (Table 3). Apparently, the stereochemistry appears to be of major influence on the organization of the hydrogen bonds in the solid state. In contrast, for L,L-PIAA and L,D-PIAA the IR values of the amide group were very similar (Table 3). However, it has to be noted that IAAT has two amide groups, whereas IAA has only one.

The CD spectra of L,L- and D,L-PIAAT are shown in Figure 16. Both spectra show a positive Cotton effect at 315 nm.

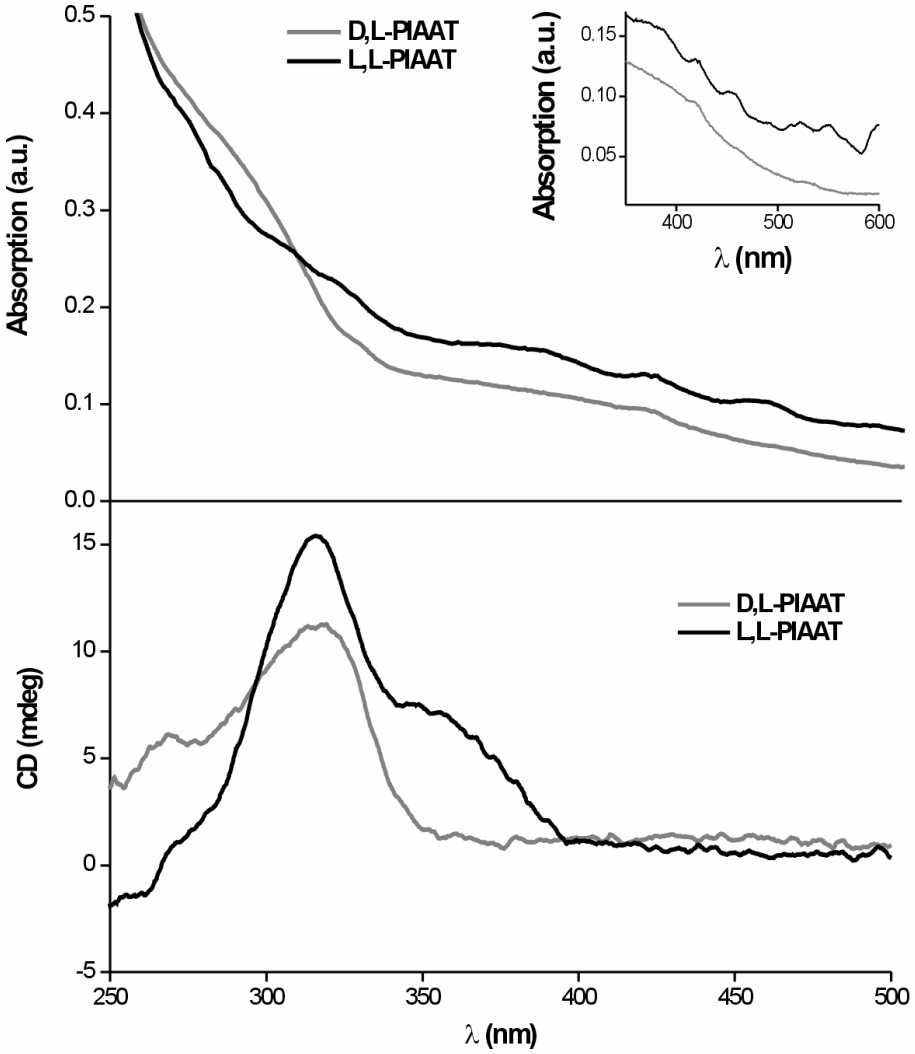

Figure 16. *UV-Vis (top) and CD spectra (bottom) in CH_2Cl_2 of L,L- and D,L-PIAAT polymerized with $Ni(ClO_4)_2$ as a catalyst. The inset shows a magnification of the region from 350 to 600 nm in the UV-Vis spectrum.*

While PIAT had a CD spectrum similar to that of PIAG, the CD spectra of L,L- and D,L-PIAAT displayed more similarity to those of L,L- and L,D-PIAA, indicating that the PIAAT backbone is more defined than the backbone of PIAT. This is due to the presence of

the second alanine group, which not only results in the formation of an extra hydrogen bond between the side groups, but also reduces the rotational freedom of these side groups, because extra methyl groups are present. The IR results indicate that D,L-PIAAT has a stronger hydrogen bonding network than L,L-PIAAT. This is reflected in the CD spectrum which shows no Cotton effect at ~360 nm in the case of the former polymer and only a weak UV absorption at wavelengths higher than 310 nm. The bands in the UV-Vis spectrum of L,L-PIAAT above 400 nm are indicative of partial uncoiling of the polyisocyanide backbone.

Fluorescence spectra were recorded for both L,L- and D,L-PIAAT. Somewhat surprisingly, only the former polymer showed appreciable fluorescence (Figure 17).

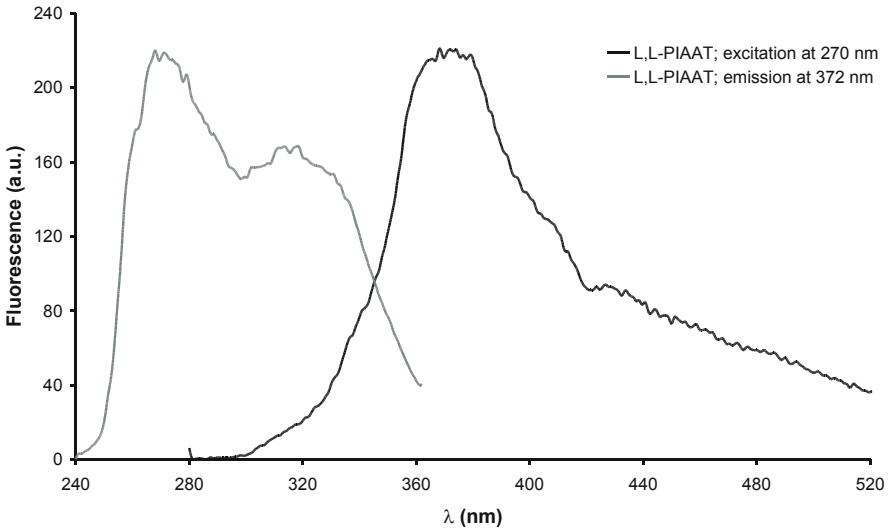

Figure 17. *Fluorescence excitation and emission spectra of L,L-PIAAT in CH_2Cl_2.*

When L,L-PIAAT was excited at 270 nm an emission peak appeared with a maximum at 372 nm. The excitation spectrum showed two peaks, viz. at 271 and 317 nm ($\lambda_{em.}$ = 372 nm). In the case of the PIAT polymers fluorescence was also observed (Figure 12), and was attributed to partial uncoiling of the polyisocyanide backbone, resulting in a conformation in which the imine bonds were conjugated (Figure 13). Whereas emission peaks at very high wavelengths were observed for PIAT, the highest emission peak of L,L-PIAAT was only at 372 nm, although above this wavelength some residual emission was observed. The excitation peak at 271 nm might be ascribed to the amide groups in the polymer, whereas the excitation peak at 317 nm may be due to the imine bonds. These results indicate that the PIAAT helices are better defined than PIAT, with D,L-PIAAT having the highest structural definition, because this polymer did not fluoresce at all.

Also in the case of PIAAT, AFM was used to visualize the polymer molecules. The AFM images of D,L-PIAAT showed long rod-like structures among shorter fragments (Figure 18).

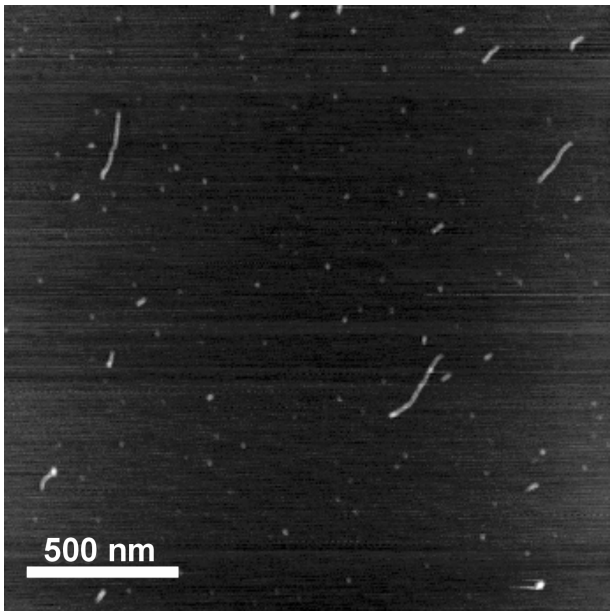

Figure 18. *AFM height image of D,L-PIAAT. The substrate used was mica.*

The lengths of the longer polymers were circa 300 nm, while the fragments were only a few nanometers in size. A length of 300 nm corresponds to circa 2.7×10^3 isocyanide repeat units and an M_n of 762×10^3 g.mol^{-1}. Not enough AFM images were at hand to determine the polydispersity of the polymer and the spread in the polymer length. Compared to the AFM images of PIAT (Figure 14), the polymer length and the level of definition of D,L-PIAAT are higher, as was already concluded from the spectroscopic measurements.

2.4 Conclusions

Polymers of isocyanides containing well-defined arrays of thiophene groups have been prepared starting from isocyanoalanylthiophene monomers using a nickel catalyzed polymerization reaction. The degree of order in the polymer backbone was found to be dependent on the optical purity of the chiral monomer and the number of alanine units present in the side groups. It was observed that both enantiomers of a partly racemized monomer become incorporated in the growing polyisocyanide chain, resulting in more flexibility and

therefore a less well defined network of hydrogen bonds between the amide groups in the polymer side chains.

The presence of a second alanine group in the side chain appeared to improve the regularity of the thiophene-containing polyisocyanides, which was concluded from their CD spectra and fluorescence studies. The fact that a second hydrogen bonding group is present and that the rotational freedom of the side chain is reduced by the presence of a methyl group on the second alanine moiety leads to this higher regularity of the polymer chain. Changing the chirality of the second alanine group altered the physical properties of the resulting polymers significantly. IR, CD, and fluorescence measurements demonstrated that the D,L-polyisocyanide was better defined than the L,L-polymer. This is probably the result of a difference in packing of the side groups in the two polymers.

The prepared polymers might be interesting materials for the preparation of conductive nanowires. For that purpose the thiophenes in the side groups have to be linked by polymerization. This approach can also be used to align other (functional) groups, such as pyridines, tetrathiafulvalenes, and sugars.

2.5 Experimental Section

General methods and materials

Diethyl ether was distilled over sodium, CH_2Cl_2 over $CaCl_2$ and methanol over CaH_2 at atmospheric pressure. DMF was dried over BaO for one week, after which it was distilled under reduced pressure. The first 25 ml of the distillate were removed. *N*-methylmorpholine was distilled under reduced pressure. All other chemicals were commercial products and used as obtained, unless stated otherwise. Silica gel from Acros was used for column chromatography and silica 60 F_{254} coated glass TLC plates were purchased from Merck. Compounds containing amine and amide groups were made visible with Cl_2/TDM. ^{1}H NMR and ^{13}C NMR spectra were recorded on Bruker DPX-200 and Bruker AC-300 instruments at room temperature. Chemical shifts are given in ppm (δ) relative to the internal standard tetramethylsilane (δ = 0.0 ppm) for measurements in $CDCl_3$, otherwise the solvent peak was used as the reference. For ^{13}C spectra the solvent peak was used as the reference. Abbreviations used are: s = singlet, d = doublet, t = triplet, q = quartet, m = multiplet, dd = doublet of doublets, and br = broad. FT-infrared spectra were recorded on a BioRad FTS 25 and a ThermoMattson IR300 spectrometer equipped with a Harrick ATR unit where the compounds were measured as a solid. Optical rotation measurements were performed on a Perkin Elmer 241 polarimeter. UV-Vis spectra were recorded on a Varian Cary 50 spectrometer. A Perkin Elmer Luminescence spectrometer LS50B was used to determine fluorescence spectra and a Jasco J600 apparatus to record CD spectra. Mass spectra were measured on a VG 7070E machine. Elemental analyses were determined with a Carlo Erba 1180 instrument. AFM measurements were carried out on a Digital Instruments Nanoscope III in tapping mode at room temperature. The polymers were spin-coated from a 10^{-5} g/ml solution on a freshly cleaved mica surface.

GPC

GPC measurements were carried out with a Shimadzu GPC with Shimadzu refractive index and UV-Vis detection, fitted with a Polymer Laboratories Plgel 5 μm mixed-D column and a PL 5 μm Guard column (separation range from 500–300,000 molecular weight) using THF as mobile phase at 35°C.

HPLC

The ratio between the enantiomers of FAT formed via route 1 and 2 were determined by HPLC using a Chiralpak AD chiral column and a UV-Vis detector operating at 250 nm. Hexane/2-propanol 8:2 (v/v) was used as eluent at a flow rate of 0.7 ml/min.

Single crystal X-ray determination of L-Isocyanoalanine(2-thiophen-3-yl-ethyl)amide (IAT)

A structure determination summary is given in Table 4 and a PLUTON[25] drawing of the molecular arrangement in the crystal is shown in Figure 6.

Table 4. ***Crystal data and structure refinement for IAT***

Crystal color	transparent, light yellow
Crystal shape	rough fragment
Crystal size [mm]	0.50 x 0.28 x 0.26
Empirical formula	$C_{10}H_{12}N_2OS$
Molecular weight	208.28
Temperature [K]	293(2)
Radiation / Wavelength [Å]	MoKα (graphite mon.) / 0.71073
Crystal system	Orthorhombic
space group	$P\ 2_12_12_1$
Unit cell dimensions [Å] (25 reflections)	$a = 4.7799(6)$, $\alpha = 90°$ $b = 9.3152(9)$, $\beta = 90°$ $c = 24.7353(19)$, $\gamma = 90°$
Range [°]	$9.740 < \theta < 14.792$
Volume [Å^3]	1101.37(19)
Z	4
Calculated density [Mg/m^3]	1.256
Absorption coefficient [mm^{-1}]	0.264
Diffractometer / scan	Enraf-Nonius CAD4 / Ω
F(000)	440
θ range for data collection [°]	2.74 to 27.48
Index ranges	$0 \le h \le 6$, $-12 \le k \le 0$, $-32 \le l \le 0$
Reflections collected / unique	1512 / 1512
Reflections observed [Io > 2σ(Io)]	723
Absorption correction	Semi-empirical from ψ-scans
Range of relative transmission factors	1.059 and 0.918
Refinement method	Full-matrix least-squares on F^2
Computing	SHELXL-97[41]
Data / restraints / parameters	1512 / 49 / 148
Goodness-of-fit on F^2	1.035
SHELXL-97 weight parameters	0.077500 0.113100
Final R indices [I > 2σ(I)]	R1 = 0.0606, wR2 = 0.1336
R indices (all data)	R1 = 0.1477, wR2 = 0.1728
Extinction coefficient	0.004(4)
Largest diff. peak and hole [Å^3]	0.173 and -0.147

Crystals of IAT suitable for X-ray diffraction studies were obtained from diethyl ether by slow evaporation of the solvent. A single crystal was mounted in air on a glass fiber. Intensity data was collected at room temperature and corrected for Lorentz and polarization effects. An Enraf-Nonius CAD4 single-crystal diffractometer (Mo-Kα radiation, omega scan mode) was used. Unit cell dimensions were determined from the angular setting of 25 reflections. Semi-empirical absorption correction (ψ-scans) was applied.[39] The structure was solved by the program CRUNCH[40] and was refined with standard methods (refinement against F^2 of all reflections with SHELXL97[41]) with anisotropic parameters for the nonhydrogen atoms. The hydrogens of the methyl group were refined as a rigid rotor with idealized sp^3 hybridization and a C-H bond length of 0.97 Å to match maximum electron density in a difference Fourier map. All other hydrogens were placed at calculated positions and were refined riding on the parent atoms. The thiophene ring was disordered over two positions. This disorder can be interpreted as a swap of the ring and can be described by a suitable disorder model.

Synthesis

(t-BuNC)$_4$Ni(ClO$_4$)$_2$,[42] β-3-thienylethylamine,[43] and *N*-formyl-L-alanine[44] were synthesized using procedures from the literature.

Boc-L-alanine(2-thiophen-3-yl-ethyl)amide (BAT)

To a stirred solution of β-3-thienylethylamine (0.45 g, 3.5 mmol) in CH_2Cl_2 was added Boc-L-alanine (0.76 g, 4.0 mmol), dimethylaminopyridine (catalytic amount) and dicyclohexylcarbodiimide (0.79 g, 3.8 mmol). This solution was stirred for 16 h after which the formed dicyclohexyl urea was filtered off and the solvent was evaporated. The product was purified by column chromatography (silica gel, eluent: 1 % (v/v) MeOH in CH_2Cl_2) and obtained as a white powder (0.92 g, 87 %). $[\alpha]_D^{20}$ (CH_2Cl_2 *c* 0.5) = -23°.cm^2.g^{-1}; ^{1}H NMR (300 MHz, $CDCl_3$) δ 7.29 (q, 1H, thiophene H-5, J = 8.0 Hz, J = 2.9 Hz), 7.01 (m, 1H, thiophene H-2, J = 2.0 Hz), 6.95 (dd, 1H, thiophene H-4, J = 6.1 Hz, J = 1.2 Hz), 6.12 and 4.89 (br, 1H, NHC(O)), 4.08 (m, 1H, NHC(O)C*H*(CH_3)), 3.52 (m, 2H, C*H*$_2$NH), 2.85 (t, 2H, C*H*$_2$-thiophene, J = 6.9 Hz), 1.42 (s, 9H, C(C*H*$_3$)$_3$), 1.32 (d, 3H, CHC*H*$_3$, J = 4.7 Hz) ppm; ^{13}C NMR (50 MHz, $CDCl_3$) δ 179.5 and 167.5 (NH*C*(O)), 139.1 (thiophene C-3), 128.2 (thiophene C-4), 126.2 (thiophene C-5), 121.6 (thiophene C-2), 80.5 (*C*(CH$_3$)$_3$), 48.6 (C(O)*C*H(CH$_3$)), 40.0 (*C*H$_2$NH), 30.3 (*C*H$_2$-thiophene), 28.5 (C(C*H*$_3$)$_3$), 18.5 (*C*H$_3$) ppm; FT-IR (cm^{-1}, KBr) 3342 (NH), 3092, 2979, 2936 and 2864 (CH), 1685 and 1655 (C=O), 1547 and 1522 (N-H); EI-MS: m/z = 298 [M]$^+$ (calcd: 298.41); El. anal. calcd for $C_{10}H_{14}N_2O_2S$ (%) C: 59.54, H: 7.85, N: 9.91, S: 11.35, found: C: 59.66, H: 7.95, N: 9.87, S: 11.19.

_N_-Formyl-L-alanine(2-thiophen-3-yl-ethyl)amide (FAT)

Route 1: β-3-Thienylethylamine (0.61 g, 4.8 mmol), _N_-formyl-L-alanine (0.56 g, 4.8 mmol), dimethylaminopyridine (catalytic amount) and dicyclohexylcarbodiimide (1.19 g, 5.8 mmol) were dissolved in 20 ml of CH_2Cl_2/EtOAc (3:1 v/v). The solution was stirred overnight, the formed dicyclohexyl urea was filtered off and the solvent evaporated. After purification by column chromatography (silica, eluent: 5 % (v/v) MeOH in CH_2Cl_2), the product was dissolved in a minimal amount of CH_2Cl_2 and precipitated in pet. ether 40–65°C yielding a white solid (0.75 g, 69 %). $[\alpha]_D^{20}$ (CH_2Cl_2 *c* 0.10) = -40°.cm^2.g^{-1}; ^{1}H NMR (300 MHz, $CDCl_3$) δ 8.13 (s, 1H, C(O)H), 7.29 (q, 1H, thiophene H-5, J = 7.8 Hz, J = 3.0 Hz), 7.01 (d, 1H, thiophene H-2, J = 2.3 Hz), 6.95 (dd, 1H, thiophene H-4, J = 9.1 Hz, J = 1.9 Hz), 6.29 and 6.08 (br, 1H, N*H*C(O)), 4.48 (m, 1H, C(O)C*H*(CH_3)), 3.52 (m, 2H, C*H*$_2$NH), 2.86 (t, 2H, C*H*$_2$-thiophene, J = 6.9 Hz), 1.37 (d, 3H, CHC*H*$_3$, J = 7.0 Hz) ppm; ^{13}C NMR (75 MHz, $CDCl_3$) δ 171.7 (NH*C*(O)), 160.9 (NH*C*(O)H), 138.9 (thiophene C-3), 128.1 (thiophene C-4), 126.3 (thiophene C-5), 121.8 (thiophene C-2), 47.8 (C(O)*C*H(CH_3)), 40.2 (*C*H$_2$NH), 30.2 (*C*H$_2$-thiophene), 18.7 (CH_3) ppm; FT-IR (cm^{-1}, KBr) 3315, 3266 (NH), 3097, 2983, 2944 and 2875 (CH), 1686 and 1642 (C=O), 1561 and 1526 (N-H); EI-MS: m/z = 226 $[M]^+$ (calcd: 226.30); El. anal. calcd for $C_{10}H_{14}N_2O_2S$ (%) C: 53.08, H: 6.24, N: 12.38, S: 14.17, found: C: 53.06, H: 6.23, N: 12.01, S: 14.37.

Route 2: The Boc-group of BAT was removed by dissolving 418 mg (1.40 mmol) of this compound in 20 ml of ethyl acetate saturated with HCl. After stirring for 4 h under an N_2 atmosphere the reaction mixture was evaporated to dryness. TLC revealed no residual starting material. The excess of HCl was removed by dissolving the product in 10 ml of *t*-BuOH and subsequent evaporation of the solvent. The residue was redissolved in 15 ml of ethylformate and 383 mg (5.63 mmol) sodium formate was added while stirring. This mixture was refluxed for 6 h after which the formed precipitate was removed by filtration. The filtrate was evaporated to dryness and the resulting viscous oil was precipitated in petroleum ether 40–65°C. The obtained product was a white powder (304 mg, 96 %). $[\alpha]_D^{20}$ (CH_2Cl_2 *c* 1.0) = -54°.cm^2.g^{-1}; ^{1}H NMR (300 MHz, $CDCl_3$) δ 8.12 (s, 1H, C(O)H), 7.29 (q, 1H, thiophene H-5, J = 8.1 Hz, J = 2.9 Hz), 7.01 (d, 1H, thiophene H-2, J = 1.8 Hz), 6.95 (dd, 1H, thiophene H-4, J = 5.9 Hz, J = 1.1 Hz), 6.35 and 6.15 (br, 1H, N*H*C(O)), 4.46 (m, 1H, C(O)C*H*(CH_3)), 3.52 (m, 2H, C*H*$_2$NH), 2.85 (t, 2H, C*H*$_2$-thiophene, J = 7.0 Hz), 1.37 (d, 3H, CHC*H*$_3$, J = 7.0 Hz) ppm.

L-Isocyanoalanine(2-thiophen-3-yl-ethyl)amide (IAT)

Route 1: To a solution of FAT (99.0 mg, 0.438 mmol) in 1.0 ml of CH_2Cl_2 *N*-methylmorpholine (0.104 ml, 0.88 mmol) was added under a N_2 atmosphere and the solution was cooled to -30°C. In a period of 10 min. diphosgene (43 mg, 0.22 mmol) in 1.0 ml of CH_2Cl_2 was added. After keeping the temperature at -30°C for an additional 30 min., the temperature was gradually brought to room temperature. A saturated $NaHCO_3$ solution (5 ml) was added and the mixture was stirred vigorously for 5 min. The organic layer was separated, extracted twice with 10 ml of water and dried using Na_2SO_4. The solvent was evaporated and the crude solid was purified by column chromatography (silica gel, eluent: 0.5 % (v/v) MeOH in CH_2Cl_2) resulting in a white solid (79 mg, 87 %). Single crystals were obtained by slow evaporation of a diethyl ether solution of the compound. Mp: 81°C; $[\alpha]_D^{20}$ (CH_2Cl_2 *c* 0.5) = +11°.cm^2.g^{-1}; ^{1}H NMR (300 MHz, $CDCl_3$) δ 7.31 (q, 1H, thiophene H-5, J = 7.6 Hz, J = 2.9 Hz), 7.04 (d, 1H, thiophene H-2, J = 2.0 Hz), 6.97 (dd, 1H, thiophene H-4, J = 6.2 Hz, J = 1.4 Hz), 6.43 (br, 1H, N*H*C(O)), 4.19 (q, 1H, C(O)C*H*(CH_3), J = 21.4 Hz, J = 7.1 Hz), 3.58 (m, 2H, C*H*$_2$NH), 2.91 (t, 2H, C*H*$_2$-thiophene, J = 6.9 Hz), 1.61 (d, 3H, CHC*H*$_3$, J = 7.1 Hz) ppm; ^{13}C NMR (75 MHz, $CDCl_3$) δ 166.1 (NH*C*(O)),

161.5 (N≡*C*), 138.5 (thiophene C-3), 128.1 (thiophene C-5), 126.7 (thiophene C-2), 122.0 (thiophene C-4), 53.7 (C(O)*C*H(CH_3)), 40.5 (*C*H_2NH), 30.1 (*C*H_2-thiophene), 20.0 (*C*H_3) ppm; FT-IR (cm^{-1}, KBr) 3282 (NH), 3095, 2928 and 2874 (CH), 2145 (CN), 1661 (C=O), 1567 (N-H); EI-MS: m/z = 208 $[M]^+$ (calcd: 208.28); El. anal. calcd for $C_{10}H_{12}N_2OS$ (%) C: 57.67, H: 5.81, N: 13.45, S: 15.40, found: C: 57.91, H: 5.89, N: 13.11, S: 15.58.

Route 2: The same method as described for IAT (route 1) was followed to synthesize this compound, but FAT (route 2) was used as the starting material. The isocyanide was obtained as a white solid in 79 % yield. $[\alpha]_D^{20}$ (CH_2Cl_2 *c* 1.0) = +17°.$cm^2.g^{-1}$; ^{1}H NMR (300 MHz, $CDCl_3$) δ 7.31 (q, 1H, thiophene H-5, J = 8.1 Hz, J = 2.9 Hz), 7.04 (d, 1H, thiophene H-2, J = 2.9 Hz), 6.97 (dd, 1H, thiophene H-4, J = 5.9, J = 1.1), 6.43 (br, 1H, N*H*C(O)), 4.19 (q, 1H, C(O)C*H*(CH_3), J = 20.9 Hz, J = 7.0 Hz), 3.58 (m, 2H, C*H*$_2$NH), 2.91 (t, 2H, C*H*$_2$-thiophene, J = 7.0 Hz), 1.61 (d, 3H, CHC*H*$_3$, J = 7.0 Hz) ppm; FT-IR (cm^{-1}, KBr) 3283 (NH), 3095, 2930 and 2878 (CH), 2145 (CN), 1661 (C=O), 1567 (N-H).

Poly(L-isocyanoalanine(2-thiophen-3-yl-ethyl)amide) (PIAT)

Ni^{2+} catalyzed polymerization. In a typical polymerization reaction the desired amount of catalyst ($Ni(ClO_4)_2$ or (*t*-BuNC)$_4$Ni(ClO_4)$_2$) was dissolved in a solution of 5 % (v/v) ethanol in CH_2Cl_2 and added to a stirred solution of IAT in CH_2Cl_2 or TCB in a flask fitted with a $CaCl_2$ tube. After complete consumption of the isocyanide, as concluded by IR spectroscopy, the solution was evaporated to dryness and the polymer redissolved in a minimal amount of CH_2Cl_2. The polymer was then precipitated by dropping this solution into 10 ml of a well-stirred mixture of methanol/water 1:1 (v/v). The product was filtered off and washed with 10 ml of methanol/water 1:1 (v/v). After drying *in vacuo* the polymer was obtained as an orange/brown solid (yields 58–79 %). ^{1}H NMR (300 MHz, $CDCl_3$) δ 7.4–7.1 (br, thiophene H-5), 7.1–6.7 (br, thiophene H-2 and H-4), 4.2–4.0 (br, C*H*(CH_3)), 3.7–3.2 (br, C*H*$_2$CH$_2$-thiophene), 3.0–2.6 (br, C*H*$_2$-thiophene), 1.9–1.0 (br, CHC*H*$_3$) ppm. See Table 1 and Table 2 for further analysis results.

Acid catalyzed polymerization. IAT (120 mg, 0.576 mmol) was dissolved in 5 ml of CH_2Cl_2 and the solution was stirred in a flask equipped with a $CaCl_2$ tube under a N_2 atmosphere. Subsequently, a solution of 1.0 ml of TFA in CH_2Cl_2 (3.3 mg, 0.05 equivalents) was added. After stirring for 5 days TLC and NMR analysis showed that partial conversion into FAT had occurred.

Boc-D-alanyl-L-alanine(2-thiophen-3-yl-ethyl)amide (D,L-BAAT)

BAT was deprotected by dissolving 581 mg (1.95 mmol) of this compound in 20 ml of ethyl acetate saturated with HCl. After stirring for 4 h under an N_2 atmosphere the reaction mixture was evaporated to dryness. The excess of HCl was removed by dissolving the product in 10 ml of *t*-BuOH and subsequent evaporation of the solvent. The residue was redissolved in 10 ml of DMF in a flask equipped with a $CaCl_2$ tube. Consecutively, DMAP (289 mg, 2.37 mmol), HOBT (355 mg, 2.35 mmol) and Boc-D-alanine (442 mg, 2.34 mmol) were added. After addition of DCC (482 mg, 2.34 mmol) the mixture was stirred at room temperature for 21 h. The formed precipitate (DCU) was removed by filtration and the solvent was removed *in vacuo*. The product was purified by column chromatography (silica gel, eluent: 5 % (v/v) MeOH in CH_2Cl_2). A final precipitation in petroleum ether 40–65°C yielded D,L-BAAT as a white crystalline material (304 mg, 57 %). $[\alpha]_D^{20}$ (CH_2Cl_2 *c* 0.5) = -15°.$cm^2.g^{-1}$; ^{1}H NMR (200 MHz, $CDCl_3$) δ 7.25 (q, 1H, thiophene H-5, J = 7.9 Hz, J = 2.7 Hz), 6.99 (br, 1H, N*H*C(O)), 6.96 (d, 1H, thiophene H-2, J = 2.0 Hz), 6.94 (dd, 1H, thiophene H-4, J = 6.1

Hz, J = 1.4 Hz), 6.51 and 4.95 (br, 1H, N*H*C(O)), 4.41 and 4.05 (m, 1H, C(O)C*H*(CH_3)), 3.49 (m, 2H, CH_2NH), 2.85 (t, 2H, CH_2-thiophene, J = 7.2 Hz), 1.45 and 1.35 (d, 3H, CHCH_3, J = 7.2 Hz), 1.34 (d, 3H, CHCH_3, J = 6.8 Hz) ppm; ^{13}C NMR (50 MHz, $CDCl_3$) δ 172.8, 172.0 155.6 (NH*C*(O)), 139.1 (thiophene C-3), 128.2 (thiophene C-4), 126.0(thiophene C-5), 121.5 (thiophene C-2), 80.5 (*C*(CH_3)$_3$), 50.5 and 49.0 (C(O)*C*H(CH_3)), 40.1 (*C*H_2NH), 30.2 (*C*H_2-thiophene), 28.5 ((*C*H_3)$_3$C), 18.1 (CH_3) ppm.

Boc-L-alanyl-L-alanine(2-thiophen-3-yl-ethyl)amide (L,L-BAAT)

Using the same procedure as described for the preparation of D,L-BAAT, L,L-BAAT was obtained in 28 % yield. $[\alpha]_D^{20}$ (CH_2Cl_2 *c* 1.0) = -33°.cm^2.g^{-1}; ^{1}H NMR (300 MHz, $CDCl_3$) δ 7.25 (q, 1H, thiophene H-5, J = 7.8 Hz, J = 2.6 Hz), 7.06 (d, 1H, N*H*C(O), J = 7.0 Hz), 6.97 (d, 1H, thiophene H-2, J = 1.8 Hz), 6.91 (dd, 1H, thiophene H-4, J = 6.0 Hz, J = 1.2 Hz), 6.84 (t, 1H, N*H*C(O), J = 5.7 Hz), 5.34 (d, 1H, N*H*C(O), J = 6.9 Hz), 4.44 and 4.17 (m, 1H, C(O)C*H*(CH_3)), 3.47 (m, 2H, CH_2NH), 2.83 (t, 2H, CH_2-thiophene, J = 6.9 Hz), 1.43 (s, 9H, C(CH_3)$_3$), 1.34 (d, 3H, CHCH_3, J = 7.2 Hz), 1.33 (d, 3H, CHCH_3, J = 6.9 Hz) ppm; ^{13}C NMR (75 MHz, $CDCl_3$) δ 172.5, 171.8 and 155.4 (NH*C*(O)), 138.9 (thiophene C-3), 127.9 (thiophene C-4), 125.6 (thiophene C-5), 121.2 (thiophene C-2), 80.3 (*C*(CH_3)$_3$), 50.6 and 49.1 (C(O)*C*H(CH_3)), 40.3 (*C*H_2NH), 30.3 (*C*H_2-thiophene), 28.6 ((*C*H_3)$_3$C), 18.7 (CH_3) ppm.

***N*-Formyl-D-alanyl-L-alanine(2-thiophen-3-yl-ethyl)amide (D,L-FAAT)**

D,L-BAAT (421 mg, 1.14 mmol) was dissolved in 20 ml of HCl-saturated ethyl acetate and stirred for 2 h. After evaporation to dryness 5 ml of *t*-BuOH was added to the flask in order to remove the excess of HCl and subsequently, the solution was evaporated to dryness again. With TLC no starting material could be detected. The residue (374 mg, 1.22 mmol) was redissolved in ethyl formate (25 ml) and 335 mg (4.93 mmol) sodium formate was added while stirring. After refluxing this mixture for 28 h in a flask equipped with a $CaCl_2$ tube the precipitate was removed by filtration and the solvent was removed *in vacuo*. This resulted in a white solid (161 mg, 44 %). $[\alpha]_D^{20}$ (MeOH *c* 1.1) = -6°.cm^2.g^{-1}; ^{1}H NMR (300 MHz, $CDCl_3$) δ 8.11 (s, 1H, C(O)H), 7.28 (q, 1H, thiophene H-5, J = 8.8 Hz, J = 2.9 Hz), 7.00 (m, 1H, thiophene H-2), 6.98 (dd, 1H, thiophene H-4, J = 6.2 Hz, J = 1.1 Hz), 4.45–4.33 (m, 2H, C(O)C*H*(CH_3)), 3.49 (m, 2H, CH_2NH), 2.85 (t, 2H, CH_2-thiophene, J = 4.5 Hz), 1.40 (d, 3H, CHCH_3, J = 4.6 Hz) and 1.35 (d, 3H, CHCH_3, J = 4.6 Hz) ppm; ^{13}C NMR (75 MHz, $CDCl_3$) δ 174.3 and 173.8 (NH*C*(O)), 163.9 (NH*C*(O)H), 140.0 (thiophene C-3), 129.0 (thiophene C-4), 126.1(thiophene C-5), 122.0 (thiophene C-2), 50.6 and 49.9 (C(O)*C*H(CH_3)), 41.3 (*C*H_2NH), 30.8 (*C*H_2-thiophene), 18.0 and 17.8 (CH_3) ppm; FT-IR (cm^{-1}, ATR) 3281 (NH), 3096, 2970, 2929 and 2874 (CH), 1637 (C=O), 1555 and 1528 (N-H); EI-MS: m/z = 297 [M]$^+$ (calcd: 297.38).

***N*-Formyl-L-alanyl-L-alanine(2-thiophen-3-yl-ethyl)amide (L,L-FAAT)**

In a similar procedure as described for the synthesis of D,L-FAAT, L,L-FAAT was obtained as a white solid in a yield of 88 %. $[\alpha]_D^{20}$ (MeOH *c* 1.7) = -87°.cm^2.g^{-1}; ^{1}H NMR (300 MHz, $CDCl_3$) δ 8.03 (s, 1H, C(O)H), 7.26 (q, 1H, thiophene H-5, J = 7.8, J = 2.7 Hz), 7.04 (m, 1H, thiophene H-2), 6.94 (dd, 1H, thiophene H-4, J = 6 Hz, J = 1.2 Hz), 4.39–4.20 (m, 2H, C(O)C*H*(CH_3)), 3.37 (m, 2H, CH_2NH), 2.80 (t, 2H, CH_2-thiophene, J = 7.2 Hz), 1.34 (d, 3H, CHCH_3, J = 7.2 Hz) and 1.29 (d, 3H, CHCH_3, J = 7.2 Hz) ppm; ^{13}C NMR (75 MHz, $CDCl_3$) δ 174.3 and 173.8 (NH*C*(O)), 163.3 (NH*C*(O)H), 140.3 (thiophene C-3), 128.9 (thiophene C-4), 126.2(thiophene

C-5), 122.0 (thiophene C-2), 50.5 and 49.8 (C(O)*C*H(CH_3)), 41.2 (*C*H_2NH), 30.8 (*C*H_2-thiophene), 18.2 (CH_3) ppm; FT-IR (cm^{-1}, ATR) 3310 and 3263 (NH), 3090, 2984 and 2874 (CH), 1691, 1663 and 1633 (C=O), 1560 and 1529 (N-H).

D-2-Isocyanoalanyl- L-alanine(2-thiophen-3-yl-ethyl)amide) (D,L-IAAT)

Starting from D,L-FAAT, D,L-IAAT was prepared following the same procedure as described for the synthesis of IAT. The product was obtained as a white crystalline material (37 %). $[\alpha]_D^{20}$ (CH_2Cl_2 *c* 4.3) = -17°.cm^2.g^{-1}; ^{1}H NMR (300 MHz, $CDCl_3$) δ 7.29 (q, 1H, thiophene H-5, J = 11.8 Hz, J = 4.6 Hz), 7.22 (br, 1H, N*H*C(O)), 7.01 (m, 1H, thiophene H-2), 6.98 (dd, 1H, thiophene H-4, J = 6.2 Hz, J = 1.5 Hz), 6.32 (br, 1H, N*H*C(O)), 4.42 (m, 1H, C(O)C*H*(CH_3)), 4.26 (q, 1H, C(O)C*H*(CH_3)NC, J = 21.3 Hz, J = 7.3 Hz), 3.53 (m, 2H, C*H*$_2$NH), 2.86 (t, 2H, C*H*$_2$-thiophene, J = 4.6 Hz), 1.62 (d, 3H, CHC*H*$_3$, J = 4.7 Hz), 1.37 (d, 3H, CHC*H*$_3$, J = 4.6 Hz) ppm; ^{13}C NMR (50 MHz, $CDCl_3$) δ 171.5 and 166.2 (NH*C*(O)), 161.1 (N≡C), 138.9 (thiophene C-3), 128.1 (thiophene C-4), 126.2 (thiophene C-5), 121.6 (thiophene C-2), 53.3 and 49.3 (C(O)*C*H(CH_3)), 40.1 (*C*H_2NH), 30.1 (*C*H_2-thiophene), 19.9 and 18.6 (*C*H_3) ppm; FT-IR (cm^{-1}, ATR) 3275 (NH), 3090, 2985 and 2933 (CH), 2142 (CN), 1666 and 1646 (C=O), 1552 (N-H).

L-2-Isocyanoalanyl-L-alanine(2-thiophen-3-yl-ethyl)amide) (L,L-IAAT)

Using the same conditions as described for the preparation of **IAT**, 90 mg (0.30 mmol) of L,L-FAAT was converted into L,L-IAAT in 54 % yield. $[\alpha]_D^{20}$ (CH_2Cl_2 *c* 0.1) = -38°.cm^2. g^{-1}; ^{1}H NMR (300 MHz, $CDCl_3$) δ 7.27 (q, 1H, thiophene H-5, J = 7.8 Hz, J = 3.0 Hz), 6.98 (m, 1H, thiophene H-2), 6.95 (br, 1H, N*H*C(O)), 6.91 (dd, 1H, thiophene H-4, J = 6.3 Hz, J = 1.5 Hz), 5.88 (br, 1H, N*H*C(O)), 4.32 (m, 1H, C(O)C*H*(CH_3)), 4.18 (q, 1H, C(O)C*H*(CH_3)NC, J = 21.3 Hz, J = 7.2 Hz), 3.56 (q, 2H, C*H*$_2$NH, J = 18.9 Hz, J = 6.3 Hz), 2.85 (t, 2H, C*H*$_2$-thiophene, J = 6.6 Hz), 1.63 (d, 3H, CHC*H*$_3$, J = 6.9 Hz), 1.37 (d, 3H, CHC*H*$_3$, J = 7.2 Hz) ppm; ^{13}C NMR (50 MHz, $CDCl_3$) δ 170.9 and 165.7 (NH*C*(O)), 162.1 (N≡C), 138.6 (thiophene C-3), 127.9 (thiophene C-4), 126.2 (thiophene C-5), 121.6 (thiophene C-2), 49.5 and 45.6 (C(O)*C*H(CH_3)), 40.2 (*C*H_2NH), 30.1 (*C*H_2-thiophene), 20.0 and 18.6 (*C*H_3) ppm; FT-IR (cm^{-1}, ATR) 3310 and 3288 (NH), 3090, 2929 and 2849 (CH), 2142 (CN), 1652 (C=O), 1551 and 1532 (N-H).

Poly(D-2-isocyanoalanyl-L-alanine(2-thiophen-3-yl-ethyl)amide) (D,L-PIAAT)

Ni^{2+} catalyzed polymerization. D,L-IAAT (16 mg, 57 μmol) was dissolved in CH_2Cl_2 (5 ml) in a flask equipped with a $CaCl_2$ tube and a stirring bar. To this stirred solution 300 μl of a 2.0 mM $Ni(ClO_4)_2$ solution in CH_2Cl_2/ethanol 94:6 (v/v) (0.020 equiv.) was added. After a few minutes the solution turned light brown. After three days of stirring the solvent was removed *in vacuo*. The residue was redissolved in a minimal amount of CH_2Cl_2 and added drop wise to 10 ml of a well-stirred mixture of methanol/water 1:1 (v/v). The precipitated product was filtrated and washed with 10 ml of methanol/water 1:1 (v/v). After drying *in vacuo* the polymer was obtained as a yellow/orange solid (yield 10 mg, 63 %). ^{1}H NMR (300 MHz, $CDCl_3$) δ 7.4–7.1 (br, thiophene H-5), 7.1–6.7 (br, thiophene H-2 and H-4), 4.7–4.1 (br, C*H*(CH_3)), 3.7–3.2 (br, C*H*$_2$CH$_2$-thiophene), 2.9–2.6 (br, C*H*$_2$-thiophene), 1.8–0.9 (br, CHC*H*$_3$) ppm; FT-IR (cm^{-1}, ATR) 3310 and 3284 (NH), 3096, 2961, 2925 and 2854 (CH), 1742 and 1645 (C=O), 1540 and 1520 (N-H).

Acid catalyzed polymerization. A solution of 21 mg (75 μmol) D,L-IAAT in CH_2Cl_2 (5 ml) was stirred in a flask equipped with a $CaCl_2$ tube while 60 μl of a 25 mM solution of TFA (0.20 equivalents) were added. After stirring over the weekend the solvent was evaporated and the residue redissolved in a minimal amount of CH_2Cl_2. This solution was then added drop wise to 10 ml of a well-stirred mixture of methanol/water 1:1 (v/v). The precipitated product was filtered off and washed with 10 ml methanol/water 1:1 (v/v). After drying *in vacuo*, the polymer was obtained as a yellow/orange solid (< 1.0 mg). As a consequence of the limited quantity of product no full characterization was conducted.

Poly(L-2-isocyanoalanyl-L-alanine(2-thiophen-3-yl-ethyl)amide) (L,L-PIAAT)

The same procedure as described for the polymerization of D,L-IAAT (14 mg, 50 μmol) with $Ni(ClO_4)_2$ was used to prepare L,L-PIAAT, resulting in a slightly yellow solid (yield 10 mg, 70 %). ^{1}H NMR (300 MHz, $CDCl_3$) δ 7.3–7.1 (br, thiophene H-5), 7.1–6.8 (br, thiophene H-2 and H-4), 4.7–4.2 (br, C*H*(CH_3)), 3.6–3.3 (br, C$H_2$$CH_2$-thiophene), 3.0–2.7 (br, CH_2-thiophene), 1.8–0.8 (br, CHCH_3) ppm; FT-IR (cm^{-1}, ATR) 3284 (NH), 3092, 2976, 2931 and 2871 (CH), 1647 (C=O), 1531 (N-H).

2.6 Notes and References

[1] G. McDermott, S. M. Prince, A. A. Freer, A. M. Hawthornewaite-Lawless, M. Z. Papiz, R. J. Gogdell, N. W. Isaacs, *Nature* **1995**, *374*, 517.
[2] W. Kühlbrandt, *Nature* **1995**, *374*, 497.
[3] R. J. M. Nolte, *Chem. Soc. Rev.* **1994**, *23*, 11.
[4] J. J. L. M. Cornelissen, A. E. Rowan, R. J. M. Nolte, N. A. J. M. Sommerdijk, *Chem. Rev.* **2001**, *101*, 4039.
[5] F. Millich, *Chem. Rev.* **1972**, *72*, 101.
[6] W. Drenth, R. J. M. Nolte, *Acc. Chem. Res.* **1979**, *12*, 30.
[7] T. J. Deming, B. Novak, *Macromolecules* **1991**, *24*, 326.
[8] R. J. M. Nolte, *Synthese en isomerisatie van polyisocyaniden*, University of Utrecht, Utrecht, **1973**.
[9] F. Takei, K. Yanai, O. Kiyotaka, S. Takahashi, *Chem. Eur. J.* **2000**, *6*, 983.
[10] N. Hida, F. Takei, K. Onitsuka, K. Shiga, S. Asaoka, T. Iyoda, S. Takahashi, *Angew. Chem. Int. Ed.* **2003**, *42*, 4349.
[11] R. J. M. Nolte, A. J. M. van Beijnen, W. Drenth, *J. Am. Chem. Soc.* **1972**, *96*, 5932.
[12] J. J. L. M. Cornelissen, J. J. J. M. Donners, R. de Gelder, W. S. Graswinckel, G. A. Metselaar, A. E. Rowan, N. A. J. M. Sommerdijk, R. J. M. Nolte, *Science* **2001**, *293*, 676.
[13] P. Samorí, C. Ecker, I. Gössl, P. A. J. de Witte, J. J. L. M. Cornelissen, G. A. Metselaar, M. B. J. Otten, A. E. Rowan, R. J. M. Nolte, J. P. Rabe, *Macromolecules* **2002**, *35*, 5290.
[14] M. D. Yoder, N. T. Keen, F. Yurnak, *Science* **1993**, *260*, 1503.
[15] U. F. Kragten, M. F. M. Roks, R. J. M. Nolte, *J. Chem. Soc., Chem. Commun.* **1985**, 1275.
[16] P. A. J. de Witte, M. Castriciano, J. J. L. M. Cornelissen, L. M. Scolaro, R. J. M. Nolte, A. E. Rowan, *Chem. Eur. J.* **2003**, *9*, 1775.
[17] R. D. McCullough, *Adv. Mater.* **1998**, *10*, 93.
[18] D. Fichou, *Handbook of oligo- and polythiophenes*, Wiley-VCH, Weinheim, **1999**.
[19] J. Roncali, *Chem. Rev.* **1992**, *92*, 711.
[20] M. A. Hempenius, B. M. W. Langeveld-Voss, J. A. E. H. van Haare, R. A. J. Janssen, S. S. Sheiko, J. P. Spatz, M. Möller, E. W. Meijer, *J. Am. Chem. Soc.* **1998**, *120*, 2798.
[21] J. Liu, E. Sheina, T. Kowalewski, R. D. McCullough, *Angew. Chem. Int. Ed.* **2002**, *41*, 329.
[22] A. Gesquiere, M. M. S. Abdel-Mottaleb, S. De Feyter, F. C. De Schryver, F. Schoonbeek, J. van Esch, R. M. Kellogg, B. L. Feringa, A. Calderone, R. Lazzaroni, J. L. Bredas, *Langmuir* **2000**, *16*, 10385.
[23] A. Gesquiere, S. De Feyter, F. C. De Schryver, F. Schoonbeek, J. van Esch, R. M. Kellogg, B. L. Feringa, *Nano Lett.* **2001**, *1*, 201.
[24] N. Sewald, H.-D. Jakubke, *Peptides: Chemistry and Biology*, Wiley-VCH, Weinheim, **2002**.

[25] A. L. Spek, *PLATON. A Crystallographic Tool*, Utrecht University, Utrecht, **2003**.
[26] G.A. Metselaar, publication in preparation.
[27] W. R. Krigbaum, T. Tanaka, G. Brelsford, A. Ciferri, *Macromolecules* **1991**, *24*, 4142.
[28] S. V. Meille, A. Farina, F. Bezziccheri, M. C. Gallazzi, *Adv. Mater.* **1994**, *6*, 848.
[29] J. J. L. M. Cornelissen, *Pure Appl. Chem.* **2002**, *74*, 2021.
[30] J. J. L. M. Cornelissen, W. S. Graswinckel, P. J. H. M. Adams, G. H. Nachtegaal, A. P. M. Kentgens, N. A. J. M. Sommerdijk, R. J. M. Nolte, *J. Polym. Sci. , Part A: Polym. Chem.* **2001**, *39*, 4255.
[31] J. J. L. M. Cornelissen, *Polymers and block copolymers of isocyanopeptides*, Ph.D. thesis, University of Nijmegen, Nijmegen, **2001**.
[32] G.A. Metselaar, publication in preparation.
[33] A. J. M. van Beijnen, R. J. M. Nolte, W. Drenth, A. M. F. Hezemans, P. J. F. M. van de Coolwijk, *Macromolecules* **1980**, *13*, 1386.
[34] A. W. Cooke, K. B. Wagener, *Macromolecules* **1991**, *24*, 1404.
[35] A. J. M. van Beijnen, R. J. M. Nolte, W. Drenth, A. M. F. Hezemans, *Tetrahedron* **1976**, *32*, 2017.
[36] M. Clericuzio, G. Alagona, C. Ghio, P. Salvadori, *J. Am. Chem. Soc.* **1997**, *119*, 1059.
[37] J. J. L. M. Cornelissen, W. S. Graswinckel, A. E. Rowan, N. A. J. M. Sommerdijk, R. J. M. Nolte, *J. Polym. Sci. , Part A: Polym. Chem.* **2003**, *41*, 1725.
[38] J.J.L.M. Cornelissen, personal communication.
[39] A. C. T. North, D. C. Philips, F. S. Mathews, *Acta Crystallogr.* **1968**, *A24*, 351.
[40] R. de Gelder, R. A. G. de Graaff, H. Schenk, *Acta Crystallogr.* **1993**, *A49*, 287.
[41] G. M. Sheldrick, *SHELXL-97. Program for the refinement of crystal structures*, University of Göttingen, Germany, **1997**.
[42] R. W. Stephany, W. Drenth, *Recl. Trav. Chim. Pays-Bas* **1972**, *91*, 1453.
[43] B. F. Crowe, F. F. Nord, *J. Org. Chem.* **1950**, *15*, 81.
[44] J. C. Sheehan, D.-D. H. Yang, *J. Am. Chem. Soc.* **1958**, *80*, 1154.

Chapter 3

Aggregation Behavior of Thiophene-Containing Rigid-Rod Diblock Copolymers Based on Styrene and Isocyanide

3.1 Introduction

In recent years the field of block copolymer self-assembly has expanded considerably, resulting in many exciting discoveries.[1-5] By careful selection of the type of blocks, the assembled architectures and the properties of these copolymers can be readily tuned, making them intriguing systems for academic studies and useful components for industrial applications. If a good solvent is chosen for only one of the blocks phase separation between the two blocks occurs and aggregation can be induced. A large number of parameters influence the aggregation architecture, viz. method of preparation, temperature, solvent, polymer concentration, block type and block length, ratio between the blocks and ion concentrations to name but a few.[2, 6-11] As a consequence of these many parameters, a wide variety of morphologies has been reported for these types of self-assembled macromolecules, ranging from spheres, rods, lamellae, and films, to three-dimensional patterned materials.[2, 12-16] Block copolymers have a great potential to be applied in many areas, e.g. (opto-) electronics and bio-medical materials.[17-19]

Block copolymer vesicles, often referred to as polymersomes, are of particular interest, because they are, from an architectural point of view, synthetic mimics of the naturally occurring cell membranes, yet have a much higher toughness and stability than classic liposomes.[20] As a consequence of this toughness and the ability to load them with synthetic or biological compounds, such as dyes and enzymes, a vast array of functional polymersome spheres can be constructed.[3, 21]

Rod-coil block copolymers, consisting of a flexible and a rigid block, constitute a special class of block copolymers.[4, 12, 22-26] Theoretical studies predict that the self-assembly characteristics of these molecules in selective solvents will differ from coil-coil block copolymers, due to the presence of the rigid blocks. Self-assembly of rod-coil polymers is no longer solely determined by phase separation, but is also affected by the aggregation of the rigid segments into (liquid-)crystalline domains.[27] It has been shown earlier in our group that polyisocyanopeptides can be used as the rigid component in such systems,[28, 29] since they possess a very high persistence length, originating from a well-defined helical β-sheet arrangement of the polymer side chains.[30] Charged diblock copolymers of styrene and L-isocyanoalanyl-L-alanine (PS-PIAA) and of styrene and L-isocyanoalanyl-L-histidine (PS-PIAH) have been prepared and found to self-assemble in water to form a variety of structures such as polymersomes, bilayer filaments and even helical aggregates (Figure 1).[28] In the latter assembly the chirality present in the helical polyisocyanide head group is reflected in the formed hierarchical structure.

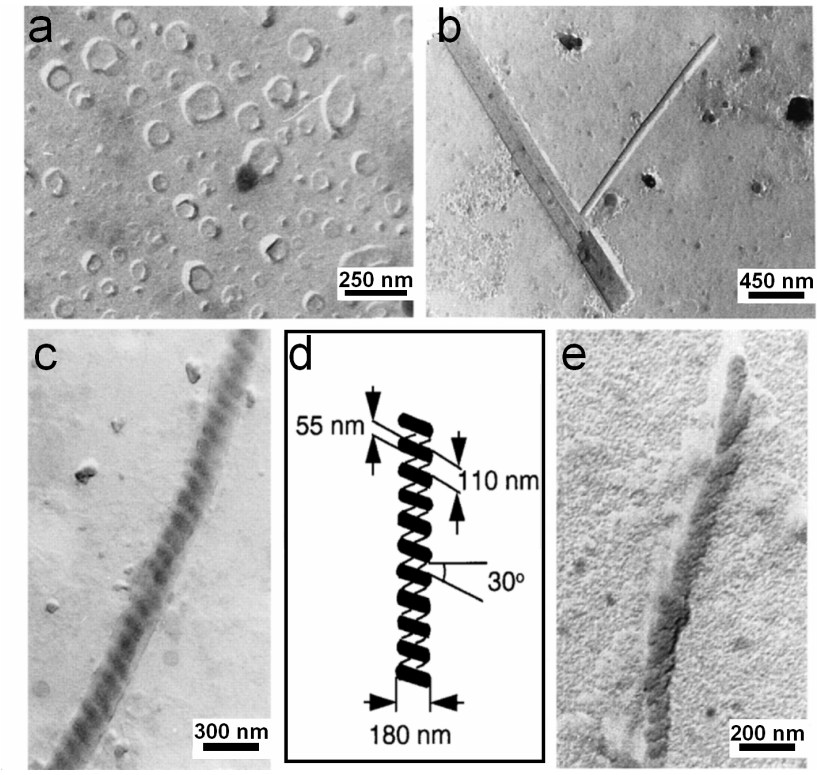

Figure 1. *Self-assembled aggregates formed by PS-PIAA$_{10}$ in a sodium acetate buffer of pH 5.6. a) Transmission electron micrograph of collapsed polymersomes, b) bilayer filaments, c) a left-handed superhelix, d) schematic representation of the helix in c) and e) right-handed superhelix of PS-PIAH$_{15}$ in the same buffer.*[28]

In this chapter we will discuss the synthesis, characterization and aggregation behavior of a new type of isocyanide diblock copolymer, namely polystyrene-*b*-poly(L-isocyanoalanine(2-thiophen-3-yl-ethyl)amide) (PS-PIAT). The rigid polyisocyanide backbone orders the thiophene groups into four offset stacks, which run parallel to the helical polymer backbone (Figure 2). The thiophene functions present in this rod-coil diblock copolymer can in principle be polymerized after aggregation has been induced, in order to form stable polymerized morphologies with possibly interesting applications, e.g. as conducting materials.

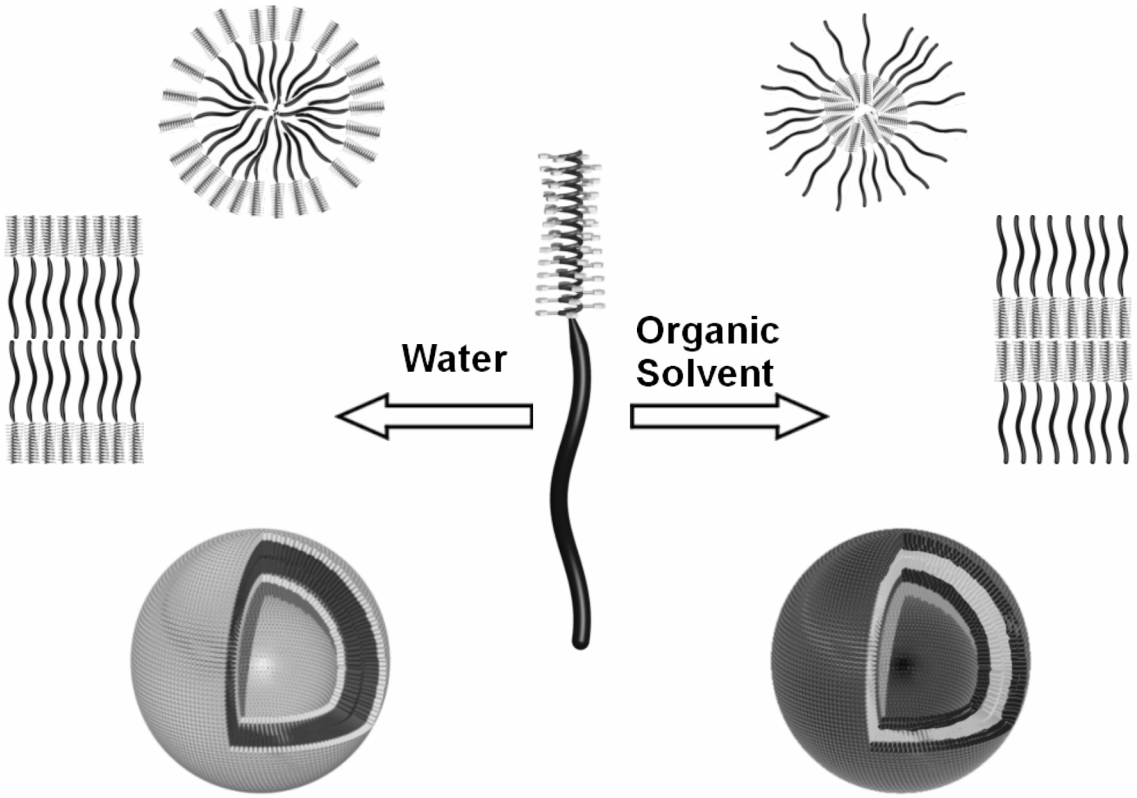

Figure 2. *Schematic representation of the super amphiphile PS-PIAT and the possible architectures it may form in organic solvents and in water, whereby the molecules will be arranged in different ways.*

3.2 Synthesis and Characterization

Isocyanides can be polymerized with Ni(II) based catalysts in combination with the addition of nucleophiles, i.e. alcohols or amines, as initiators.[31] Since the initiating nucleophile also becomes the first residue of the resulting polyisocyanide,[32] block copolymers can be prepared merely by using a polymer with an alcohol or amine end group as

the initiator. The diblock copolymers studied in this chapter are derived from an amine-terminated polystyrene and L-isocyanoalanine(2-thiophen-3-yl-ethyl)amide (IAT) (Scheme 1). The synthesis and polymerization of IAT have been described in Chapter 2. In order to prepare diblock copolymers of this compound an initiator complex was formed by the addition of amine-functionalized polystyrene (n = 40) to an equimolar amount of tetrakis(*t*-butyl isocyanide)nickel(II) perchlorate.[28] Both molecules were prepared by methods previously reported.[33, 34] Under the conditions used, the resulting complex was stable and could be isolated. Addition of the initiator complex to a stirred solution of IAT led to PS-PIAT (Scheme 1). This molecule exhibited an enhanced solubility in chlorinated solvents and tetrahydrofuran (THF) compared to the PIAT homopolymer, which was poorly soluble in all tested solvents.

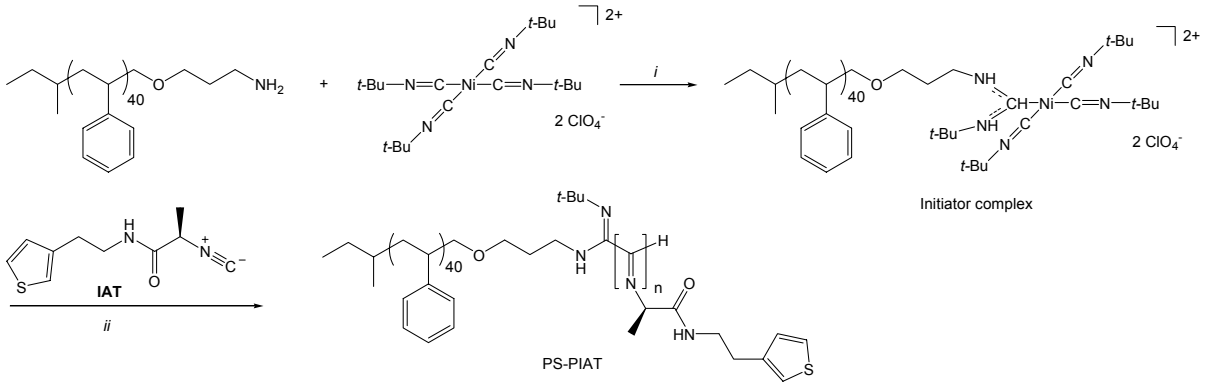

Scheme 1. *Scheme for the synthesis of PS-PIAT; i) CH_2Cl_2; ii) CH_2Cl_2.*

As was described in Chapter 2, IAT was prepared via two different methods. One route resulted in partial racemization of IAT, whilst the other gave optically pure IAT. The diblock copolymer was prepared from IAT synthesized via both these methods, and resulted in either partly racemized or optically pure PS-PIAT. It was observed that the polymerization of optically pure IAT proceeded for approximately one day before all monomers were converted, whilst the polymerization of the racemized IAT monomer needed more than two days to be completed, thus indicating that the polymerization is disturbed by the presence of both enantiomers. This suggests that when both enantiomers of the isocyanide are coordinated to the nickel center during polymerization, the growth of the polymer chain is inhibited, probably as a result of steric hindrance from the alanine methyl group in IAT. Work up of the reaction was performed by first precipitating the polymer in methanol/water (1:1, v/v), followed by filtration and washing with methanol/water (1:1 v/v). After drying *in vacuo* the

product was obtained in moderate to good yields (59–85 %). For both routes characterization by size exclusion chromatography (Sephadex LH20) gave only one band, indicating that no PIAT homopolymer or free polystyrene were present. ^{1}H NMR and IR spectroscopy both revealed the presence of the polystyrene and polyisocyanide blocks. It was therefore concluded that the resulting PS-PIAT diblock copolymers were indeed formed. While the length of the styrene block was fixed at 40 units, the polyisocyanide block length was varied by simply changing the ratio of initiator complex to monomer. For the polymers prepared with epimerized IAT three different ratios of monomer to catalyst were used: 17:1, 50:1 and 100:1. The resulting polymers were observed to be soluble in dichloromethane (CH_2Cl_2), chloroform ($CHCl_3$) and THF. This is in stark contrast to PS-PIAT prepared from optically pure IAT. When a ratio of 50:1 was used a high percentage of the resulting diblock copolymer was found to be insoluble. A ratio of 10:1 monomer to initiator yielded PS-PIAT with a good solubility in all of the three above mentioned solvents. All the prepared polymers were highly colored, varying from pale orange to dark brown/orange. This color is thought to be due to the presence of conjugated imine groups in the backbone of the isocyanide polymer.[35]

The polymers were studied by IR spectroscopy. The amide groups in PS-PIAT displayed shifts to lower wavelengths when compared to the amide functions in IAT. This is indicative of the formation of hydrogen bonds between these groups in the formed diblock copolymers (Table 1). Stronger hydrogen bonding was apparently present in the diblock copolymers prepared with optically pure IAT, as was concluded from the larger shifts to lower wavelengths. This is an indication that PS-PIAT prepared from optically pure IAT has a better defined polyisocyanide block.

Table 1. ***IR spectroscopy data of PS-PIAT prepared with different ratios of IAT/catalyst***[a]

Compound	N-H stretch	C=O stretch	N-H bend
IAT	3282	1661	1567
PS-PIAT$_{17}$[b]	3268	1659	1536
PS-PIAT$_{50}$[b]	3288	1660	1532
PS-PIAT$_{100}$[b]	3285	1655	1540
PS-PIAT$_{10}$[c]	3270	1661	1540
PS-PIAT$_{50}$[c]	3265	1658	1533

[a] The values are given in cm^{-1}. Measured as a solid in KBr. The indices indicate the ratio IAT/initiator complex. [b] Prepared with epimerized IAT. [c] Prepared with optically pure IAT.

A standard method for the determination of the molecular weight of polymers is gel permeation chromatography (GPC). For the homopolymers of IAT, described in Chapter 2, the molecular weights could be measured with the help of this technique. Unfortunately, GPC did not work for the PS-PIAT polymers. The retention times of the polymers were significantly longer than the retention time of the eluent itself. However, the prepared PS-PIAT polymers were built up from relatively short polyisocyanides. It is not clear, therefore, why GPC chromatograms could be obtained from the PIAT homopolymers, as described in Chapter 2, but not from the diblock copolymers.

Another method to estimate the polymer length is by ^{1}H NMR, namely by measuring the ratios of the integrals of both the polystyrene and polyisocyanide blocks. The number average molecular weight (M_n) of the used polystyrene block in PS-PIAT was already known and could therefore be used to calibrate the integrals.[36] The M_n of PS-PIAT was determined by comparing the integrals of the tertiary protons (I) in the polystyrene block with those of the secondary protons (II) on the carbon atom next to the thiophene group of PIAT (Figure 3, Table 2). Although integration is not a precise method of measurement, the obtained values can give an approximate guide to the M_n.

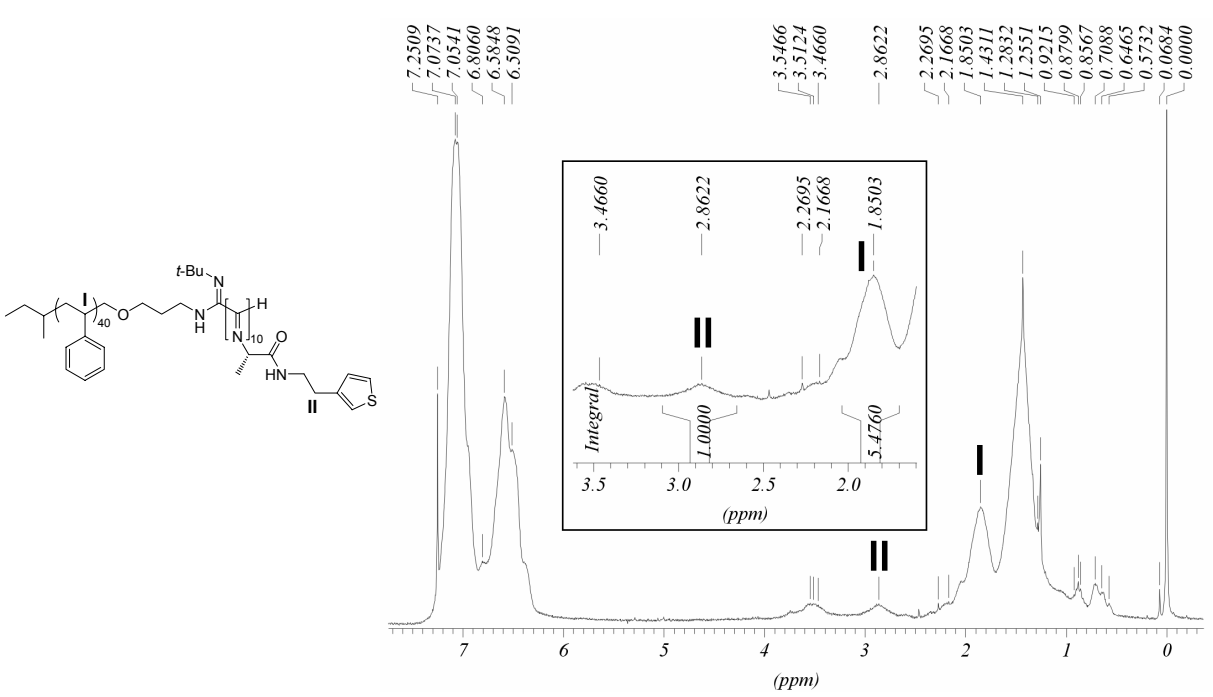

Figure 3. *^{1}H NMR spectrum of PS-PIAT$_{10}$ (structure given on the left) showing the integrals of tertiary protons (I) in the polystyrene block and the protons next to the thiophene group of PIAT (II). The inset shows an expanded part of the spectrum.*

Table 2. ***Molecular weights of different batches of PS-PIAT determined by ^1H NMR***

Polymer[a]	IAT units[b]	M_n[b]
PS-PIAT$_{17}$[c]	18	8.1×10^3
PS-PIAT$_{50}$[c]	31	11×10^3
PS-PIAT$_{100}$[c]	> 40	$> 13\times10^3$
PS-PIAT$_{10}$[d]	3.7	5.2×10^3

[a] The catalyst used was the initiator complex shown in Scheme 1. [b] The estimated error is 25 %. [c] Prepared with epimerized IAT. [d] Prepared with optically pure IAT.

As expected, upon increasing the ratio IAT/initiator complex, the M_n of PS-PIAT also increases (Table 2). Due to the broadening of the peaks, some signals were overlapping. The error in the determination of M_n was therefore estimated to be circa 25 %.

The polymers were further characterized by CD spectroscopy. The results are shown in Figure 4.

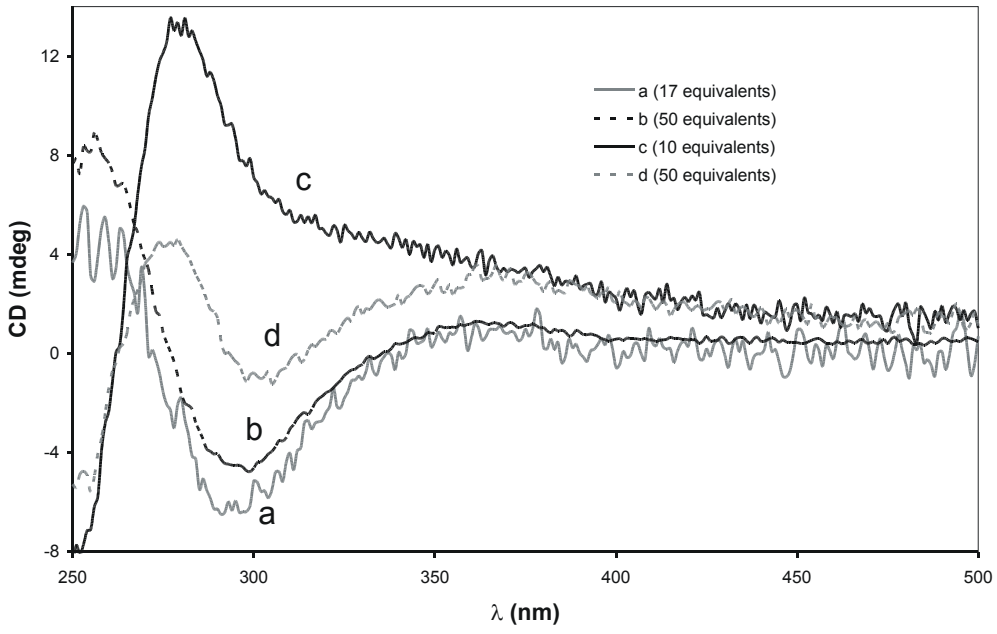

Figure 4. *Typical CD spectra of PS-PIAT in CH_2Cl_2, synthesized with epimerized (a and b) and optically pure IAT (c and d). The IAT/initiator complex ratio is shown in brackets. It should be noted that for d, much of the resulting polymer was insoluble.*

In the case of the optically pure PS-PIAT$_{50}$ the CD spectrum could only be recorded for the soluble part of the product; its spectrum, therefore, is only representative for the lower molecular weight fractions of this polymer. The short PS-PIAT$_{10}$ did not give a negative CD effect at 300 nm, which is probably the result of the fact that its polyisocyanide block length is not long enough to form a helix. The CD spectra revealed that the positions of the signals of the racemized polymers were shifted to lower wavelengths compared to those of the optically pure PS-PIAT$_{50}$. The reason for these shifts may be related to the differences in hydrogen bonding strength within the studied polyisocyanides. The racemized PS-PIAT molecules probably have less well-defined hydrogen bonding arrays, in contrast to the optically pure PS-PIAT molecules, as was also concluded from the IR spectroscopy measurements (Table 1). This results in a difference in the conformation of the polyisocyanide backbone, with the optically pure polymers likely having a better defined helical structure.

In Chapter 2 it was concluded that the PIAT homopolymers were fluorescent due to the presence of conjugated imine bonds in the polymer backbone. Clericuzio *et al.* have predicted that the polyisocyanide backbone can be arranged in such a way that conjugation between the imine bonds becomes possible.[35] The existence of conjugated imine bonds in the PS-PIAT block copolymers is reflected in the color of the polymers, which varied from pale orange to dark orange/brown. In the absorption spectrum of racemized PS-PIAT$_{50}$ (solid line in Figure 5) no significant absorption peaks could be observed.

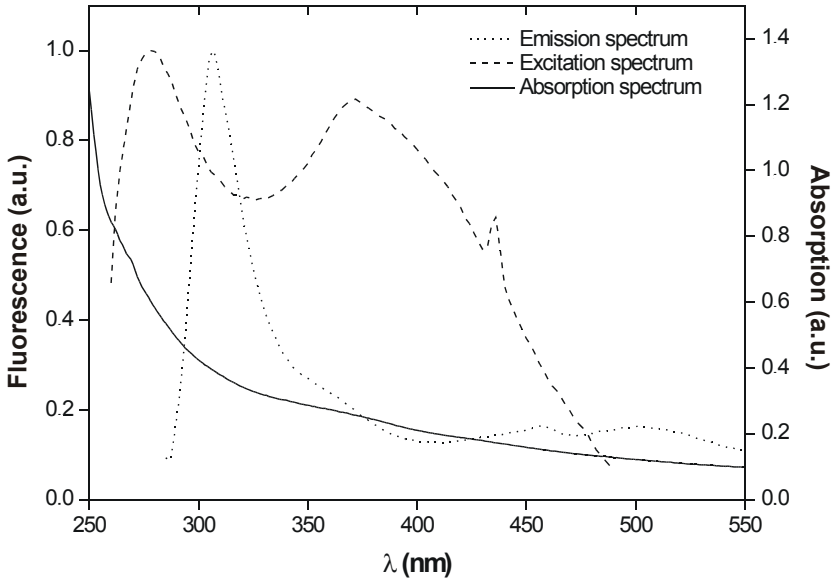

Figure 5. *Absorption, fluorescence emission and fluorescence excitation spectra of racemized PS-PIAT$_{50}$ in THF. The emission spectrum was recorded using a $\lambda_{exc.}$ of 285 nm; the emission wavelength ($\lambda_{em.}$) in the excitation spectrum was 500 nm.*

When, however, an emission wavelength ($\lambda_{exc.}$) of 500 nm was used to record the excitation spectrum, three peaks could be seen, viz. at 280, 372 and 436 nm. Normally, the absorption and excitation spectra are well comparable. The peak at 436 nm is likely the result of Raman scattering. This phenomenon produces scattered photons that differ in frequency from the radiation source and the difference is related to vibrational and/or rotational properties of the molecules from which the scattering occurs.[37] The peaks at 280 nm and 372 nm are thought to arise from the n–π* transitions of the carbonyl and imine groups, respectively. Monomeric thiophene groups normally do not show any fluorescence. When the polymer was excited at 280 nm, a strong fluorescence emission was observed at 307 nm and weaker bands at 457 and 501 nm, originating from the imine groups. When $\lambda_{exc.}$ was varied the positions of these peaks shifted, which was the result of the absence of discrete chromophores, due to the spread in conjugation length of the imine groups, various emission peaks could be observed.

3.3 Aggregation Behavior

3.3.1 Aggregates in organic solvents

PS-PIAT possesses amphiphilic behavior, as a result of a difference in polarity of its two blocks. It can be expected, therefore, that this macromolecule forms aggregates depending on the solvent used. $CHCl_3$ was chosen, because the PIAT block is known to have a low solubility in this solvent (Chapter 2), whilst the polystyrene block solubility in this solvent is very good. PS-$PIAT_{50}$, prepared from epimerized IAT, was added to $CHCl_3$ and shaken for several minutes until all the material had dissolved. Transmission electron microscopy (TEM) studies on this solution revealed the presence of vesicular aggregates. Upon preparation for electron microscopy the spherical shape of the polymersomes was not retained, as could be concluded from the disk-shaped structures that were visible after platinum shadowing of the TEM samples (Figure 6). The observed circular structures, upon closer examination, appeared to have an inner wrinkled surface, which was thought to be the collapsed polymersome membrane (Figure 6, inset). In contrast, no such membrane-like structure was observed outside the circular structures, further confirming this hypothesis.

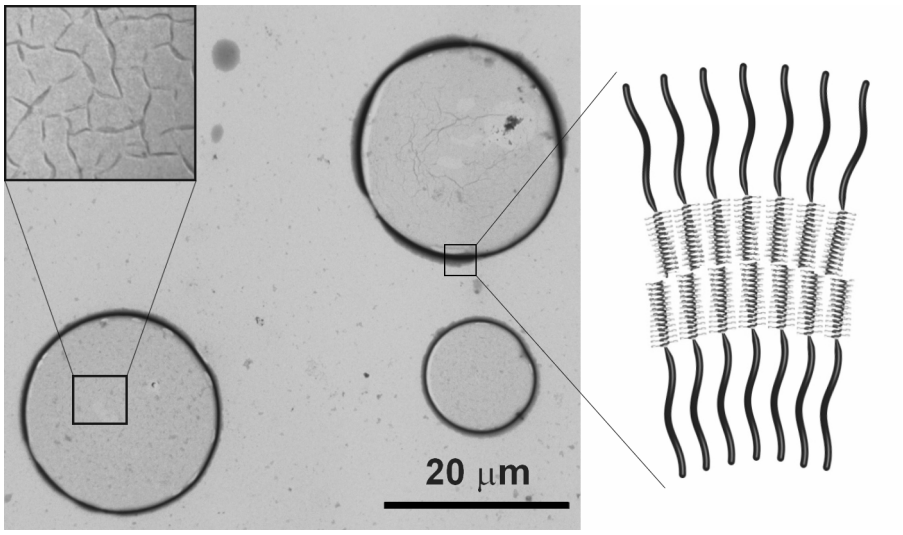

Figure 6. *Left: TEM micrograph of dried polymersomes of PS-PIAT$_{50}$ prepared in CHCl$_3$, the inset shows the wrinkled film, which is only seen inside the area of the collapsed polymersome. Right: schematic representation of the polymersome membrane, with polystyrene tails on the outside and inside surfaces.*

Aggregation of the diblock copolymer molecules is driven by the poor solubility in $CHCl_3$ of the polyisocyanide block of PS-PIAT$_{50}$, which prefers to aggregate. The formed polymersomes were found to have a relatively high polydispersity, with diameters varying between 2 and 22 μm, and an average diameter of 7 μm, as determined from statistical studies of numerous TEM micrographs. The average membrane thickness was measured to be 27±5 nm, which is approximately twice the length of a single, stretched, PS-PIAT$_{50}$ molecule. The length of the polystyrene block when completely extended is estimated to be ca. 10 nm and the polyisocyanide block, which is ca. 31 units long (see Table 2), has an estimated length of 3.1 nm. This results in a maximum chain length for PS-PIAT$_{50}$ of 13 nm. We therefore tentatively propose that the polymersome membrane is composed of a bilayer of molecules with the polyisocyanide blocks located in the center of the membrane and the polystyrene blocks directed towards the solvent (Figure 6, right).

Aggregates of PS-PIAT$_{10}$ were also prepared in ethyl acetate, using the injection method,[38] since the direct dissolving route, as described for $CHCl_3$, did not give any well-defined aggregates. A 1.0 mg.ml^{-1} THF solution of the polymer was injected into ethyl acetate, with the resulting dispersion having a final ethyl acetate/THF ratio of 5:2 (v/v). THF is a good solvent for both blocks and therefore suitable to inject the amphiphilic polymers into a poor solvent. TEM studies of the resulting dispersion revealed many circular aggregates.

These assembled rings had a low transmission and an interior of higher transmission, indicating that the observed structures were also collapsed polymersomes (Figure 7).

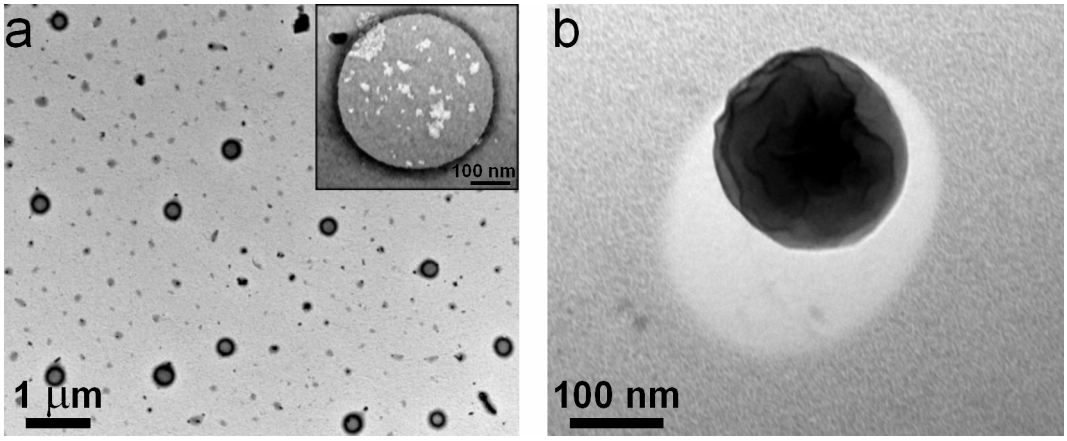

Figure 7. *Aggregates preparared by injection of a THF solution of PS-PIAT$_{10}$ into ethyl acetate. a) Circular aggregates with an average diameter of 223 nm. The inset shows an aggregate which was irradiated for several minutes by the electron beam of the TEM. b) Pt shadowing of the grids highlights the vesicular architecture of the aggregates.*

It was often seen that the aggregates shrunk when placed in the focus of the electron beam. Upon irradiation by the beam of the TEM for several minutes, the material on the inside of the aggregates was observed to be damaged by the high energy of the penetrating electrons (Figure 7 a, inset). Pt shadowed grids showed that all shrunken particles had a spherical shadow, proving that they were indeed spherical in nature, viz. polymersomes. The size distribution of the polymersome diameter was relatively narrow, with diameters ranging from 170 to 350 nm and an average diameter of 223 nm.

Dynamic light scattering (DLS) is a suitable technique to determine the particle size distribution in dispersions and colloids.[39] When a beam of light passes through a dispersion, the particles or droplets scatter some of the light in all directions. When the particles are very small compared to the wavelength of the light, the intensity of the scattered light is uniform in all directions (Rayleigh scattering); for larger particles (above 250 nm diameter), the intensity is angle dependent (Mie scattering). If the light is coherent and monochromatic, as from a laser for example, it is possible to observe time-dependent fluctuations in the scattered intensity using a suitable detector such as a photomultiplier capable of operating in the photon counting mode. These fluctuations arise from the fact that the particles are small enough to undergo random thermal (Brownian) motion and the distance between them is therefore constantly varying. Constructive and destructive interference of light scattered by neighboring

particles within the illuminated zone gives rise to the intensity fluctuation at the detector plane which, as it arises from particle motion, contains information about this motion. Analysis of the time dependence of the intensity fluctuation can therefore yield the diffusion coefficient of the particles from which, via the Stokes-Einstein equation, knowing the viscosity of the medium, the hydrodynamic radius or diameter of the particles can be calculated.[39]

Dynamic light scattering experiments carried out with the prepared dispersion of PS-$PIAT_{10}$ in ethyl acetate also confirmed the presence of well-defined aggregates. They were shown to have an average hydrodynamic radius of 198 nm (Figure 8).

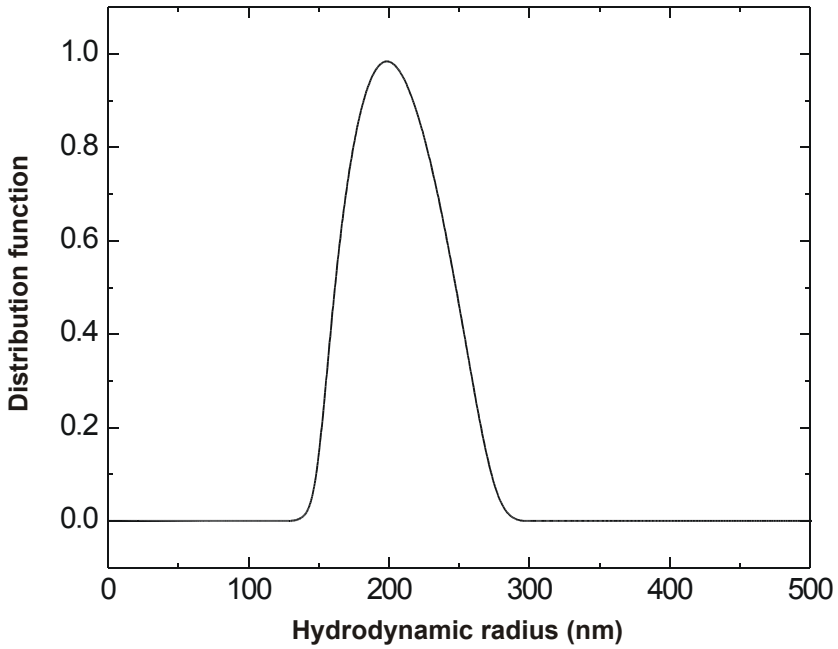

Figure 8. *DLS experiments on PS-$PIAT_{10}$ polymersomes formed in ethyl acetate. The average diameter of the aggregates is 198 nm.*

Aggregates were also prepared in toluene, but in this solvent no defined assemblies could be observed. This is thought to be a result of the fact that toluene solubilizes both blocks, therefore no phase separation will occur.

3.3.2 Aggregates in aqueous solutions, prepared using the injection method

An ideal technique for inducing aggregate formation in aqueous solutions is the injection method.[38] A 1.0 $mg.ml^{-1}$ solution of PS-$PIAT_n$ in THF was injected into ultra pure water, until a final water to THF ratio of 5:1 (v/v) was achieved. For all four polymer batches

the dispersions became immediately turbid and the resulting assemblies were studied by transmission electron microscopy (TEM, Figure 9).

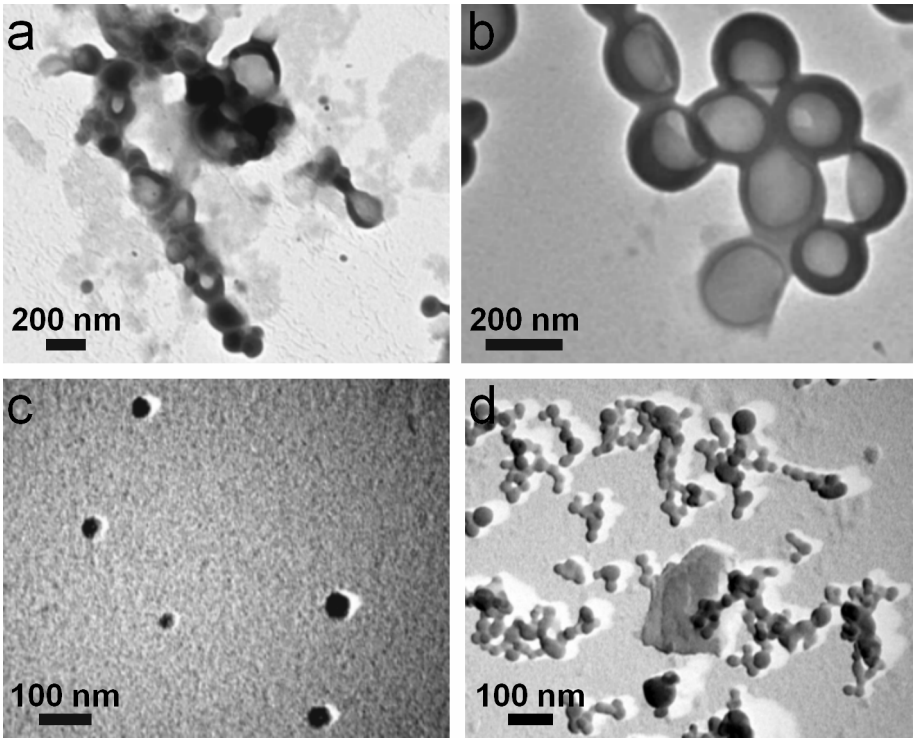

Figure 9. *TEM micrographs of freshly prepared dispersions of PS-PIAT$_n$ in water/THF (5:1, v/v): a) PS-PIAT$_{17}$, b) PS-PIAT$_{50}$, c) PS-PIAT$_{100}$ (all prepared with epimerized IAT), and d) PS-PIAT$_{10}$ (prepared with enantiomerically pure IAT). Pt shadowing was applied to the samples shown in c) and d).*

A range of morphologies could be observed for these macromolecular amphiphiles directly after injection. Both PS-PIAT$_{17}$ and PS-PIAT$_{50}$ formed vesicle-like structures (Figure 9, a and b). The polymersomes formed by the latter polymer appeared to be more stable and better defined than the polymersomes formed by the former polymer, which were also more disperse in size. From the analysis of 25 micrographs an average diameter (D) of 150 nm was calculated for PS-PIAT$_{17}$ and 80 nm for PS-PIAT$_{50}$. Studies on a PS-PIAT$_{100}$ dispersion showed that this polymer formed spherical structures with an average diameter of 35 nm (Figure 9 c). Based on the length of this macromolecule (>14 nm), it is postulated that the aggregates are micellar in nature. All these samples were prepared from epimerized IAT. In contrast, samples of PS-PIAT$_{10}$, prepared from enantiomerically pure IAT, showed the co-existence of spherical aggregates and multilayer assemblies (Figure 9 d). The average diameter of the spherical aggregates was 32 nm. When PS-PIAT$_{10}$ is completely extended, the

length of the molecule is 11 nm. If the observed spherical aggregates were micellar in nature, they probably would have been smaller than 22 nm and less disperse in size. It is more likely, therefore, that these aggregates are solid spheres. When amine-functionalized polystyrene was dispersed from DMF into pure water, the same type of spheres were formed.[40]

The aggregates of PS-PIAT$_{50}$ prepared from epimerized IAT were further examined by cryogenic scanning electron microscopy (cryo-SEM) and SEM (Figure 10).

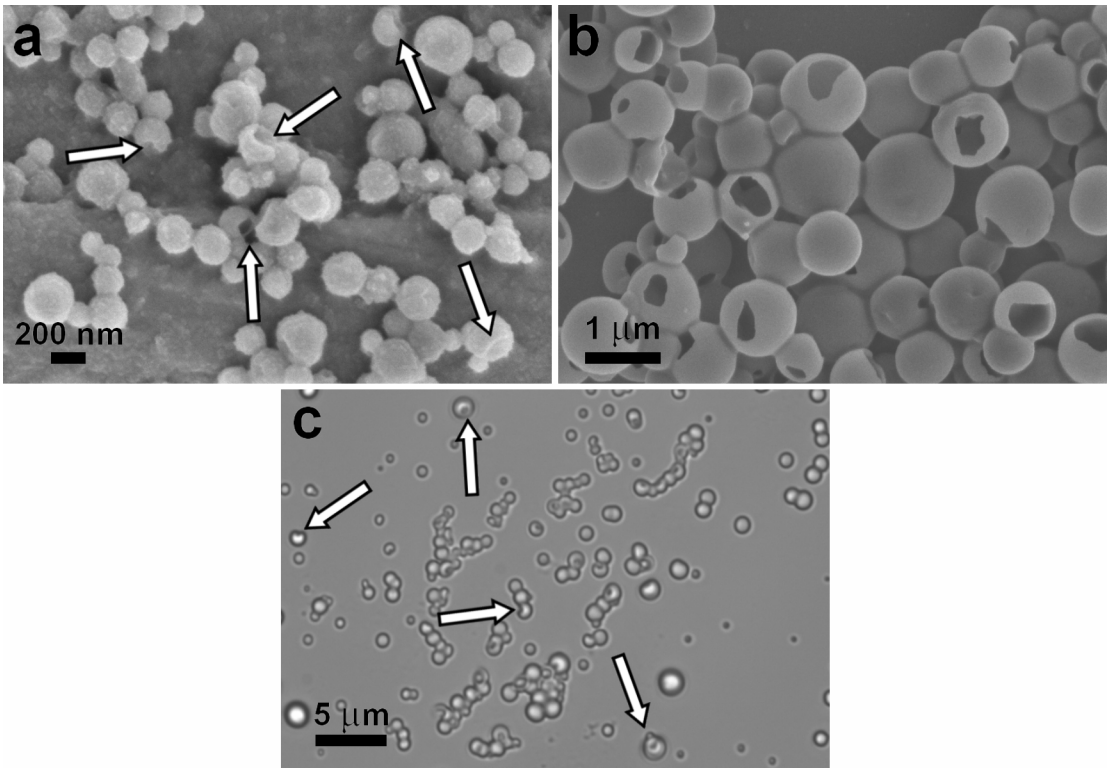

Figure 10. *a) Cryo-SEM and b) SEM micrographs of PS-PIAT$_{50}$ polymersomes freshly prepared by the injection method in an aqueous mixture of water/THF (5:1, v/v). c) Light micrograph of this sample after two days. The arrows point to several polymersomes with holes in their membranes.*

Both techniques showed the presence of aggregates that contained holes, revealing their hollow interior, thus confirming the vesicular nature of the architectures. It was not possible to cleave a polymersome by cryo-SEM, a standard procedure to obtain information about the membrane structure of liposomes, e.g. lamellarity. This indicated that the membranes were too stable and too rigid to allow their splitting. Several explanations can be given for the observed holes in the membranes: (*i*) a drying-in effect, (*ii*) an artifact resulting from the high vacuum in the microscope,[41] and (*iii*) an effect which is related to the process of polymersome formation.[5] The first two explanations can be excluded, because

polymersomes with holes were also observed by cryo-SEM (Figure 10 a); using this technique any change in aggregate morphology is prevented due to the deeply frozen state of the aggregates. Interestingly, using a light microscope at atmospheric pressure polymersomes with similar defects were clearly visible (Figure 10 c). The most likely explanation is that polymersomes are formed when very large bilayer sheets, having a low bending energy and a high surface tension, close to form a vesicle (Figure 11).[5] If the process of polymersome formation is stopped before completion, for instance by removal of the solvent, aggregates possessing holes remain.

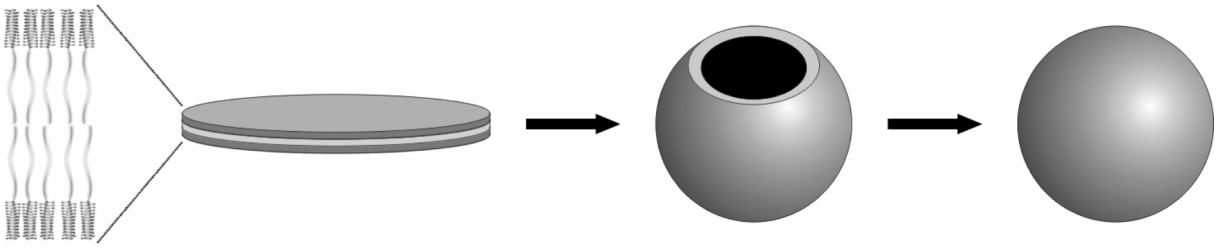

Figure 11. *Schematic illustration of the closure of membranes during the process of polymersome formation.*

Inclusion experiments with the water-soluble fluorescence probe ethidium bromide, followed by size exclusion chromatography using Sephadex, ultimately confirmed that the spherical particles of PS-PIAT$_{50}$ were indeed polymersomes. Two fractions containing the dye, with a large difference in retention time (3 h vs. 50 h), could be collected from the column. The faster running fraction was the ethidium bromide encapsulated in the polymersomes and the slower fraction the free dye. Fluorescence microscopy studies on polymersomes filled with ethidium bromide and of polymersomes filled with methylene blue, after dialysis (Figure 12), also proved that polymersomes were formed. The empty polymersomes were observed to fluoresce as well, but only at the membranes, whilst the polymersomes filled with the dyes were observed to fully fluoresce. The origin of the fluorescence of PS-PIAT$_{50}$ was previously discussed in paragraph 3.2 and it is probably the consequence of the presence of conjugated imine bonds in the polymer backbone. It is noteworthy that the encapsulation of a dye also influences the aggregate formation; in the presence of the dye smaller polymersomes were formed with an average diameter of 410 nm.

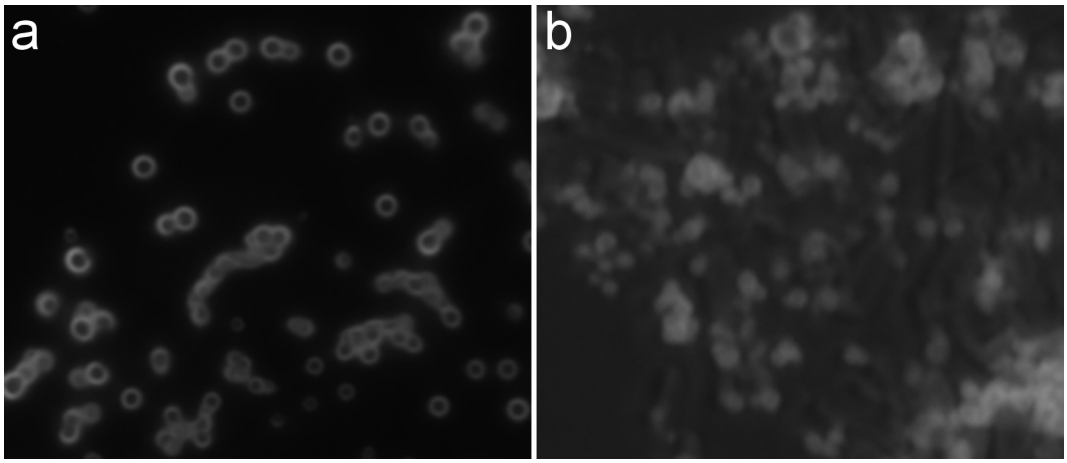

Figure 12. *Fluorescence images ($\lambda_{exc.}$ of 488 nm) of PS-PIAT$_{50}$ after two days, a) without and b) with methylene blue encapsulated. The widths of images a) and b) correspond to 25 μm and 14 μm, respectively.*

The polymersomes of PS-PIAT$_{50}$ formed in water retained their shape even after drying. They must have, therefore, a much higher rigidity than the PS-PIAT$_{50}$ polymersomes formed in $CHCl_3$. This increased stability may be the result of a different architecture of the polymersome membrane in water when compared to $CHCl_3$ (see Figure 2). In pure water, or when only a small amount of organic solvent is present, the polystyrene blocks are not dissolved and exist below their glass transition temperature (T_g), inhibiting any reorganization. Consequently, upon evaporation of the water the polymersomes preserve their shape. In $CHCl_3$, on the other hand, the polystyrene blocks are in direct contact with the solvent, which gives them a high degree of flexibility, allowing the polymersomes to collapse when the solvent evaporates.

From the SEM micrograph in Figure 13, a membrane thickness of 30±10 nm could be determined, which roughly corresponds to twice the length of an extended PS-PIAT$_{50}$ molecule. The most likely membrane structure of the polymersomes in water is thought to be a bilayer of PS-PIAT$_{50}$ molecules in which the polystyrene blocks are pointing towards the center of the membrane and the polyisocyanide blocks towards the solvent (Figure 13, right). However, it can be seen by TEM that the membrane thickness is not completely uniform and more studies are therefore needed to confirm the bilayer arrangement. X-ray diffraction studies were performed on the PS-PIAT$_{50}$ polymersomes, but these unfortunately did not reveal a defined packing between the molecules.

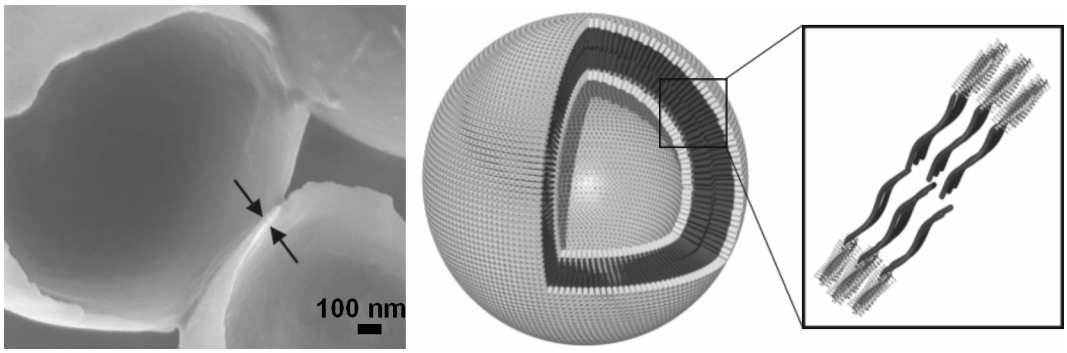

Figure 13. *Left: SEM micrograph of a close up of the polymersome membrane of PS-PIAT$_{50}$, revealing a thickness of 30±10 nm; middle: schematic representation of a bilayer polymersome; right: schematic representation of the membrane structure with isocyanide blocks at the surface.*

An absorption spectrum of the polymersomes, either in dispersion or dried on a glass surface could not be obtained, probably due to scattering phenomena. It was possible, however, to measure the CD spectrum of a dispersion of PS-PIAT$_{50}$ polymersomes in water/THF (Figure 14 a).

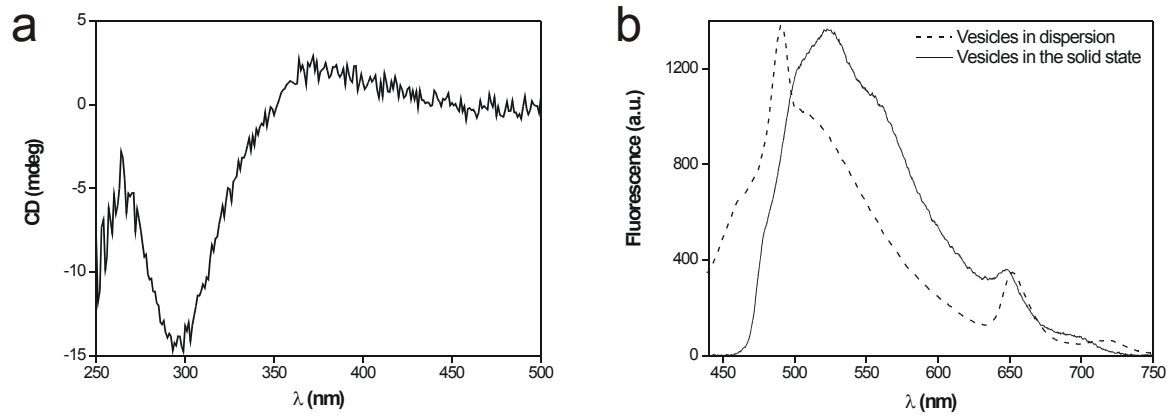

Figure 14. a) *CD spectrum of PS-PIAT$_{50}$ polymersomes in water/THF (5:1, v/v) and b) fluorescence spectra ($\lambda_{exc.}$ of 420 nm) of PS-PIAT$_{50}$ polymersomes dried on glass and in dispersion.*

The CD spectrum of a dispersion of PS-PIAT$_{50}$ in water/THF (5:1, v/v) was similar to the CD spectrum of the diblock copolymer in CH_2Cl_2 (Figure 4), showing that the helical arrangement of the polyisocyanide backbone remained unaltered in the two solvents. Fluorescence spectra of the polymersomes could be recorded both in dispersion and dried on a glass plate (Figure 14 b). In Figure 12 a) it was already shown that the polymersomes

displayed fluorescence in the solid state. At a $\lambda_{exc.}$ of 420 nm the observed maximum $\lambda_{em.}$ was 525 nm for the polymersomes in the solid state and 492 nm for the polymersomes in dispersion. In both spectra a peak at 650 nm, caused by Raman scattering, could be observed. The observed peaks at wavelengths below 600 nm are probably due to the presence of conjugated imine groups.

The polymersomes of PS-PIAT$_{50}$ formed in water/THF (5:1, v/v), were found to fuse upon standing, yielding polymersomes of approximately 20 times larger size. Membrane fusion is known to occur for natural, closed membrane systems, i.e. cells, and is of great importance for many life processes.[42] Fusion of polymersomes of block copolymers has also been reported before,[43, 44] but the increase in size upon fusion was not as dramatic as seen for the polymersomes of PS-PIAT$_{50}$. Eisenberg *et al.* induced fusion of polymersomes by increasing the amount of water in their solvent mixture. In the case of PS-PIAT$_{50}$ the polymersomes were found to fuse without any external stimuli. Directly after preparation, the average polymersome diameter amounted to 80 nm, but within a few hours, larger polymersomes could be observed. After 50 hours the fusion process was found to be complete and only large polymersomes, with an average diameter of 1.5 μm, could be observed (Figure 15).

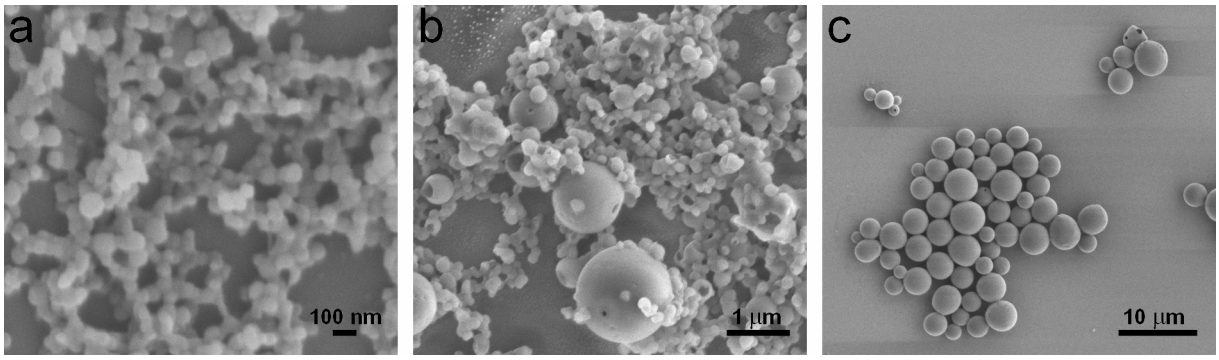

Figure 15. *Scanning electron micrographs of PS-PIAT$_{50}$ polymersomes at increasing times in dispersion. a) Directly after preparation of the dispersion, b) after being in dispersion for 19 h and c) after 50 h.*

The growth curve of the polymersomes as a function of time is shown in Figure 16. The increase in polymersome diameter was very slow in the first 15 h. After this initiation period a sharp increase was observed, which ended 10 h later. No further increase was observed after 50 h.

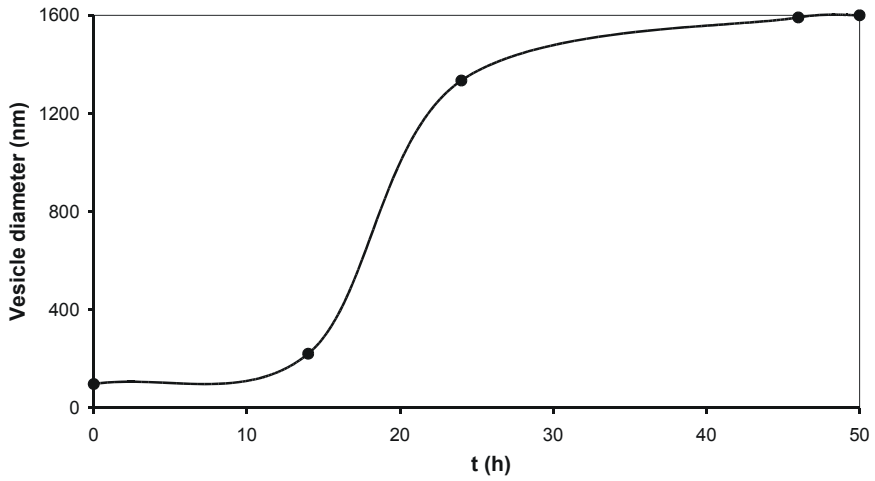

Figure 16. *Plot of the polymersome diameter vs. time of PS-PIAT$_{50}$ polymersomes in water/THF (5:1, v/v).*

These types of fusion processes are known to be driven by (*i*) the high membrane curvature energy of the initially formed vesicles, which causes strain in the amphiphiles, and (*ii*) a large number of defects in the vesicle membrane.[45] By fusing into larger vesicles, the curvature energy can be decreased, leading to a thermodynamically more stable state for the particles.[46] A factor that helps the fusion process is the flexibility of the polystyrene block, which is the result of the presence of THF, allowing the polymeric amphiphiles to reorganize. Dialysis against ultra pure water of the PS-PIAT$_{50}$ polymersomes prepared in water/THF directly after preparation, which removed the THF, showed that the polymersomes remained small. In addition, many polymersomes could be seen that were in an intermediate stage of fusion, which indicated that the increase in polymersome diameter was truly a fusion process and was not due to Ostwald ripening (Figure 17).

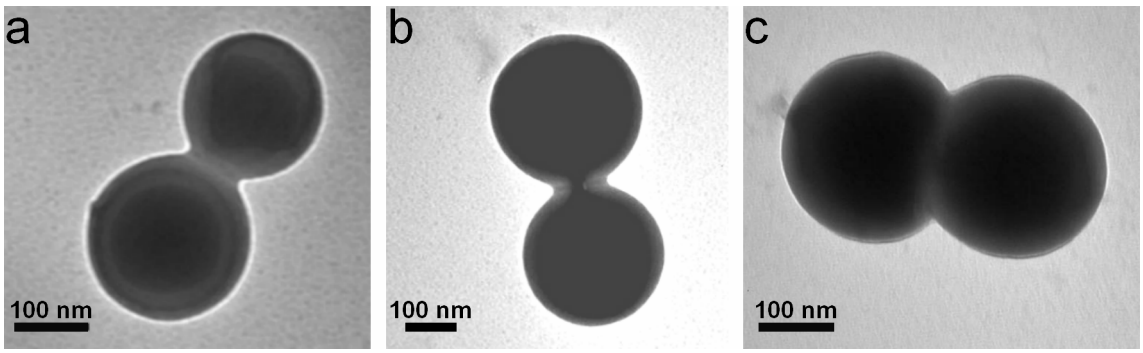

Figure 17. *PS-PIAT$_{50}$ polymersomes trapped in intermediate stages of the fusion process. a) Polymersomes in an early stage, b) creation of a fusion pore between the polymersomes and c) almost completely fused polymersomes.*

The formation of a fusion pore between two fusing polymersomes, also known as stalk formation, was also observed (Figure 17 b). This type of geometry is predicted in the stalk mechanism, and has often been predicted for the fusion of liposomes.[47] The timescale of amphiphile reorganization in these polymer based membranes is several orders of magnitude slower than in liposomes and this allows the intermediate stages of fusion to be observed.[48]

For the optically pure PS-PIAT$_{10}$ changes in the dimensions of the aggregates were also seen when a dispersion of this diblock copolymer was followed in time. On standing larger spheres were observed and their average diameter increased from 32 nm directly after formation to 119 nm after four days. It appeared that there were two populations of spherical aggregates for this diblock copolymer: small spheres with a diameter around 100 nm and large spheres with an average diameter around 500 nm, which had a very low transmission, making it difficult to determine if they had a hollow interior. Inclusion experiments, in which fluorescently labeled enzymes were encapsulated, could demonstrate that these large spheres were indeed hollow (see Chapter 5 for further details). After two weeks the smaller spheres were still by far the most abundant species (Figure 18).

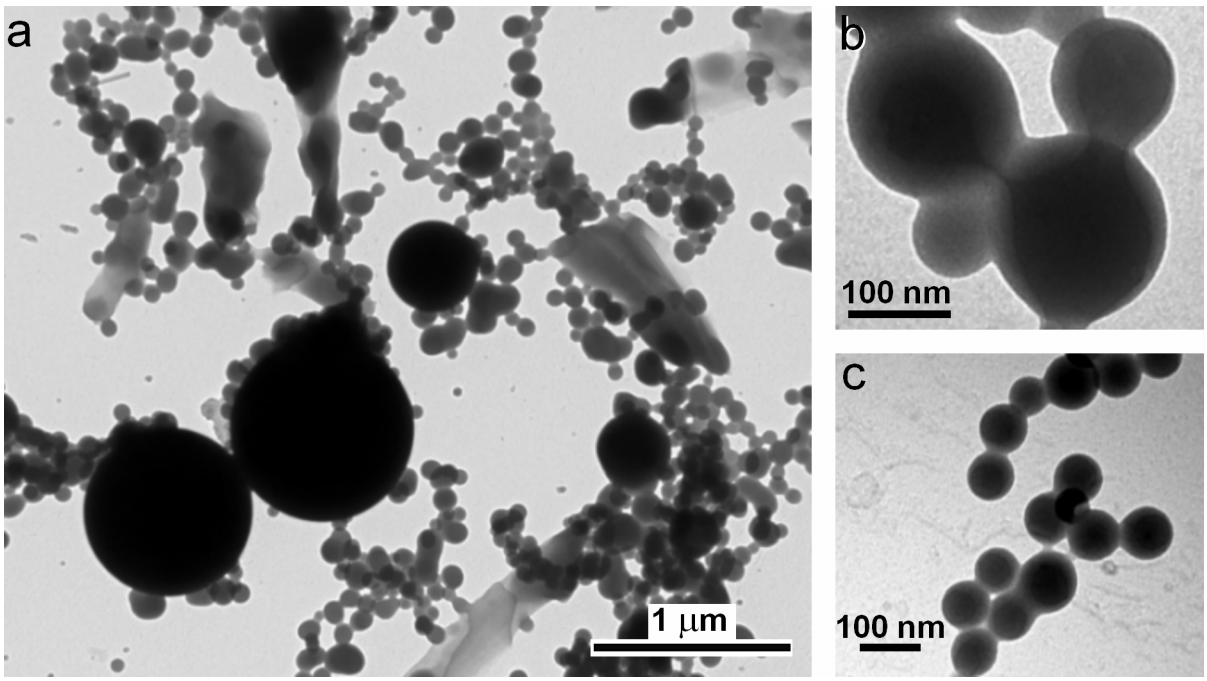

Figure 18. *a) Large spherical aggregates present in dispersions of PS-PIAT$_{10}$ after standing at room temperature (the micrograph is of an eight days old dispersion); b) and c) are micrographs of the same batch at higher magnification. In b) a channel is visible between two spheres.*

A complete disappearance of the small spherical aggregates, however, was not observed. Dispersions of PS-PIAT$_{10}$ started to precipitate already after a few days and complete precipitation took place in less than three weeks, whilst dispersions of PS-PIAT$_{50}$ remained stable and in solution for many months. The multilayer films that were observed immediately after preparation of the dispersion did not disappear in time, nor did their dimensions change significantly. The differences in aggregation behavior between these two amphiphiles seemed to be the result of a difference in the definition of the polyisocyanide blocks. In Chapter 2 it was already concluded that optically pure PIAT has a better defined backbone than racemized PIAT. The packing of PS-PIAT in a membrane will also be affected by this difference in definition. Optically pure PS-PIAT$_{10}$ can probably adopt a more crystalline-type of packing, whereas the more flexible racemized PS-PIAT$_{50}$ will be less densely packed in the membrane.

To obtain more insight in the aggregation behavior of racemized PS-PIAT L-IAT and D-IAT monomers were mixed during polymerization in the ratios 99:1, 90:10, 75:25, 50:50, and 10:90 (L-IAT:D-IAT). For the polymerization reaction a ratio of isocyanide to polystyrene-nickel initiator complex of 50:1 was used. The results of these experiments are shown in Table 3.

Table 3. ***Analysis data of racemized PS-PIAT block copolymers***

Entry	Ratio L-IAT/D-IAT	IAT units[a]	M_n[a]	CD effect[b]
1	99:1	11	6.7×10^3	-44
2	90:10	29	10×10^3	-32
3	75:25	35	12×10^3	-25
4	50:50	35	12×10^3	-2
5	10:90	35	12×10^3	28

[a] In g.mol^{-1}, determined by ^{1}H NMR, the estimated error is 25 %, see Figure 3 for details, [b] intensity of the Cotton effect at λ =288 nm.

The block length of the diblock copolymer prepared at an L-IAT/D-IAT ratio of 99:1 is smaller than the block lengths of the polymers prepared at other L/D monomer ratios (compare entries 1 and 2-5 in Table 3). As mentioned before, at high ratios of isocyanide to polymerization catalyst, the resulting polymer is insoluble and precipitates prematurely from solution. At a high molecular ratio of one enantiomer (entry 1) the polymer rigidity is high

and as a result the diblock copolymer precipitates and the reaction stops, in this way explaining a shorter PIAT block length than expected. The product of the polymerization of L- and D-IAT in a ratio of 1:1 displayed the expected CD effect close to zero. Probably due to a small difference in the ratio of these enantiomers a small CD effect was observed. The IR spectra of these diblock copolymers showed marginal differences in the values of the amide vibrations compared to PS-PIAT$_{50}$ prepared with epimerized IAT.

Initial aggregation experiments with the polymers mentioned in Table 3 were carried out. The aggregates were prepared using the injection method in the same way as described for the previously studied PS-PIAT diblock copolymers. Electron microscopy studies of the resulting dispersions showed that all diblock copolymers formed spherical aggregates, with average diameters ranging from 150 to 300 nm immediately after preparation. Some of the observed aggregates had holes exposing a hollow interior, indicating that also these aggregates were vesicular architectures. However, differences were observed in the stability of the dispersions and in the average diameter of the aggregates. It was noticed that the size of the initially formed aggregates strongly depended on the rate of injection of the PS-PIAT solution into water. Performing the injection with higher pressures resulted in larger spheres. Since these larger spheres were only characterized by electron microscopy it is uncertain if they are vesicular in nature. Due to the high pressure during injection, macrophase separated solid spheres, instead of vesicles, might be formed. For the preparation of well-defined polymersomes a ratio of 75:25 L-IAT:D-IAT gave the most satisfying results.

Dispersions of PS-PIAT$_{17}$ and PS-PIAT$_{100}$ (both prepared from epimerized IAT) were also followed in time, but even after one month no changes in morphology could be observed compared to the initially formed aggregates of these polymeric amphiphiles. This could indicate that the aggregates are in a thermodynamically stable state and therefore no driving force is present for morphological changes. Another possibility is that the aggregates are kinetically trapped structures. This is however unlikely, because the amount of THF present in dispersions of PS-PIAT$_{50}$ was high enough to induce polymersome fusion. Moreover, the head group interactions in polymersomes of PS-PIAT$_{17}$ will be weaker, making that less energy would be needed for a reorganization of the membrane. For the moment no explanation can be given for the deviating behavior of the two diblock copolymer systems.

3.3.3 Aggregates in aqueous solutions, prepared under thermodynamic control

It was already mentioned in the introduction section that many parameters can be varied during the preparation of the polymersomes. The method of inducing aggregate formation determines if an aggregate is prepared under thermodynamic or kinetic control. Over the years many procedures have been developed,[49] like the already mentioned injection method.[38] This technique, however, results in aggregates that are formed under kinetic control. Other methods are, amongst others, the rehydration method, in which a film of aggregates is dried on a surface and submersed into water, sonication, electroformation, and slow addition of a poor solvent to the amphiphile in a good solvent. The latter method results in continuous aggregate formation under thermodynamic control, therefore allowing the amphiphiles to adopt the most favorable morphology.[10, 13, 50]

Optically pure PS-PIAT$_{10}$ was dissolved in THF and at room temperature water was slowly added with the help of a peristaltic pump. Increasing the amount of water led to an increase in turbidity of the polymer solution. The concomitant morphological changes during this addition were followed by TEM (Figure 19).

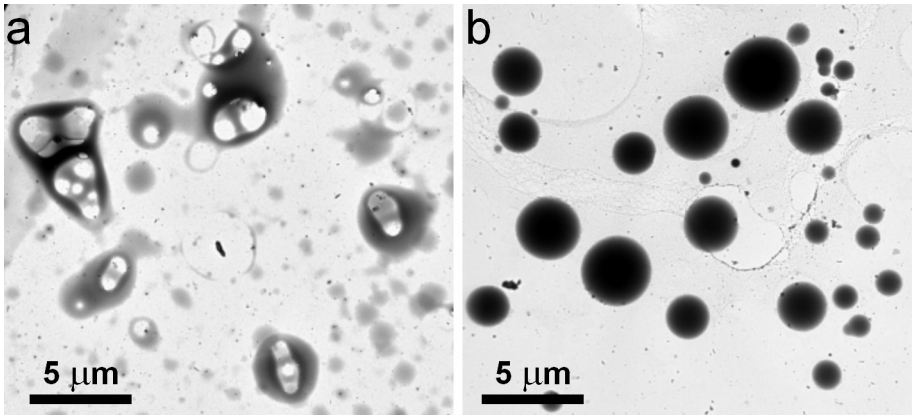

Figure 19. *Aggregates formed after the slow addition of water to a PS-PIAT$_{10}$ solution in THF. a) 55 % (v/v) of water added, b) 67 % (v/v) of water added.*

At low water fractions only phase separated structures could be observed, whilst at intermediate solvent fractions spherical aggregates became visible. When the fraction of water reached a value of 74 % (v/v) precipitation occurred. At this stage spherical aggregates could still be observed with electron microscopy, but also significant amounts of phase separated assemblies were present.

These experiments indicate that the formation of well-defined aggregates under thermodynamic control is only possible in a narrow water fraction range (55 – 74 % (v/v)). It was expected in this experiment that different morphologies would be found upon increasing the amount of water, allowing the formulation of a phase diagram. Studies carried out in the group of Eisenberg on polystyrene based diblock copolymers have previously demonstrated that upon increasing the fraction of water, transitions from spheres, to rods, to polymersomes could be observed. It was also reported that some of these transitions took place within 1 % (v/v) difference in the fraction of water,[16] highlighting the very subtle processes which control self-assembly. In our case different types of aggregates apparently are not formed.

3.3.4 Aggregates in aqueous solutions, prepared under various conditions

The influence of Ca^{2+} ions on the fusion of liposomes and biological cells has been widely investigated.[51, 52] In the presence of Ca^{2+}, fusion of phosphatidylserine vesicles was observed to proceed in less than 5 s.[48] Induction of fusion by Ca^{2+} is believed to be due to a decrease in the electrostatic repulsion between the phospholipid head groups, allowing for a more rapid reorientation of the vesicle bilayer. It has been well-documented that phospholipid vesicle fusion induced by Ca^{2+} proceeds more smoothly than fusion induced by other divalent cations.[52]

It has been found that certain block copolymer aggregates can also undergo shape changes when electrolytes or other solutes are added. Aggregates of the polymeric amphiphile polystyrene-*b*-poly(acrylic acid) (PS-PAA) have been reported to change morphology upon the addition of $CaCl_2$, HCl, and NaCl.[6] Depending on the type of salt added, spherical, rod-like, vesicular or lamellar aggregates could be obtained. The changes in aggregate morphology are a result of reduced electrostatic repulsion among charged head groups due to counterion binding. The specific detailed causes of the effect of added ions on the aggregate morphology probably differ for each additive. For the neutral diblock copolymer polystyrene-*b*-poly(ethylene oxide) (PS-PEO) morphological changes could also be induced by the addition of ions.[53] The main reason why the addition of electrolytes induces morphogenic effects in aggregates of these diblock copolymers is believed to be a decrease in the effective dimension of the PEO block, and also a change in the surface tension between the polystyrene core and the solvent. Another electrolyte responsive diblock copolymer is polystyrene-*b*-poly[2-(β-D-glucosyloxy)ethyl acrylate] (PS-PBGEA), which undergoes morphological changes in aqueous media when solutes like glucose, HCl and $CaCl_2$ are added.[10]

The influence of $CaCl_2$ and $FeCl_2$, both divalent cations, on the aggregation behavior of PS-$PIAT_{50}$ in aqueous solutions was studied. The influence of $CaCl_2$ on the fusion behavior of PS-$PIAT_{50}$ polymersomes was investigated, because it is a commonly applied salt (see above), whilst $FeCl_2$ was employed, because Fe^{2+} has affinity to bind with the sulfur atoms, which are present in the thiophene groups. These ions might therefore alter the packing of the polymeric amphiphiles in the polymersome membranes.

The aggregates of PS-$PIAT_{50}$ were formed using the injection method. $CaCl_2$ and $FeCl_2$ solutions with a concentration of 10^{-6} M were prepared and to these solutions a 1.0 $mg.ml^{-1}$ THF solution of the polymer was injected. The resulting aggregates were examined by SEM, which revealed the formation of polymersomes that had similar dimensions (Figure 20).

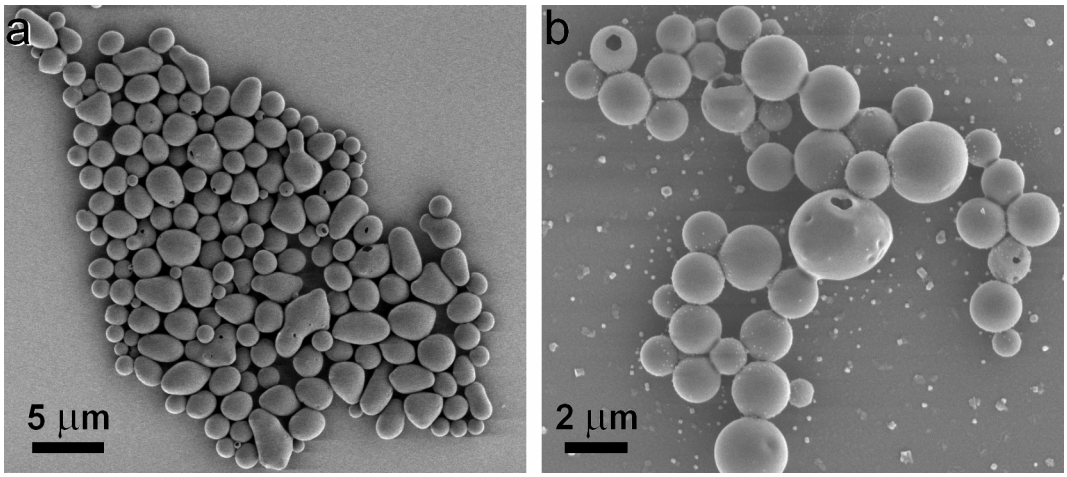

Figure 20. *Formation of aggregates in the presence of divalent metal ions. Dispersions of PS-$PIAT_{50}$ after 18 h containing a) $CaCl_2$, and b) $FeCl_2$.*

Fusion also occurred in the presence of the ions, because the dimensions of the vesicles in the dispersions after 2 days were similar to those of the polymersomes prepared in the absence of the ions (see Figure 15 c). In Figure 20 a), corresponding to the dispersion containing $CaCl_2$, a significantly higher number of imperfect polymersomes are observed, the deformations were almost exclusively found in the larger polymersomes, while the polymersomes with diameters ≤ 1.5 μm were perfectly spherical. A possible explanation for the observed morphogenic effects in the dispersion containing $CaCl_2$ is that Ca^{2+} ions bind to the amide groups in the polyisocyanide blocks, resulting in repulsion between these blocks, leading to the creation of membrane defects. The shapes of the imperfect polymersomes were more oval and seemed to be built up from more than one polymersome. It is possible that

these aggregates are trapped intermediates of a fusion process. $FeCl_2$ didn't seem to have a significant influence on the shape of the polymersomes (Figure 20 b). It might be that larger morphological changes can be obtained at higher electrolyte concentrations, but these experiments were not performed. For the previously mentioned PS-PAA and PS-PEO diblock copolymers salt concentrations of 10^{-3} – 10^{-4} M were used. Moreover, these literature experiments with PS-PAA and also with PS-PBGEA were carried out differently, viz. using the slow addition method, in which the added water already contained the salt.[7, 10]

Dispersions containing $CaCl_2$ were almost completely precipitated after five days. The turbidity of dispersions containing $FeCl_2$ was lower after five days than after two days and some precipitation had occurred. After a week all material had precipitated. As already mentioned, that in the presence of $CaCl_2$ and $FeCl_2$ fusion occurs as well. At a certain diameter the resulting aggregates will be too large to stay dispersed, in the presence of $CaCl_2$, resulting in their precipitation.

Increasing the temperature at which the aggregates are prepared can have a significant influence on the resulting morphology. For phospholipids and other amphiphiles, which possess small aliphatic tails, it is common to prepare vesicles at temperatures above the melting point of the apolar tails.[54] The glass transition temperature (T_g) of the polystyrene$_{40}$ block, as determined by differential scanning calorimetry (DSC), was found to be 68°C.[40] It was decided, therefore, to prepare aggregates of PS-PIAT$_{50}$ above this temperature, namely by injecting the polymeric amphiphile dissolved in THF into water of 70°C, then holding the dispersion at this temperature for 5 min. It was observed that the turbidity of dispersions following this procedure was significantly higher than the turbidity of dispersions prepared at room temperature. SEM micrographs of dispersions prepared at 70°C showed large vesicular assemblies with diameters up to 9 μm, many of which were incompletely formed (Figure 21). Two possible explanations for the presence of either incomplete polymersomes or polymersomes with holes can be proposed. The first is that upon application of the vacuum inside the SEM the entrapped solvent inside the polymersomes evaporates and a nano-explosion occurs.[41] If the holes were created by the vacuum of the microscope, it would be expected that remnants of the membranes would be found in the vicinity of the polymersomes, which was not the case. The second and most probable explanation is that the vesicular assemblies are incompletely formed and exist in a meta-stable state. The mechanism of formation is then similar to the mechanism shown in Figure 11.[5]

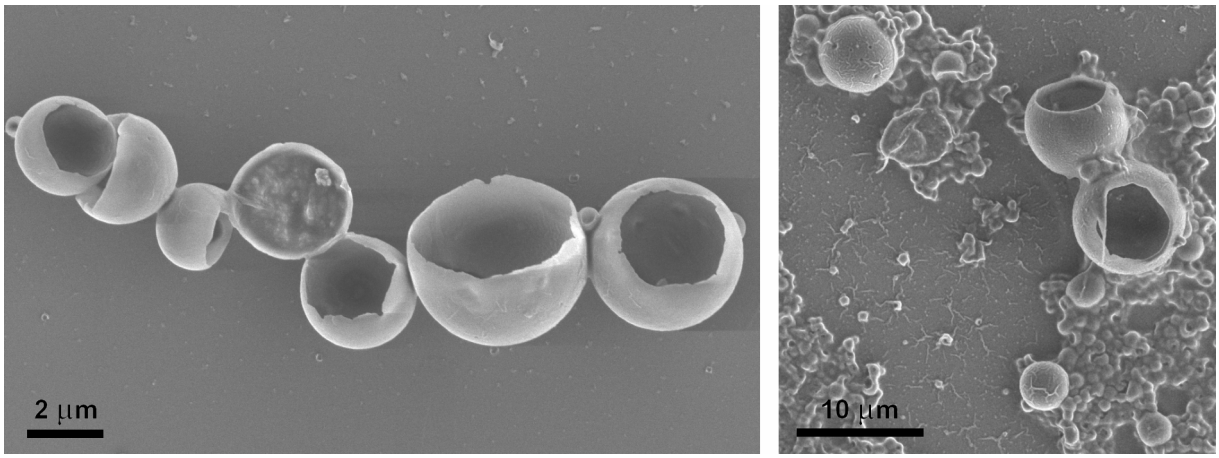

Figure 21. *Aggregates of PS-PIAT$_{50}$ prepared at 70°C. Micrographs were taken from the same sample.*

It was mentioned in Section 3.3.2 that at room temperature the presence of THF was proven to be necessary for the polymersomes to fuse and grow. At 70°C the polystyrene block is very flexible, which allows the diblock copolymers to more readily rearrange themselves into the thermodynamically preferred architecture. Since the system is much more dynamic than at room temperature, the fusion process occurs at an enhanced rate and larger polymersomes are generated immediately, however, at this temperature not in full form.

For PS-PIAT$_{10}$ a similar experiment was performed as described above for PS-PIAT$_{50}$. The polymer was dissolved in THF and injected into water of 70°C. After 6 min the very turbid dispersion was cooled down to room temperature and samples were prepared for electron microscopy studies (Figure 22).

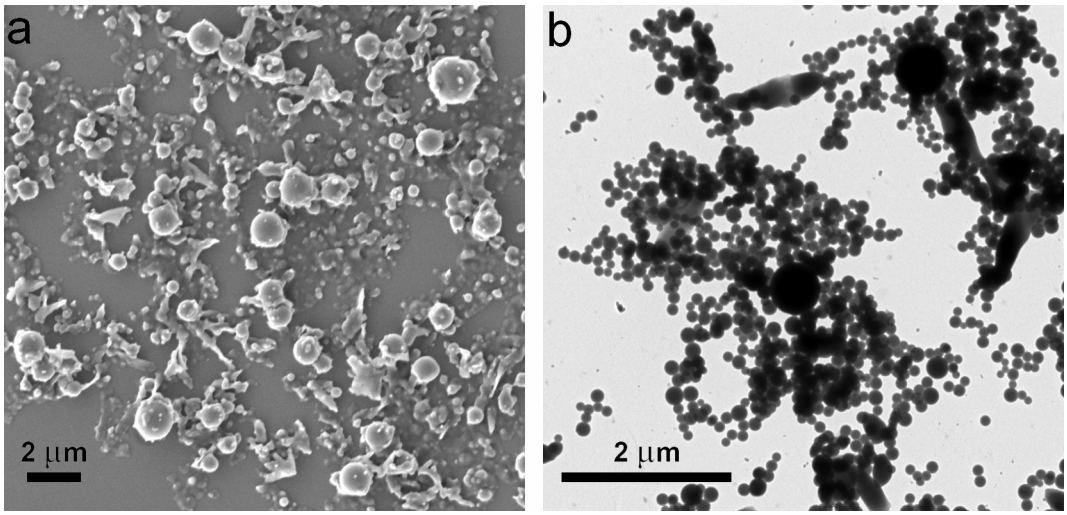

Figure 22. *a) SEM and b) TEM micrographs of spherical aggregates and multilayer films of PS-PIAT$_{10}$ prepared at 70°C.*

It can be concluded from Figure 22 that fusion is accelerated at 70°C when it is compared to the fusion of the dispersions at room temperature (Figure 9 d). Many large spheres could already be observed despite the very short aging time of the dispersion. For dispersions of this diblock copolymer at room temperature it took a few days to detect any change in aggregate dimension. The amount of multilayer films present in the dispersion before and after increasing the temperature seemingly was the same.

The toughness for solvent of the polymersome membranes was investigated by drying polymersomes of PS-PIAT$_{50}$ on a glass plate, which was then submersed into acetonitrile for 30 min. The polymersomes subsequently were examined by SEM (Figure 23).

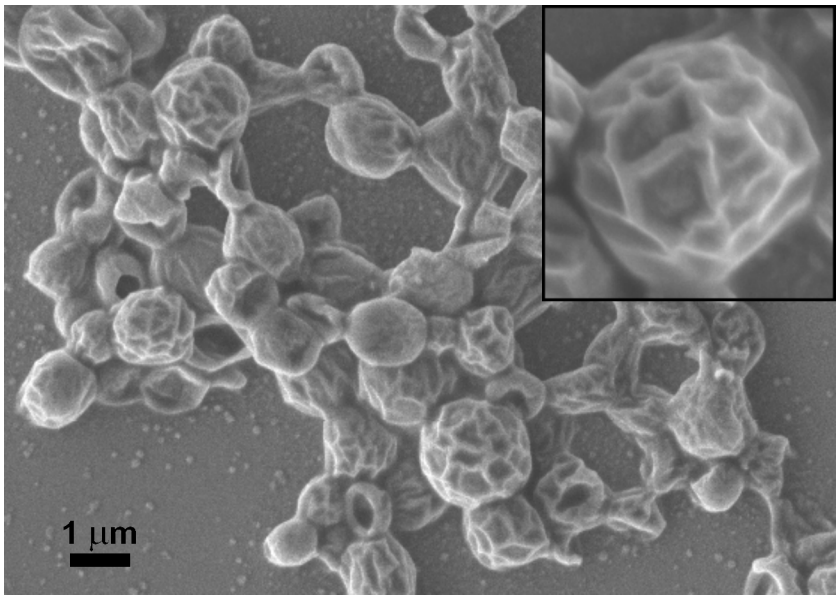

Figure 23. *SEM micrograph of PS-PIAT$_{50}$ polymersomes after being submersed in acetonitrile for 30 min, revealing the dehydrated appearance of the nanospheres. The inset shows an enlargement of a 'raisin-like' polymersome.*

The micrograph revealed that the vesicular architecture was retained, however, the polymersome surface was clearly disrupted. The aggregates had the appearance of a dehydrated grape, and can be described as 'raisin' polymersomes. This appearance is probably caused by the fact that water, which is trapped inside these polymersomes, is extracted by the acetonitrile, which allows it to migrate through the membrane. It is postulated that the polystyrene block of PS-PIAT$_{50}$, which is soluble in acetonitrile, is flexible enough to allow the polymeric amphiphiles to rearrange themselves in the polymersome membranes. As a result the water is released via small pores and the membranes partly collapse, giving them their 'raisin-like' appearance under the electron microscope. This result is in contrast to the

structures of fully collapsed polymersomes observed for the diblock copolymers prepared in $CHCl_3$ (Figure 6). This difference in 'solvent toughness' is a result of the difference in membrane architecture between polymersomes prepared in organic and aqueous solvents, in the sense that the organization of the amphiphiles inside the membrane is inverted in the two solvent systems (Figure 2).

3.3.5 Aggregates prepared by electroformation

Over the last few years several methods have been developed for the construction of giant vesicles with diameters in the range of 10 to 200 μm.[55, 56] Electroformation has proven to be one of the most useful approaches in this respect, since it allows the preparation of giant vesicles from a large variety of neutral, charged and zwitterionic lipids.[57] This technique, invented by Angelova and Dimitrov,[58] involves the use of two Pt wires, serving as electrodes, onto which a thin film of the amphiphile is dried. The two coated wires are then submersed in an aqueous solution. An alternating current is then applied, and the vesicles are grown on the electrodes. In Figure 24 a typical electroformation setup is shown.

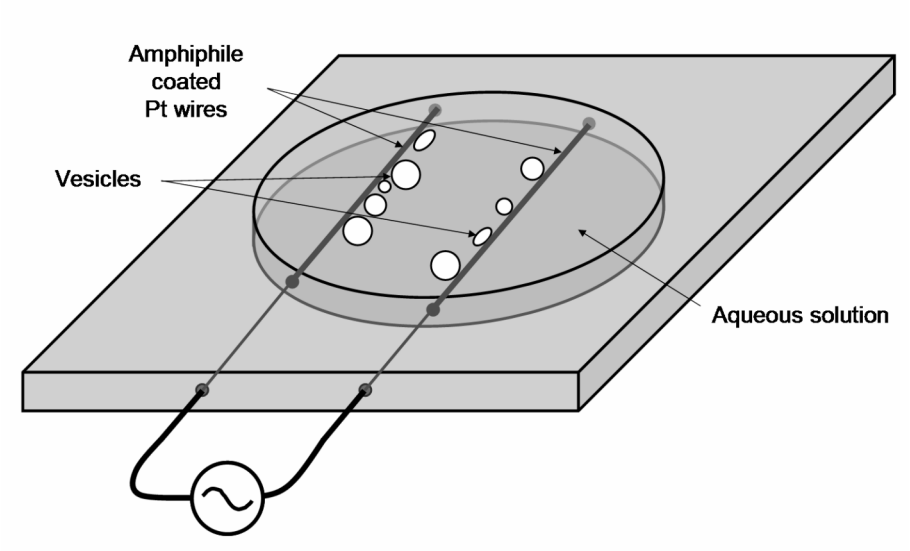

Figure 24. *Typical electroformation setup; two Pt wires are submersed in an aqueous bath and an alternating current is applied, resulting in the growth of the vesicles on the electrode surfaces.*

Interestingly, the size of the vesicles can also be readily controlled by the electroformation technique, viz. varying the voltage and frequency of the electric field.[56] It

has been shown that this technique can also be applied to amphiphilic block copolymers. Discher *et al*. demonstrated the feasibility of such an approach and constructed giant polymersomes from polyethyleneoxide-*b*-polyethylethylene (PEO-PEE) with diameters (D) in the range of 20–50 μm.[3] Dimova and coworkers have used the same approach to prepare giant polymersomes of polybutadiene-*b*-polyethyleneoxide (PB-PEO) and have studied their shear surface viscosity.[59] In general, the combination of electroformation and block copolymers may offer an ideal route to prepare stable giant polymersomes with potentially unique properties.

Given the information in the literature it was decided to investigate the possibility of preparing giant polymersomes from PS-PIAT$_{50}$ diblock copolymers by electroformation. Indeed, it was observed that this diblock copolymer also readily formed large quantities of well-defined vesicular aggregates, with diameters ranging from $1 \leq D \leq 100$ μm (Figure 25). The obtained polymersomes were considerably larger than the polymersomes prepared via the injection method and were approximately 2 times larger than the polymersomes reported by both Discher and Dimova.[3, 59]

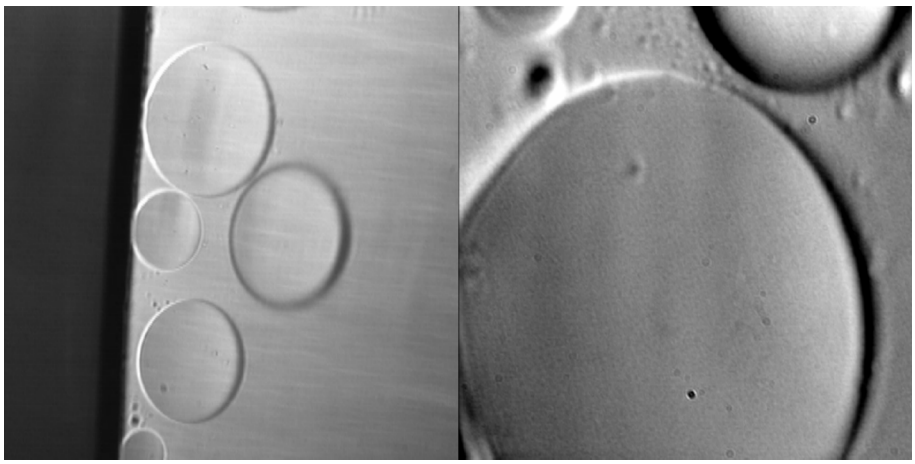

Figure 25. *Optical micrographs of electroformed giant polymersomes of PS-PIAT$_{50}$; the image width corresponds to 60 μm. In the left image polymersome growth from the electrode surface can be seen.*

A standard method for the preparation of vesicles from low molecular weight amphiphiles, such as dioleoylphosphatidylcholine (DOPC), is the hydration method.[60] This technique was also used to construct polymersomes from PS-PIAT$_{50}$. A drop of a PS-PIAT$_{50}$ solution in $CHCl_3$ was dried on a roughened teflon surface and subsequently immersed into a 0.1 M sucrose solution of 40°C. After one day, no polymersome formation could be observed.

The lack of polymersome formation by the hydration method is attributed to the low mobility of the polystyrene chains in the diblock copolymers at 40°C, which is below their T_g (~70°C). In contrast, applying an alternating electric current to the dried PS-PIAT$_{50}$ sample readily led to the formation of polymersomes. The hydration experiment highlights the importance of an alternating electric current for polymersome formation. The mechanism of the electroformation of giant vesicles is not yet fully understood, however, it is believed that the electro-osmotic motion of water induces bilayer separation and vesicle growth.[57] Since the electroformation experiments were done at a temperature below the T_g of polystyrene$_{40}$ it is assumed that the applied alternating current supplies the required energy needed to plasticize the polystyrene chains, resulting in the growth of the polymersome particles.

Although constructed from rigid diblock copolymers, fusion of two giant polymersomes was observed to be possible, when they were brought in close proximity using a micropipette. This suggests that in spite of the high T_g value of the polystyrene block the polymersome membranes are still sufficiently fluidic in nature to behave in a similar manner as simple lipid membranes (Figure 26).

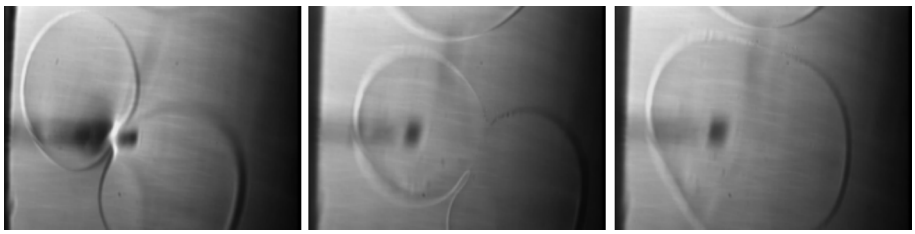

Figure 26. *Optical micrographs of two giant polymersomes fused into one polymersome with the help of a micropipette. The width of the optical micrographs amounts to 80 μm.*

Due to the mechanical force acting upon the diblock copolymers within the polymersome membranes, the copolymers were able to rearrange themselves. This process is different from the fusion process of polymersomes prepared via the injection method, where THF is an essential component for fusion, since it solvates the polystyrene block, allowing the diblock copolymers to reorganize.

These giant polymersomes may also have the potential to be used as micro-capsules, as was demonstrated in a separate experiment. Giant polymersomes of PS-PIAT$_{50}$ were prepared by electroformation in a 0.1 M sucrose solution containing fluorescein labeled dextran (M_w = 10^4 g/mol). The polymersomes where grown from the surface, and found to encapsulate the dye, as could be observed by fluorescence microscopy. The encapsulation of

the labeled biopolymer allowed the observation of two distinct types of giant polymersomes, viz. multicompartment polymersomes (Figure 27 a) and multilamellar polymersomes (Figure 27 b).

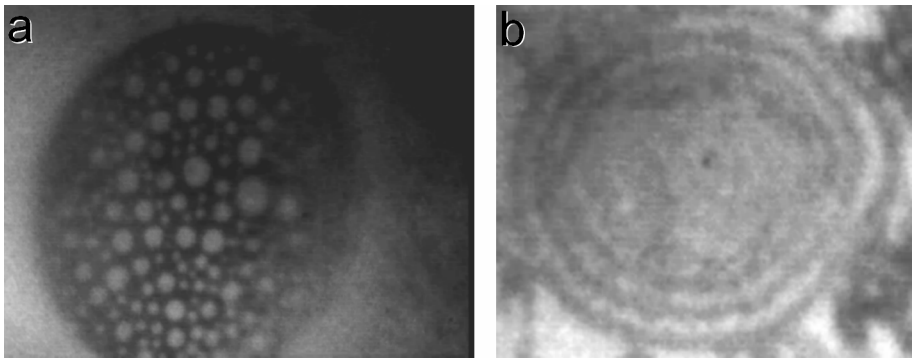

Figure 27. *Fluorescence micrographs ($\lambda_{exc.}$ of 488 nm) of fluorescein labeled dextran inside electroformed giant polymersomes of PS-PIAT$_{50}$. a) Multicompartmental giant polymersome, the width of the image corresponds to 80 μm. b) Multilamellar giant polymersome; the width of the image corresponds to 45 μm.*

These above results are in contrast to experiments carried out with classical phospholipids and experiments performed by Discher *et al.* using diblock copolymers. In both cases the giant vesicles were unilamellar in nature.[3, 61] The mechanism of the formation of the compartmental polymersomes shown in Figure 27 requires further study, but it is likely that the unique structural properties of PS-PIAT$_{50}$ play an important role. In contrast to the classical phospholipids and the PEO-PEE diblock copolymers studied by Discher and coworkers,[3] both blocks of PS-PIAT$_{50}$ have a very low solubility in water. The multilamellar polymersomes are probably formed from a multilayer sheet of PS-PIAT$_{50}$, which shrinks at a rate that is similar for the whole sheet, yielding the observed "onion type" polymersomes.[62] Encapsulation of smaller, clustered polymersomes on the electrode surface by a giant polymersome is a likely explanation for the formation of the multicompartmental polymersomes. It is clear that many fundamental studies are still required to understand the relationship between the self-assembled architecture and the polymer building block structure.

3.4 Conclusions

A series of diblock copolymers based on styrene and isocyanoalanine(2-thiophen-3-yl-ethyl)amide has been prepared in aqueous dispersions and their aggregation behavior has been

studied under various conditions. By varying the ratio between polystyrene and polyisocyanide block length, aggregates with different morphologies could be readily prepared. It was also possible to prepare aggregates of the same polymeric amphiphile in non-aqueous solvents, resulting in the formation of polymersomes. In aqueous dispersions the polymersomes were found to fuse, resulting in the formation of polymersomes with diameters that were 20 times higher than the diameters of the initially formed polymersomes. When aggregate formation was performed at temperatures around the T_g of polystyrene an increased rate of the fusion process was observed. The presence of ions in the preparation led to the formation of polymersomes with a high number of membrane defects. Finally, the electroformation method was found to be an excellent technique to prepare giant polymersomes with diameters up to 100 μm.

The performed experiments have resulted in a better understanding of the aggregation behavior of these rod-coil diblock copolymers, which differs significantly from the well-known classic amphiphiles like phospholipids. Using this knowledge in the future new encapsulation materials based on polymeric amphiphiles can be created for applications in the fields of sensor technology and drug-release.

3.5 Experimental Section

General methods and materials

THF was distilled over sodium, $CHCl_3$ and CH_2Cl_2 over $CaCl_2$, ethyl acetate over K_2CO_3, and methanol over CaH_2. Polystyrene$_{40}$-carboxylic acid was kindly provided by Dr. J.J.L.M. Cornelissen. Amine-functionalized polystyrene$_{40}$,[33] and (tBuNC)$_4$Ni(ClO$_4$)$_2$[34] were synthesized following procedures from the literature. The synthesis of the monomer (IAT) is described in Chapter 2. All other chemicals were used as obtained unless stated otherwise. For the aggregation studies in aqueous solutions ultra pure water ($R > 18\times10^6$ Ω) was used. ^{1}H NMR spectra were recorded on Bruker DPX-200 and Bruker AC-300 instruments at room temperature and on the latter spectrometer ^{13}C NMR spectra were recorded as well. Chemical shifts are given in ppm (δ) relative to tetramethylsilane. Abbreviations used are s = singlet, d = doublet, t = triplet, q = quartet, m = multiplet and br = broad. Infrared spectra were recorded on a BioRad FTS 25 spectrometer. CD spectra were measured on a Jasco J600. A Perkin Elmer LS 50B was used to record fluorescence spectra. GPC measurements were carried out with a Shimadzu GPC with Shimadzu refractive index and UV-Vis detectors, equipped with a Polymer Laboratories Plgel 5 μm mixed-D column and a PL 5 μm guard column (separation range from 500–300,000 molecular weight) using THF or DMSO as mobile phases at 35°C, respectively.

Preparation of Aggregates

In organic solvents.

Dispersions of enantiomerically impure PS-PIAT$_{50}$ in $CHCl_3$ with a concentration of 0.1 mg.ml^{-1} were prepared in a flask. The flask was shaken until no solid particles of polymer could be observed with the naked eye.

Aggregate formation in ethyl acetate was induced by the injection of 1.0 ml of a 1.0 mg.ml^{-1} solution of PS-PIAT$_{10}$ in THF into 2.5 ml of ethyl acetate. The resulting mixture was shaken by hand to obtain a homogeneous mixture. No further method was used to induce the formation of aggregates.

In aqueous solvents.

(*i*) In a typical aggregation experiment 1.0 ml of a 1.0 mg.ml^{-1} PS-PIAT$_n$ solution in THF was injected into 5.0 ml of ultra pure water at room temperature. In order to homogenize the obtained dispersion, it was shaken by hand. No additional energy was used to induce aggregate formation.

(*ii*) Aggregates were prepared by injecting a PS-PIAT$_n$ solution of 0.5 mg.ml^{-1} in THF into 5.0 ml of ultra pure water at 70°C. After 45 min the dispersion was cooled to room temperature.

To study the influence of ions on the morphology, aqueous solutions containing $CaCl_2$ and $FeCl_2$, both at a concentration of 10^{-6} M were prepared. Into 5.0 ml of these solutions a 0.5 mg.ml^{-1} PS-PIAT$_{50}$ solution in THF was injected.

(*iii*) Ultra pure water was slowly added (1.3 ml.h^{-1}) with the help of a peristaltic pump to 1.0 ml of a 1.0 mg.ml^{-1} PS-PIAT$_n$ solution in THF which was very slowly stirred. The addition of water was ended after reaching a water/THF ratio of 1.4.

Electroformation

The electroformation setup used consisted of a bath with 2 platinum electrode wires (5 x 1 mm), which were separated 5 mm from each other and were connected to an external alternating or direct current supply. A thin film of PS-PIAT in $CHCl_3$ was dried onto both electrodes, the bath was filled with a 0.1 M sucrose solution and an alternating current potential of 10 V with a frequency of 10 Hz was applied for 6 h. Thereafter, the frequency was lowered to 2 Hz for 12 h to release the polymersomes from the electrodes, followed by dilution into an iso-osmotic sucrose solution. The setup was mounted on the stage of a Zeiss Axiovert 100 light microscope, for optical and fluorescence observation.

Microscopy studies

For the SEM and TEM studies JEOL JSM-6330F and JEOL JEM-1010 instruments were used respectively. Samples for TEM were prepared by drying a drop of the dispersion on a carbon-coated copper grid. When grids of aqueous samples were prepared the excess of water was blotted away with a filter paper after 2 min. For Pt shadowing the grids were placed in an Edwards coater Model 306 under an angle of 45° with respect to the Pt source. SEM samples were prepared by drying a drop of the dispersion on microscopy glass which was cleaned prior to use by sonication for 15 min. in CH_2Cl_2. The samples were left to dry for a day in the fume hood

before study. A 1.5 nm layer of Pd/Au was sputtered on the SEM samples before studying by using a Cressington 208 HR sputter coater fitted with a Cressington layer thickness controller.

Light and fluorescence micrographs of polymersomes dried on glass were prepared with a Zeiss Axiovert 135 TV, fitted with a monochromatic light source for the fluorescence measurements. The fluorescence spectra of dried-in polymersomes were recorded with a Nikon Microscope fitted with Ocean Optics equipment.

Encapsulation of dyes

A PS-PIAT$_{50}$ solution of 0.5 mg.ml^{-1} in THF was injected into a 10^{-4} M solution of ethidium bromide in ultra pure water, with a final water/THF ratio of 5 (v/v). This mixture was allowed to equilibrate for 50 h before it was brought on a Sephadex G50 column. A fluorescence detector working at 280 nm was used to monitor the fractions. Ultra pure water was used as eluent. The polymersomes containing the encapsulated dye had a retention time of 3 h, whilst the free dye had a retention time of 56 h.

In 3.5 ml of an aqueous solution of 4×10^{-7} M methylene blue, 0.5 ml PS-PIAT$_{50}$ solution of 0.5 mg.ml^{-1} in THF was injected. After 2 days 1.0 ml of this dispersion was transferred to a dialysis bag with a molecular weight cut off of 3500 D and dialyzed over the weekend in ultra pure water.

Dynamic light scattering

These experiments were carried out in the High Field Magnet Laboratory in Nijmegen with a home-built setup fitted with a He-Ne laser at 632.8 nm. An amount of 1.0 ml of the dispersion was transferred into a spherical glass cuvet and placed in a very stable and accurate thermostat set to 25°C. The angle of detection was 90°. After stabilization of the temperature 3 measurements of 10 minutes each were performed and the average hydrodynamic radius of the aggregates in these runs was calculated.

Synthesis

Initiator complex 1

While stirring, 1.02 g (0.242 mmol) of PS-NH_2 dissolved in 10 ml of CH_2Cl_2 was added to a solution of 0.143 g (0.242 mmol) (*t*BuNC)$_4$Ni(ClO_4)$_2$ in 25 ml of CH_2Cl_2 under a nitrogen atmosphere. After an additional hour of stirring the solvent was evaporated, yielding a yellow solid (yield 1.16 mg, 100 %). ^{1}H NMR (300 MHz, $CDCl_3$) δ 7.82 (s, CH_2NH), 7.3–6.3 (br, CH*Ph*), 3.7 (br, $OCH_2CH_2CH_2NH$), 3.3–2.9 (br, CH_2OCH_2 and CH_2OCH_2), 2.3–1.7 (br, CHPh), 1.54 (s, $C(CH_3)_3$), 1.7–1.2 (br, CH_2CHPh), 1.26–0.58 (*Bu*($CH_2CHPh)_{40}$) ppm; ^{13}C NMR (75 MHz, $CDCl_3$) δ 178 (NCN), 146.5–145 (br, CH*Ph*$_{ipso}$), 130–127 (br, (CH*Ph*$_{ortho+meta}$), 127–124 (br, CH*Ph*$_{para}$), 123 (br, Ni-C=N), 75 (br, $CH_2OCH_2CH_2CH_2NH$), 68 (br, $CH_2OCH_2CH_2CH_2NH$), 54.9 ($CH_2OCH_2CH_2CH_2NH$), 41 (CHPh), 46–40 (br, CH_2CHPh), 31.7 ($CH_2CH(CH_3)(CH_2CHPh)_{40}$), 30.3 (($CH_3)_3CN$), 29.5 (($CH_3)_3CNH$), 28.2 (br, $CH_2CH(CH_3)(CH_2CHPh)_{40}$), 26.9 ($OCH_2CH_2CH_2NH$), 22.3 ($CH_2CH(CH_3)(CH_2CHPh)_{40}$), 13.9 ($CH_3CH_2CH(CH_3)(CH_2CHPh)_{40}$) ppm; FT-IR (cm^{-1}, KBr) 3282 (NH), 3061, 3026, 2923, 2850 (CH), 2253 + 2226 (C=N), 1602 (C-C aryl), 1575 (NCN), 1493, 1453 (C-C aryl), 1097 (ClO_4). The data listed here are in good agreement with previous reports.[40]

PS-PIAT$_n$

In a typical polymerization reaction the desired amount of initiator complex **1** dissolved in 5.0 ml of CH_2Cl_2 was added to a stirred solution of IAT in 10 ml of CH_2Cl_2. Complete consumption of isocyanide, as observed by IR spectroscopy, was obtained after 2 days. The polymer was evaporated to dryness and redissolved in a minimal amount of CH_2Cl_2. The polymer was then precipitated by dropping this solution into a well-stirred mixture of methanol/water (1:1 v/v). The product was filtered off and washed with methanol/water (1:1 v/v). After drying *in vacuo* the polymer was obtained as an orange/brown solid (yields 58–79 %). Analysis results for PS-PIAT$_{50}$: ^{1}H NMR (300 MHz, $CDCl_3$) δ 7.3–6.3 (br, CH*Ph*, thiophene H-5, thiophene H-2, thiophene H-4), 4.3–4.1 (br, C=NC*H*(CH_3)), 3.9–3.3 (br, C*H*$_2$CH$_2$-thiophene), 3.7 (br, $OCH_2CH_2CH_2NH$), 3.3 - 2.9 (br, C*H*$_2$OCH$_2$ and CH_2OCH_2), 3.1–2.6 (br, C*H*$_2$-thiophene), 2.1–1.7 (br, CH_2CHPh), 1.7 (br, C(CH_3)$_3$), 1.7–1.2 (br, C*H*$_2$CHPh), 1.62 (br, NHCH(C*H*$_3$)C(O)), 1.0–0.6 (*Bu*($CH_2CHPh)_{40}$) ppm; ^{13}C NMR (75 MHz, $CDCl_3$) δ 155.2 (C=N), 147–143 (br, CH*Ph*$_{ipso}$), 140 (thiophene C-3), 130–127 (br, (CH*Ph*$_{ortho+meta}$), 127–124 (br, thiophene C-4, C-5 and CH*Ph*$_{para}$), 113 (br, thiophene C-2), 72 (br, *C*$H_2OCH_2CH_2CH_2NH$), 68 (br, $CH_2OCH_2CH_2CH_2NH$), 63 (br, C=N*C*H(CH_3)), 42–38 (br, *C*HPh and *C*H_2CHPh), 39.8 (br, $CH_2CH_2NHC(O)$), 37.5–34 (br, $CH_2OCH_2CH_2CH_2NH$), 32–30 (C=NC(*C*H$_3$)$_3$) and $CH_2CH(CH_3)(CH_2CHPh)_{40}$), 28.7 (*C*$H_2CH_2NHC(O)$), 25.9 (br, *C*$H_2CH(CH_3)(CH_2CHPh)_{40}$), 22.6 ($CH_2CH(CH_3)(CH_2CHPh)_{40}$), 21.4 (CH(*C*H$_3$)), 13.4 ($CH_3CH_2CH(CH_3)(CH_2CHPh)_{40}$) ppm; FT-IR (cm^{-1}, KBr) 3288 (NH), 3060, 3027, 2950, 2924, 2850 (CH), 1660 (amide I), 1604 (C-C aryl), 1532 (amide II).

3.6 References and Notes

[1] S. I. Stupp, V. LeBonheur, K. Walker, L. S. Li, K. E. Huggins, M. Keser, A. Amstutz, *Science* **1997**, *276*, 384.
[2] N. S. Cameron, M. K. Corbierre, A. Eisenberg, *Can. J. Chem.* **1999**, *77*, 1311.
[3] B. M. Discher, Y.-Y. Won, D. S. Ege, J. C.-M. Lee, F. S. Bates, D. E. Discher, D. A. Hammer, *Science* **1999**, *284*, 1143.
[4] M. Lee, B.-K. Cho, W.-C. Zin, *Chem. Rev.* **2001**, *101*, 3869.
[5] M. Antonietti, S. Förster, *Adv. Mater.* **2003**, *15*, 1323.
[6] L. Zhang, K. Yu, A. Eisenberg, *Science* **1996**, *272*, 1777.
[7] L. Zhang, A. Eisenberg, *Macromolecules* **1996**, *29*, 8805.
[8] J. Ding, G. Liu, M. Yang, *Polymer* **1997**, *38*, 5497.
[9] E. Fossum, K. Matyjaszewski, S. S. Sheiko, M. Möller, *Macromolecules* **1997**, *30*, 1765.
[10] Z.-C. Li, Y.-Z. Liang, F.-M. Li, *New J. Chem.* **2002**, *26*, 1805.
[11] S. Pispas, N. Hadjichristidis, *Langmuir* **2003**, *19*, 48.
[12] S. A. Jenekhe, X. L. Chen, *Science* **1998**, *279*, 1903.
[13] L. Zhang, A. Eisenberg, *Macromolecules* **1999**, *32*, 2239.
[14] Y.-Y. Won, A. K. Brannan, H. T. Davis, F. S. Bates, *J. Phys. Chem . B* **2002**, *106*, 3354.
[15] S. Jain, F. S. Bates, *Science* **2003**, *300*, 460.
[16] O. Terreau, L. Luo, A. Eisenberg, *Langmuir* **2003**, *19*, 5601.
[17] U. Stalmach, B. de Boer, C. Videlot, P. F. van Hutten, G. Hadziioannou, *J. Am. Chem. Soc.* **2000**, *122*, 5464.
[18] E. Liu, J. Sheina, T. Kowalewski, R. D. McCullough, *Angew. Chem. Int. Ed.* **2002**, *41*, 329.
[19] B. Jeong, Y. H. Bae, D. S. Lee, S. W. Kim, *Nature* **1997**, *392*, 860.
[20] D. E. Discher, A. Eisenberg, *Science* **2002**, *297*, 967.
[21] A. Graff, M. Sauer, P. van Gelder, W. Meier, *Proc. Natl. Acad. Sci. U.S.A.* **2002**, *99*, 5064.
[22] J. T. Chen, E. L. Thomas, C. K. Ober, G.-P. Mao, *Science* **1996**, *273*, 343.
[23] X. L. Chen, S. A. Jenekhe, *Macromolecules* **2000**, *33*, 4610.
[24] B. de Boer, U. Stalmach, H. Nijland, G. Hadziioannou, *Adv. Mater.* **2000**, *12*, 1581.

[25] N. A. J. M. Sommerdijk, S. J. Holder, R. C. Hiorns, R. G. Jones, R. J. M. Nolte, *Macromolecules* **2000**, *33*, 8289.
[26] H.-A. Klok, J. F. Langenwalter, S. Lecommandoux, *Macromolecules* **2000**, *33*, 7819.
[27] A. Halperin, *Macromolecules* **1990**, *23*, 2724.
[28] J. J. L. M. Cornelissen, M. Fischer, N. A. J. M. Sommerdijk, R. J. M. Nolte, *Science* **1998**, *280*, 1427.
[29] J. J. L. M. Cornelissen, J. J. J. M. Donners, R. de Gelder, W. S. Graswinckel, G. A. Metselaar, A. E. Rowan, N. A. J. M. Sommerdijk, R. J. M. Nolte, *Science* **2001**, *293*, 676.
[30] P. Samorí, C. Ecker, I. Gössl, P. A. J. de Witte, J. J. L. M. Cornelissen, G. A. Metselaar, M. B. J. Otten, A. E. Rowan, R. J. M. Nolte, J. P. Rabe, *Macromolecules* **2002**, *35*, 5290.
[31] R. J. M. Nolte, *Chem. Soc. Rev.* **1994**, *23*, 11.
[32] P. C. J. Kamer, R. J. M. Nolte, W. Drenth, *J. Am. Chem. Soc.* **1988**, *110*, 6818.
[33] J. C. M. van Hest, D. A. P. Delnoye, M. W. P. L. Baars, C. Elissen-Roman, M. H. P. van Genderen, E. W. Meijer, *Chem. Eur. J.* **1996**, *12*, 1616.
[34] R. W. Stephany, W. Drenth, *Recl. Trav. Chim. Pays-Bas* **1972**, *91*, 1453.
[35] M. Clericuzio, G. Alagona, C. Ghio, P. Salvadori, *J. Am. Chem. Soc.* **1997**, *119*, 1059.
[36] The carboxylic acid end-capped PS_{40} used to synthesize the amine-functionalized polystyrene had an M_n and polydispersity of 4170 and 1.05, respectively, as determined by (GPC).
[37] S. T. Thornton, A. Rex, *Modern Physics for Scientists and Engineers*, Saunders College Publishing, Fort Worth, **1993**.
[38] A. S. Domazou, P. L. Luisi, *J. Liposome Res.* **2002**, *12*, 205.
[39] W. Burchard, *Adv. Polym. Sci.* **1983**, *48*, 1.
[40] J. J. L. M. Cornelissen, PhD Thesis thesis, University of Nijmegen (Nijmegen), **2001**.
[41] F. Caruso, R. A. Caruso, H. Möhwald, *Science* **1998**, *282*, 1111.
[42] H. Harris, *Cell fusion*, Oxford University Press, London, **1970**.
[43] L. Luo, A. Eisenberg, *Langmuir* **2001**, *17*, 6804.
[44] M. Maskos, J. R. Harris, *Macromol. Rapid Commun.* **2001**, *22*, 271.
[45] J. Zimmerberg, L. V. Chernomordik, *Adv. Drug Delivery Rev.* **1999**, *38*, 197.
[46] J.-K. Lee, B. R. Lentz, *Biochemistry* **1997**, *36*, 6251.
[47] P. I. Kuzmin, J. Zimmerberg, Y. A. Chizmadzhev, F. S. Cohen, *Proc. Natl. Acad. Sci. U.S.A.* **2001**, *98*, 7235.
[48] D. Hoekstra, *Biochemistry* **1982**, *21*, 2833.
[49] P. Walde, S. Ichikawa, *Biomol. Eng.* **2001**, *18*, 143.
[50] L. Luo, A. Eisenberg, *J. Am. Chem. Soc.* **2001**, *123*, 1012.
[51] D. Papahadjopoulos, S. Nir, N. Düzgünes, *J. Bioenerg. Biomembr.* **1990**, *22*, 157.
[52] G. Cevc, H. Richardson, *Adv. Drug Delivery Rev.* **1999**, *38*, 207.
[53] K. Yu, A. Eisenberg, *Macromolecules* **1998**, *31*, 3509.
[54] D. D. Lasic, Elsevier Science, Amsterdam, **1993**.
[55] A. D. Bangham, Academic Press, London, **1983**.
[56] P. L. Luisi, P. Walde, *Giant vesicles*, John Wiley & Sons, Chichester, **2000**.
[57] F. M. Menger, M. I. Angelova, *Acc. Chem. Res.* **1998**, *31*, 789.
[58] M. I. Angelova, D. S. Dimitrov, *Faraday Discuss. Chem. Soc.* **1986**, *81*, 303.
[59] R. Dimova, U. Seifert, B. Pouligny, S. Förster, H.-G. Döbereiner, *Eur. Phys. J. E* **2002**, *7*, 241.
[60] M. Goulian, O. N. Mesquita, D. K. Fygenson, C. Nielsen, O. S. Andersen, A. Libchaber, *Biophys. J.* **1998**, *74*, 328.
[61] L. Mathivet, S. Cribier, P. F. Devaux, *Biophys. J.* **1996**, *70*, 1112.
[62] H. Shen, A. Eisenberg, *Angew. Chem. Int. Ed.* **2000**, *39*, 3310.

Chapter 4

Membrane Cross-linking of Thiophene-Containing Diblock Copolymer Vesicles

4.1 Introduction

Biomembranes have played a crucial role in the origin of life by supplying a protective shell in which biological phenomena could take place. The cell membrane is vital in transport, energy metabolism, cell division and the synthesis of biomacromolecules. Especially the surface of the cell is essential in processes like immunology, cell-cell interactions and cell differentiation.[1, 2] The amphiphiles in the cell membrane are phospholipids and Bangham already described in the 1960s that aqueous dispersions of phospholipids spontaneously form closed bilayers, which he called *liposomes*.[3] This has led to a more fundamental understanding of the cell membrane, because many of its unique properties could be mimicked by these simple liposome model systems.[4, 5]

The membranes of liposomes are dynamic systems; their amphiphiles undergo rapid lateral diffusion and display slow translocations from one side of the membrane to the other, also called "flip-flop".[6] The half-life of the latter process ranges from hours to days depending on the type of amphiphile.[7] For the transport in and out of the cells the membrane needs to be dynamic, especially during exo- and endocytosis. In these two processes solutes are excreted or enclosed, respectively, via the temporal formation of vesicles.[8] Detailed studies have revealed that the biological membrane is stabilized by the incorporation of membrane spanning proteins and the presence of the cytoskeleton (Figure 1).[1]

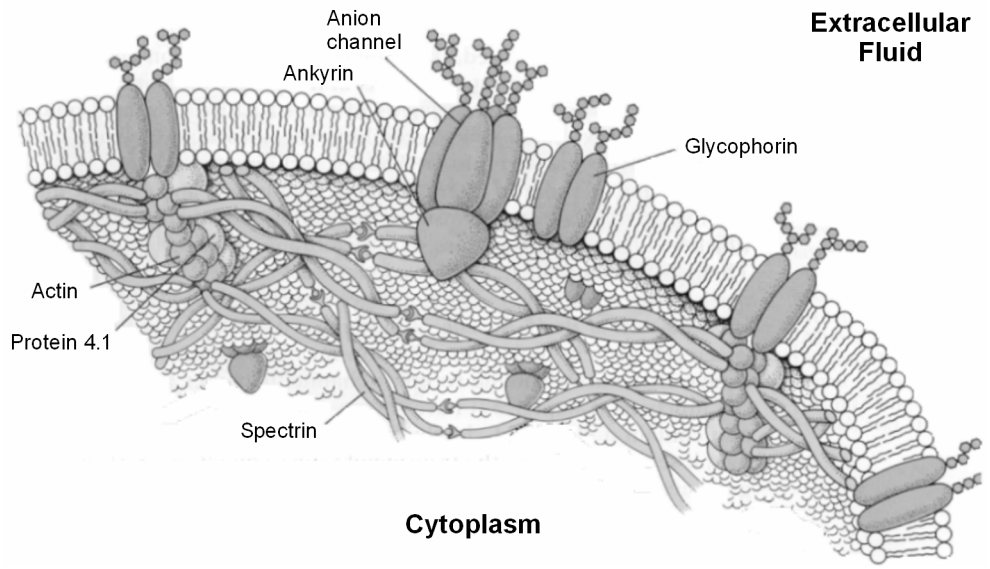

Figure 1. *Schematic diagram of the erythrocyte membrane skeleton, showing nature's solutions to anchor the phospholipids and to stabilize the membrane. The cytoskeleton is formed by the proteins on the inner side of the membrane.*[1]

Various methods have been developed over the years to increase the stability of synthetic closed bilayers, as can be seen in Figure 2.[9]

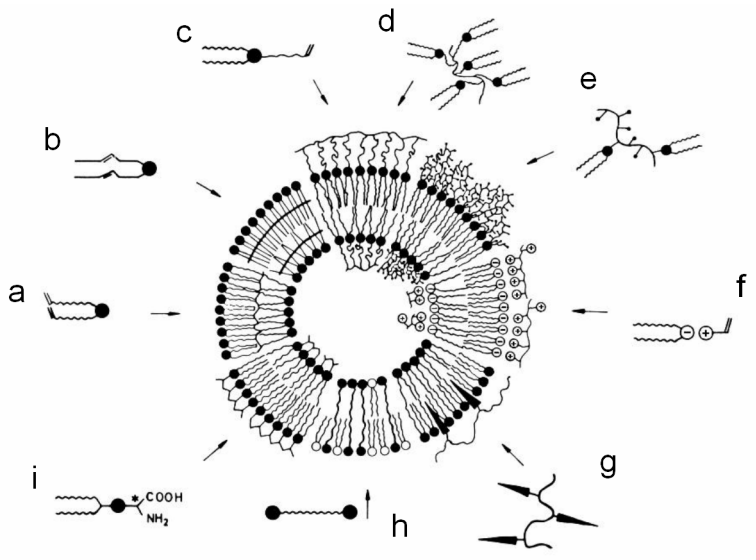

Figure 2. *Overview of the possibilities to stabilize vesicular membranes.*[9] *In the text below each approach is mentioned.*

Most of the work described in the literature deals with the polymerization or cross-linking of the amphiphiles.[9-12] Aggregates that consist of cross-linked amphiphiles can be

prepared in two different ways, either by polymerizing the amphiphiles after aggregation (Figure 2 a-c), or by first polymerizing them and then allowing them to form aggregates (Figure 2 d).[9, 10] Other approaches that have been developed involve the use of amphiphilic polymers (Figure 2 e), cross-linkable counter ions (Figure 2 f), coating of the vesicle outer shell with polymers (Figure 2 g), mixing-in of membrane spanning amphiphiles (Figure 2 h), or the use of amphiphiles with amino acid head groups (Figure 2 i).[13, 14]

A relatively new development in the field of amphiphiles is the study of the aggregation behavior of large, block copolymer based amphiphiles, which has resulted in the discovery of several new morphologies.[15-20] Diblock copolymers have the same basic architecture as lipids, in that they possess a hydrophobic tail and a hydrophilic head. Generally, they consist of distinct polymer chains covalently linked in a series of two or more segments. Interestingly, many amphiphilic block copolymers have been shown to be able to form vesicles.[21] These vesicles, also referred to as polymersomes, are less dynamic than the vesicles formed by classic lipid amphiphiles, due to the larger dimensions of the amphiphiles and their lower critical aggregation concentration.[18, 22, 23]

In a similar fashion to the low molecular weight amphiphiles, cross-linking of vesicle membranes built up from block copolymers has been studied.[24, 25] One approach has been developed in the group of Meier; they made use of poly(2-methyloxazoline)-*b*-poly(dimethylsiloxane)-*b*-poly(2-methyloxazoline) (PMOXA-PDMS-PMOXA) triblock copolymers carrying methacrylate groups at both chain ends.[26] After formation of the vesicular morphologies in aqueous solutions, the methacrylate end groups were polymerized within the aggregate using a UV-induced free radical process. The cross-linking did not lead to morphological modifications of these polymersomes as evidenced by light scattering and electron microscopy techniques (Figure 3 a). Discher and coworkers have prepared giant polymersomes of poly(ethylene oxide)-*b*-polybutadiene (PEO-PBD) and cross-linked them by free radical polymerization as well.[28] The resulting particles proved to be exceptionally stable in chloroform and could also be dehydrated and re-hydrated without destroying the membrane core. Experiments using the micropipette aspiration technique demonstrated that the surface elastic modulus of these polymersomes was many orders of magnitude higher than that of lipid membranes (Figure 3 b).[18]

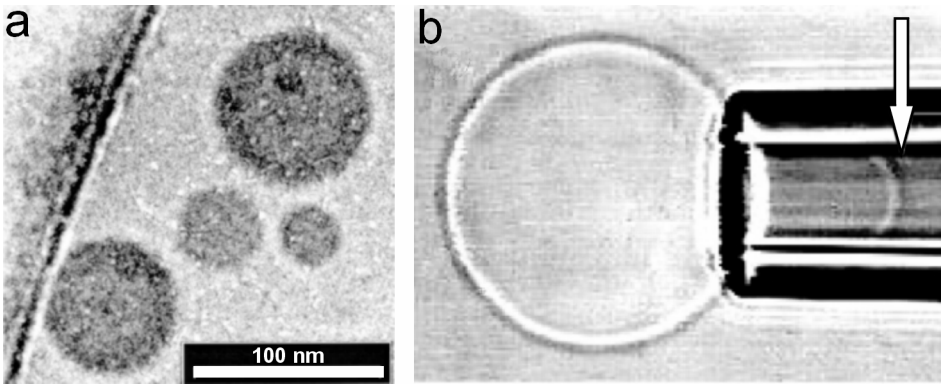

Figure 3. *Micrographs of cross-linked polymersomes of a) PMOXA-PDMS-PMOXA,[27] and b) PEO-PBD.[18] A part of the polymersome membrane is sucked into a micropipette to determine the surface elastic modulus.*

Compared to polymerizable phospholipids or to the triblock copolymers described by Meier *et al.*, the use of polybutadiene offers many more reactive groups for cross-linking and consequently makes the system much more stable. Organic/inorganic hybrid polymersomes, built up from poly(ethylene oxide)-*b*-poly(3-trimethoxysilyl)propyl methacrylate), have been stabilized using another method, namely a polycondensation reaction after hydrolysis of the trimethoxysilyl groups.[29]

In Nijmegen diblock copolymers based on styrene and isocyanopeptides have been prepared and in these macromolecules the polyisocyanide block forms a rigid rod segment.[17] These block copolymers were found to self-assemble into super helices as a result of the chirality of the head group-forming polyisocyanide; a right-handed polyisocyanide resulted in a left-handed super helix and vice versa. In addition, these polymeric amphiphiles were found to form polymersomes and bilayer fragments.

A helix is the most favorable conformation for the polyisocyanide backbone due to steric hindrance between its side groups.[30] When they are sufficiently bulky the polymer is locked in its helical conformation. The rigidity of polyisocyanides can be further increased by making use of amino acids as side groups in the polymers, as a result of which hydrogen bonding arrays are formed within the polymer strands.[31]

In this chapter polymersomes with an electron conducting membrane are described. They are prepared by cross-linking the thiophene functions in the membrane of polymersomes constructed from polystyrene-*b*-poly(isocyanoalanine(2-thiophen-3-yl-ethyl)amide) (PS-PIAT) (Figure 4).

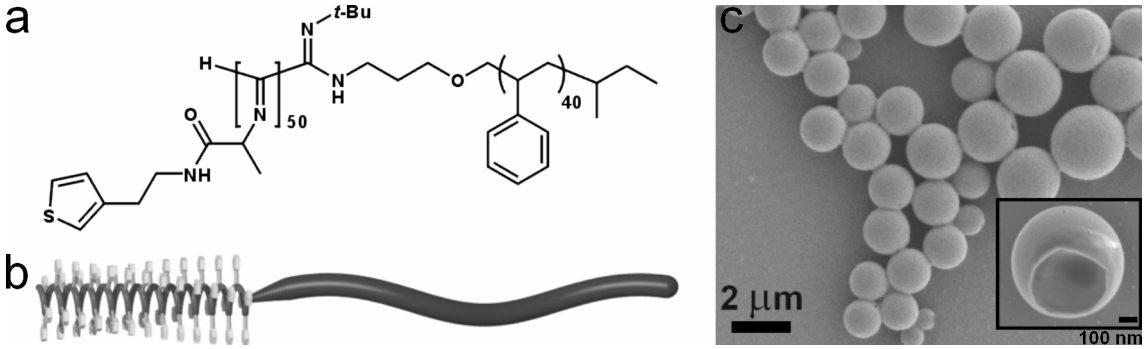

Figure 4. *a) Structure formula and b) schematic representation of PS-PIAT. c) SEM micrograph of PS-PIAT polymersomes.*

Conducting polymersomes are of great interest since they can provide a protective conducting shell for the encapsulation of solutes, e.g. redox compounds, allowing the development of redox active systems that can be used in sensory applications. Until now no publications have appeared that describe electron conducting polymersomes. In living systems biological redox reactions that occur in the cell membrane are well known.[1] Electrochemical gradients across mitochondrial membranes are maintained by the transport of electrons and protons through the membrane bilayer via naturally occurring ubiquinones. In the literature several systems have been described that deal with transmembrane electron transfer in vesicles. In general, two approaches can be distinguished, viz. the use of mediators such as viologens,[32] or fully conjugated, membrane spanning molecules that function as a molecular wire.[33] With these systems electrons produced outside the vesicle can be transferred to its interior to reduce encapsulated substrates. In the case of PS-PIAT, by cross-linking the thiophenes after vesicle formation, a conducting outer skin (and also inner skin) can be formed, which may lead to potentially useful applications.

4.2 Results and Discussion

4.2.1 Electrochemical cross-linking

Computer modeling studies performed on PIAT revealed that it is possible to form four columns of polythiophenes in a parallel fashion to the polyisocyanide backbone without large deviations of the helical conformation of this polymer. The computer generated structure of the polymer showed that at least five thiophene groups, connected to the polyisocyanide backbone, could be linked together without significant alterations in the

helical arrangement of the polyisocyanide backbone. These studies revealed that the pentamer did not adopt a planar configuration. Planarity is a pre-requisite for good electron conductivity (Figure 5).

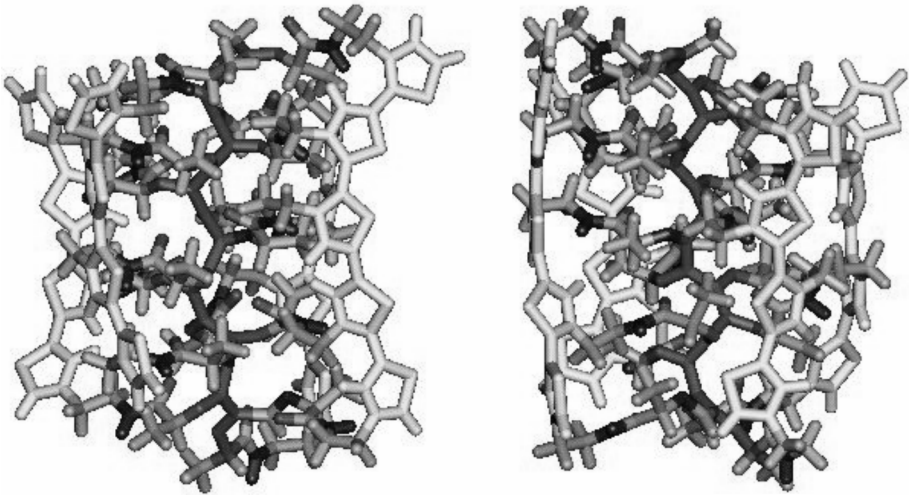

Figure 5. *Computer modeled images of a block of PIAT, having the thiophene groups polymerized.*

When the polymerization of thiophenes is carried out in the polymersome membrane, the probability of coupling thiophenes from neighboring diblock copolymers is high and will lead to cross-linking of the whole polymersome membrane surface. Each diblock copolymer possesses around 30 thiophene groups, making it highly likely that cross-linking will occur. In Figure 6 various possibilities of thiophene coupling are shown.

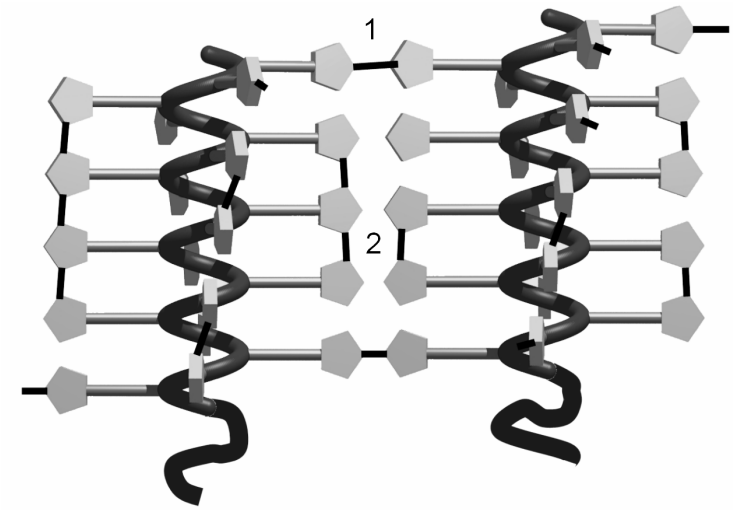

Figure 6. *Schematic impression of the different possibilities of inter- (1) and intramolecular (2) thiophene coupling in neighboring PIAT blocks.*

The most commonly used method to prepare polythiophenes is oxidative anodic electropolymerization, because it has several advantages. These are: (*i*) the absence of a catalyst, (*ii*) direct grafting of the conducting polymer onto the electrode surface occurs, and (*iii*) the possibility to directly monitor and characterize the growing polymer film.[34] In suitable electrolyte solutions, either aqueous or non-aqueous, the polythiophenes can be formed at a constant potential, at a constant current, or by cycling the potential.[34]

In a first series of experiments polymerization of the thiophene functions in the skin of PS-PIAT polymersomes formed in water was investigated by electrochemical anodic oxidation. Initially, blank experiments with *N*-formyl-L-alanine(2-thiophen-3-yl-ethyl)amide **(**FAT**),** using cyclic voltammetry, were carried out to estimate the oxidation potential necessary for thiophene polymerization inside the polymersomes; this potential amounted to 1.55 V (vs. ferrocene/ferrocenium) (Fc/Fc^+). Upon increasing the number of cycles in this experiment the heights of both the oxidation and reduction peaks increased, indicating the formation of a polymer on the surface of the electrode (Figure 7 a).

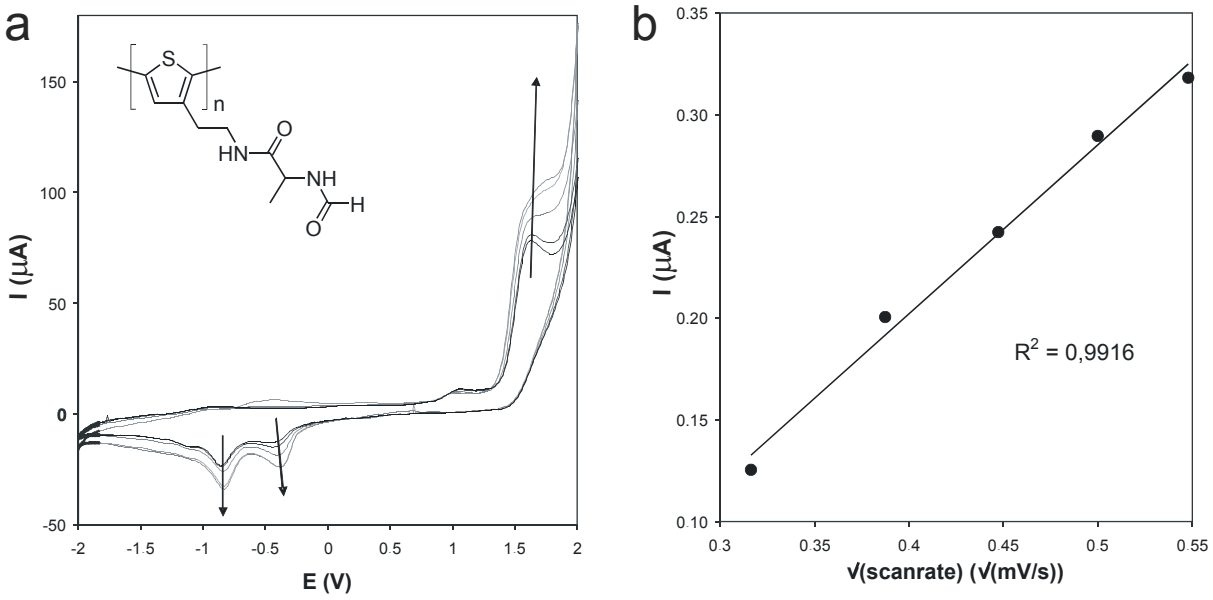

Figure 7. *a) Cyclic voltammograms of FAT. The increasing peak heights indicate the formation of a polymer on the electrode. The structure in the left corner is that of PFAT. b) Plot of the current against the square root of the scan rate. The straight line is indicative for the formation of a conductive polymer.*

The electrode on which poly(*N*-formyl-L-alanine(2-thiophen-3-yl-ethyl)amide **(**PFAT) was formed, was placed in a fresh electrolyte solution and the grafted polymer was analyzed with increasing scan rate, which is the rate of potential variation. In these experiments the

scan rate was varied from 100 to 300 $mV.s^{-1}$. For PFAT a linear relationship was found between the oxidation peak height and the square root of the scan rate. (Figure 7 b), which is indicative for a diffusion controlled process of electron transfer from the polymer to the electrode.[35, 36] If a linear relationship is observed between the current and the scan rate, the process is kinetically controlled.[37]

Electrochemical cross-linking polymerizations of the thiophene groups in polymersomes of PS-$PIAT_{50}$ were subsequently carried out by drying a drop of a polymersome dispersion in water/THF (5:1, v/v) on an indium tin oxide (ITO) plate, which served as the working electrode in the electrochemical setup. This plate was submersed into an acetonitrile solution containing an electrolyte together with a reference and a counter electrode. A constant potential of 1.6 V was applied to the ITO plate for 60 s. SEM studies on the ITO plates after polymerization showed that the polymersomes were highly deformed, due to extensive intervesicular cross-linking, indicating that the polymerization of the thiophene groups readily occurred, but not in a selective fashion (Figure 8).

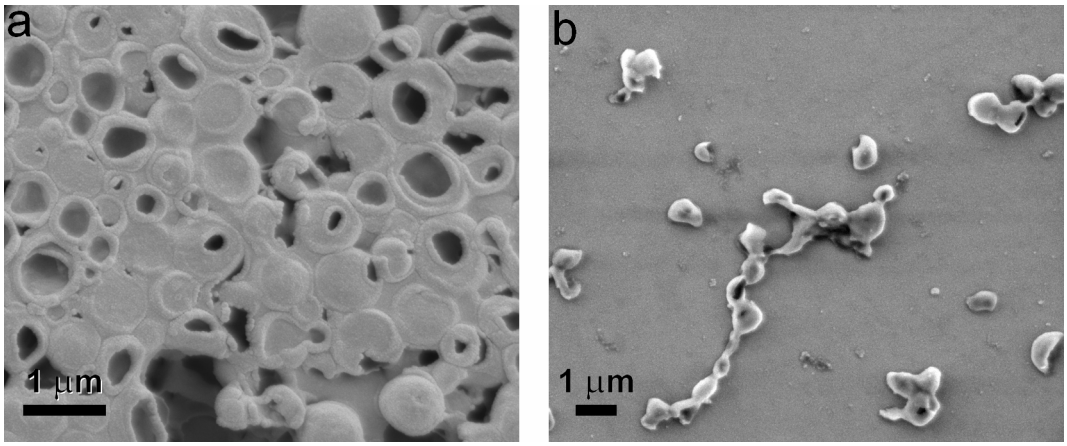

Figure 8. *SEM micrographs of the structures formed after electrochemical cross-linking polymerization of the thiophene groups inside polymersomes of PS-$PIAT_{50}$ on an ITO plate.*

In separate experiments, as described in Chapter 3, it was confirmed that the shape change of the polymersomes was not due to the presence of the solvent acetonitrile. Although the polymersomes were observed to shrink in this solvent, no collapse or degradation of the membranes was seen.

4.2.2 Chemical oxidative cross-linking

Since electrochemical cross-linking of the thiophenes within the polymersome membranes of PS-PIAT resulted in the disruption of the polymersomes, it was decided to abandon this method. In order to achieve more control during cross-linking, chemical oxidation was investigated. Attempts were made to use iron(III) chloride ($FeCl_3$), a known polymerization agent for thiophenes, in combination with polymersomes prepared in chloroform. No polymerization of the thiophene groups could be observed, however, with IR spectroscopy. TEM studies on these samples revealed that only small polymersomes had been formed, containing entrapped $FeCl_3$ with high concentrations located near or in their membranes, as judged by the differences in transmission (Figure 9).

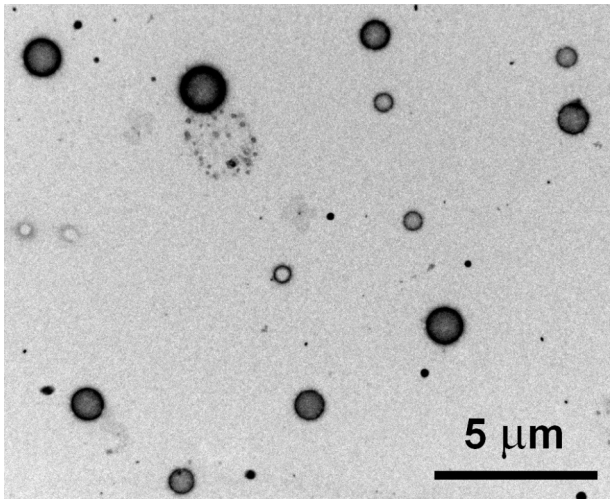

Figure 9. *TEM micrograph of polymersomes of PS-PIAT$_{50}$ prepared in a $CHCl_3$ dispersion containing $FeCl_3$.*

It has been reported that polymerization of thiophene groups occurs at active sites on the surface of solid $FeCl_3$, while dissolved $FeCl_3$ is inactive.[38] This approach is therefore incompatible with a dispersion of polymersomes. For the polymersomes in aqueous solutions $FeCl_3$ would not be suitable, since this complex is inactive as cross-linker in water. Ultimately, the complex [bis(2,2'-bipyridine)ruthenium(II)bis(pyrazolyl)] (BRP) was chosen as a possible catalyst for cross-linking in water from a long list of oxidation catalysts, because of its ideal oxidation potential.[39] It is soluble in hot water, but insoluble in dichloromethane. BRP is a strong base and the pK_a of the conjugate acid $[(bpy)_2Ru(pz)(pzH)]^+$ ($BRPH^+$) is probably > 13 (Scheme 1).[40]

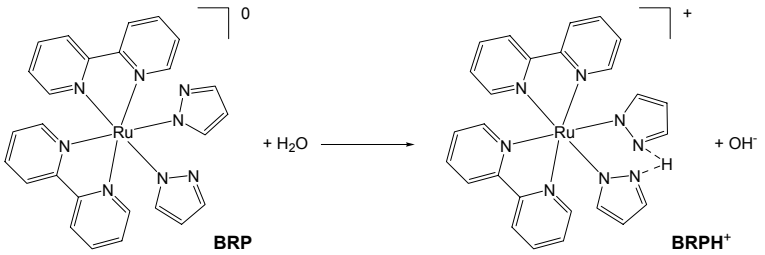

Scheme 1. *In the presence of water, BRP takes up a proton and forms $BRPH^+$.*[40]

In water BRP extracts a proton, forming $BRPH^+$, in which the proton interacts with both pyrazole groups by hydrogen bonding. The pK_a of $BRPH_2^{2+}$ is considerably lower and the latter species is deprotonated even by very weak bases to give back the $BRPH^+$. The oxidation potential of $BRPH^+$ is 1.60 V (vs. Fc/Fc^+), which makes it suitable to polymerize the thiophene groups in PS-PIAT, which have an oxidation potential of 1.55 V (vs. Fc/Fc^+). Initial experiments revealed that $BRPH^+$ is a good polymerization catalyst for other thiophenes, *e.g.* 3-dodecyl-thiophene. Polymersomes of PS-PIAT were prepared by injecting a THF solution of the diblock copolymer into an aqueous solution of BRP at 70°C. A concentration of BRP was chosen that was comparable to the amount of thiophene groups present (2×10^{-7} M).[41] The cross-linking was carried out at elevated temperatures (70°C) to increase the solubility of the metal complex. After standing for three days, SEM studies were carried out, which showed that well-formed polymersomes, retaining their original spherical shape were present (Figure 10 a).

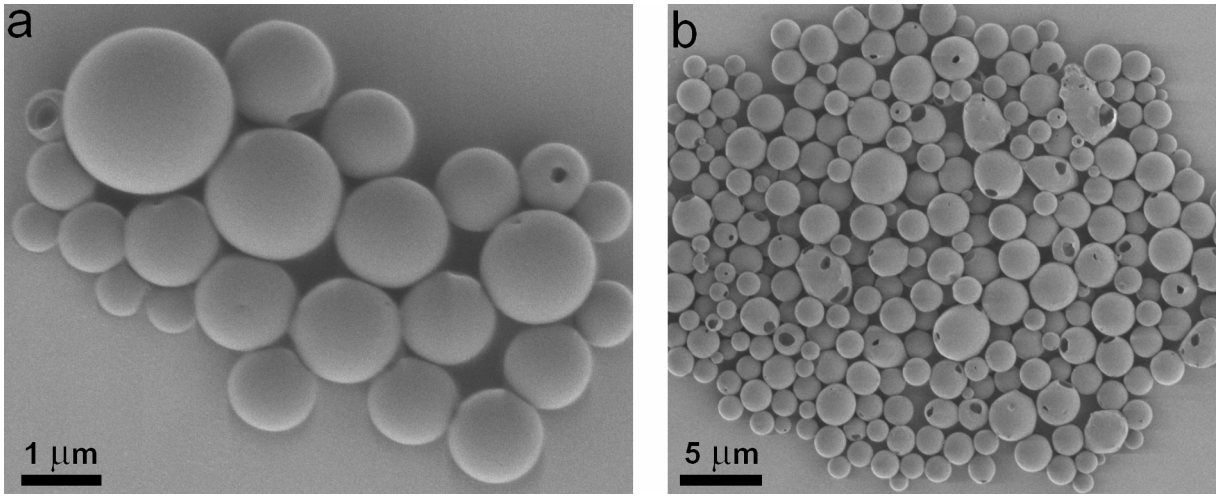

Figure 10. *SEM micrographs of PS-$PIAT_{50}$ polymersomes cross-linked using different concentrations of $BRPH^+$. a) [BRP] = 2×10^{-7} M, b) [BRP] = 2×10^{-6} M. At this concentration many polymersomes with defects can be seen.*

It is presumed that $BRPH^+$ will reside in the polar region of the polymersome membrane at room temperature, because its solubility in water of ambient temperature is very limited. Once in the membrane the complex is able to cross-link the large number of thiophene groups present. When a 10 times higher concentration of BRP was used, polymersomes, which possessed a large number of membrane defects (Figure 10 b), were formed, presumably due to accumulation of this complex inside the polymersome membrane. The observed behavior is very reminiscent to that observed for the addition of salts to polymersomes (see Chapter 3).

The generally accepted mechanism for the oxidative coupling of thiophenes is that of a process involving radicals, in an analogous way to the electrochemical polymerization of this compound.[42] Currently, the only method to prepare polythiophenes in a chemical oxidative manner, is by using $FeCl_3$, which, as mentioned earlier, acts as a heterogeneous catalyst. The advantage of $BRPH^+$ is the low amount of catalyst required, whereas in the case of $FeCl_3$ a 3- to 4-fold excess is necessary.[39] Due to the low concentrations of thiophene groups used during the cross-linking of the polymersomes it was difficult to identify the structure of the Ru complex after the reaction, making that the mechanism of polymerization of the thiophenes by $BRPH^+$ cannot be yet elucidated.

The presence of polythiophene was investigated by electrochemical measurements on a sample of dried-in polymersomes. The polymersomes showed a new oxidation peak at 0.523 V (vs. Fc/Fc^+), and a broad reduction peak at 0.23 V ($E^{1/2}$ = 0.38 V), indicative of the presence of polymerized thiophene groups (Figure 11).[43] Infrared studies on the same sample revealed a new vibration at 802 cm^{-1}, again confirming the presence of polythiophene in the polymersomes.[44] In order to definitively prove the formation of cross-linked polymersomes, fluorescence experiments were carried out on single polymersomes deposited on a surface, formed with and without $BRPH^+$. Due to scattering effects, it was not possible to record a UV-Vis spectrum of a single polymersome or a suspension of polymersomes. However, the presence of cross-linked polymersomes could be confirmed by fluorescence spectroscopy upon excitation at 460 nm (Figure 12 a). The emission spectrum of a single polymersome cross-linked using the ruthenium complex $BRPH^+$ displayed a maximum at 725 nm (Figure 12 b, black trace).

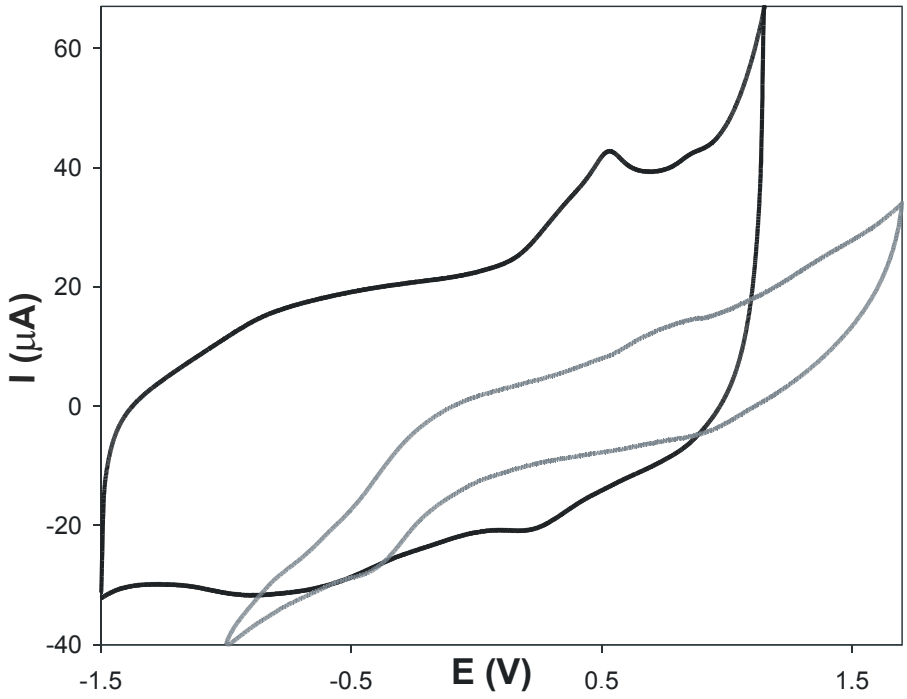

Figure 11. *Cyclic voltammograms of polymersomes before (grey trace) and after cross-linking (black trace) with $BRPH^+$; the scan-rate was 250 $mV.s^{-1}$ (potential vs. Fc/Fc^+).*

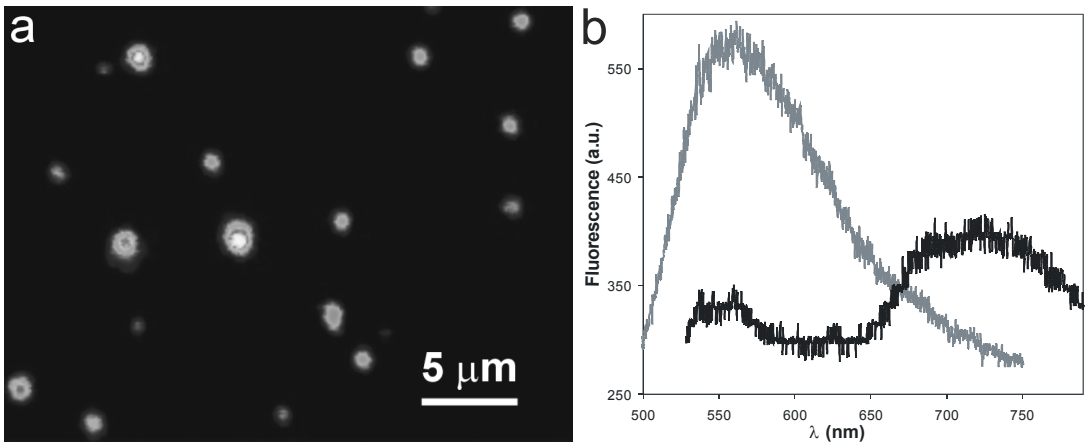

Figure 12. *Single polymersome fluorescence spectroscopic studies on cross-linked PS-PIAT polymersomes dried on glass. a) Observed fluorescence micrograph of polymersomes, b) emission spectra of polymersomes before (grey) and after cross-linking (black) ($\lambda_{exc.}$ = 460 nm).*

Blank experiments confirmed that this shift in emission was in agreement with the presence of polymerized thiophene groups and not due to the ruthenium complex.[43] Interestingly, single polymersomes before cross-linking also displayed an emission spectrum, viz. with a maximum located at 550 nm (Figure 12 b, grey trace). This fluorescence cannot be attributed to the monothiophene functions in the side groups, because they are known not to

exhibit any fluorescence. Instead, the fluorescence is thought to originate from domains of conjugated imine groups in the polyisocyanide backbone, as a result of partially unfolded chains or small defects in the strands, which are emissive when excited at 460 nm. The helical arrangement of polyisocyanides is probably not the thermodynamically most stable state, and when the backbone unfolds the imine groups can adopt a more planar orientation in which they become conjugated. In Chapter 2 this phenomenon was also described for PIAT homopolymers.

4.2.3 Patch clamp technique

The direct measurement of the electron conductivity of cross-linked PS-PIAT polymersomes would give considerable insight in the cross-linking efficiency, e.g. if the complete surface of the polymersomes is conductive, or whether only domains are formed in the membrane, capable of transporting electrons. Due to the dimensions of PS-PIAT polymersomes, the direct determination of the conductivity before and after cross-linking cannot be readily carried out. Scanning probe techniques, e.g. atomic force microscopy (AFM), with electrochemical tips, and scanning tunneling microscopy (STM), have the potential to measure such conductivities. The latter technique has the disadvantage that the distance between the tip and the surface is normally less than 1 nm. Since the PS-PIAT polymersomes have an average diameter of 1.5 μm, the possibility to detect a tunneling current between the tip and the surface is very small. The use of an electrochemical AFM in these measurements would also not be trivial, again due to the large dimensions of the polymersomes.

One approach to measure conductivities, developed for the micrometer regime, is the micropipette method, better known as the “patch clamp” technique. It was developed in the mid 1970’s by the German scientists Neher and Sakmann, who received the Nobel Prize in 1991 for their work, and has revolutionized the study of ion channels in cell membranes.[45] With this technique, transport through a single ion channel protein can be recorded and the ion flux measured. For this purpose a micropipette is placed on the cell wall with the help of a micromanipulator (Figure 13). The micropipette is connected to a tube and by suction either a patch is removed from the membrane or a pore is created in the cell and an insulating seal is formed around the micropipette. This seal is essential to prevent any side effects during the measurements (Figure 13 a). The micropipette is equipped with an electrode sensitive enough

to detect minute changes in potential. In a normal setup, cells are submersed in a well filled with a physiological buffer solution, and mounted under a light microscope (Figure 13 b).

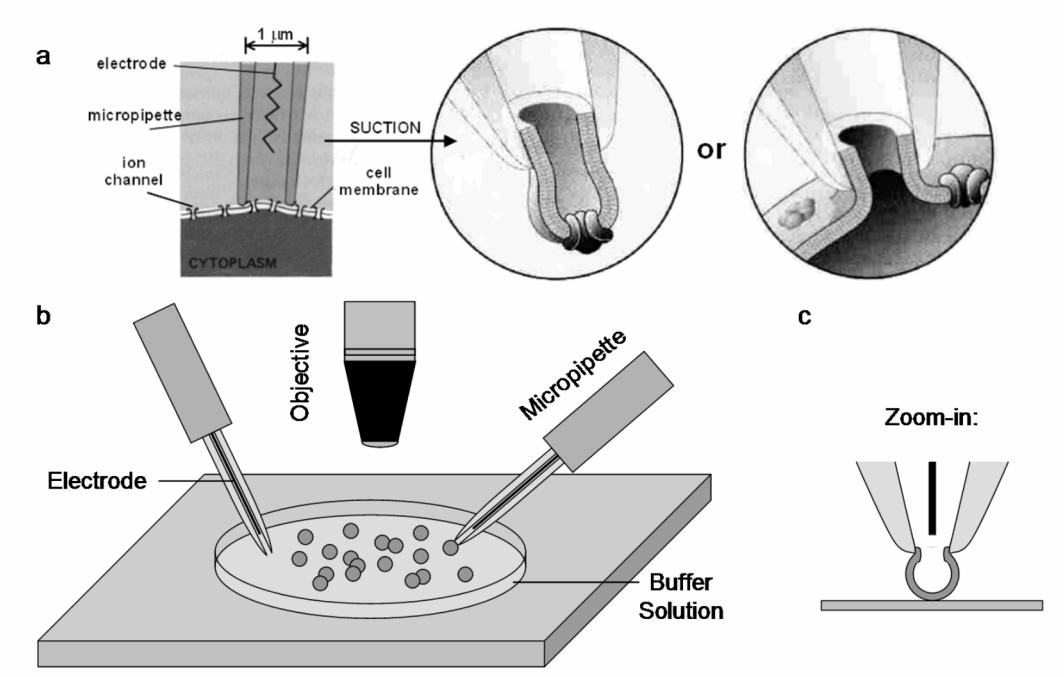

Figure 13. *a) Schematic representation of a patch clamp setup in which a micropipette is placed on the cell wall and by suction either a patch is taken from the membrane or a pore is created in the cell wall. b) Schematic drawing of the patch clamp setup used to measure the PS-PIAT polymersomes. c) Zoom-in of the side-view of a clamped polymersome.*

Using the patch clamp approach, it would in principle be possible to determine the conductivity of the polymersome membrane when a difference in potential would be created between an electrode in an electrolyte solution and a micropipette fitted with an electrode placed on the membrane of a polymersome, which is also filled with an electrolyte solution. As already mentioned, an insulating seal is formed around the micropipette on the membrane. In order for electrons to reach the electrode in this micropipette they have to pass the polymersome membrane, which is only possible when it is conductive. For this purpose cross-linked polymersomes of PS-PIAT were dried on microscopy glass and placed in the well of the microscope. After positioning the micropipette on the surface of a polymersome, attempts were made to suck the membrane into the micropipette, but these experiments failed as a result of the higher membrane toughness of the PS-PIAT polymersomes compared to phospholipid based cell membranes (Figure 14).

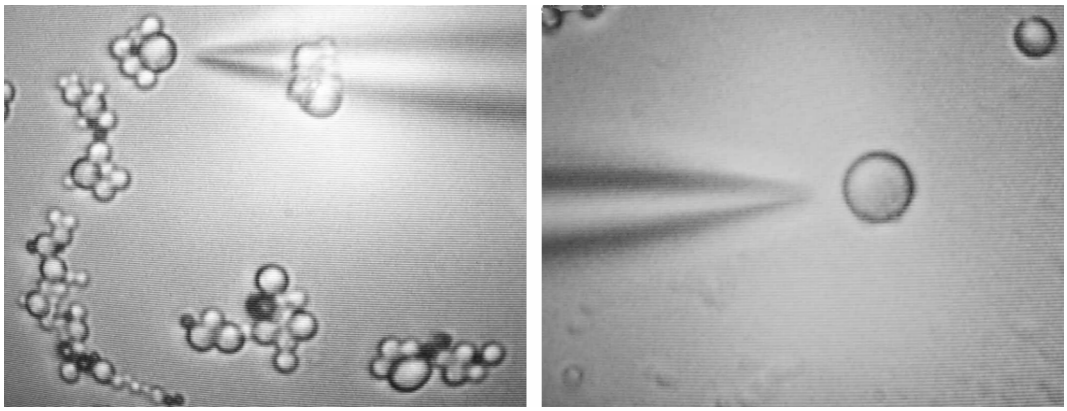

Figure 14. *Optical micrographs of a micropipette on the surface of a PS-PIAT polymersome.*

It must be noted that the vacuum created in the micropipette is by manual suction which is not sufficient enough to form a pore in the membrane. While a micropipette easily penetrates the wall of a cell without any damage to the rest of the wall, it was impossible to do so for the polymersomes of PS-PIAT, even not for the non-polymerized ones. The fluidity of cell membranes is much higher than the fluidity of the wall of these polymersomes, which is the result of the polystyrene blocks in PS-PIAT being in the glass state at room temperature. It would be more convenient to place two bare electrodes on the polymersome surface and measure the conductivity after applying a potential between the electrodes. This is impossible, however, because the diameters of the electrodes are too large (~1 mm).

4.2.4 Bulk resistivity measurements

Due to the difficulties in measuring the conductivity of a single polymersome, a bulk technique was subsequently chosen. Simple conductivity measurements on these polymersomes before and after cross-linking were carried out by drying a drop of a polymersome dispersion between two ITO plates with their conducting sites facing each other. By using a simple multimeter the resistivity between the two plates was measured (Figure 15). The measured difference in resistivity for polymersomes before and after cross-linking was significant, see Table 1.

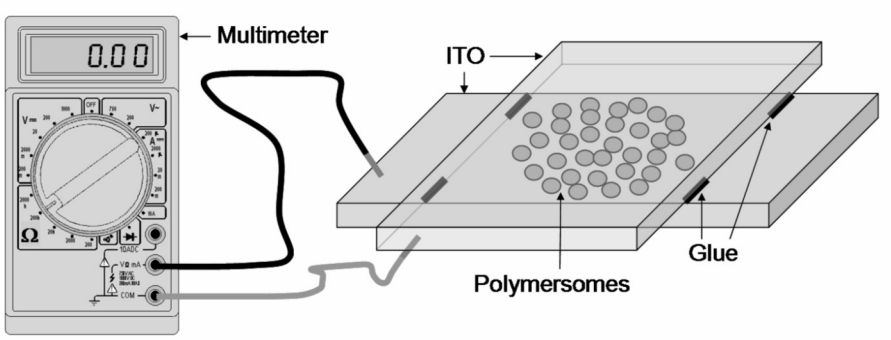

Figure 15. *Set up for the measurement of the bulk resistivity of dried polymersomes using two ITO plates.*

Table 1. ***Difference in resistivity between PS-PIAT polymersomes before and after cross-linking***

Polymersomes	Before doping	After doping[a]
non-cross-linked	120×10^6 Ω	40×10^6 Ω
cross-linked	150×10^3 Ω	6.2×10^3 Ω

[a] I_2 was used to dope the polymersomes.

The values of the resistivity of the polymersomes before cross-linking were almost three orders of magnitude higher than after cross-linking. The observed difference in resistivity is thought to be a direct result of the formation of conducting pathways involving polymerized thiophene groups in the polymersome membranes upon cross-linking. Blank experiments confirmed that the measured differences in resistivity were a direct result of the different polymersome architectures. Two ITO plates glued together had a resistivity of less than 1 Ω, while two ITO plates glued together with a plastic spacer of 1 μm in between had an infinite resistivity. After doping of the polymersomes between the ITO plates with I_2, the resistivity dropped further to 40×10^6 Ω for non-cross-linked polymersomes and to 6.2×10^3 Ω for cross-linked polymersomes, which corresponded to a 3- and 24-fold decrease in resistivity respectively. This significant reduction in resistivity after doping of the cross-linked polymersomes strongly suggests the presence of large arrays of conjugated polythiophene chains over the complete surface of the polymersomes. The three-fold decrease in resistivity for non-cross-linked polymersomes might be due to doping of polythiophenes formed by autopolymerization.

Great caution needs to be taken with above results, because no estimation can be made about the number of polymersomes that are conductive. The electrons have to cross a distance

of at least 1 μm, which means that a single chain mechanism can be excluded, therefore, many polymer chains are probably involved in the electron transport. It is very well possible that all polymersomes have large conductive domains in their membrane, but when a polymersome is touching the ITO plates with a non-cross-linked part of its membrane it is inactive in electron transport. Any comparison with values of systems reported in the literature is therefore not possible.

Additional proof for the conductivity of these polymersomes was obtained by SEM studies carried out on cross-linked polymersomes dried on an ITO plate. A standard procedure with SEM studies is to coat samples before study with a conducting metal layer to prevent damage to the samples due to charging by energy rich electrons. It was observed, however, that cross-linked PS-PIAT polymersomes did not require such a layer, as a result of their conductive surface, whereas non-cross-linked PS-PIAT polymersomes turned black upon irradiation unless they were pre-coated with Pd/Au.

4.3 Conclusions

The results presented in this chapter show that the thiophene groups of PS-PIAT can be polymerized, either electrochemically or chemically, while this diblock copolymer is aggregated into a vesicular architecture. The latter method proved to be the most suitable one, because it did not alter the morphology of the polymersomes, in contrast to the former method. The presence of polythiophene chains was proven by different techniques, e.g. IR spectroscopy, electrochemistry and single polymersome fluorescence.

Several methods were tried to determine the conductivity of these polymersomes after cross-linking. Their resistance was measured between two ITO plates containing either cross-linked or non-cross-linked PS-PIAT polymersomes. These studies revealed that the cross-linked polymersomes had a much lower resistance. When the polymersomes were doped with I_2 the difference in resistance between the polymersomes before and after cross-linking was even larger.

The present systems may find various applications. For instance, in the case of encapsulation of redox active compounds, such as redox enzymes, the electron conductive properties of the polymersome membranes might be used to switch on or off reactions, e.g. by applying an external potential, or to transport electrons produced within the polymersomes.

The cross-linked polymersomes also form a cage of Faraday and as such they can protect electrostatically sensitive particles.

4.4 Experimental Section

General methods and materials

THF was distilled over sodium, $CHCl_3$ over $CaCl_2$, and acetonitrile over CaH_2. For the aggregation studies in aqueous solutions ultra pure water ($R > 18\times10^6$ Ω) was used. The synthesis of FAT and PS-PIAT are described in Chapters 2 and 3 respectively, while BRP was prepared following a procedure from the literature.[40] All other chemicals were used as received, unless stated otherwise. Infrared spectra were recorded on a BioRad FTS 25 spectrometer. A Varian Cary 50 spectrophotometer was used to measure UV-Vis spectra. TEM and SEM studies were performed with JEOL JEM-1010 and JEOL JSM-6330F instruments respectively. Samples for TEM were dropped on carbon-coated copper grids and dried for several hours in the fume hood. The SEM samples were prepared by drying a drop of a dispersion on a clean substrate, which was left to dry in the fume hood before a 1.5 nm layer of Pd/Au was applied using a Cressington 208 HR sputter coater fitted with a Cressington layer thickness controller.

Electrochemical experiments

An electrochemical cell was used, fitted with an $Ag/AgNO_3$ reference electrode, and platinum counter and working electrodes, of which the potential was varied. The experiments were conducted in an acetonitrile solution containing 0.10 M tetrabutylammonium hexafluorophosphate as the electrolyte. The electrodes were calibrated using ferrocene. All measurements were carried out under an inert atmosphere of N_2. The potentiostat used in these measurements was an Eco Chemie Autolab PGSTAT10.

FAT was polymerized by cycling the voltage 50 times from -2.0 to 2.0 V with a scan rate of 100 $mV.s^{-1}$, using a Pt working electrode. After refreshing the electrolyte solution the polymer formed on the working electrode was studied at various scan rates to determine its conductivity.

Cross-linking of PS-PIAT polymersomes was performed by drying a drop of a 0.10 $mg.ml^{-1}$ dispersion in water/THF (5:1, v/v) on an ITO plate and using this plate as the working electrode on which a constant potential of 1.6 V was applied. The resulting polymersomes on the ITO plates were examined by SEM.

Chemical oxidative cross-linking

BRP

Polymersomes of PS-PIAT were prepared by injecting a 0.50 $mg.ml^{-1}$ solution of this diblock copolymer in THF into a solution of 2.0×10^{-7} M BRP in ultra-pure water at 70°C. After 5 min. the dispersion was left for 1 h to cool down to room temperature. A drop of the resulting dispersion was dried on a Pt electrode to carry out the cyclic voltammetry measurements, in order to prove the presence of polythiophene in the polymersomes. This electrode was then used as the working electrode. The scans were made at a scan rate of 250 $mV.s^{-1}$ from -1.5 to 1.15 V.

$FeCl_3$

To a dispersion of 4.0 mg PS-PIAT in 8.0 ml $CHCl_3$, 5.0 mg $FeCl_3$ was added, resulting in a change of color from faint yellow to deep yellow. After 10 min. samples were prepared for TEM studies.

Single polymersome fluorescence

The fluorescence studies on single polymersomes were performed with a home built setup fitted with an argon ion laser beam, operating at 458 nm. The laser light was focused by a 25× microscope objective to a 50 μm diameter spot on the sample. The fluorescence emission was imaged by a 50× objective on a CCD camera.

Bulk conductivity measurements

A drop of a dispersion containing cross-linked PS-PIAT polymersomes, prepared as described above, was dried on an ITO plate and a second ITO plate was glued on top of it. The resistance between the ITO plates was measured with a Digi-Tool Digi-16 multimeter.

4.5 References and Notes

[1] L. Stryer, *Biochemistry*, W. H. Freeman, New York, **1988**.
[2] P. L. Luisi, P. Walde, T. Oberholzer, *Curr. Opin. Colloid Interface Sci.* **1999**, *4*, 33.
[3] A. D. Bangham, R. W. Horne, *J. Mol. Biol.* **1964**, *8*, 660.
[4] R. R. C. New, *Liposomes: a practical approach*, Oxford University Press, Oxford, **1990**.
[5] A. D. Bangham, *Chem. Phys. Lipids* **1993**, *64*, 275.
[6] B. D. Smith, T. N. Lambert, *Chem. Commun.* **2003**, 2261.
[7] J. M. Boon, B. D. Smith, *Med. Res. Rev.* **2002**, *22*, 251.
[8] W. T. Keeton, C. Hardy McFadden, *Elements of biological science*, third ed., W. W. Norton, New York, **1983**.
[9] H. Ringsdorf, B. Schlarb, J. Venzmer, *Angew. Chem. Int. Ed. Engl.* **1988**, *27*, 113.
[10] B. A. Armitage, D. E. Bennett, H. G. Lamparski, D. F. O'Brien, *Adv. Polym. Sci.* **1996**, *126*, 53.
[11] G. E. Lawson, Y. Lee, A. Singh, *Langmuir* **2003**, *19*, 6401.
[12] B. J. Ravoo, W. D. Weringa, J. B. F. N. Engberts, *Langmuir* **1996**, *12*, 5773.
[13] Y. Okahata, T. Kunitake, *J. Am. Chem. Soc.* **1979**, *101*, 5231.
[14] J.-H. Fuhrhop, K. Ellermann, H. H. David, J. Mathieu, *Angew. Chem. Int. Ed. Engl.* **1982**, *21*, 440.
[15] J. C. M. van Hest, D. A. P. Delnoye, M. W. P. L. Baars, C. Elissen-Roman, M. H. P. van Genderen, E. W. Meijer, *Chem. Eur. J.* **1996**, *12*, 1616.
[16] L. Zhang, A. Eisenberg, *Science* **1995**, *268*, 727.
[17] J. J. L. M. Cornelissen, M. Fischer, N. A. J. M. Sommerdijk, R. J. M. Nolte, *Science* **1998**, *280*, 1427.
[18] B. M. Discher, Y.-Y. Won, D. S. Ege, J. C.-M. Lee, F. S. Bates, D. E. Discher, D. A. Hammer, *Science* **1999**, *284*, 1143.
[19] N. S. Cameron, M. K. Corbierre, A. Eisenberg, *Can. J. Chem.* **1999**, *77*, 1311.
[20] S. Jain, F. S. Bates, *Science* **2003**, *300*, 460.
[21] D. E. Discher, A. Eisenberg, *Science* **2002**, *297*, 967.
[22] R. Dimova, U. Seifert, B. Pouligny, S. Förster, H.-G. Döbereiner, *Eur. Phys. J. E* **2002**, *7*, 241.
[23] H. Bermudez, A. K. Brannan, D. A. Hammer, F. S. Bates, D. E. Discher, *Macromolecules* **2002**, *35*, 8203.
[24] W. Meier, *Chem. Soc. Rev.* **2000**, *29*, 295.
[25] F. Chécot, S. Lecommandoux, H.-A. Klok, Y. Gnanou, *Eur. Phys. J. E* **2003**, *10*, 25.
[26] C. Nardin, J. Widmer, M. Winterhalter, W. Meier, *Eur. Phys. J. E* **2001**, *4*, 403.
[27] C. Nardin, S. Thoeni, J. Widmer, M. Winterhalter, W. Meier, *Chem. Commun.* **2000**, 1433.
[28] B. M. Discher, H. Bermudez, D. A. Hammer, D. E. Discher, Y.-Y. Won, F. S. Bates, *J. Phys. Chem. B* **2002**, *106*, 2848.
[29] J. Du, Y. Chen, Y. Zhang, C. C. Han, K. Fischer, M. Schmidt, *J. Am. Chem. Soc.* **2003**, *125*, 14710.
[30] R. J. M. Nolte, *Chem. Soc. Rev.* **1994**, *23*, 11.

[31] J. J. L. M. Cornelissen, J. J. J. M. Donners, R. de Gelder, W. S. Graswinckel, G. A. Metselaar, A. E. Rowan, N. A. J. M. Sommerdijk, R. J. M. Nolte, *Science* **2001**, *293*, 676.
[32] L. Hammerström, H. Berglund, M. Almgren, *J. Phys. Chem.* **1994**, *98*, 9588.
[33] S.-I. Kugimiya, T. Lazrak, M. Blanchard-Desce, J.-M. Lehn, *J. Chem. Soc., Chem. Commun.* **1991**, 1179.
[34] J. Roncali, *Chem. Rev.* **1992**, *92*, 711.
[35] A. J. Bard, L. R. Faulkner, *Electrochemical Methods*, John Wiley, New York, **1980**.
[36] M. Skompska, *Electrochim. Acta* **1998**, *44*, 357.
[37] A. R. Hillman, E. F. Mallen, *J. Electroanal. Chem.* **1991**, *309*, 159.
[38] V. M. Niemi, P. Knuutila, J.-E. Österholm, J. Korvola, *Polymer* **1992**, *33*, 1559.
[39] A. Juris, V. Balzani, F. Barigelletti, S. Campagna, P. Belser, A. Von Zelewsky, *Coord. Chem. Rev.* **1988**, *84*, 85.
[40] B. P. Sullivan, D. J. Salmon, T. J. Meyer, J. Peedin, *J. Inorg. Chem.* **1979**, *18*, 3369.
[41] By ^{1}H NMR the number average molecular weight was determined to be $(11 \pm 3)\times10^{3}$ g.mol^{-1}, which corresponds to 31 thiophene groups per molecule. In Chapter 3 further details are given.
[42] R. D. McCullough, *Adv. Mater.* **1998**, *10*, 93.
[43] D. Fichou, *Handbook of oligo- and polythiophenes*, Wiley-VCH, Weinheim, **1999**.
[44] D. Dini, F. Decker, F. Andreani, E. Salatelli, P. Hapiot, *Polymer* **2000**, *41*, 6473.
[45] B. Alberts, D. Bray, J. Lewis, M. Raff, K. Roberts, J. D. Watson, *Molecular biology of the cell*, second ed., Garland Publishing, New York, **1989**.

Chapter 5

Nanoreactors Based on Enzyme-Containing Diblock Copolymer Vesicles

5.1 Introduction

Enzymes are essential catalysts in many processes, both in nature and in industry. They combine high efficiency with high specificity. Although some enzymes, like the extremophiles, are known to withstand harsh conditions, i.e. high/low temperatures or extreme pHs, most enzymes are only active in a narrow environmental window, requiring buffered solutions, ambient temperatures and protection from harmful solutes.[1] How can enzymes be protected against denaturation and proteolysis while keeping them in a fully functional state? Nature has solved this problem by compartmentalization. Cells contain membranes which separate the enzyme-containing cell plasma from the environment. These membranes are involved in protection, transport and communication tasks in cells.[2]

A number of research groups have adopted immobilization of enzymes as a means to stabilize these biomacromolecules, but also to prepare recoverable and specific catalysts. The methods developed over the years to immobilize enzymes are numerous, and include covalent bonding to activated polymers, copolymerization with multifunctional reagents, physical adsorption, and entrapment in cross-linked polymer particles (Figure 1).[3] Much research has been focused on the use of artificial cell membranes to encapsulate enzymes and other biomolecules. For this purpose phospholipids and synthetic surfactants have been used, the objective being to construct models for living cell structures and to investigate biochemical processes involving enzymes.[4, 5] Advances have been made in realizing RNA replication,[6] polypeptide formation,[7] mRNA synthesis,[8] and protein synthesis[9] within vesicles and even the polymerase chain reaction could be performed.[10] It was shown that compartmentalization

had a pronounced effect on gene expression, which took place more efficiently inside vesicles than in solution, and on protection of the encapsulated compounds by attack of externally added proteases and nucleases.[9]

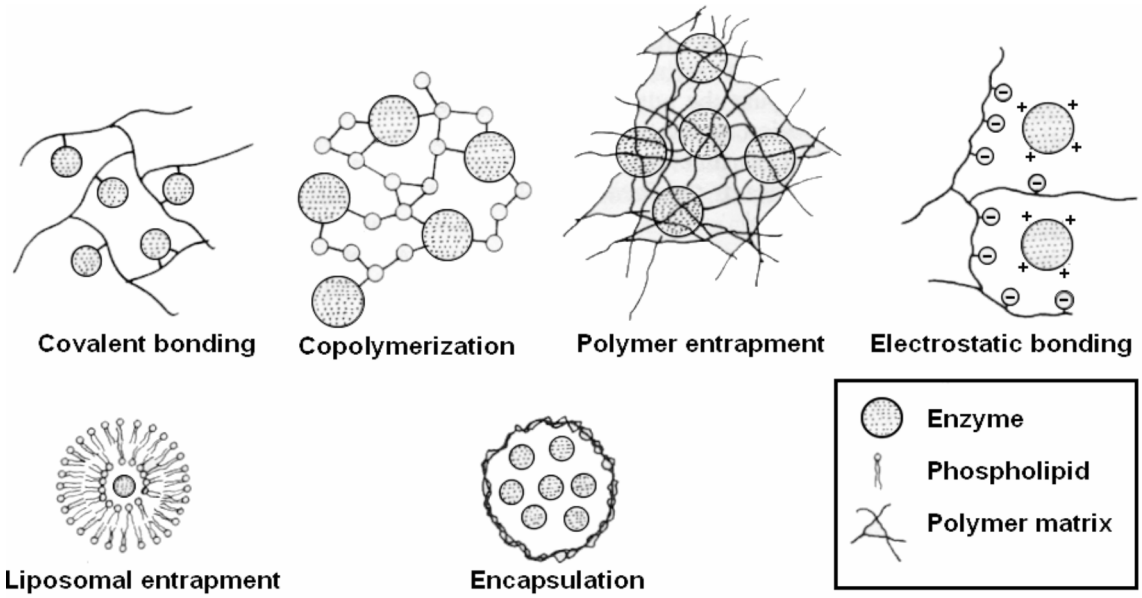

Figure 1. *Overview of possibilities to immobilize enzymes.*[3]

Enzymes have not only been encapsulated inside vesicles to mimic cell functions. Most applications utilize the vesicle as a container to release enzymes in a controlled manner.[11] Especially in the field of drug delivery much research has been carried out in the use of vesicular architectures. The encapsulated compounds can either be enzymes, pharmaceutics or genetic material. In the cosmetics industry vesicles are used in beauty products, e.g. skin creams.[12]

In most studies involving the encapsulation of enzymes, phospholipid-based vesicles, or liposomes, have been used. However, some studies also involved vesicles constructed from polymers. These so called polymersomes possess a higher membrane toughness than liposomes.[13] Furthermore, the rich diversity in available monomers and polymerization methods make it possible to precisely tune the properties of the resulting polymersomes. In Chapter 1 an overview was given of polymersomes containing enzymes. Two examples already mentioned in that chapter are discussed briefly below. Nardin *et al.* prepared polymersome nanoreactors of cross-linkable triblock copolymers which incorporated channel proteins in their membrane and encapsulated lactamase enzymes inside their water pool.[14] They showed that an externally added substrate was converted inside these polymersomes and that the channel protein activity was retained upon cross-linking of the membrane.

The compartmentalization of glucose oxidase enzymes within poly(ethylene glycol)-*b*-poly(propylene sulfide)-*b*-poly(ethylene glycol) (PEG-PPS-PEG) polymersomes led to the formation of oxidation-responsive capsules.[15] The hydrogen peroxide which is produced during the oxidation of glucose, oxidizes the thioether groups in the PPS block, resulting in destabilization of the polymersome membrane and thus release of its content. One drawback in the use of polymersomes is the increased membrane thickness which drastically reduces the permeability,[16] and thus the activity of the enzyme entrapped in the polymersomes.

In Chapter 3 it was discussed that the diblock copolymer polystyrene-*b*-poly(L-isocyanoalanine(2-thiophen-3-yl-ethyl)amide) (PS-PIAT) is able to form very stable and well-defined polymersomes in water and organic solvents (Figure 2).[17, 18]

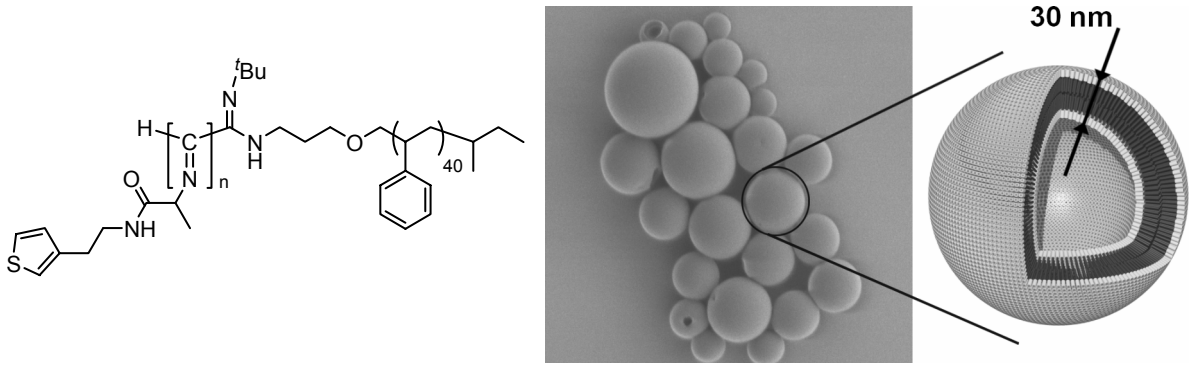

Figure 2. *Left: structure formula of PS-PIAT, middle: SEM micrograph of PS-PIAT$_{50}$ polymersomes formed in an aqueous solution, right: schematic representation of a polymersome, indicating the membrane thickness of 30 nm.*

This amphiphilic macromolecule contains a rigid helical polyisocyanide head group and a flexible polystyrene tail, making it a rod-coil type of diblock copolymer. The membrane thickness of 30±10 nm for polymersomes prepared from PS-PIAT$_{50}$ was determined by SEM by examining incompletely formed polymersomes. The thiophene side groups present in the side chain can be polymerized either electrochemically or by chemical oxidation, resulting in cross-linking of the polymersome membrane.[17] Initial studies have shown that the electron conducting properties of the PS-PIAT polymersomes improve after cross-linking.[19]

In this chapter we report on the encapsulation of three different enzymes inside polymersomes of PS-PIAT and on enzyme activity studies. It was discussed in Chapter 3 that the aggregation behavior of PS-PIAT depended on the amount of enantiomeric access of the isocyanide monomers during polymerization. In this chapter different PS-PIAT block

copolymers, varying in the ratio of L-isocyanoalanine(2-thiophen-3-yl-ethyl)amide) (L-IAT) and D-IAT, were used. The influence of cross-linking on the permeability of the enzyme-containing polymersomes has also been studied, namely by comparing the rates of substrate conversions as a function of degree of cross-linking.

5.2 Results and Discussion

5.2.1 Encapsulation of *Candida antarctica* lipase B

The possibility to encapsulate enzymes inside aggregates of PS-PIAT was first tested with *Candida antarctica* lipase B (CAL B, Figure 3a). This enzyme of 33 kDa has been well-studied both in aqueous solutions, where it hydrolyses esters, and in anhydrous organic solvents, in which it performs amidation, esterification, and transesterification reactions in an enantioselective manner.[20] Most lipases display almost no hydrolysis activity when they are in a dissolved state. In the absence of a (lipid) interface several varieties of the enzyme are in an inactive state, since a part of the enzyme, an α-helix, covers the active site. Upon contact with the hydrophobic interface the α-helix is folded back, thus allowing substrates to reach the active site.[20] The crystal structure of CAL B has revealed that this enzyme does not have a lid that shields the active site,[21] making it suitable for our studies. Lipases have been immobilized by anchoring them onto a solid support and by cross-linking them in order to increase their stability and to simplify recovery. The activity of immobilized CAL B is in general much higher than that of the free enzyme due to better solvatation and stabilization of the immobilized biomacromolecule.[22]

The encapsulation of CAL B was carried out by applying two different methods. In the first one injection was used as a tool,[23] and in the second one lyophilization.

5.2.1.1 Preparation of PS-PIAT/CAL B biohybrids via the injection method

The PS-PIAT used was prepared by polymerization of a mixture of 78 % L-IAT and 22 % D-IAT, as concluded from studies on the monomer using an HPLC equipped with a chiral column. It was determined by ^{1}H NMR that the PIAT block had a length of 31 units. A solution of PS-PIAT in THF was injected into an aqueous solution of CAL B. The solution became slightly turbid after injection and the non-encapsulated enzymes were removed by

filtration. When the dispersion was examined by TEM, dark and light polymersomes could be seen (Figure 3 b). In order to visualize the presence of the enzyme with a fluorescence microscope, CAL B enzymes were labeled with the fluorescent dye Alexa Fluor® 488 (Alexa-488). Again two types of polymersomes were observed: polymersomes that showed fluorescence and others that did not (Figure 3, c and d). From these combined experiments it was concluded that the dark polymersomes in the TEM micrographs contained entrapped enzymes and the light polymersomes were empty. Since not all polymersomes have closed membranes, enzymes inside these aggregates were washed out during the filtration step.

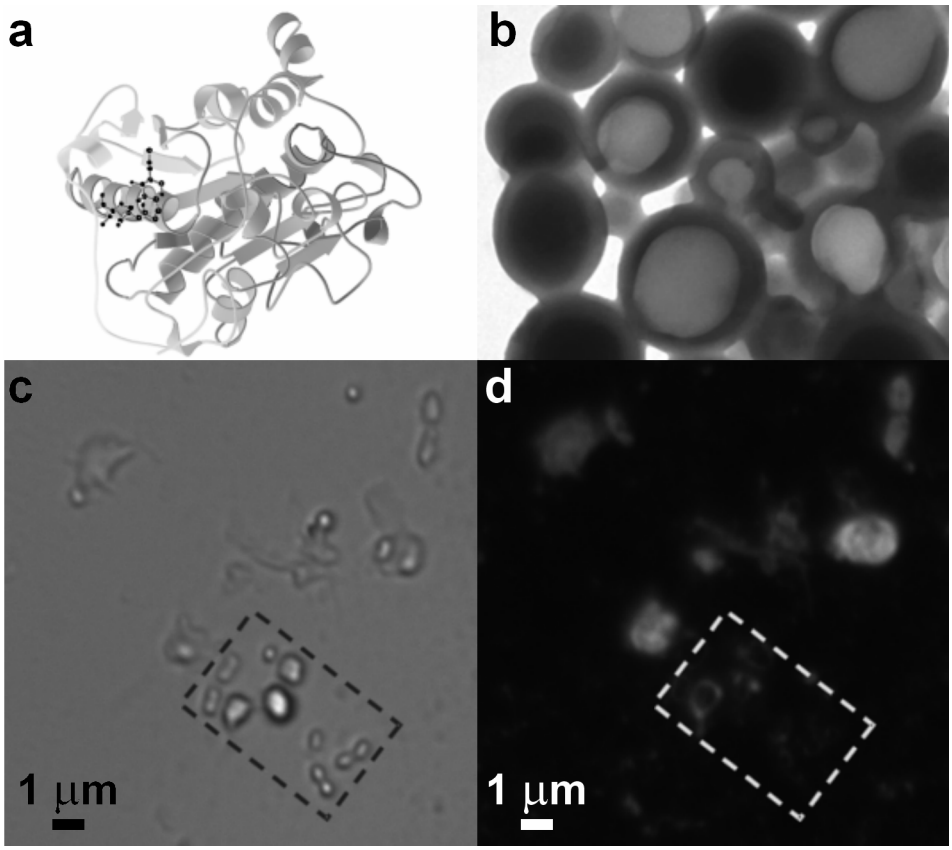

Figure 3. *Inclusion of CAL B enzymes inside polymersomes of PS-PIAT using the injection method. a) Crystal structure of CAL B, b) TEM micrograph of a dried drop of this mixture on a carbon-coated copper grid revealing dark and light polymersomes, c) optical micrograph of PS-PIAT polymersomes containing Alexa-488 labeled enzymes. Polymersomes without enzymes are indicated by the rectangle, d) fluorescence micrograph ($\lambda_{exc.}$ = 488 nm) of the same area revealing that not all polymersomes fluoresce.*

The activity of the included enzymes was tested by the external addition of the substrate 6,8-difluoro-4-methylumbelliferyl octanoate (DiFMU octanoate) to the PS-

PIAT/CAL B aggregates. This compound starts to fluoresce when the DiFMU group, a coumarin type of fluorophore ($\lambda_{exc.}$ = 358 nm, $\lambda_{em.}$ = 450 nm), is formed upon CAL B catalyzed hydrolysis (Scheme 1).

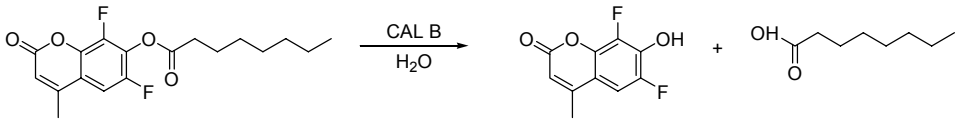

Scheme 1. *Hydrolysis of DiFMU octanoate catalyzed by CAL B.*

Initial experiments with fluorescence microscopy, in which the PS-PIAT/CAL B dispersion was deposited on glass, revealed a significant increase in fluorescence intensity around the single polymersomes upon addition of the DiFMU octanoate substrate. Blank experiments involving empty polymersomes under the same conditions confirmed that the increase in fluorescence was due to the enzymatic activity and not to background hydrolysis (Figure 4).

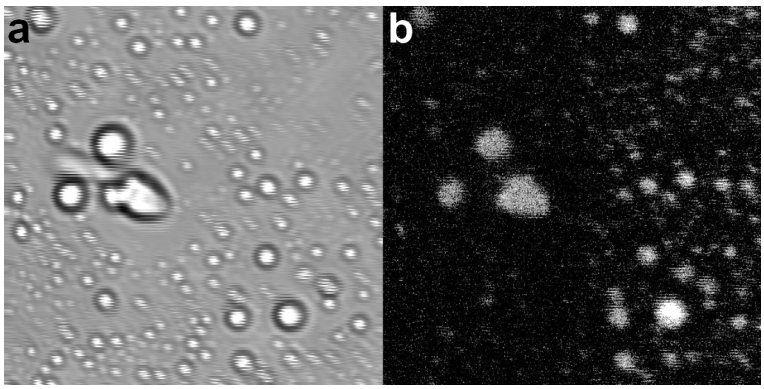

Figure 4. *Fluorescent emission of the product formed from DiFMU octanoate hydrolysis by CAL B entrapped in PS-PIAT polymersomes. a) Optical micrograph before addition of DiFMU octanoate, b) fluorescence micrograph ($\lambda_{exc.}$ = 358 nm) 30 min. after addition of the substrate, revealing that emission was localized around the polymersomes.*

This above assay proved that the entrapped enzymes were still active and that the substrate could permeate through the polymersome membrane. The same assay was applied in a dispersion of PS-PIAT/CAL B where the increase in fluorescence (Figure 5) was conveniently monitored using a fluorescence spectrophotometer. In order to determine if the membrane was permeable for DiFMU the polymersome dispersion was filtrated 1 h after the addition of DiFMU octanoate. It was observed that the filtrate had approximately the same

intensity in fluorescence as before filtration. This showed that the fluorescent DiFMU product could leak out of the polymersomes. Interestingly, the polymersomes prepared by Nardin *et al.* required a channel protein in order to obtain diffusion of the substrate.[14] Enzymes compartmentalized with PS-PIAT polymersomes were found to be active even after being in dispersion for 1.5 months.

The membranes of PS-PIAT polymersomes containing CAL B were also cross-linked using the metal complex [bis(2,2'-bipyridine)ruthenium(II)bis(pyrazolyl)] (BRP, Scheme 2).[24]

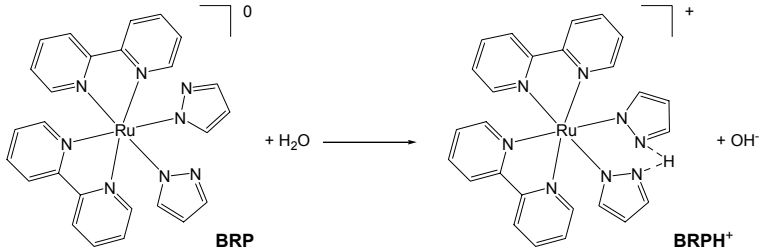

Scheme 2. *BRP is protonated in water and forms $BRPH^+$, which has a high oxidation potential.*[24]

In water, one of its pyrazolyl groups is protonated and the resulting species $[(bpy)_2Ru(pz)(pzH^+)]$ ($BRPH^+$) has an oxidation potential of 1.60 V (vs. Fc/Fc^+), making it suitable to polymerize the thiophene groups in PS-PIAT.[17] More details can be found in Chapter 4. The rate of cross-linking is higher when it is performed at elevated temperatures.

In a first set of experiments the enzyme activity of CAL B was studied after a treatment of 30 min. at a temperature of 60°C in the presence and in the absence of the oxidative Ru complex (Figure 5). The activity was determined by fluorescence spectroscopy using the DiFMU octanoate assay as described above. The experiments revealed that the activity of the enzyme was reduced to 33 % after a treatment of 30 min. at 60°C compared to the enzyme at room temperature, while the enzyme after a treatment of 30 min. at 60°C and in the presence of BRP had 37 % of its initial activity left.[25] From these numbers it could be concluded that denaturation of the enzyme was considerable at the used temperature, whereas the presence of the Ru complex had no significant effect on the performance of the enzyme.

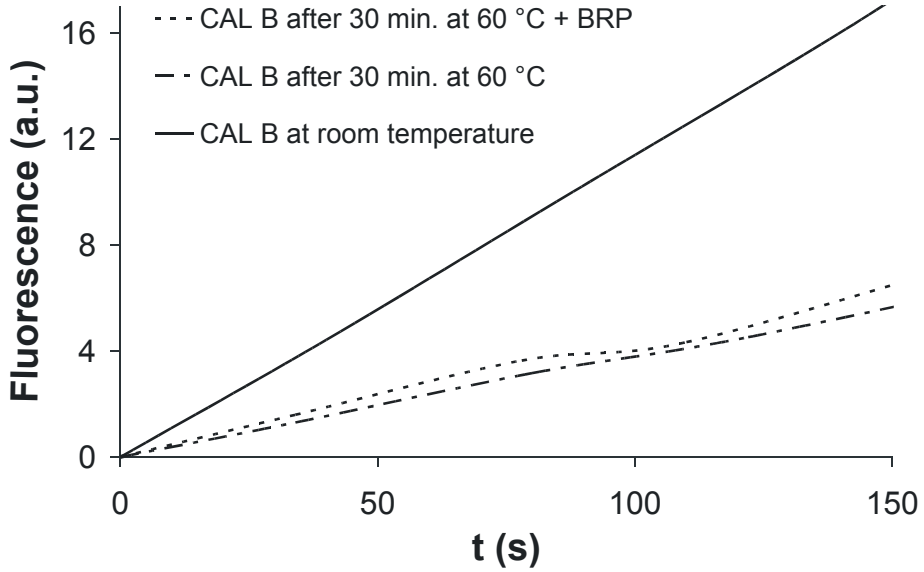

Figure 5. *Fluorescence emission as a function of time for several enzyme systems, revealing the conversion of substrate by free enzyme under cross-linking conditions. The measurements were carried out at room temperature.*

The activity of CAL B inside PS-PIAT polymersomes was subsequently determined with the same assay as described above, see Figure 6. The curve for the autohydrolysis of DiFMU octanoate in water is also given in this figure.

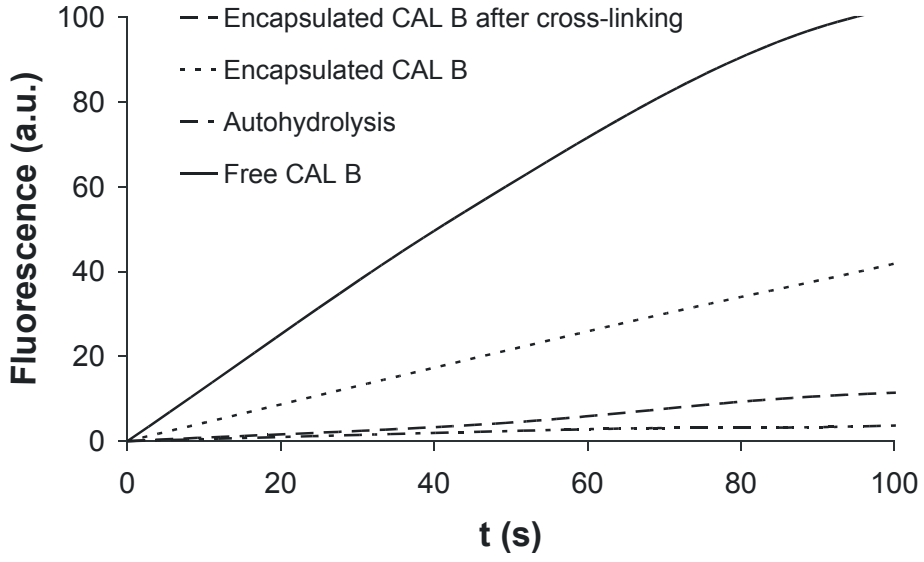

Figure 6. *Substrate conversion by PS-PIAT/CAL B biohybrids and blank reactions. The measurements were carried out at room temperature.*

The rate at which the substrate was converted by compartmentalized CAL B was reduced to 37 % compared to free CAL B, while the rate for CAL B inside cross-linked

polymersomes was 9.3 % of that of free CAL B. This difference strongly suggested that substrate conversion is reduced as a result of a reduction in the diffusion of the substrate through the membrane and not because of thermal enzyme denaturation. Interestingly, an initiation period due to substrate diffusion through the membrane was not observed. The influence of the degree of cross-linking on the enzyme-catalyzed hydrolysis of DiFMU octanoate was investigated in more detail by varying both the cross-linking time and the concentration of $BRPH^+$ (Figure 7).

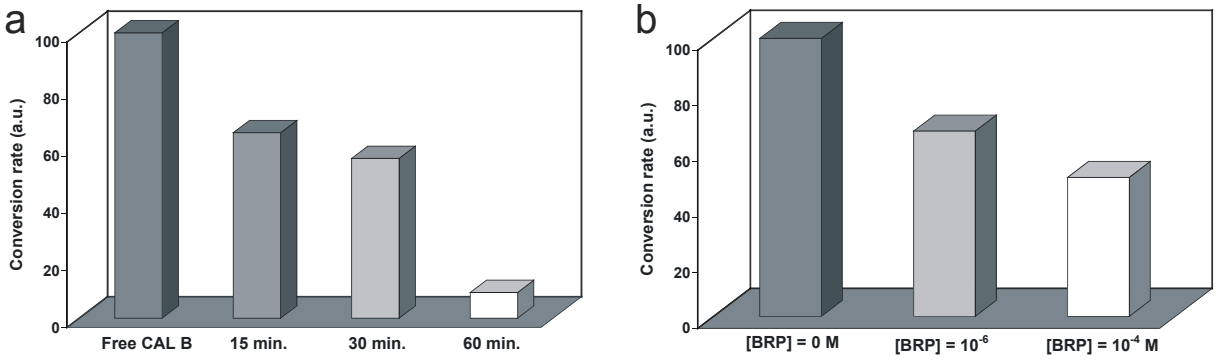

Figure 7. *Effect of varying the cross-linking conditions. a) Effect of increasing cross-linking time on the rate of substrate conversion by PS-PIAT/CAL B biohybrids, b) effect of the BRP concentration on the rate of substrate conversion by PS-PIAT/CAL B biohybrids.*

From the two graphs in Figure 7 it can be concluded that the rate of DiFMU octanoate hydrolysis becomes lower when either the cross-linking time is extended or the cross-linker concentration is increased. It is tentatively proposed that this effect is caused by the closing of pores present in the polymersome membrane by the cross-linking reaction (Figure 8). These pores have to be smaller than the enzymes, because leakage of enzymes was not observed over a period of one week. This was determined by filtrating one week old dispersions of polymersomes filled with CAL B, which had been filtrated after preparation. The same DiFMU octanoate assay (Scheme 1) as used in the previous experiments gave a rate of hydrolysis for the filtrate comparable to the rate of autohydrolysis. This result could also indicate that the enzymes had decomposed, due to partial denaturation during the treatment of the dispersion at 60°C. When the residue was tested, however, enzyme activity was observed. Separate experiments revealed that the polymersomes remained active for periods up to 1.5 months. The methods of varying cross-linking time or cross-linker concentration offer a way to tune the permeability of the PS-PIAT polymersomes.

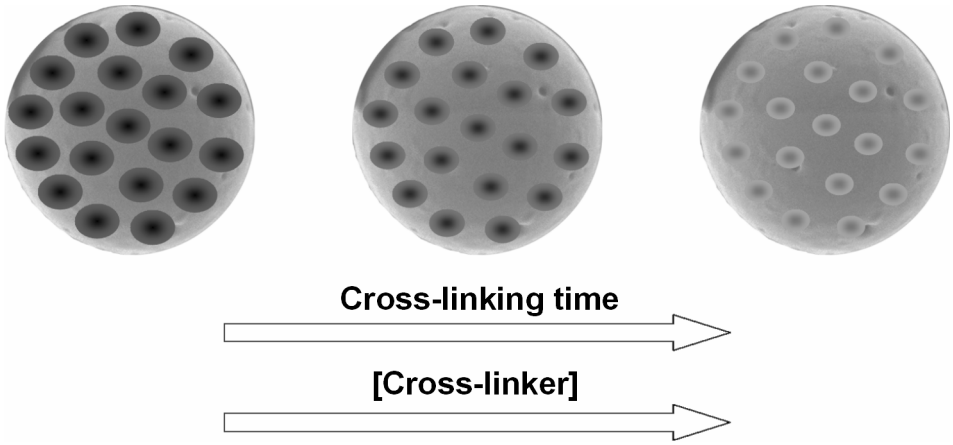

Figure 8. *Schematic representation of the change in polymersome structure upon increasing the cross-linking time or increasing the cross-linker concentration: pores which are present in the membrane are closed during the cross-linking reaction. The drawings do not show the pores in the right dimensions, since they cannot be observed microscopically.*

5.2.1.2 Preparation of PS-PIAT/CAL B biohybrids via lyophilization

Lyophilization, or freeze-drying, of enzymes with polymers and surfactants has been adopted as a technique to introduce enzymes in organic solvents or to protect the enzymes.[22, 26] After lyophilization the enzyme is coated with the polymer or the surfactant which has a stabilizing effect on the enzyme's conformation. Furthermore, the solubility and hence the activity in organic solvents is significantly increased.

The initial idea of the study presented in this section was to improve the solubility of CAL B in organic solvents by co-lyophilizing it with PS-PIAT, however, it turned out that the formed biohybrid displayed interesting aggregation behavior itself in aqueous solvents. For these experiments PS-PIAT that was synthesized from 100 % L-IAT was used. The length of the PIAT block was determined by ^{1}H NMR to be 4 units. A solution of PS-PIAT in THF was introduced in an aqueous solution of CAL B by injection, in a similar way as described in Section 5.2.1.1. This mixture was then lyophilized, resulting in a fluffy off-white powder, which was redissolved in THF to give a clear solution. In the same way as described above, the THF solution was injected into pure water, resulting in the formation of a turbid dispersion. The same experiment was carried out with PS-PIAT polymersomes without CAL B present. Electron micrographs of the prepared PS-PIAT aggregates with and without CAL B present are shown in Figure 9.

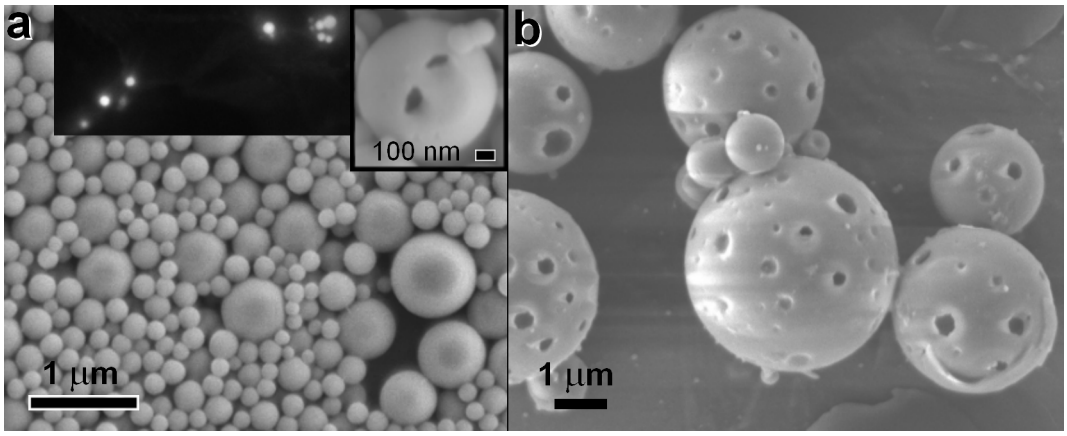

Figure 9. *Aggregates of PS-PIAT/CAL B biohybrids formed prior to the lyophilization treatment. a) SEM micrograph of PS-PIAT polymersomes. The dark inset is a fluorescence micrograph ($\lambda_{exc.}$ = 488 nm) of polymersomes encapsulating 5(6)-carboxyfluorescein (CF), the right inset shows a micrograph of a punctured polymersome exposing its hollow interior. b) SEM micrograph of aggregates of PS-PIAT/CAL B biohybrids.*

To confirm the vesicular nature of the PS-PIAT aggregates by lyophilization, the polar and hydrophilic probe 5(6)-carboxyfluorescein (CF) was encapsulated. To this end the sample was studied by fluorescence microscopy, which clearly revealed that the fluorescence came from the aggregate interior (Figure 9 a, left inset), precisely as expected for an aggregate with a vesicle architecture.

The spherical aggregates of the lyophilized PS-PIAT/CAL B complexes were much larger than the non-lyophilized ones. Moreover, they contained many holes on their surface (Figure 9 b). Boerakker *et al.* prepared a protoporphyrin IX with a polystyrene tail attached and this compound self-assembled in water to give spherical aggregates with similar holes on their surface.[27] An explanation for this phenomenon was not given. In our case it is obvious that the enzyme plays a role in the formation of the holes, since the aggregates of PS-PIAT formed in the absence of CAL B were perfectly spherical (Figure 9 a). In the same way as described above, CAL B enzymes labeled with the fluorescent dye Alexa-488 were used to visualize the enzymes within the biohybrid aggregate prepared by lyophilization. Analysis of the sample by fluorescence microscopy revealed that the enzymes were accumulated within the membrane (Figure 10).

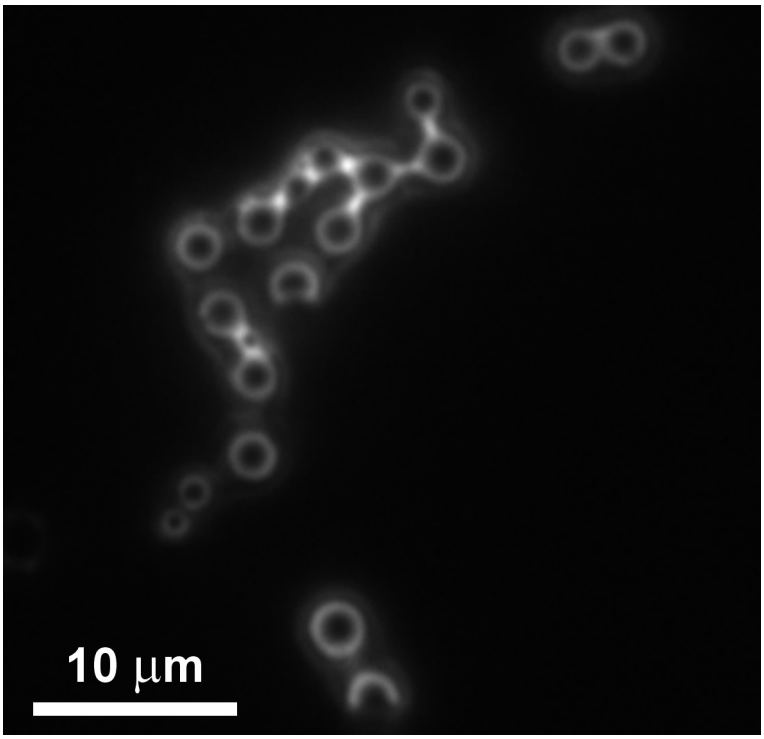

Figure 10. *Fluorescence micrograph ($\lambda_{exc.}$ = 488 nm) of PS-PIAT polymersomes encapsulating CAL B enzymes which are labeled with Alexa-488. These complexes were prepared by prior lyophilization.*

An explanation for the fact that the enzymes are only present in the membrane of PS-PIAT polymersomes might be that during lyophilization these biomacromolecules are coated by PS-PIAT. When these enzyme-PS-PIAT clusters are redissolved in THF, the amphiphilic diblock copolymers remain present around the enzymes. Injection of the THF solution into water will then lead to aggregates of PS-PIAT with membranes containing entrapped CAL B enzymes. THF will aid in the rearrangement of the amphiphiles by solubilizing the polystyrene tails. The presence of THF and the tendency of PS-PIAT to form polymersomes, eventually lead to the aggregates shown in Figure 9 b). A closer look to the biohybrids in Figure 9 b) shows that the membranes are not very regular and probably have a multilayer structure, indicating that they are built up in a different manner than the CAL B containing PS-PIAT polymersomes shown in Figure 3 b). It has to be noted that fluorescence micrographs of PS-PIAT polymersomes, as discussed in Chapter 3, resemble closely Figure 10, but the excitation time necessary to record a micrograph of an empty PS-PIAT polymersome is a factor of 10 longer than for the polymersomes containing labeled CAL B. Furthermore, addition of an aqueous solution of DiFMU octanoate to PS-PIAT/CAL B biohybrids dried on glass showed that there was enzyme activity, indicating that the enzymes

are indeed present in the membrane. Detailed studies still have to be performed in order to compare the enzyme activity with that of the PS-PIAT/CAL B complexes prepared without prior lyophilization. In principle the difference in location of the enzyme within the aggregate, viz. in the membrane or in the inner aqueous compartment of the polymersome, could result in a difference in activity of the enzyme.

The above presented procedure allows the preparation of biohybrids in which the capsule is built up from PS-PIAT macromolecules, CAL B is present in the membrane and a second enzyme is encapsulated within the water pool. In order to investigate this possibility, two batches of CAL B enzymes were labeled, one with Alexa-488 dye and the other with Alexa-633 dye. The CAL B labeled with Alexa-488 was lyophilized together with PS-PIAT, while the Alexa-633 was encapsulated when the PS-PIAT/CAL B (Alexa-488) biohybrid was injected into an aqueous solution of this enzyme. The location of the two different enzymes could be visualized by fluorescence microscopy using excitation wavelengths of 488 and 633 nm, respectively (Figure 11).

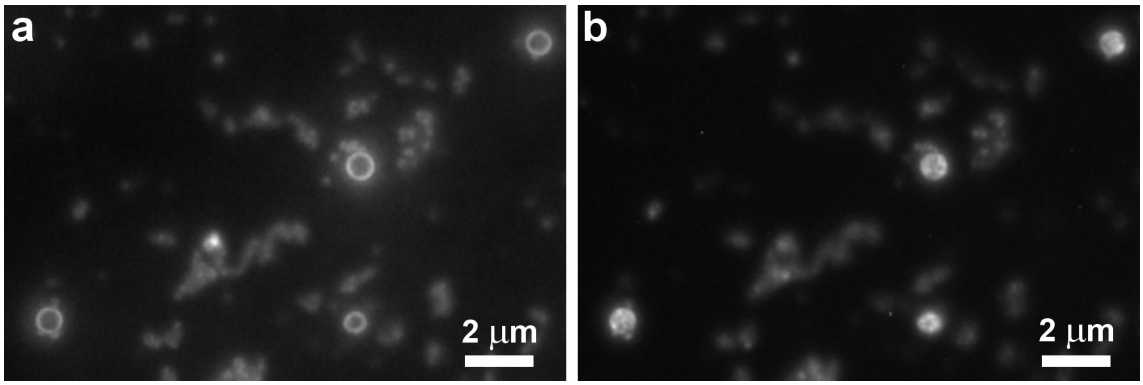

Figure 11. *Fluorescence micrographs of the same area of polymersomes containing CAL B enzymes with two different Alexa labels dried on glass. a) Excitation at 488 nm, b) excitation at 633 nm.*

It is clearly visible in Figure 11 a) that the highest fluorescence intensity is located in the membrane, as was also the case for the aggregates shown in Figure 10, while in Figure 11 b) a higher intensity is present in the center of the polymersomes.

The above approach allows one to perform cascade reactions in the polymersome nanoreactors, e.g. when two completely different enzymes are incorporated. Interesting combinations can be created, capable of catalyzing complex reactions. Immobilization of the polymersomes on a surface and preparation of arrays of these systems with different compartmentalized enzymes opens the way to construct lab-on-a-chip devices.

5.2.2 Encapsulation of horseradish peroxidase

Horseradish peroxidase (HRP, Figure 12 a) is a 44 kDa enzyme found in plants. It has a heme group as the active center and catalyzes the oxidation of compounds using hydrogen peroxide (H_2O_2).[28] In the presence of specific substrates, which act as hydrogen donors, the action of HRP converts colorless or nonfluorescent molecules into colored and/or fluorescent moieties, respectively (Scheme 3).

Scheme 3. *Mechanism for the reduction of H_2O_2 by HRP. The substrate, 2,2'-azino-bis-(3-ethylbenzthiazoline-6-sulfonic acid) (ABTS), is oxidized during the reduction and the resulting radical cation has a maximum absorption at 420 nm.*

Liposomes are commonly applied in immunodiagnostic assays as a means to obtain signal enhancement and thus increased sensitivities. The water pool of liposomes can entrap many marker molecules while to their polar outer surface receptor molecules can be attached.[29, 30] HRP is generally used in these assays to perform a colorimetric reaction for detection.

Encapsulation of HRP inside PS-PIAT polymersomes was performed in the same manner as described in Section 5.2.1.1. The used PS-PIAT was prepared by polymerization of 100 % L-IAT. In a phosphate buffered solution of HRP a solution of PS-PIAT in THF was injected. The resulting dispersion turned cloudy instantly, indicating the formation of aggregates. A buffered solution was used, because HRP is more prone to denaturation than CAL B. Both TEM and fluorescence microscopy studies proved that the resulting aggregates were vesicular in nature (Figure 12 b and c). For these studies HRP labeled with rhodamine isothiocyanate was used. The fluorescence in the polymersomes shown in Figure 12 c) appears to be concentrated within the membrane. However, a small amount of fluorescence inside the central water pool can be seen. It is possible that the HRP enzymes have an affinity for PS-PIAT and are therefore more concentrated in the membrane. Unfortunately, the resolution of the optical microscope did not allow higher magnification.

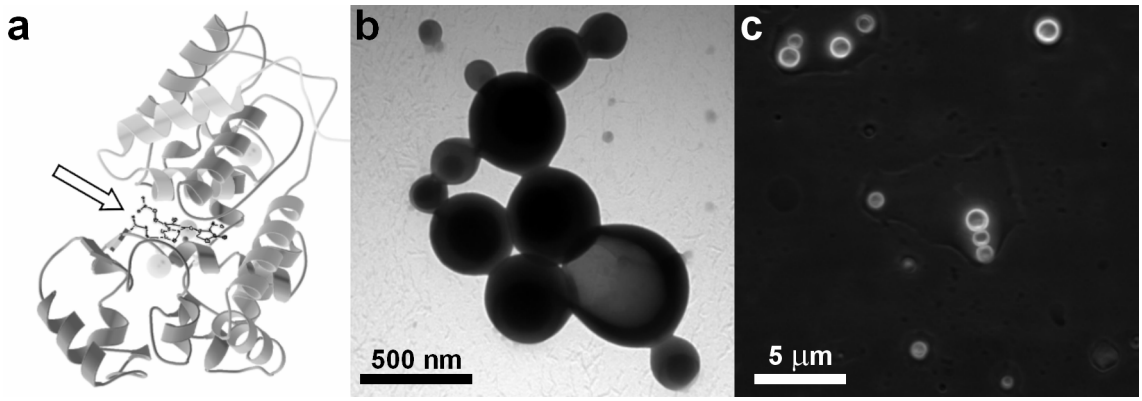

Figure 12. *Encapsulation of HRP inside PS-PIAT polymersomes. a) Crystal structure of HRP, the arrow indicates the enzyme's active center, b) TEM micrograph of the enzyme encapsulated polymersome complex, c) fluorescence micrograph ($\lambda_{exc.}$ = 488 nm) of the same sample.*

The activity of the encapsulated HRP enzymes was tested with a colorimetric assay using an ABTS/H_2O_2 solution (Scheme 3). In this assay, ABTS is oxidized during the reduction of H_2O_2 by the present HRP, resulting in the formation of an ABTS radical cation which has a λ_{max} at 420 nm, in this way coloring the solution blue/green.[31] The increase in absorption in the bulk solution is conveniently monitored at 420 nm. The activity of the compartmentalized HRP is shown in Figure 13.

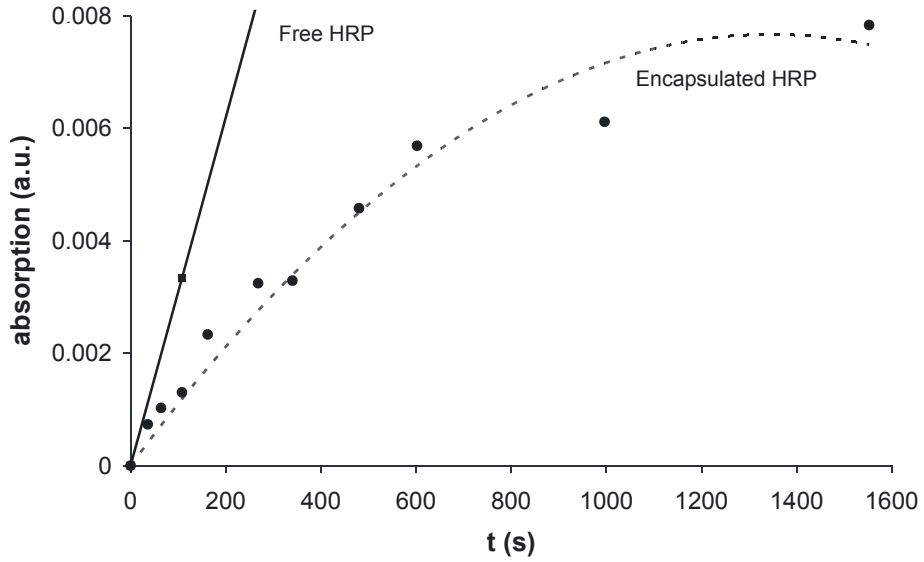

Figure 13. *Activity experiments on free HRP and on HRP present within PS-PIAT polymersomes using an ABTS/H_2O_2 assay.*

As can be seen in Figure 13 the encapsulated enzymes are still active, while the polymersome membrane is permeable for the solutes ABTS and H_2O_2. The ratio of the rate of the initial conversion of ABTS by encapsulated HRP and by free HRP was 0.39:1. This experiment shows that the substrate can migrate through the PS-PIAT membrane. The leveling-off observed in the case of the HRP encapsulated inside the polymersomes might be due to limited diffusion of the ABTS substrate across the liposome membrane. Oxidation of thiophenes by H_2O_2 does not occur in the absence of a catalyst,[32] and the other functional groups in the polymersome membrane are not expected to be oxidized under the used conditions.

5.2.3 Encapsulation of glucose oxidase

The enzyme glucose oxidase (GOx) is a 160 kDa large protein, which is highly specific for the oxidation of β-D-glucose (Figure 14).

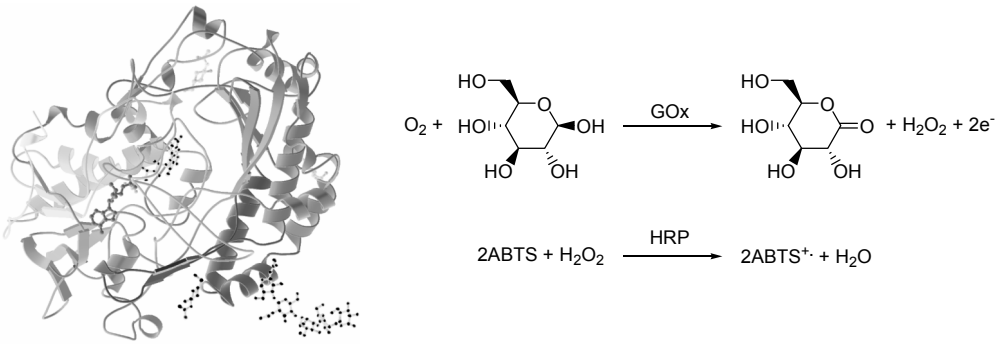

Figure 14. *Left: crystal structure of GOx, right: oxidation of β-D-glucose by GOx. The presence of HRP and ABTS facilitate the determination of the enzyme activity.*

The biomacromolecule is built up from two identical polypeptide units, each containing a flavine-adenine dinucleotide (FAD) unit. GOx is generally used in sensor applications,[33] because the glucose conversion can be monitored by recording the H_2O_2 formation,[34] the consumption of oxygen,[35] or the current of the produced electrons.[36, 37] In the Nolte group several approaches have been followed to develop a glucose sensor for patients with diabetes. A successful method was the incorporation of GOx in the pores of a track-etch membrane coated with an electron conductive polymer, e.g. polypyrrole,[38] or polythiophene.[39] The addition of glucose to a flow cell containing the coated membrane and

two electrodes resulted in a detectable electron current, hence a working glucose sensor (Figure 15).

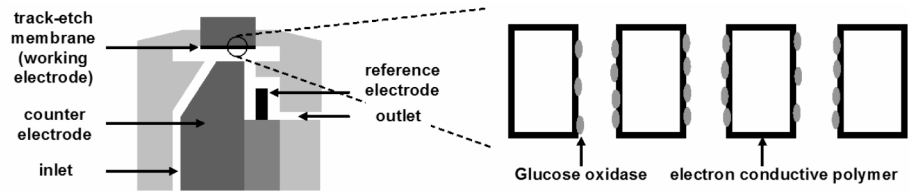

Figure 15. *A working glucose sensor based on a track-etch membrane coated with an electron conductive polymer of which the pores are filled with GOx.*[39]

Glucose sensors have also been developed by encapsulation of GOx inside vesicles.[11, 36, 40] Kim *et al.* have constructed a promising insulin release system by coencapsulating GOx and insulin within pH sensitive vesicles. Externally added glucose led to the formation of gluconic acid, resulting in a decrease of pH and concomitant vesicle destabilization and therefore the release of insulin.[41] Taylor and coworkers have studied various parameters that influenced the performance of glucose sensors based on electrodes coated with GOx-containing vesicles. It turned out that ruptured vesicles were an important cause for the loss of electrode response.[42] Increasing the bilayer permeability by changing the composition of the amphiphiles in the membrane increased the response of the electrode, but with the unfavorable side-effect of reducing the linear range of the enzyme.[36] In the introduction of this chapter the formation of oxidation-responsive capsules prepared by encapsulating GOx inside oxidation-sensitive polymersomes was mentioned.[15] This type of capsule might also be applied as a controlled release container.

In a similar approach as described for the encapsulation of CAL B and HRP, GOx was encapsulated inside PS-PIAT aggregates by the injection method.[23] The used PS-PIAT was synthesized by polymerizing a mixture of 90 % L-IAT and 10 % D-IAT. A solution of PS-PIAT in THF was injected into a solution of GOx in phosphate buffer (20 mM, pH 7), resulting in a turbid dispersion. For the same reason as mentioned in the case of the experiments with HRP, i.e. preventing denaturation, buffered solutions were used to dissolve GOx. Free enzymes were removed from the PS-PIAT/GOx aggregates by a Sephadex column. TEM micrographs of the resulting aggregates are shown in Figure 16.

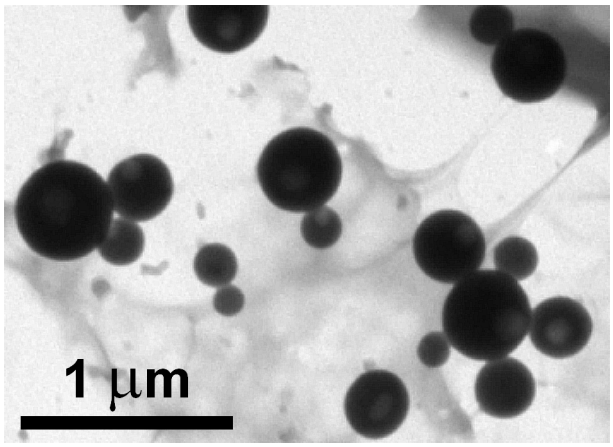

Figure 16. *TEM micrograph of the aggregates formed by the compartmentalization of GOx within PS-PIAT polymersomes.*

The observed aggregates appeared to have a lighter interior than the membrane, confirming their vesicular nature. Further characterization is required to fully determine the composition of the GOx-containing polymersomes. Fluorescence microscopy is an ideal technique, since the GOx enzymes contain FAD units, which are fluorescent themselves. Another option would be to disrupt the aggregates, for instance by adding THF, and measure the release of enzyme molecules.

Initial qualitative enzyme activity studies were performed by adding a solution of glucose, ABTS, and HRP to the PS-PIAT/GOx dispersion. The formation of a green color, indicative of the formation of $ABTS^{+\cdot}$ confirmed the presence of H_2O_2. This green color was visible with the naked eye after a few minutes, indicating that GOx was present in the PS-PIAT aggregates and also revealing that the enzymes remained active after compartmentalization. In depth studies are needed to clarify if a reduction in enzyme activity occurs upon encapsulation.

Cross-linking of the PS-PIAT polymersome membrane results in systems in which the electronic resistance is three orders of magnitude lower than before cross-linking.[19] In combination with the electron-producing capacity of GOx a nanobattery system might be developed, at least in principle, which is capable of generating electricity. The electrons have to be transported through the membrane to an electrode in order to create a potential. Each polymersome with GOx inside would then behave as a fuel cell. When a system can be designed in which glucose is able to migrate through the membrane in a continuous manner and no built up of gluconolactone occurs, a working fuel cell might be possible.

5.3 Conclusions

The compartmentalization of enzymes within aggregates of PS-PIAT leads to biohybrids in which the enzyme activity remains appreciable. It appears that diffusion of substrates through the polymersome membrane is fast enough to measure enzyme activity. The compartmentalization approach has been successfully applied to CAL B, HRP and GOx enzymes, which makes it plausible that this is a general method to prepare PS-PIAT/enzyme hybrids. Although detailed comparative studies were not performed, the amount of L-IAT and D-IAT present in PS-PIAT seemed of little influence on the structure of the resulting aggregates, since all prepared PS-PIAT/enzyme complexes were spherical and appeared vesicular in nature.

For the entrapment of CAL B inside PS-PIAT aggregates two different methodologies were developed, which resulted in the formation of biohybrids in which the enzymes were present at different locations within the polymersomes. Direct injection of PS-PIAT into a solution of enzymes yielded polymersomes with enzymes primarily located inside their water pool. Aggregates of PS-PIAT and CAL B, which were first lyophilized and then reinjected in water, gave systems in which the enzyme was primarily present in the membrane. Initial studies suggested that it is possible to prepare polymer/enzyme complexes in which two types of enzymes are located in different parts of the aggregate. This may lead to the development of cascade catalysts capable of performing two different reactions on the same substrate, mimicking in a primitive way the functioning of a cell.

5.4 Experimental Section

General methods and materials

Candida antarctica Lipase B, recombinant from *Aspergillus oryzae* (E.C. 3.1.1.3), peroxidase labeled with rhodamine isothiocyanate, prepared from type VI horseradish peroxidase (E.C. 1.11.1.7), and glucose oxidase (E.C. 1.1.3.4) type X-S from *Aspergillus niger* were purchased from Sigma. 5(6)-Carboxyfluorescein was supplied by Eastman-Kodak and purified using a literature procedure.[43] Succinimidyl ester disodium salts of Alexa Fluor® 488 and 633 were obtained from Molecular Probes. THF was distilled over Na. The synthesis of PS-PIAT has been published elsewhere.[18] For the aggregation studies ultra pure water ($R > 18\times10^6$ Ω) was used. All other chemicals were used as received. UV-Vis spectra were recorded on a Varian Cary 50 spectrophotometer. A Perkin Elmer LS 50B fluorescence spectrophotometer was used to measure fluorescence spectra. TEM micrographs were recorded on a JEOL JEM-1010 instrument. The samples were prepared by drying a drop of the dispersion on a carbon-coated copper grid and the excess of water was blotted away after 2

min. with a filter paper. For SEM studies a JEOL JSM-6330F was used. The samples were prepared by drying a drop of the dispersion on microscopy glass which was cleaned by sonication for 15 min. in CH_2Cl_2. The samples were left to dry for a day in the fume hood before study. A 1.5 nm layer of Pd/Au was sputtered on the SEM samples before studying by using a Cressington 208 HR sputter coater fitted with a Cressington layer thickness controller. Optical and fluorescence microscopy experiments were carried out with a Zeiss Axiovert 135 TV, fitted with a monochromatic light source for the fluorescence measurements.

Synthesis of Alexa-labeled CAL B

To 0.50 ml of a 1.0 $g.l^{-1}$ solution of CAL B in 20 mM phosphate buffer (pH 8.0), 50 µl of a 1.0 M sodium bicarbonate solution was added. To this solution 1.0 mg of the reactive succinimidyl ester disodium salt of Alexa-488 or Alexa-633 was added and the coupling was allowed to proceed for ~2 h at room temperature. The conjugates were purified by size-exclusion chromatography using Sephadex G-25, followed by extensive dialysis (molecular weight cutoff 7 kDa). The coupling of the dye was verified by polyacrylamide gel electrophoresis.

Encapsulation of CAL B

A 0.50 $g.l^{-1}$ solution of PS-PIAT dissolved in THF was injected into a 30 $mg.l^{-1}$ solution of CAL B enzymes; the final water to THF ratio amounted to 12:1 (v/v). After two days of equilibrating the mixture was filtrated to dispose all non-included enzymes with the help of an eppendorf equipped with a 100 kDa cutoff filter. After centrifugation until the filter was dry the same volume of water was added to the filter and centrifugation was continued until dryness. This step was repeated one more time. The PS-PIAT/CAL B biohybrid was redispersed in the same volume of water.

CAL B activity assay

From the purified PS-PIAT/CAL B dispersion 0.50 ml was transferred to a cuvettete containing 0.50 ml of water. Immediately after the addition of 1.0 ml of 1.5 µM DiFMU octanoate solution in water, the cuvette was placed in the fluorescence spectrophotometer and the increase in fluorescence was followed ($\lambda_{exc.}$ = 358 nm, $\lambda_{em.}$ = 450 nm).

Cross-linking of PS-PIAT membrane

Into an aqueous solution prepared by mixing 0.20 ml of 30 $mg.l^{-1}$ CAL B and 1.0 ml of 1.3 µM BRP was injected 0.10 ml of a solution containing 0.50 $g.l^{-1}$ PS-PIAT solution in THF, resulting in a final water/THF ratio of 12:1 (v/v). Subsequently, the dispersion was placed in a water bath of 60°C for the desired period of time. After cooling to room temperature 0.50 ml of the dispersion was transferred to an eppendorf having a filter unit with a cutoff of 100 kDa. The dispersion was centrifuged to dryness after which 0.50 ml of pure water was added and the dispersion was centrifuged again to dryness. After repeating this step a second time, 0.50 ml of water was added to redisperse the cross-linked aggregates.

Preparation of aggregates by lyophilization

A solution of 1.0 ml of 1.0 $g.l^{-1}$ PS-PIAT in THF was injected into 0.20 ml of a 0.10 $g.l^{-1}$ CAL B solution in water, resulting in a dispersion with a PS-PIAT/CAL B molar ratio of 50:1. To this solution a tenfold excess of pure water was added after which it was lyophilized. The resulting fluffy off-white powder was redissolved in THF and injected into water having a final PS-PIAT/CAL B concentration of 0.50 $g.l^{-1}$ in water/THF (8:5, v/v). Aggregates of PS-PIAT in the absence of enzymes were prepared in the same manner.

Encapsulation of two enzymes inside PS-PIAT aggregates

In the same manner as described above CAL B labeled with an Alexa-488 dye was lyophilized with PS-PIAT and the resulting powder was redissolved in THF and injected into water containing 30 $mg.l^{-1}$ of CAL B labeled with an Alexa-633 dye. Non-encapsulated enzymes were removed by column chromatography using Sephadex G-50.

Encapsulation of 5(6)-carboxyfluorescein inside PS-PIAT aggregates

A phosphate buffered solution (20 mM, pH 7.4) of CF with a concentration between 0.010 and 0.10 M was prepared. Into this solution 0.50 $g.l^{-1}$ lyophilized PS-PIAT dissolved in THF was injected, yielding a dispersion with a water/THF ratio of 8:5 (v/v). The free CF was separated from the polymersomes by column chromatography using Sephadex G-50.

Encapsulation of HRP

A solution of HRP, labeled with rhodamine isothiocyanate, was prepared by dissolving 0.90 mg of the enzyme in 10 ml aqueous phosphate buffered solution (20 mM, pH 7.5). Into this solution a 1.0 $mg.ml^{-1}$ solution of PS-PIAT in THF was injected. The dispersion was left to equilibrate for a day prior to study. In order to remove the non-encapsulated enzymes 0.50 ml of the dispersion was transferred to an eppendorf fitted with a 100 kDa cutoff filter unit. The eppendorf was centrifuged until all buffer had passed the filter. Fresh aqueous phosphate buffered solution (0.50 ml, 20 mM, pH 7.5) was added to the filter and the eppendorf was centrifuged again until dryness. This step was repeated a second time. The content of the filter was redispersed in 0.50 ml aqueous phosphate buffer (20 mM, pH 7.5).

HRP activity assay

An amount (0.50 ml) of the purified PS-PIAT/HRP dispersion was transferred to a cuvette. An ABTS/H_2O_2 solution was prepared by adding an H_2O_2 solution in phosphate buffer (50 µl, 0.070 %, pH 7.5) to an aqueous solution of ABTS (2.2 ml, 0.33 µM). From this solution, 0.50 ml was added to the cuvette. The enzyme activity was monitored by measuring the absorption at 420 nm with UV-Vis spectroscopy.

Encapsulation of GOx

A solution of 48 $mg.l^{-1}$ GOx dissolved in phosphate buffer (20 mM, pH 7.0) was prepared. Into this solution a 1.0 $mg.ml^{-1}$ solution of PS-PIAT in THF was injected resulting in a final buffer to THF ratio of 6:1 (v/v). The free enzyme was removed by size exclusion chromatography using Sephadex G-50 and an aqueous phosphate buffer (pH 7.5) as eluent.

GOx activity assay

To the above described dispersion of PS-PIAT/GOx polymersomes a solution of glucose (1.1 M), ABTS (1.8 mM), and HRP (0.40 $g.l^{-1}$) in phosphate buffer (20 mM, pH 7.0) was added. Detection was performed visually.

5.5 References and Notes

[1] P. Gacesa, J. Hubble, *Enzyme technology*, Open University Press, Milton Keynes, **1987**.
[2] L. Stryer, *Biochemistry*, W. H. Freeman, New York, **1988**.
[3] M. D. Trevan, *Immobilized enzymes*, John Wiley & Sons, Chichester, **1980**.
[4] T. Oberholzer, P. L. Luisi, *J. Biol. Phys.* **2002**, *28*, 733.
[5] P.-A. Monnard, *J. Membr. Biol.* **2003**, *191*, 87.
[6] T. Oberholzer, R. Wick, P. L. Luisi, C. K. Biebricher, *Biochem. Biophys. Res. Commun.* **1995**, *207*, 250.
[7] T. Oberholzer, K. H. Nierhaus, P. L. Luisi, *Biochem. Biophys. Res. Commun.* **1999**, *261*, 238.
[8] A. Fischer, A. Franco, T. Oberholzer, *ChemBioChem* **2002**, *3*, 409.
[9] S. M. Nomura, K. Tsumoto, T. Hamada, K. Akiyoshi, Y. Nakatani, K. Yoshikawa, *ChemBioChem* **2003**, *4*, 1172.
[10] T. Oberholzer, M. Albrizio, P. L. Luisi, *Chem. Biol.* **1995**, *2*, 677.
[11] P. Walde, S. Ichikawa, *Biomol. Eng.* **2001**, *18*, 143.
[12] G. Redziniak, *Pathol. Biol.* **2003**, *51*, 279.
[13] B. M. Discher, Y.-Y. Won, D. S. Ege, J. C.-M. Lee, F. S. Bates, D. E. Discher, D. A. Hammer, *Science* **1999**, *284*, 1143.
[14] C. Nardin, S. Thoeni, J. Widmer, M. Winterhalter, W. Meier, *Chem. Commun.* **2000**, 1433.
[15] A. Napoli, M. J. Boerakker, N. Tirelli, R. J. M. Nolte, N. A. J. M. Sommerdijk, J. A. Hubbell, *Langmuir* **2004**, *20*, 3487.
[16] D. E. Discher, A. Eisenberg, *Science* **2002**, *297*, 967.
[17] D. M. Vriezema, J. Hoogboom, K. Velonia, K. Takazawa, P. C. M. Christianen, J. C. Maan, A. E. Rowan, R. J. M. Nolte, *Angew. Chem. Int. Ed.* **2003**, *42*, 772.
[18] D. M. Vriezema, A. Kros, R. de Gelder, J. J. L. M. Cornelissen, A. E. Rowan, R. J. M. Nolte, *Macromolecules* **2004**, *37*, 4736.
[19] D. M. Vriezema, A. Kros, J. Hoogboom, A. E. Rowan, R. J. M. Nolte, *Polym. Prepr.* **2004**, *45*, 749.
[20] K. Faber, *Biotransformations in organic chemistry*, Springer-Verlag, Berlin, **1992**.
[21] J. Uppenberg, N. Öhrner, M. Norin, K. Hult, G. J. Kleywegt, S. Patkar, V. Waagen, T. Anthonson, T. A. Jones, *Biochemistry* **1995**, *34*, 16838.
[22] F. Secundo, G. Carrea, *J. Mol. Catal. B: Enzym.* **2002**, *19-20*, 93.
[23] A. S. Domazou, P. L. Luisi, *J. Liposome Res.* **2002**, *12*, 205.
[24] B. P. Sullivan, D. J. Salmon, T. J. Meyer, J. Peedin, *J. Inorg. Chem.* **1979**, *18*, 3369.
[25] These percentages were determined by dividing the tangents over the first 100 s of the respective plots.
[26] Y. Okahata, Y. Fujimoto, K. Ijiro, *J. Org. Chem.* **1995**, *60*, 2244.
[27] M. J. Boerakker, J. M. Hannink, P. H. H. Bomans, P. M. Frederik, R. J. M. Nolte, E. M. Meijer, N. A. J. M. Sommerdijk, *Angew. Chem. Int. Ed.* **2002**, *41*, 4239.
[28] P. Tijssen, *Practice and theory of enzyme immunoassays*, Elsevier, Amsterdam, **1985**.
[29] A. K. Singh, P. K. Kilpatrick, R. G. Carbonell, *Biotechnol. Prog.* **1995**, *11*, 333.
[30] H. A. H. Rongen, A. Bult, W. P. van Bennekom, *J. Immunol. Methods* **1997**, *204*, 105.
[31] N. P. Groome, *J. Clin. Chem. Clin. Biochem.* **1980**, *18*, 345.
[32] K. N. Brown, J. H. Espenson, *Inorg. Chem.* **1996**, *35*, 7211.
[33] M. Gerritsen, J. A. Jansen, A. Kros, R. J. M. Nolte, J. A. Lutterman, *J. of Invest. Surg.* **1998**, *11*, 163.
[34] D. Olea, C. Faure, *J. Chem. Phys.* **2003**, *119*, 6111.
[35] M. Gerritsen, J. A. Jansen, A. Kros, D. M. Vriezema, N. A. J. M. Sommerdijk, R. J. M. Nolte, J. A. Lutterman, S. W. F. M. van Hövell, A. van der Gaag, *J. Biomed. Mater. Res.* **2001**, *54*, 69.
[36] M. A. Taylor, M. N. Jones, P. M. Vadgama, S. P. J. Higson, *Biosens. Bioelectron.* **1997**, *12*, 467.
[37] K. Mitsubayashi, Y. Wakabayashi, S. Tanimoto, D. Murotomi, T. Endo, *Biosens. Bioelectron.* **2003**, *19*, 67.
[38] C. G. J. Koopal, B. de Ruiter, R. J. M. Nolte, *J. Chem. Soc., Chem. Commun.* **1991**, 1691.
[39] A. Kros, S. W. F. M. van Hövell, N. A. J. M. Sommerdijk, R. J. M. Nolte, *Adv. Mater.* **2001**, *13*, 1555.

[40] M. Kaszuba, M. N. Jones, *Biochim. Biophys. Acta.* **1999**, *1419*, 221.
[41] C.-K. Kim, E.-B. Im, S.-J. Lim, Y.-K. Oh, S.-K. Han, *Int. J. Pharm.* **1994**, *101*, 191.
[42] M. A. Taylor, M. N. Jones, P. M. Vadgama, S. P. J. Higson, *Biosens. Bioelectron.* **1995**, *10*, 251.
[43] R. R. C. New, Oxford University Press, Oxford, **1990**.

Chapter 6

Aggregation Studies of Thiophene-Containing Octadecene-*Block*-Polyisocyanide Copolymers

6.1 Introduction

The morphology of amphiphilic block copolymer aggregates can be tuned in a relatively easy manner by varying different parameters, e.g. solvent,[1, 2] concentration,[3-6] method of aggregation,[7] temperature,[6, 8, 9] and presence of solutes.[6, 9-11] Other parameters, which are less easy to change, such as block length,[12-14] type of block[15] and the ratio between the blocks,[15, 16] also play an important role in the morphology. It has been shown for certain types of amphiphilic block copolymers that it is possible to obtain a range of aggregate types, for instance micelles, micellar rods, bilayer sheets, polymersomes (polymer-based vesicles), vesicular rods and other morphologies never seen before, by changing the parameters mentioned above.[14-19]

Previous studies have revealed that diblock copolymers of isocyanides can also form a variety of aggregate architectures, depending on the length and type of their head group,[20] or the size of their apolar tail.[21] In this way polymersomes, bilayer filaments, micellar rods, nanoarrays and superhelices were prepared.

Polyisocyanides can be synthesized via a Ni(II) catalyzed polymerization reaction, in which the monomers first coordinate around the nickel ion.[22] The reaction starts when a nucleophile, e.g. an alcohol or amine, attacks one of the coordinated isocyanide molecules. This results in the formation of a highly reactive carbene complex, which reacts with a neighboring coordinated isocyanide molecule (Scheme 1). During propagation the carbene ligands are continuously generated and react with neighboring isocyanide molecules on the nickel center in a merry-go-round manner, resulting in the formation of a helix which grows

always from the nickel catalyst. When bulky isocyanides are used, the helix is a stable conformation and in the case of *t*-butyl isocyanide the polymer could be separated into its left- and right-handed helical forms.[23] Since the nucleophile is always the group that starts the polymerization reaction,[24] the possibility exists to use an alcohol- or amine-functionalized polymer as an initiator, resulting in the formation of polyisocyanide block copolymers. Using this simple approach, diblock copolymers of polyisocyanides have been prepared with e.g. polystyrene tails,[20] or carbosilane dendrimers.[21]

In Chapter 3, the synthesis and aggregation behavior of polystyrene$_{40}$-*b*-poly(isocyano-L-alanine(2-thiophen-3-yl-ethyl)amide) (PS-PIAT) were discussed.[25] In this chapter the aggregation properties of 9-octadecene-*b*-poly(isocyano-L-alanine(2-thiophen-3-yl-ethyl)amide) (OD-PIAT) will be described. Although this molecule is not a block copolymer, it is referred to as such in this chapter in order to compare it with PS-PIAT. The tail of this amphiphile is much smaller than that of PS-PIAT. The difference in volume of the apolar groups can be seen in Figure 1.

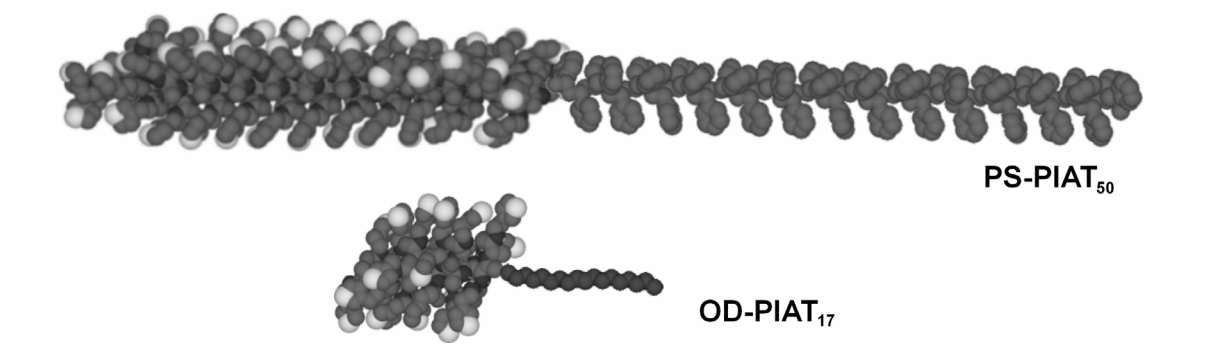

Figure 1. *Space filling representations of PS-PIAT$_{50}$ and OD-PIAT$_{17}$, highlighting the difference in tail volume. The indices refer to the length of the isocyanide block.*

Compound OD-PIAT was prepared in order to determine the influence of the apolar tail on the morphology of the resulting aggregate. An apolar tail with a significantly smaller volume than polystyrene was chosen to more clearly see the potential effect.

6.2 Synthesis and Characterization

The OD-PIAT polymers were prepared by adding the desired amount of 9-octadecene-1-amine-tetrakis(*t*-butyl isocyanide)nickel(II)perchlorate initiator complex to a stirred solution of the monomer isocyano-L-alanine(2-thiophen-3-yl-ethyl)amide (IAT, Scheme 1).

The amount of initiator complex was varied in order to obtain polymers with different polyisocyanide block lengths. In total four different polymers were prepared: OD-PIAT$_{10}$, OD-PIAT$_{17}$, OD-PIAT$_{100}$ and OD-PIAT$_{500}$, where the indices refer to the ratio of isocyanide versus initiator complex at the start of each polymerization reaction.

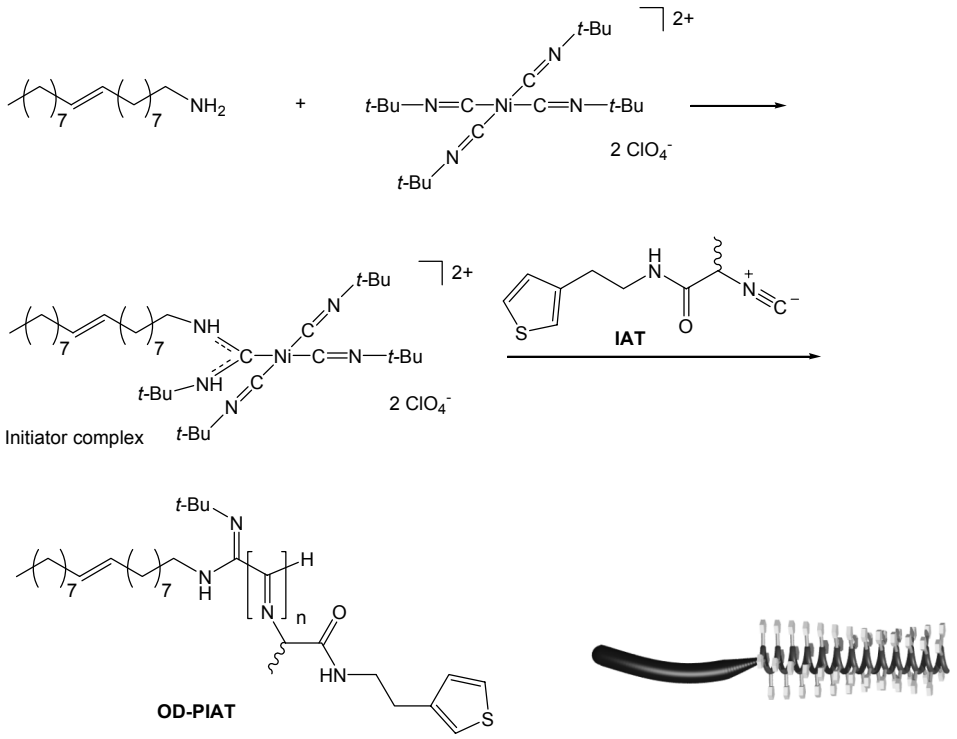

Scheme 1. *Synthetic route of OD-PIAT. Bottom right: a schematic representation of the polymeric amphiphile.*

The synthesis of IAT, using the initial route which results in epimerization of this compound, has already been described in Chapter 2. The initiator complex was prepared by the addition of equimolar amounts of 9-octadecene-1-amine (OD-NH_2) to tetrakis(*t*-butyl isocyanide)nickel(II)perchlorate (Ni(CN-*t*-Bu)$_4$(ClO_4)$_2$). IR spectroscopy revealed the successful formation of this compound as confirmed by a broad vibration at ν = 2227 cm^{-1}, with a shoulder at 2254 cm^{-1}, originating from the isocyanide bonds and vibrations at ν = 1584 and 1546 cm^{-1} resulting from the carbene ligand. The broadening of the isocyanide bond vibration and the two signals for the N-C-N bonds are indicative of the presence of more than one conformation of the initiator complex, as a result of the hindered rotation around the N-C-N bonds. This phenomenon was already observed for other initiator complexes,[24, 26] but not for the initiator complex prepared with amine-functionalized polystyrene, probably due to the bulkiness of the polymer. OD-NH_2 is much smaller and hence less bulky.

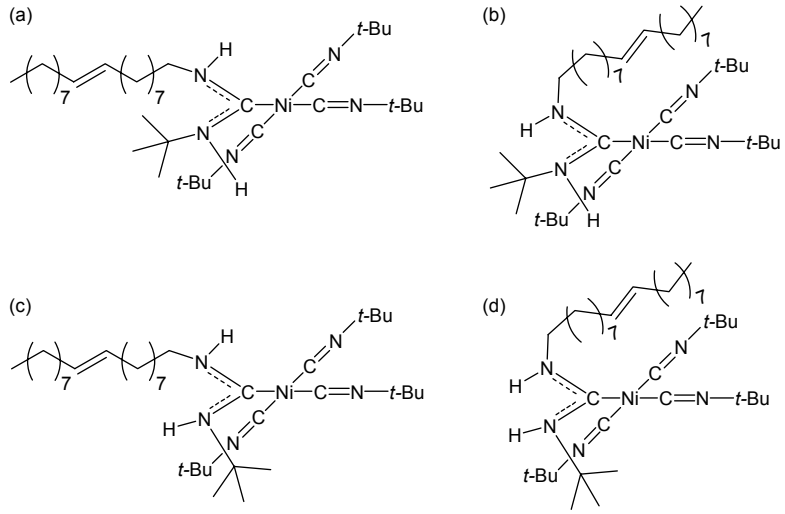

Figure 2. *The four possible conformations of the OD-NH_2/Ni initiator complex.*

The initiator complex can in principle exist in at least four different conformations (Figure 2). In the ^{1}H NMR spectrum it was evident that two conformations are predominant, giving rise to peaks at 8.13 and 6.81 ppm for one conformation and at 7.99 and 7.00 ppm for the other (Figure 3). Some less intense, broader resonances between 7.3 and 7.8 ppm could be observed, possibly corresponding to a third conformation. Based on previous findings using NMR spectroscopy, where a carbene complex prepared from Ni(CN-*t*-Bu)$_4$(ClO$_4$)$_2$ and an amine-functionalized carbosilane dendrimer was studied, the major conformations are thought to be (b) and (c), see Figure 2, with the minor conformation corresponding to conformation (d).[26] Conformation (a) is unlikely, due to steric hindrance between the octadecyl and *t*-butyl groups. The solubility of the resulting OD-PIAT polymers was considerably higher than of the PIAT homopolymers, which were only soluble in TCB and warm toluene.

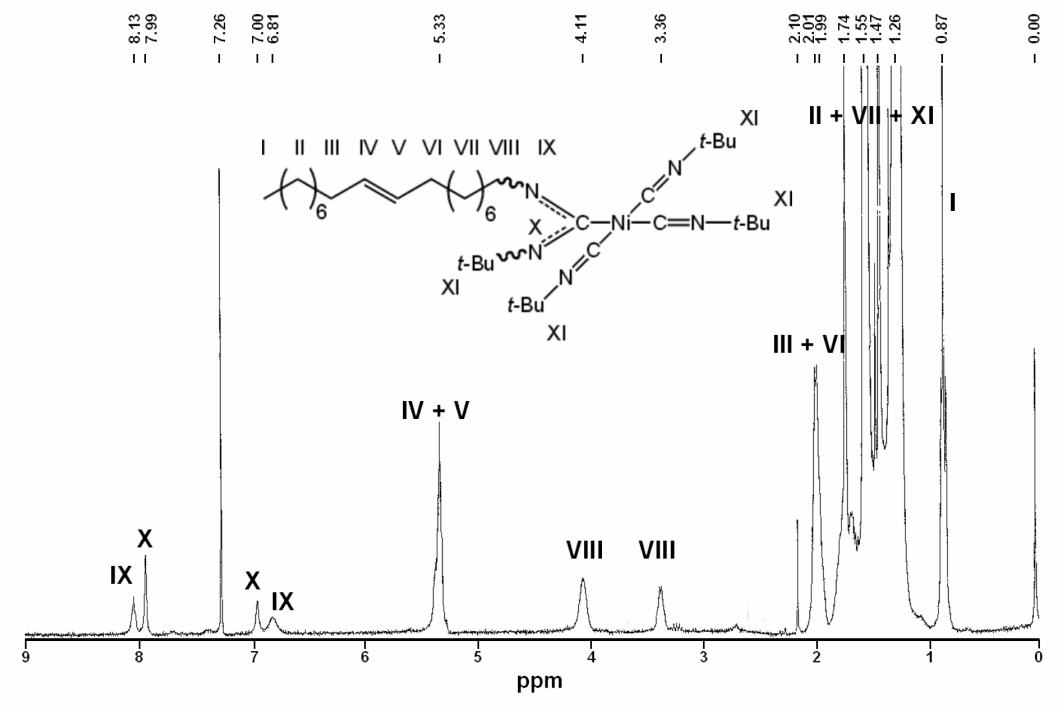

Figure 3. *^{1}H NMR spectrum of the initiator complex.*

The polymers were characterized by circular dichroism (CD) and NMR spectroscopy, mass spectrometry and optical rotation (OR) measurements. Electrospray ionization mass spectrometry (ESI-MS) of OD-PIAT$_{17}$ revealed a broad distribution of peaks with all lengths up to 34 isocyanide units present, suggesting that this polymer is polydisperse. The polydispersity index cannot be deduced, however, from the mass spectrum, because it is unknown if polymers with different lengths have the same behavior in the mass spectrometer, making that the true abundance of the longer polymers in the mass spectrum cannot be determined.

IR spectroscopy revealed that there were only weak hydrogen bonds present between the amide groups within the side chains of the polymers (Table 1), unlike in the case of the diblock copolymers of PS-PIAT prepared with enantiomerically pure IAT (Chapter 3). Upon formation of a hydrogen bond the amide vibrations are expected to shift to lower wavelengths and as can be concluded from Table 1 in these polymers only slightly shifted amide vibrations are observed. The data suggest that OD-PIAT$_{100}$ has the weakest hydrogen bonds, possibly because this polymer was ill-defined. This may be attributed to the presence of both enantiomers of IAT during the polymerization reaction, resulting in an ill-defined polymeric backbone. It has been shown by Metselaar *et al.* that diastereomeric isocyanides can be readily incorporated into the polymer chain, as was concluded from CD measurements of the

acid catalyzed polymerization of a racemic mixture of L-isocyanoalanyl-L-alanine (L,L-IAA) and (L,D-IAA).[27] The consequence of the use of a racemic mixture of isocyanides is a decrease in rigidity of the resulting polyisocyanide backbone when compared to the corresponding optically pure polymers.

Table 1. ***IR data of OD-PIAT in the solid state, measured in KBr***[a]

Compound	N-H stretch	C=O stretch	CN stretch[b]	N-H bend
IAT	3282	1661	2145	1567
OD-PIAT$_{10}$	3280	1654	1617	1525
OD-PIAT$_{17}$	3278	1652	1618	1527
OD-PIAT$_{100}$	3284	1660	1620	1531
OD-PIAT$_{500}$	3278	1654	1617	1531

[a] Measured as a solid in KBr, values are given in cm^{-1}. [b] For the monomer the C≡N stretch is given, while the C=N stretch is reported for the polymers.

The OR data showed that an increase in the ratio of monomer/initiator resulted in a stronger optical rotation, as expected when longer polymers are formed (Table 2).

Table 2. ***Optical rotation, circular dichroism and molecular weight data of the studied polymers***

Polymer	$[\alpha]_D^{20}$ [a]	$\Delta\varepsilon$[b]	M_p[c]
OD-PIAT$_{10}$	-19	-0.046	1.74
OD-PIAT$_{17}$	-22	-0.047	1.96
OD-PIAT$_{100}$	-62	-0.057	2.96
OD-PIAT$_{500}$	-83	-0.065	4.40

[a] In °.cm^2.g^{-1}, measured in CH_2Cl_2 (*c* 0.1). [b] In l.mol^{-1}.cm^{-1} at 288 nm. [c] In kg.mol^{-1}, Mp is the molecular weight at the maximum peak height, see text for details.

These measurements indicate that the polymers are chiral and probably have a helix structure. OR values have been used frequently to draw conclusions about conformations of polymer chains in solution,[28] however, care has to be taken with isocyanide polymers since their rigid backbone might affect the conformation of the side groups and thus their contribution to the overall OR. The change in the magnitude of the OR of the polymer, when

compared to the monomer, is not necessarily due to a change in the conformation of the backbone exclusively. CD spectroscopy is usually more informative than OR measurements and enables one to distinguish better the various contributions to the overall chirality.[29] All polymers showed a negative Cotton effect at 288 nm which is attributed to the n–π* transitions of the imine bonds. The intensity of the Cotton effect increased with increasing monomer/initiator complex ratio, i.e. when the polymer becomes longer (Table 2). In contrast to the IR results, the OR and CD data of OD-PIAT$_{100}$ are in line with those of the other polymers (see Table 2).

The Cotton effect corresponding to the imine bonds in a well-defined polyisocyanide backbone is normally observed at wavelengths around 310 nm and such a Cotton effect is lacking in the spectra of polymers of OD-PIAT.[26] It is therefore doubtful whether the OD-PIAT polymers have a well-defined helical structure extending over the whole PIAT block, as was already concluded from the IR measurements (Table 1). Probably parts of the polyisocyanide block are arranged in a well-ordered helical fashion, in this way contributing to an increase in optical activity compared to the monomer. As an example the UV-Vis and CD spectra of OD-PIAT$_{500}$ are shown in Figure 4.

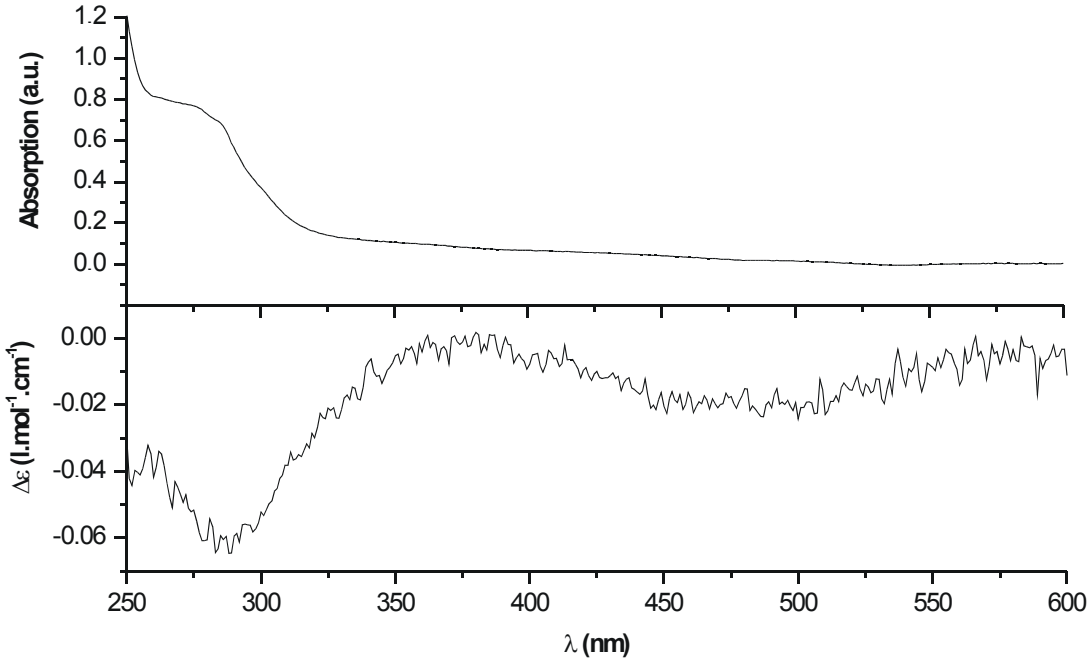

Figure 4. *UV-Vis absorption spectrum (top) and CD spectrum (bottom) of OD-PIAT$_{500}$ in CH_2Cl_2.*

With the help of CD spectroscopy it is possible to determine the helix sense of isocyanide polymers. Van Beijnen *et al.* have studied this topic intensively.[29, 30] Based on

CD calculations it was postulated that a Z-shaped (negative) couplet in the 300 nm region of the CD spectrum (n–π* transition of the imine bonds in the polyisocyanide) corresponded to a right-handed helical conformation, whereas an S-shaped (positive) couplet corresponded to a left-handed one. For poly(L-isocyanoalanyl-glycine) (L-PIAG), which closely resembles PIAT, a *P* helical conformation was assigned.[31] Since both polymers have a comparable CD spectrum with a negative couplet and a negative optical rotation, it is proposed that the polyisocyanide block of OD-PIAT is predominantly in a right-handed helical conformation as well. For the PIAT homopolymer a right-handed helix was postulated as well.

Gel permeation chromatography (GPC) was used to determine the molecular weight of the OD-PIAT polymers (Table 2). Calibration was performed with polystyrene samples. Since the rigidity of a polyisocyanopeptide chain is much higher than that of a polystyrene chain,[32] while the diameters of the OD-PIAT polymers are also larger, a different behavior on a GPC column can be expected. The molecular weight at the maximum peak height (M_p), therefore, is given instead of the weight average (M_w) and number average (M_n) molecular weights, which would be calibrated against the polystyrene standards. Attempts to also determine the molecular weights of other types of polyisocyanides (peptide-based polyisocyanides and the diblock copolymers described in Chapter 3) failed, because the polymers were found to adhere to the GPC column, which is thought to be the result of their relatively high rigidity. The molecular weights found for the OD-PIAT molecules can therefore only be used in a relative manner.

A rough estimation of the degree of polymerization of the PS-PIAT diblock copolymers as described in Chapter 3 could be made with the help of ^{1}H NMR. Due to overlap of the signals of both the OD tail and the PIAT block and the low intensities of the signals of the OD tail compared to the PIAT block, this approach failed in the case of the OD-PIAT polymers.

Fluorescence experiments revealed that the OD-PIAT polymers exhibited fluorescence when they were excited at wavelengths between 280 and 480 nm (Figure 5). The highest fluorescence intensity was obtained using an excitation wavelength of 280 nm. The precursor to the isocyanide, *N*-formyl-L-alanine(2-thiophen-3-yl-ethyl)amide, was found to fluoresce weakly when excited at 280 nm, as a result of the n–π* transition of the amide bonds. The observation of fluorescence of the OD-PIAT polymers at 280 nm is therefore attributed to the imine bonds in the polyisocyanide backbone. The fluorescence at higher wavelengths is very likely due to the presence of conjugated imine bonds.

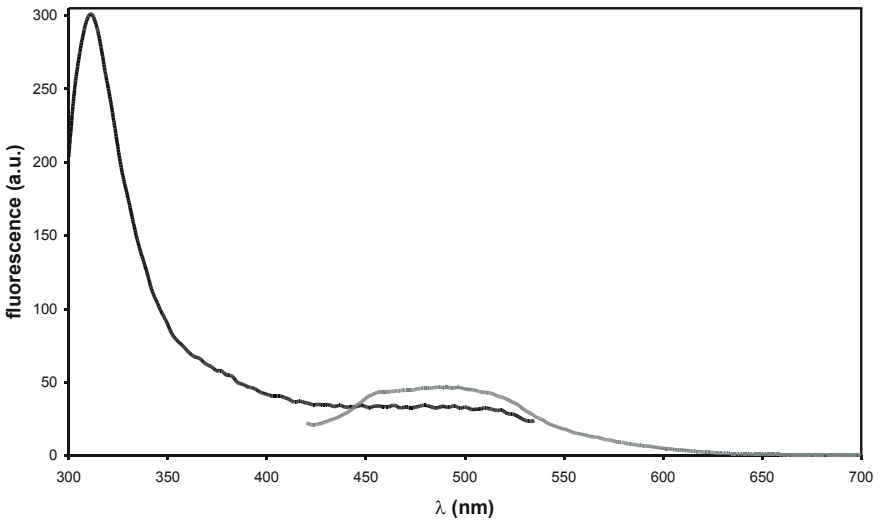

Figure 5. *Fluorescence emission spectra of OD-PIAT$_{17}$ using excitation wavelengths of 280 nm (black trace) and 400 nm (grey trace).*

It has already been described in Chapter 2 that partial uncoiling of the polyisocyanide backbone might occur when the hydrogen bonding network is not well-defined, leading to the formation of domains of conjugated imine bonds. This was also reflected in the color of the OD-PIAT samples, which displayed an orange/brown color. Structurally well-defined polyisocyanides are white.

6.3 Aggregation Behavior

Aggregation studies were carried out in water using the injection method.[33] For all the polymeric amphiphiles the dispersions turned turbid immediately upon injection in water. A range of morphologies could be observed when the samples were studied by transmission (TEM) and scanning electron microscopy (SEM). In freshly prepared dispersions of OD-PIAT$_{10}$ micrometers long micellar fibers, which had an average diameter of 16 nm, were visible (Figure 6 a). In contrast to OD-PIAT$_{10}$, no defined aggregates could be observed in dispersions of OD-PIAT$_{17}$ immediately after injection (Figure 6 b). The longer polymers, OD-PIAT$_{100}$ and OD-PIAT$_{500}$ both formed ill-defined rings, likely due to phase separation on the surface (Figure 6 c).

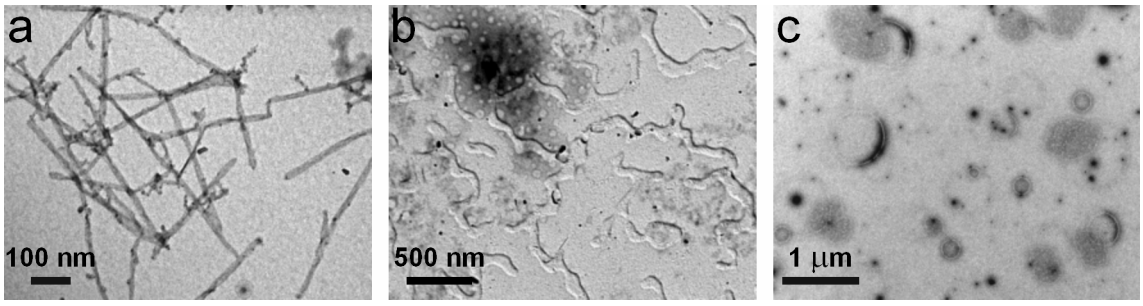

Figure 6. *TEM micrographs of freshly prepared dispersions of a) OD-PIAT$_{10}$, b) OD-PIAT$_{17}$, and c) OD-PIAT$_{500}$.*

Significant shape changes of block copolymer aggregates, induced by altering the dispersion, i.e. by addition of electrolytes or solvents, have been reported in the literature.[18] For the OD-PIAT aggregates, major morphological changes were observed merely upon ageing of the dispersions. In all of the studied aqueous dispersions 17 % (v/v) of tetrahydrofuran (THF) was present. In previous studies with PS-PIAT$_{50}$ it had been observed that this amount of organic solvent is high enough to prevent kinetic trapping of the formed aggregates.[25] After 14 days the amount of fibers in dispersions of OD-PIAT$_{10}$ was reduced and two new types of aggregates were visible, i.e. spherical micelles and network structures (Figure 7), which is an indication that the initially formed fibers are not the thermodynamically most favorable structures.

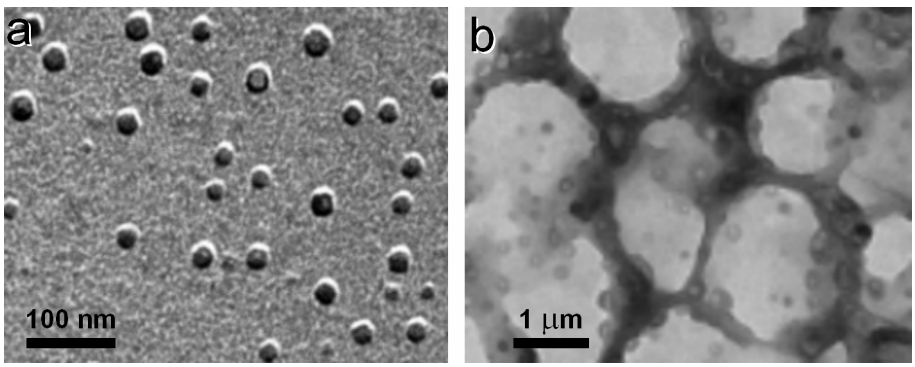

Figure 7. *Aggregates of OD-PIAT$_{10}$ after standing in dispersion for 14 days. a) Pt shadowed micelles and b) network structures.*

Surprisingly, dispersions of OD-PIAT$_{17}$, which initially had formed ill-defined aggregates, turned more turbid in time. After 16 hours polymersomes with diameters of circa 100 nm were observed, as well as larger polymersomes of several hundred nanometers in size (Figure 8 a).

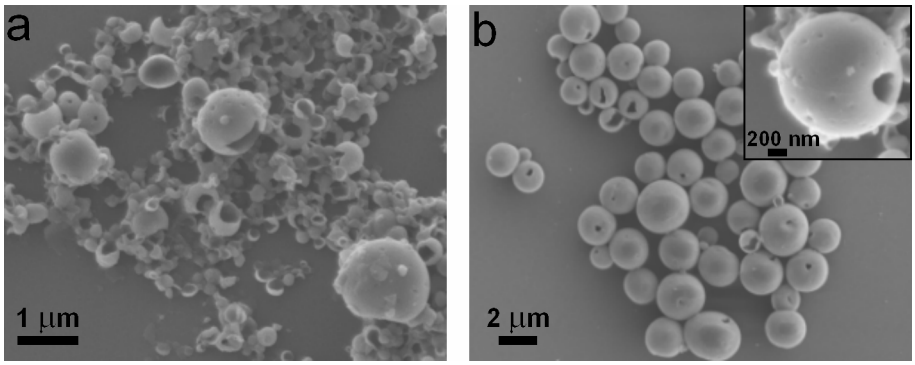

Figure 8. *a) Large and small polymersomes coexisting in a dispersion of OD-PIAT$_{17}$ after standing for 23 hours. b) Large polymersomes present after 6 days in dispersions of OD-PIAT$_{17}$; the inset shows a magnification of a polymersome.*

After 6 days electron microscopy studies on the dispersion revealed that all small polymersomes had disappeared as the result of a fusion process and that only large polymersomes with diameters ranging from 0.2 to 4 μm, and an average diameter of 1.6 μm had remained (Figure 8 b). The OD-PIAT$_{17}$ polymersomes are very similar to those observed for PS-PIAT$_{50}$.[25] The latter polymeric amphiphile initially formed polymersomes with an average diameter of 80 nm, which then fused in a period of two days to give polymersomes with an average diameter of 1.5 μm. In contrast to OD-PIAT$_{17}$, PS-PIAT$_{50}$ immediately formed polymersomes after preparation of the dispersion and the process of fusion was three times faster than the fusion process of the polymersomes of the former amphiphile. When the sizes of the two polymers are compared, it is remarkable that the larger PS-PIAT$_{50}$ is more dynamic than OD-PIAT$_{17}$. From the space filling models of OD-PIAT$_{17}$ and PS-PIAT$_{50}$ (see Figure 1), it is clear that the shape of these polymeric amphiphiles is very different. It is therefore believed that the aggregation process to a large extend is controlled by the polyisocyanide blocks, which can adopt a more crystalline type of packing as a result of their higher rigidity compared to the apolar blocks. This allows them to pack in a more close manner, thus favoring the formation of the polymersome membrane.

Fusion processes are known to be driven by the high curvature energy of the initially formed vesicles, which causes strain in the polymer chains, and by the presence of packing defects in the vesicle membrane.[34] Fusing into larger systems reduces the strain and the packing of the polymers is optimized, resulting in a lower surface energy. Dialysis of a freshly prepared dispersion of PS-PIAT$_{50}$ against water, which removes the THF present, followed by EM studies, showed that the polymersomes became kinetically trapped because of the removal of THF.[25] Their average diameter remained 80 nm over a period of weeks.

This experiment proved that only in the presence of THF the apolar PS block is flexible enough to allow rearrangement. Some PS-PIAT$_{50}$ polymersomes that were in an intermediate stage of fusion could be observed, demonstrating that the increase in polymersome diameter was truly by fusion and not by ripening.

OD-PIAT$_{100}$ did not show any morphological changes in time and after three weeks the polymers merely precipitated from solution. Interestingly, aggregates of OD-PIAT$_{500}$ did change in morphology over time and studies on a 14 days old dispersion revealed the formation of small, poor-defined, disk-shaped aggregates with an average diameter of 75 nm (Figure 9).

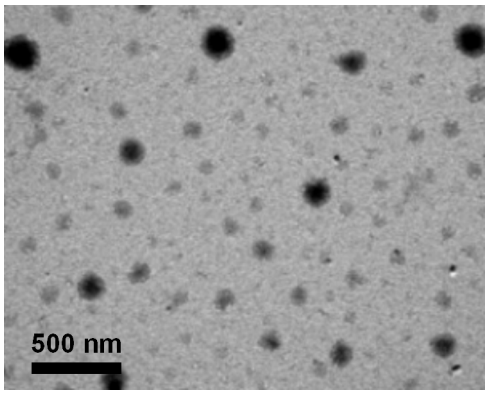

Figure 9. *Disk-shaped aggregates of OD-PIAT$_{500}$ after 14 days in dispersion.*

Considering the length of the polar head group of OD-PIAT$_{500}$ it is doubtful whether the apolar tail has a significant influence on the aggregation behavior of this polymer. It is therefore likely that the aggregation behavior of this compound is similar to that of the PIAT homopolymer, although it is known that amphiphiles with a very small head group can undergo changes in aggregate geometry.[18]

The theory of the critical packing parameter (P) developed by Israelachvili predicts the aggregate morphology of small amphiphiles by taking into account the ratio between the diameters of the head group and tail (Table 3).[35] For OD-PIAT$_{17}$ and PS-PIAT$_{50}$ this parameter must be very different when both molecules are completely extended (Figure 1), but when the apolar tails are curled up the P values might be more similar, resulting in the formation of the same type of aggregates, i.e. polymersomes. However, Israelachvili's theory was developed for small amphiphiles and therefore care has to be taken to implement this theory to block copolymer-based amphiphiles.

Table 3. ***Overview of the formed morphologies at different values of P***

Critical Packing Shape	P (v/a_0l_c)	Formed Structures
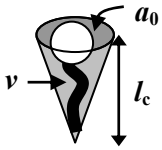	< 0.33	Spherical Micelles 
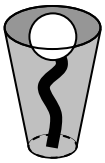	0.33 - 0.5	Cylindrical Micelles 
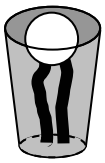	0.5 - 1	Vesicles 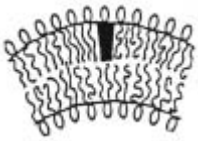
	= 1	Planar Bilayers 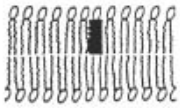
	> 1	Inverted Micelles 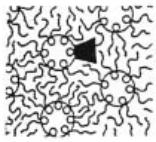

One of the reasons for a possible discrepancy is that the shape of the hydrophilic head group of a block copolymer can differ completely from that of a lipid amphiphile. In general, the head group of a classic amphiphile is much smaller than the apolar tail, while the polar head group of an amphiphilic block copolymer can be larger than the apolar block. Other interactions can also play a role in the case of polymers, such as entanglement of the chains or attraction between the head groups, which are absent in aggregates of small amphiphiles. Despite these differences a series of block copolymer amphiphiles based on polystyrene and poly(propylene imine) dendrimers prepared by Van Hest *et al*. was found to change aggregate morphology from vesicular to micellar rods to spherical micelles upon increasing the head group size (increasing number of dendrimer generations),[13] a trend analogous to lowering Israelachvili's P value.

The derivatives of OD-PIAT with short head group sizes can be considered as classic amphiphiles, but for larger head group sizes the OD tail will be of minor influence. Due to the short length of the polyisocyanide block in OD-$PIAT_{10}$ its head group is not well-defined, because of the limited number of hydrogen bonds that keep the structure. Therefore, the head group in this compound could in principle occupy more space than the head group of OD-$PIAT_{17}$, resulting in a lower P-value. This is a possible explanation for the fact that the former compound aggregated into micellar fibers and spherical micelles and the latter into polymersomes. By increasing the length of the PIAT block the influence of the apolar tail is reduced and this leads to a decrease in the amphiphilic character of the longer polymers, hence in less control during aggregation, as is demonstrated by OD-$PIAT_{100}$ and OD-$PIAT_{500}$.

The effect of concentration on the morphological changes was investigated with dispersions of OD-$PIAT_{10}$. Both the concentration of polymer in THF and the final water/THF ratio were varied. When solutions of 1.0 $mg.ml^{-1}$ or higher of OD-$PIAT_{10}$ in THF were injected into water no well-defined aggregates were obtained, independent of the final water/THF ratio and precipitation of these dispersions occurred within a day. With OD-$PIAT_{10}$ concentrations lower than 0.1 $mg.ml^{-1}$ in THF, stable dispersions could be prepared, but no aggregates could be observed by electron microscopy. At low ratios of water/THF no aggregates could be prepared either, probably as a result of the high THF concentration, which inhibits the formation of aggregates. The optimum conditions to prepare dispersions of OD-$PIAT_{10}$ were to use a concentration of 0.2 $mg.ml^{-1}$ polymer in THF and inject this solution into water with a final water/THF ratio of 5:1. It is possible that for the other three amphiphilic polymers better conditions can be found than the ones described here. However, this point was not studied further.

Samples were prepared from an OD-$PIAT_{10}$ dispersion of four weeks old, having a final OD-$PIAT_{10}$ concentration in water/THF that was 1.5 times lower than the dispersion which initially formed fibers (Figure 6 a). TEM studies revealed that in this case a new type of fiber, which appeared to be built up from bundles of much smaller fibers, was generated (Figure 10). It is not yet clear how these structures are built up. It might be possible that the observed fibers are the result of folding of a bilayer tape or another type of aggregate.

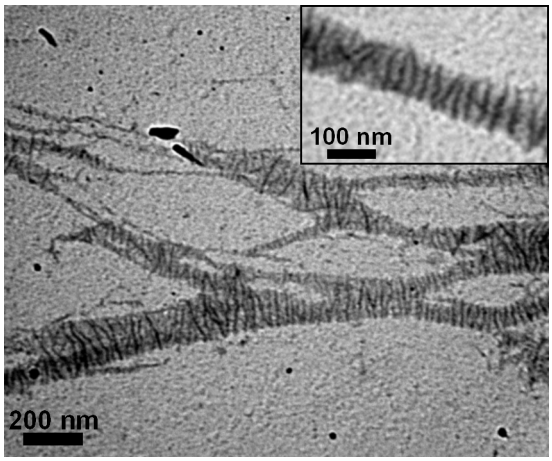

Figure 10. *Aggregates of OD-PIAT$_{10}$ in a dispersion of 0.02 mg.ml^{-1} in water/THF (5:1 v/v) after being 4 weeks in dispersion. The inset shows a magnification.*

Various attempts were made to prepare aggregates with DMF instead of THF as a co-solvent, in order to investigate the influence of the solvent on the formation of aggregates. Solutions with a range of concentrations of OD-PIAT$_{10}$ in DMF were prepared and these solutions were injected into water in an identical manner as described before. Unfortunately, no well-defined aggregates could be obtained by this approach, highlighting the strong effect of the co-solvent on the aggregate formation. This different result is thought to be related to the better solubility of OD-PIAT$_{10}$ in DMF than in THF, which keeps this polymer dissolved in water, even at low DMF concentrations.

6.4 Conclusions

OD-PIAT polymers with increasing PIAT length have been synthesized and their aggregation behavior in water studied in detail. The purpose of this study was to compare the OD-PIAT system with the PS-PIAT diblock copolymer system, in particular to determine the influence of the apolar block length on the aggregation behavior of the amphiphiles. A range of morphologies could be obtained from the amphiphilic OD-PIAT macromolecules upon increasing the head group size, some of which were not seen with PS-PIAT, thus showing the importance of the apolar block in the aggregation process.

Ageing of the dispersions was found to result in a change of morphology. For instance, OD-PIAT$_{17}$ initially formed no well-defined structures, but after several hours polymersomes were observed to form, which fused to even larger polymersomes after 6 days. Remarkably, this behavior is identical to that seen for PS-PIAT$_{50}$, which is a considerably larger molecule,

suggesting that the head group in the diblock copolymer amphiphile determines the aggregate morphology. In the case of the two longest OD-PIAT polymers the influence of the apolar tail on the aggregation behavior appeared to be negligible, since for both compounds no well-defined aggregates could be observed.

Both the concentration of the initial OD-PIAT$_{10}$ solution in THF and the final amphiphile concentration in dispersions of water/THF proved to be critical for a controlled aggregation process. Stable dispersions containing well-defined aggregates, could only be prepared from OD-PIAT$_{10}$ in a small concentration range (0.1 g.ml^{-1} – 1.0 g.ml^{-1}).

The formation of polymersomes by OD-PIAT$_{17}$ is promising for applications, e.g. the construction of electron conducting spheres containing redox active enzymes. The previously prepared polymersomes of PS-PIAT$_{50}$ had a relatively thick insulating layer of polystyrene which may be unfavorable for the transport of electrons from the electron conducting polymersome to an external electrode (see Chapter 3). The polymersomes of OD-PIAT$_{17}$ have a thinner bilayer and are much better in that respect, although it remains to be proven that the thiophene functions can be polymerized to give an electron conducting sphere.

6.5 Experimental Section

General methods and materials

THF was distilled over sodium and CH_2Cl_2 over $CaCl_2$. DMF was first dried for a week on BaO before it was distilled under reduced pressure. For the synthesis of (tBuNC)$_4$Ni(ClO$_4$)$_2$ a literature procedure was followed.[36] The synthesis of the monomer (IAT) is described in Chapter 2. The route that led to racemization was used. All other chemicals were used as received unless stated otherwise. For all aggregation studies ultra pure water (R > 18×10^6 Ω) was used. ^{1}H NMR and ^{13}C NMR spectra were recorded on a Bruker AC-300 instrument at room temperature. Chemical shifts are given in ppm (δ) relative to tetramethylsilane. Abbreviations used are s = singlet, d = doublet, t = triplet, q = quartet, m = multiplet and br = broad. A MAT900 mass spectrometer was used for the preparation of ESI mass spectra. Infrared spectra were recorded on a BioRad FTS 25 spectrometer. A Varian Cary 50 spectrometer was used to prepare UV-Vis spectra. CD spectra were measured on a Jasco J600 machine. A Perkin Elmer LS 50B instrument was used to record fluorescence spectra. Optical rotations were determined with a Perkin Elmer 241 polarimeter. GPC measurements were carried out with a Shimadzu GPC instrument with Shimadzu refractive index and UV-Vis detectors, equipped with a Polymer Laboratories Plgel 5 μm mixed-D column and a PL 5 μm Guard column (separation range from 500 – 300,000 molecular weight). THF was used as a mobile phase at 35°C.

Preparation of aggregates

In a typical aggregation experiment 1.0 ml of a 1.0 mg.ml^{-1} OD-PIAT solution in THF was injected into 5.0 ml ultra pure water. In order to homogenize the obtained dispersion it was shaken by hand. No additional energy was used to induce aggregate formation.

Microscopy studies

For the SEM and TEM studies JEOL JSM-6330F and JEOL JEM-1010 microscopes were used, respectively. Samples for TEM were prepared by drying a drop of the dispersion on a carbon-coated copper grid. The excess of water was blotted away with a filter paper after 2 min. For Pt shadowing the grids were placed in an Edwards coater Model 306 under an angle of 45° with respect to the Pt source. SEM samples were prepared by drying a drop of the dispersion on microscopy glass that had been cleaned by sonication for 15 min. in CH_2Cl_2. The samples were left to dry for a day in the fume hood before study. A 1.5 nm layer of Pd/Au was sputtered on the SEM samples before study using a Cressington 208 HR sputter coater fitted with a Cressington layer thickness controller.

Synthesis

Initiator complex

To a stirred solution of 53 mg (0.090 mmol) of (tBuNC)$_4$Ni(ClO_4)$_2$ in 10 ml of CH_2Cl_2 was added 0.29 ml (0.090 mmol) of OD-NH_2 under a N_2 atmosphere. After stirring for 1 h, thin layer chromatography showed complete consumption of OD-NH_2. The reaction mixture was evaporated to dryness, resulting in an orange oil (yield 100 %). ^{1}H NMR (300 MHz, $CDCl_3$) δ 8.13 (s, N*H*), 7.99 (s, N*H*), 7.00 (s, N*H*), 6.81 (s, N*H*), 5.33 (m, 2H, CH_2CH=$CH$$CH_2$), 4.11 and 3.36 (2s, 2H, CH_2NH), 2.01 (m, 4H, CH_2C=C), 1.74-1.26 (m, remaining H), 0.89 (t, 3H, CH_2CH_3) ppm; ^{13}C NMR (75 MHz, $CDCl_3$) δ 177.4 (NCN), 124–123 (br, Ni-*C*=N), 130.2, 130.0, 129.8 (CH_2*C*H=*C*HCH_2), 60.6, 56.5, 55.8 (Ni-C=N-*C*(CH_3)$_3$), 51.5 (CH_2CH_2*C*H_2NH), 32.0 (*C*H_2CH=CHCH_2), 31.2 (CH_3CH_2*C*H_2), 30.6 ($CH_3CH_2CH_2$*C*H_2), 29.7 ((*C*H_3)$_3$CN), 29.5–26.9 (remaining hydrogen atoms of OD tail), 22.8 (CH_3*C*H_2CH_2), 14.3 (*C*$H_3CH_2CH_2$) ppm; FT-IR (cm^{-1}, KBr) 3283 (NH), 2986, 2958, 2923, 2854 (CH), 2254, 2227 (C=N), 1637 (C=C), 1584 (NCN), 1546 (CNC), 1463 (C-C), 1095 (ClO_4).

OD-PIAT

In a typical polymerization reaction the desired amount of initiator complex, dissolved in 5.0 ml of CH_2Cl_2, was added to a stirred solution of IAT in 10 ml of CH_2Cl_2. Complete consumption of isocyanide, as observed by IR spectroscopy, was obtained after 2 days. The reaction mixture was evaporated to dryness and the resulting product redissolved in a minimal amount of CH_2Cl_2. The polymer was then precipitated by adding the CH_2Cl_2 solution into a well-stirred mixture of methanol/water (1:1 v/v). The product was filtered off and washed with methanol/water (1:1 v/v). After drying *in vacuo* the polymer was obtained as an orange/brown solid (yields 58–79 %). The IR, CD and optical rotation data of the prepared polymers are summarized in Table 1 and Table 2. As an example the NMR data of OD-PIAT$_{10}$ are given: ^{1}H NMR (300 MHz, $CDCl_3$) δ 7.3–6.9 (br, thiophene H-5), 6.9–6.4 (br, thiophene H-2 and thiophene H-4), 5.5–5.2 (br, 2H, C*H*=C*H*), 4.6–4.1 (br, C=NC*H*(CH_3)), 3.9–3.3 (br, CH_2CH_2-thiophene), 3.1–2.6 (br, CH_2-thiophene), 1.8–1.5 (br, C=NC(*C*H_3)$_3$), 2.1–1.9 (br,

CH_2C=C), 1.7–1.1 (remaining H), 1.0–0.8 (br, $CH_2CH_2CH_3$); ^{13}C NMR (75 MHz, $CDCl_3$) δ 175–170 (br, *C*(O)NH), 167–161 (br, *C*=NCH(CH3)C(O)), 139 (br, thiophene C-3), 136.0 (*C*H=*C*H), 127.9 (br, thiophene C-4), 125.6 (br, thiophene C-5), 121.1 (br, thiophene C-2), 68–62 (br, C=N*C*H(CH_3)C(O)), 40.4 (br, CH_2CH_2NHC(O)), 32–30 (C=NC(CH_3)$_3$) and CH_2CH=CHCH_2), 29.6 (br, CH_2CH_2NHC(O)), 24–18 (br, OD tail), 21.9 (br, C=NCH(CH_3)C(O)), 14.1 ($CH_2CH_2CH_3$) ppm.

6.6 References and Notes

[1] K. Yu, A. Eisenberg, *Macromolecules* **1998**, *31*, 3509.
[2] I. C. Riegel, A. Eisenberg, *Langmuir* **2002**, *18*, 3358.
[3] S. E. Burke, A. Eisenberg, *Polymer* **2001**, *42*, 9111.
[4] A. A. Choucair, A. H. Kycia, A. Eisenberg, *Langmuir* **2003**, *19*, 1001.
[5] L. Luo, A. Eisenberg, *Langmuir* **2001**, *17*, 6804.
[6] S. Pispas, N. Hadjichristidis, *Langmuir* **2003**, *19*, 48.
[7] B. M. Discher, Y.-Y. Won, D. S. Ege, J. C.-M. Lee, F. S. Bates, D. E. Discher, D. A. Hammer, *Science* **1999**, *284*, 1143.
[8] S. Liu, N. C. Billingham, S. P. Armes, *Angew. Chem. Int. Ed.* **2001**, *40*, 2328.
[9] Z.-C. Li, Y.-Z. Liang, F.-M. Li, *New J. Chem.* **2002**, *26*, 1805.
[10] L. Zhang, K. Yu, A. Eisenberg, *Science* **1996**, *272*, 1777.
[11] L. Zhang, A. Eisenberg, *Macromolecules* **1996**, *29*, 8805.
[12] L. Zhang, A. Eisenberg, *Science* **1995**, *268*, 1728.
[13] J. C. M. van Hest, D. A. P. Delnoye, M. W. P. L. Baars, M. H. P. van Genderen, E. W. Meijer, *Science* **1995**, *268*, 1592.
[14] O. Terreau, L. Luo, A. Eisenberg, *Langmuir* **2003**, *19*, 5601.
[15] J. Ding, G. Liu, M. Yang, *Polymer* **1997**, *38*, 5497.
[16] Y.-Y. Won, A. K. Brannan, H. T. Davis, F. S. Bates, *J. Phys. Chem . B* **2002**, *106*, 3354.
[17] S. Förster, M. Antonietti, *Adv. Mater.* **1998**, *10*, 195.
[18] N. S. Cameron, M. K. Corbierre, A. Eisenberg, *Can. J. Chem.* **1999**, *77*, 1311.
[19] M. Antonietti, S. Förster, *Adv. Mater.* **2003**, *15*, 1323.
[20] J. J. L. M. Cornelissen, M. Fischer, N. A. J. M. Sommerdijk, R. J. M. Nolte, *Science* **1998**, *280*, 1427.
[21] J. J. L. M. Cornelissen, R. van Heerbeek, P. C. J. Kamer, J. N. H. Reek, N. A. J. M. Sommerdijk, R. J. M. Nolte, *Adv. Mater.* **2002**, *14*, 489.
[22] R. J. M. Nolte, *Chem. Soc. Rev.* **1994**, *23*, 11.
[23] W. Drenth, R. J. M. Nolte, *Acc. Chem. Res.* **1979**, *12*, 30.
[24] P. C. J. Kamer, R. J. M. Nolte, W. Drenth, *J. Am. Chem. Soc.* **1988**, *110*, 6818.
[25] D. M. Vriezema, J. Hoogboom, K. Velonia, K. Takazawa, P. C. M. Christianen, J. C. Maan, A. E. Rowan, R. J. M. Nolte, *Angew. Chem. Int. Ed.* **2003**, *42*, 772.
[26] J. J. L. M. Cornelissen, *Polymers and block copolymers of isocyanopeptides*, Ph.D. thesis, University of Nijmegen, Nijmegen, **2001**.
[27] G.A. Metselaar, manuscript in preparation.
[28] G. Z. Gao, F. Sanda, T. Masuda, *Macromolecules* **2003**, *36*, 3938.
[29] A. J. M. van Beijnen, R. J. M. Nolte, W. Drenth, A. M. F. Hezemans, P. J. F. M. van de Coolwijk, *Macromolecules* **1980**, *13*, 1386.
[30] A. J. M. van Beijnen, R. J. M. Nolte, A. J. Naaktgeboren, J. W. Zwikker, W. Drenth, *Macromolecules* **1983**, *16*, 1679.
[31] J. J. L. M. Cornelissen, W. S. Graswinckel, A. E. Rowan, N. A. J. M. Sommerdijk, R. J. M. Nolte, *J. Polym. Sci. , Part A: Polym. Chem.* **2003**, *41*, 1725.
[32] P. Samorí, C. Ecker, I. Gössl, P. A. J. de Witte, J. J. L. M. Cornelissen, G. A. Metselaar, M. B. J. Otten, A. E. Rowan, R. J. M. Nolte, J. P. Rabe, *Macromolecules* **2002**, *35*, 5290.
[33] A. S. Domazou, P. L. Luisi, *J. Liposome Res.* **2002**, *12*, 205.
[34] J. Zimmerberg, L. V. Chernomordik, *Adv. Drug Delivery Rev.* **1999**, *38*, 197.
[35] J. N. Israelachvili, *Intermolecular & Surface Forces*, second ed., Academic Press, London, **1992**.
[36] R. W. Stephany, W. Drenth, *Recl. Trav. Chim. Pays-Bas* **1972**, *91*, 1453.

Chapter 7

Towards Electron Conducting Polyisocyanide Nanowires

7.1 Introduction

Electron conducting wires of nanometer dimensions have been often proposed as ideal materials for application in electronic devices or as building blocks for transport layers in electrocopying machines or electrophotographic instruments. For such purposes self-assembled columns or wires with high carrier mobilities, capable of rapid one-dimensional charge transport would be of interest. These properties can, however, only be obtained when the electro-active units are arranged in a precise manner. Any defect will very rapidly inhibit electron transfer. In Chapter 2 the synthesis and characterization of polyisocyanides bearing thiophene side groups were presented. The polyisocyanide backbone functioned as a scaffold onto which the thiophene groups were ordered in a precise fashion. All carbon atoms in the backbone of a polyisocyanide bear substituents, resulting in a high degree of steric crowding of the side groups, which significantly decreases the rotational freedom of the atoms forming the polymer backbone.[1] Both theoretical and experimental studies have revealed that the polyisocyanide backbone adopts a helical arrangement with a high rotational barrier when the side groups are sufficiently bulky. The rigidity of polyisocyanides can be further increased by the introduction of hydrogen bond-forming moieties like amides. Cornelissen *et al.* prepared polyisocyanides from amino acids and have demonstrated that the resulting polymers are very stiff, due to the formation of hydrogen bonds between the amide groups in the side chains.[2, 3] De Witte *et al.* have shown that large chromophoric dyes, i.e. porphyrins and perylenes, can be attached as side groups to polyisocyanides.[4]

In this chapter we discuss the possibilities to prepare nanowires based on rigid polyisocyanides having electroactive side groups that are well-arranged in a columnar

fashion. In addition to rigidity the functional side-arms have to be oriented in such a way that they form well-ordered stacks. Molecules possessing a large aromatic surface already have the tendency to arrange themselves into stacks to maximize π–π overlap. Porphyrins and phthalocyanines are large dye molecules with an aromatic core ranging from 10–20 Å, which are known to stack to give discotic liquid crystals if long aliphatic tails are present. Crown ether functionalized phthalocyanines, which are even larger, are known to form electron conductive stacks,[5, 6] while phthalocyaninato-polysiloxane systems have been shown to form rigid electron conductive nanowires.[7] In this chapter attempts to prepare hexabenzocoronene (HBC) and tetrathiafulvalene (TTF) polyisocyanide molecules will be described (Figure 1).

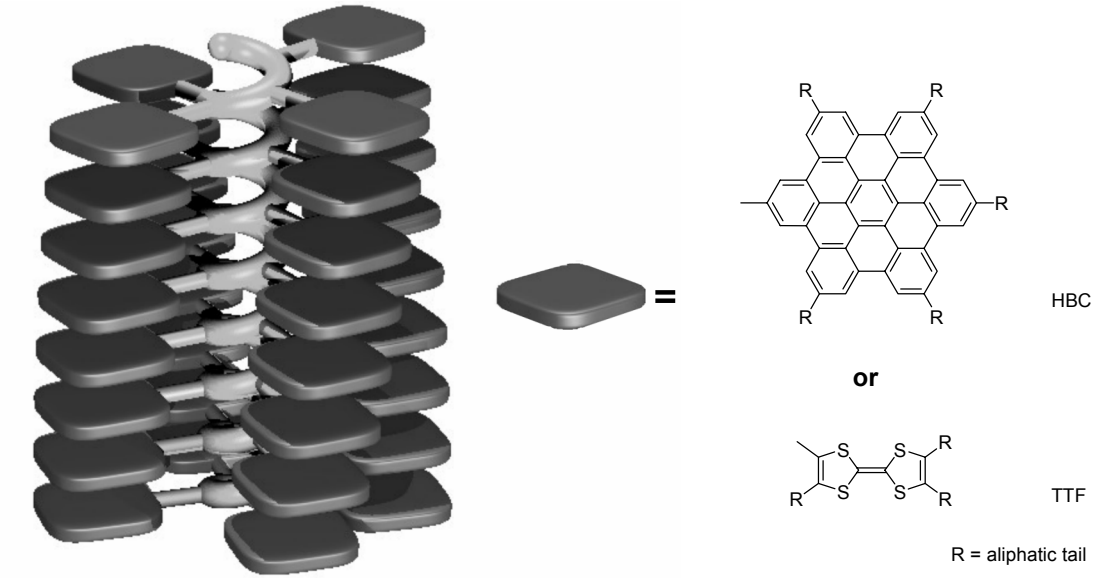

Figure 1. *Schematic representation of a polyisocyanide containing electro-active side groups (HBCs or TTFs).*

7.1.1 Hexabenzocoronenes

HBCs are flat, disk-shaped, polyaromatic hydrocarbons.[8-11] Alkyl- or phenyl-alkyl substituted HBCs form discotic liquid crystalline materials with mesophases extending over a large temperature range. These mesophases are very stable due to the very large aromatic core of the mesogens, which favor π–π overlap.[12] Self-assembled columns of HBCs are known to have high charge carrier mobilities along the columnar axis (1.13 $cm^2.V^{-1}.s^{-1}$).[13]

In the group of Müllen polymeric architectures of HBCs have been prepared, both in a covalent and non-covalent manner. One method was the polymerization of a

hexaphenylbenzene containing a vinyl group (4'-(4-vinylphenylene)hexaphenylbenzene, 4VPHBC), of which both homo- and copolymers were prepared(Scheme 1).[14]

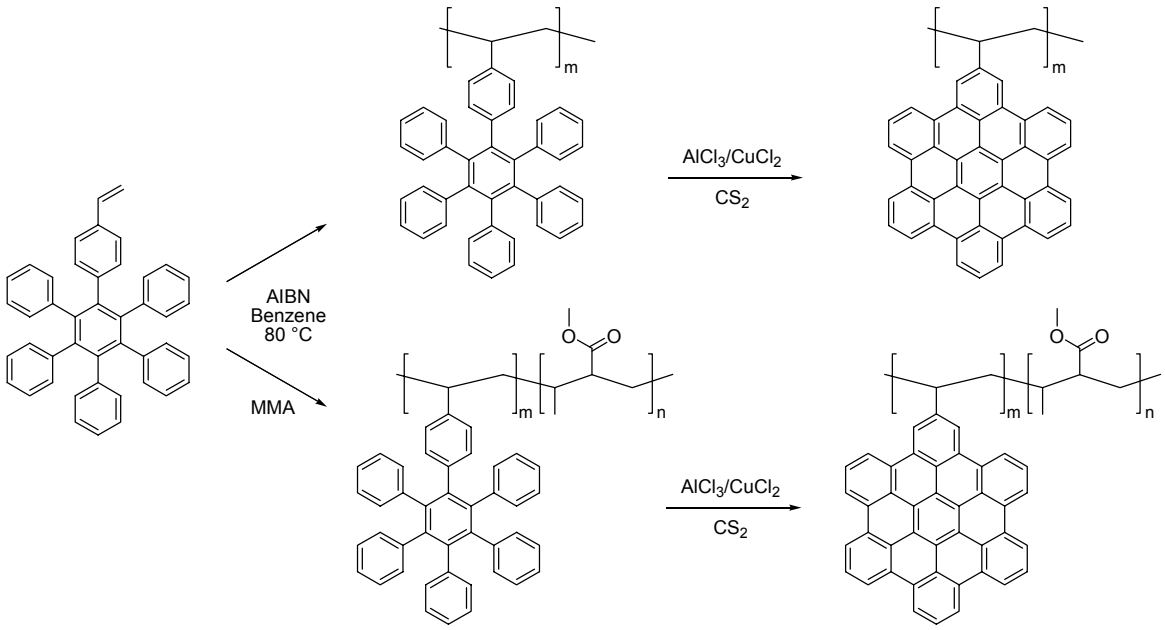

Scheme 1. *Preparation of homo- and block copolymers with an HBC side group.[14]*

Both types of polymers were prepared by a radical polymerization reaction with azobis(izobutyronitrile) (AIBN) as the initiator in refluxing benzene. The copolymer was obtained by polymerizing a mixture of methylmethacrylate (MMA) and 4VPHBC. After this reaction a cyclodehydrogenation of the hexaphenylbenzene groups was conducted with the help of $AlCl_3$ and $CuCl_2$ in CS_2. In the case of the homopolymer a completely insoluble brown solid was obtained, in which 90 % of the hexaphenylbenzene groups were converted into HBC groups as determined by elemental analysis and IR studies. The copolymer was also subjected to the cyclodehydrogenation conditions and again an insoluble material was obtained, but extraction with 1,1,2,2-tetrachloroethane yielded a soluble fraction of the HBC-containing polymer. The degree of cyclodehydrogenation in this fraction was determined to be 18 % using UV-Vis measurements, however, the total degree of cyclodehydrogenation could not be determined. It is obvious that this approach is not suitable for HBCs containing no solubilizing aliphatic tails. It is likely that the use of more soluble HBCs will lead to more satisfying results, however, complete conversion of all hexaphenylbenzene groups seems difficult, and thus the formation of well-defined electron conductive stacks may not be possible by this approach.

Complexation of carboxylate functionalized hexabenzocoronenes with ionic polymers has been used to study their thermotropic liquid-crystalline behavior.[15] Two different HBCs and three different ionic polymers were investigated (Scheme 2).

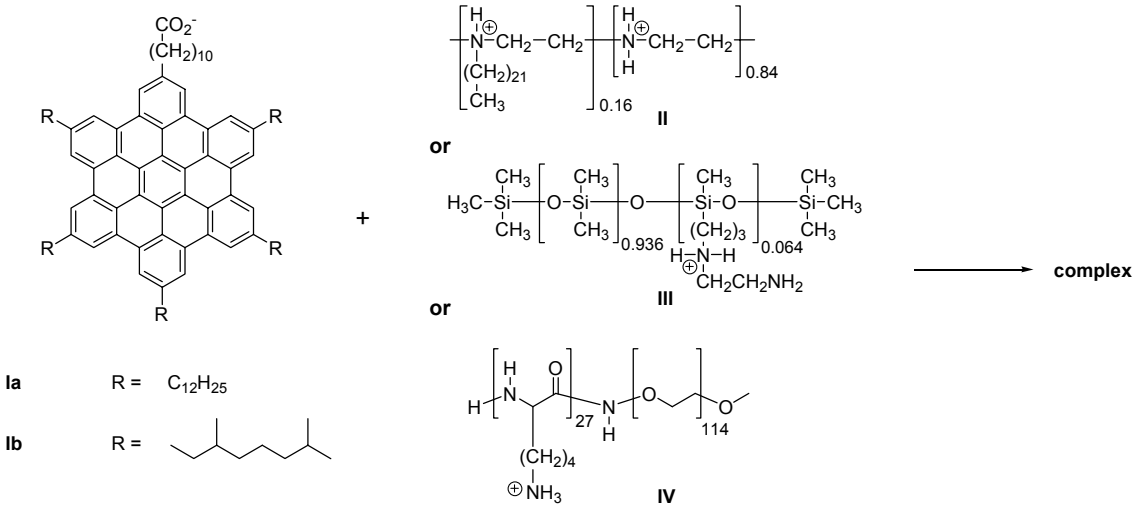

Scheme 2. *Overview of HBCs and ionic polymers used to prepare polymeric complexes of HBCs.[15]*

For the stoichiometric complex of **Ia** and polyethyleneimine **II** a rectangular centered lattice was found at room temperature, whilst at higher temperatures the columns were oriented in a hexagonal columnar mesophase (Figure 2).[15]

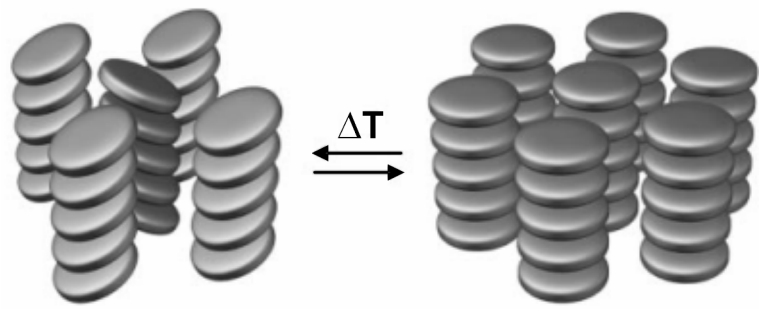

Figure 2. *Two different columnar mesophases formed by complexes of **Ia** and **II**. The left arrangement was found at room temperature, while at higher temperatures the right arrangement was observed.[15]*

In the absence of ionic polymer **II** compound **Ia** formed columnar liquid-crystalline structures as well, with the same columnar mesophases. The intra-molecular order of the stoichiometric complex was found to be low, whereas the inter-molecular order was high.

Complexation of **Ia** with amino-functionalized polysiloxane **III** also resulted in a polymeric complex, which gave two highly ordered columnar mesophases.[16] At lower temperatures the disk-like aromatic cores were tilted with respect to the columnar axis, while at higher temperatures the cores were perpendicular to the column axis as determined by small-angle X-ray scattering. Diblock copolymer **IV** (poly(ethylene oxide)-*b*-poly(L-lysine) (PEO-PLL) was used to complex compound **Ib**.[17] The PLL blocks formed an α-helical secondary structure around which six discotic columns of **Ib** were arranged (Figure 3).

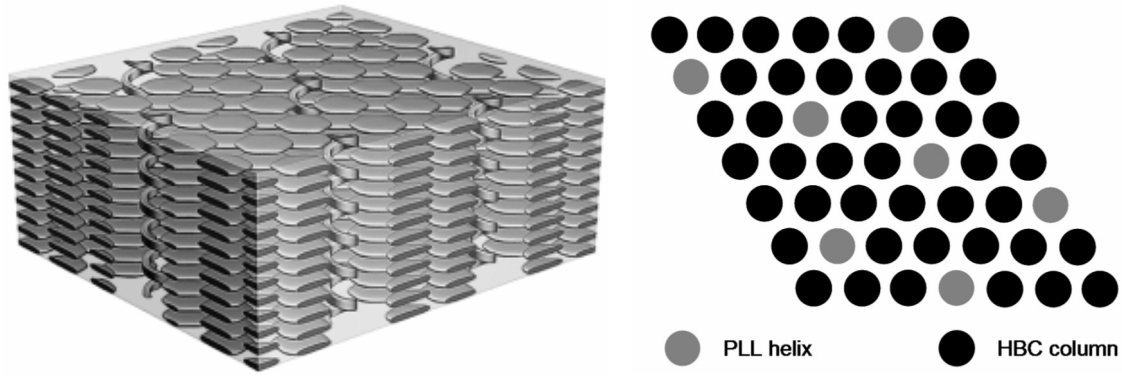

Figure 3. *Left: model of a stoichiometric complex of **Ib** and **IV** showing the α-helical structure of the PLL blocks which are symmetrically surrounded by six columns of **Ib**. Right: top view of the model.*

This complex formed a thermotropic liquid crystal and like the above mentioned polymer-HBC complexes it underwent phase-transitions upon heating. Temperature-dependent small-angle X-ray scattering showed that the phase at higher temperature is of higher structural order, due to a better intracolumnar packing of the HBC disks.

Recently Hill *et al.* described the self-assembly of an amphiphilic hexa-*peri*-hexabenzocoronene into discrete graphitic nanotubular objects.[18] TEM studies suggest that the tubes are built up from bilayers of HBCs. Upon oxidation, an electrical conductivity of 2.5 MΩ was reported for this nanotube which is comparable to that of an inorganic semiconductor nanotube composed of gallium nitride.

7.1.2 Tetrathiafulvalenes

TTF and its derivatives are reversible, stable two-electron donors (Scheme 3), and have been widely applied in supramolecular chemistry, since it was discovered 30 years ago that a chloride salt of a TTF had a high electrical conductivity.[19-23]

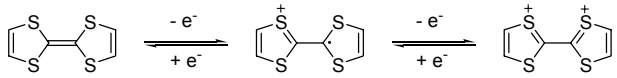

Scheme 3. *Reversible oxidations of TTF.*

The strong electron donating abilities of TTFs have been exploited in the catalysis of radical reactions,[24] and the construction of redox active supramolecular host-guest systems in order to function as sensors, catalysts and molecular switches.[25-27] In the groups of Stoddart and Becher molecular shuttles and molecular switches from TTF-containing (pseudo)rotaxanes and catenanes have been prepared and studied (Figure 4).[19, 23, 28, 29]

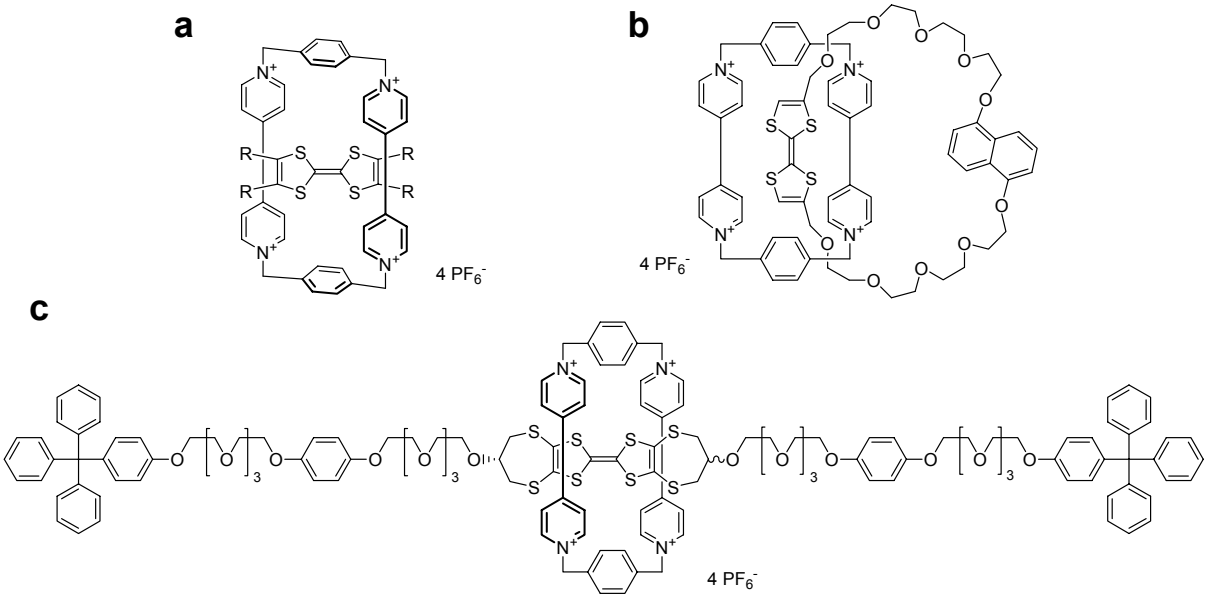

Figure 4. *a) Pseudorotaxane, b) catenane, and c) rotaxane containing TTF groups.*

Other areas where TTFs have been applied are organic ferromagnets,[30] molecular electronics,[31] nonlinear optics (NLO),[32] and fullerene chemistry. In the latter case fullerenes functionalized with TTF groups were prepared which displayed photophysical properties leading to charge-separated states with remarkable lifetimes.[33]

Polymers containing TTF units as side groups or as part of the polymer main chain have been prepared.[33] Several procedures have been developed, with varying amounts of success, to introduce TTFs in the main chain of the polymer.[34] Reducing the conformational freedom of the TTF groups helps improving the electron conducting properties. For that purpose different research groups have prepared polymers with either non-conjugated or π-conjugated backbones (Figure 5).[35, 36]

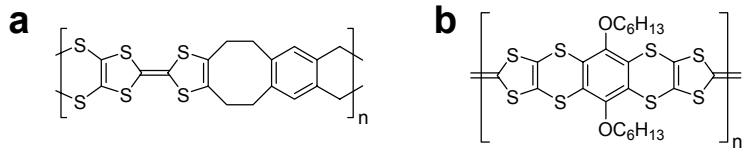

Figure 5. *Examples of polymers having TTF units in the main chain, a) ladder-type polymer, b) fully conjugated ribbon-type polymer.*

In another attempt to incorporate TTF moieties into a conjugated polymer backbone the TTF group was attached to an electropolymerizable thiophene compound. After polymerization a conjugated polymer with pendant TTF groups was formed. This method was originally developed by Bryce *et al.* to control the long-range order of the polythiophene by using the strong propensity of TTF to self-assemble into π–π stacks (Figure 6 a).[37] Roncali and coworkers prepared bithiophenes with TTF side groups to lower the electropolymerization potential (Figure 6 b).[38]

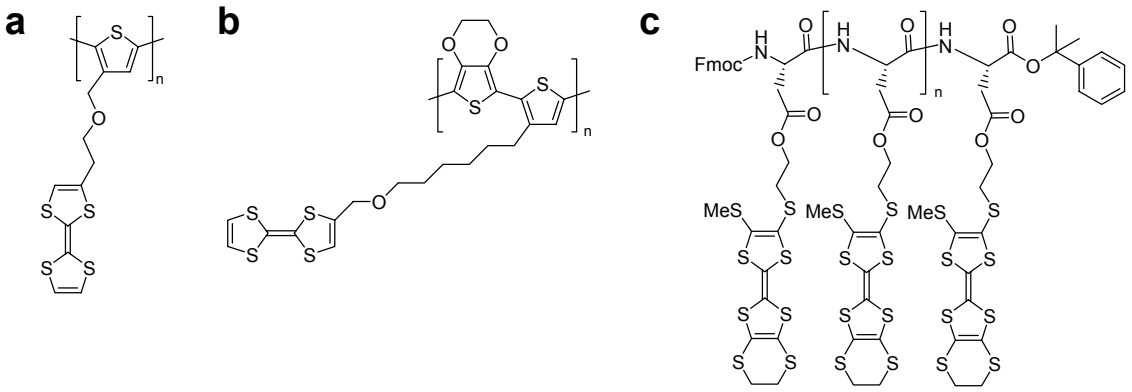

Figure 6. *Examples of polymers with pending TTF side groups, a) polythiophene,[37] b) poly(bithiophene),[38] and c) polypeptide with TTF side groups.[39]*

In the group of Kilburn TTF-bearing amino acids were incorporated into a polypeptide where the role of the backbone would be to control the spatial arrangements of the TTF groups (Figure 6 c).[39] They proposed that the incorporation of TTF units into an α-helical structure might allow the alignment of these groups into a conducting stack on one face of the helix. Although they have not been able to prepare characterizable charge transfer salts of these polymers, their electrochemical studies indicate that the polymers may well undergo conformational reorganization upon oxidation of the TTF moieties, presumably as a result of repulsion between the TTFs.

Because of their unique properties the HBC and TTF groups described above were chosen as possible candidates for the construction of functional polyisocyanide nanowires.

7.2 Polyisocyanides with Hexabenzocoronene Side Groups

For the synthesis of a polyisocyanide with HBC side groups the approach depicted in Scheme 4 was used.

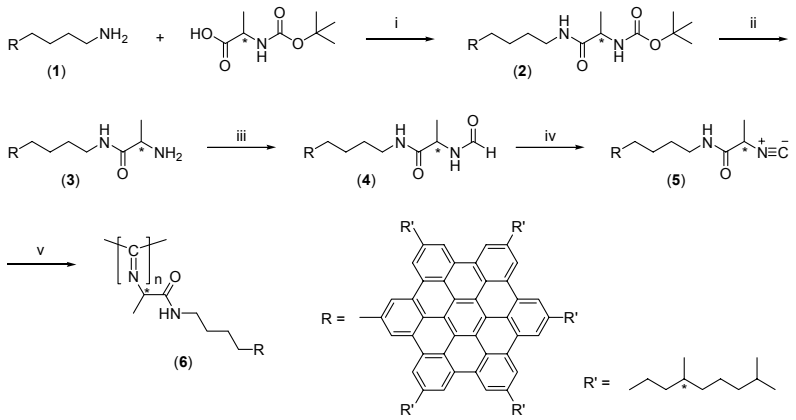

Scheme 4. *Synthesis of poly(HBC-L-isocyanoalanine); i) EDC, DMAP, CH_2Cl_2; ii) CF_3CO_2H, CH_2Cl_2; iii) diisopropylethylamine,* p-*nitrophenylformate, THF; iv) diphosgene,* N-*methylmorpholine, CH_2Cl_2; and v) $Ni(ClO_4)_2$, EtOH, CH_2Cl_2.*

Amine-functionalized HBC **1** was coupled to Boc-L-Ala-OH using 1-(3-dimethylaminopropyl)-3-ethylcarbodiimide (EDC) as activating agent. After deprotection of the Boc group with trifluoroacetic acid, compound **3** was converted into formamide **4** using *p*-nitrophenylformate. Dehydration of **4** with diphosgene and *N*-methylmorpholine resulted in isocyanide **5**. Work up of the dehydration reaction proved to be troublesome because addition of a saturated $NaHCO_3$ solution, a standard procedure in the preparation of isocyanides,

resulted in the regeneration of formamide **4**. Before addition of the aqueous $NaHCO_3$ solution a strong vibration at 2123 cm^{-1} originating from the formed isocyanide group could be observed in the IR spectrum of the crude reaction mixture. This vibration disappeared after addition of the $NaHCO_3$ solution. In a second attempt both IR and mass spectroscopy showed that the isocyanide was formed. It was then decided to polymerize isocyanide **5** without prior work up.

In order to prevent racemization of the α-carbon of the Ala group the HBC group was introduced at the beginning of the synthesis. A more versatile approach would be, however, to introduce the HBC group at a later stage. One can argue that it is better to do initial experiments with racemized compounds, just to show a proof-of-principle, but it is not sure whether a racemized polyisocyanide with HBC side groups would give a well-defined column of HBCs parallel to the polyisocyanide backbone.

Although the formed isocyanide was not purified before polymerization (see above), it could be demonstrated by CD spectroscopy that a helical polyisocyanide is formed upon addition of a catalytic amount of $Ni(ClO_4)_2$ (Figure 7).

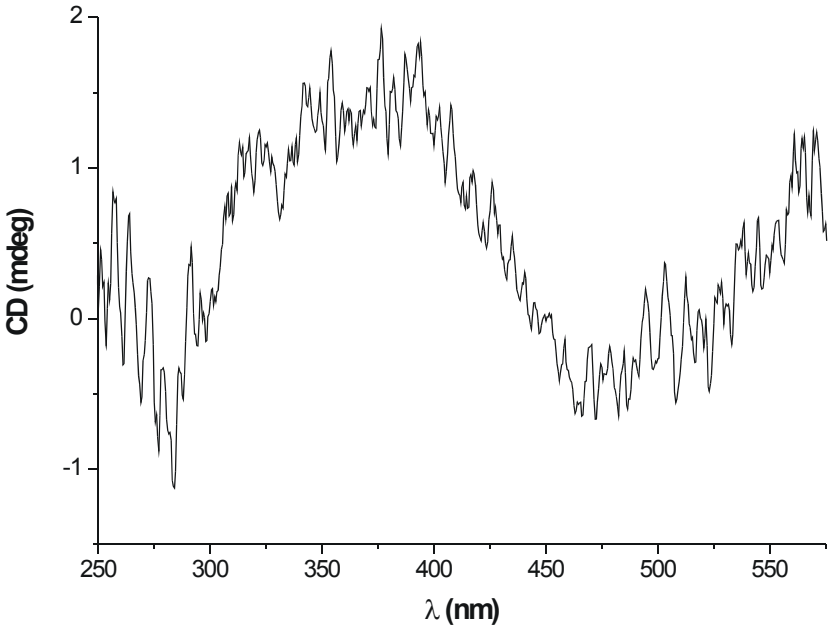

Figure 7. *CD spectrum of polyisocyanide **6** in CH_2Cl_2.*

The CD spectrum shows a negative signal effect at 284 and 482 nm and a broad positive signal around 370 nm. In general, the CD spectra of polyisocyanides with a well-

defined hydrogen bonding network display a single strong Cotton effect around 310 nm.[40] The CD spectrum of **6** indicates that such a hydrogen bonding pattern is obscured, either due to the presence of more than one conformation of the polymer backbone or due to the effect of the HBCs on the n–π* transitions of the N=C chromophores. It is very well possible that there is competition between the π–π stacking of the HBC cores and hydrogen bond formation between the amide groups in the side chains, resulting in a complex architecture.

The IR spectrum of polymer **6** revealed the disappearance of the isocyanide group, indicating complete polymerization of **5**. The amide vibrations in the polymer were shifted between 3 and 11 cm^{-1} to lower wave numbers, suggesting that hydrogen bonds were present between these groups, however, the IR and CD data indicated that no strong hydrogen bonding arrays were formed between the side groups. Other characterization methods were not tried, because of the low yield of the polymerization reaction, but are necessary to elucidate the structural arrangement of polyisocyanide **6** in the future. It is remarkable in itself that such a large molecule as HBC is, can be incorporated as a side group in a polyisocyanide chain. These preliminary results suggest that further studies are warranted.

7.3 Polyisocyanides with Tetrathiafulvalene Side Groups

For the synthesis of a polyisocyanide containing TTF side chains an approach different from that of HBC was used, due to the limited availability of TTFs with a functional group. A TTF carrying an alcohol could be easily accessed, therefore the side groups were linked to the polyisocyanide backbone via an ester bond instead of a stronger amide bond (Scheme 5).

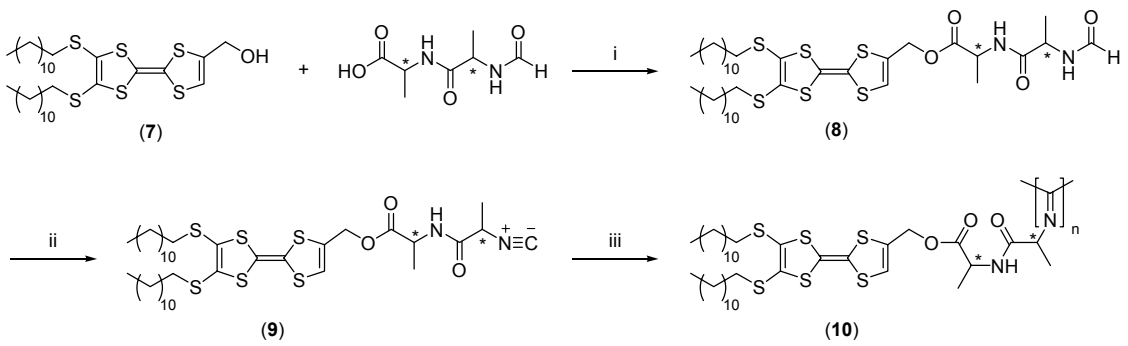

Scheme 5. *Synthesis of poly(L-isocyanoalanyl-L-alanyl-TTF); i) DCC, HOBT, CH_2Cl_2, DMF; ii) diphosgene, Et_3N, CH_2Cl_2; and iii) $NiCl_2$, EtOH, CH_2Cl_2.*

For the preparation of the TTF-bearing polyisocyanide it was chosen to couple a TTF-alcohol to dialanine instead of alanine, because of potential hydrogen bond formation by the

amide group in the dipeptide. Coupling of TTF **7** to *N*-formyl-L-alanyl-L-alanine proceeded via activation with dicyclohexyl carbodiimide (DCC). The use of a base as a catalyst yielded only a very small amount of ester, while acids should be avoided when working with TTFs, because of the chance of oxidation of the TTF units. It is known that *N*-acyl amino acids are sensitive to racemization when activated.[41] In Chapter 2 it was described that coupling of *N*-formyl-L-alanine to β-3-thienylethylamine using DCC as an activating agent resulted in 22 % racemization. With the help of NMR spectroscopy it could be estimated, by comparison of the integrals, that 9±1 % of formamide **8** had been racemized. Another synthetic strategy would have resulted in more reaction steps and more loss of the valuable TTF compound. Therefore the use of an activating agent was unavoidable. The isocyanide was prepared by dehydration of formamide **8** using diphosgene and was subsequently polymerized with $NiCl_2$. Polymerization of isocyanide **9** proceeded very slowly and did not go to completion. After 2 days 5±2 % of the isocyanide had remained, as was estimated by IR spectroscopy. The weight average molecular weight (M_w) of the polymer was determined with gel permeation chromatography (GPC) to be 42.9×10^3 g.mol^{-1}, corresponding to 54 repeat units and a length of ~5 nm. This is quite a large number when the molecular weight of the monomer (787.3 g.mol^{-1}) is considered. The optical rotation of the polymer was higher than that of formamide **8**, suggesting that a helix had been formed. This hypothesis was confirmed by CD spectroscopy; a negative couplet at 320 nm was observed in the spectrum of polymer **10** (Figure 8).

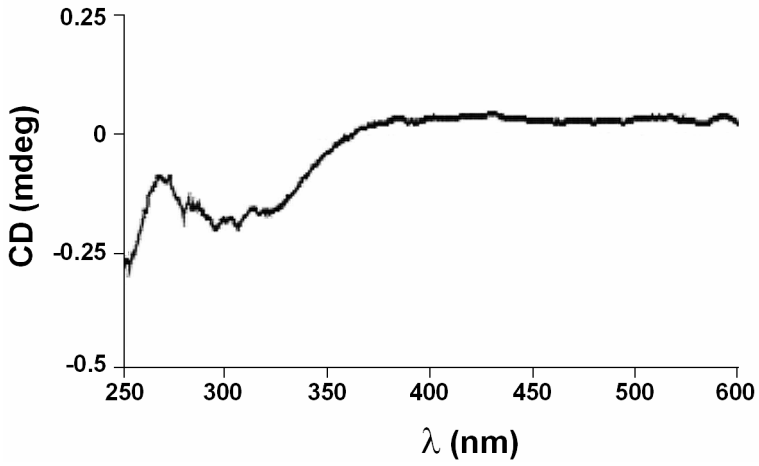

Figure 8. *CD spectrum of TTF-polyisocyanide **10** in CH_2Cl_2.*

By correlating the optical rotation and CD results, the helicity of **10** was tentatively assigned to be right-handed.[42] The vibrations corresponding to the amide groups in the IR

spectrum of **10** were shifted between 4 and 29 cm^{-1} to lower wavenumbers when compared to **9**, suggesting that stronger hydrogen bonds were formed between these groups. Due to the presence of both diastereomers during polymerization of **9** it is not expected that the hydrogen bonding pattern is well-defined. It is likely that diastereomerically pure monomers will give TTF-containing polyisocyanides with a higher degree of order. Due to lack of time and the availability of only limited quantities of isocyanide no further experiments could be performed. However, these initial studies suggest that further work may lead to promising results.

7.4 Conclusions

The preliminary studies described in this chapter indicate that electroactive groups can be attached to a polyisocyanide backbone. Considering the large molecular weight of the HBC and TTF derivatives (1376 and 787 $g.mol^{-1}$ respectively), it is remarkable that these groups can be built in so readily into the polymer. Detailed characterization of the HBC-containing polymer is lacking, due to the low yields obtained during the synthesis. Optimization of the reaction conditions surely will lead to higher yields. In the case of the TTF polyisocyanides polymers with on average 55 repeat units could be prepared. Because of racemization during the synthesis of the monomer the resulting polymer was not diastereomerically pure, resulting in a decrease in order of the polymer side chains. A further limiting factor is the complex and laborious synthesis of the electroactive HBC and TTF groups. Further studied are required to prove that the approach of using rigid polyisocyanides as scaffolds for the preparation of electron conductive nanowires is successful.

7.5 Experimental Section

General methods and materials

THF was distilled over sodium, $CHCl_3$ and CH_2Cl_2 over $CaCl_2$, ethyl acetate over K_2CO_3, and methanol over CaH_2. DMF was first dried for a week on BaO before it was distilled under reduced pressure. 4-Aminobutyl-5,8,11,14,17-penta(3,7-dimethyloctanyl)-hexa-*peri*-hexabenzocoronene (compound **1**) was kindly provided by Dr. N. Tchebotareva and Prof. K. Müllen from the MPI in Mainz, while 2,3-bis-dodecylthio-6-methanol-tetrathiafulvalene (compound **7**) was donated by E. Gomar-Nadal and Dr. D.B. Amabilino from the ICMAB in Barcelona. All other chemicals were used as received unless stated otherwise. ^1H NMR spectra were recorded at room temperature on Bruker DMX-200 and DPX-250 instruments. Chemical shifts are given in ppm (δ) relative to tetramethylsilane. Abbreviations used are s = singlet, d = doublet, t = triplet, q = quartet, m =

multiplet and br = broad. Mass spectra were measured on a VG Instruments ZAB 2-SE-FPD apparatus using FD, while MALDI-TOF spectra were recorded using a Kratos Kompact MALDI 4 instrument. Infrared spectra were recorded on a BioRad FTS 25 spectrometer. CD spectra were measured on a Jasco J600 machine. Optical rotations were determined with a Dr. Kernchen Optik+Elektronik Propol polarimeter using a 1 cm cell. GPC measurements were carried out at room temperature with a Shimadzu GPC with a Shimadzu UV-Vis detector, equipped with a Supelco TOSOHAAS TSK-gel G4000HXL column and a TSK guard column (separation range from 500–300,000 molecular weight), using THF as a mobile phase. Polystyrene samples were used for calibration.

Synthesis

2-(Boc-L-alanyl-4-aminobutyl)-5,8,11,14,17-penta(3,7-dimethyloctanyl)-hexa-*peri*-hexabenzocoronene (2).

To a stirred solution of **1** (0.40 g, 0.31 mmol) in 2.0 ml of CH_2Cl_2 was added a solution of Boc-L-Ala-OH (0.35 g, 1.9 mmol), dimethylaminopyridine (catalytic amount), and EDC (0.35 g, 1.8 mmol) in 2.0 ml of CH_2Cl_2. This mixture was stirred for 1 h and filtered. The crude product was purified by column chromatography (silica gel, eluent: first 100 % CH_2Cl_2, followed by hexane/THF 6:4 (v/v)) to yield 0.39 g (86 %) of **2** as a yellow solid. ^{1}H NMR (250 MHz, $C_2D_2Cl_4$) δ 8.24 (s, 12H, C*H* (HBC)), 6.45 (s, 1H, CH_2NH), 5.12 (s, 1H, N*H*C(O)), 4.10 (m, 1H, C(O)C*H*CH_3), 3.37 (br, 2H, C*H*$_2$NH), 2.96 (br, 12H, CC*H*$_2$), 1.94-1.36 (m, 52H), 1.33 (s, 9H, (C*H*$_3$)$_3$C), 1.28-1.22 (m, 15H), 1.17 (d, 15H, C*H*$_3$, J = 6.7 Hz), 0.91 (d, 30H, C*H*$_3$) ppm; FT-IR (cm^{-1}, KBr) 3301 (NH), 2954, 2925 and 2855 (CH), 1684 and 1655 (C=O), 1559 and 1529 (N-H); MALDI-TOF (m/z, %) = 1465.19 [M$^+$] (calcd for $C_{104}H_{140}N_2O_3$ = 1466.2).

2-(L-Alanyl-4-aminobutyl)-5,8,11,14,17-penta(3,7-dimethyloctanyl)-hexa-*peri*-hexabenzocoronene (3).

Trifluoroacetic acid (3.0 ml) was added to a stirred solution of **2** (109 mg, 0.0743 mmol) in 3.0 ml of CH_2Cl_2 under argon. After stirring for 2 h the reaction was quenched with an aqueous saturated K_2CO_3 solution. The organic layer was separated, extracted 2 times with water and dried on Na_2SO_4 for 16 h. The crude product was precipitated in methanol and after filtration 80 mg (86 %) of **3** was obtained as a yellow solid. ^{1}H NMR (250 MHz, $C_2D_2Cl_4$) δ 8.35 (s, 12H, C*H* (HBC)), 7.26 (br, 1H, CH_2NH), 3.38 (m, 4H, C*H*CH_3+C*H*$_2$NH), 3.01 (br, 12H, CC*H*$_2$), 1.95 (br, 9H, C*H*$_2$) 1.71-1.14 (m, 49H), 0.87 (d, 45H, C*H*$_3$, J = 6.3 Hz) ppm; FT-IR (cm^{-1}, KBr) 3287 (NH), 2954, 2924 and 2854 (CH), 1649 (C=O), 1582 (N-H); MS (FD, 8 kV, m/z, %) = 1367.6 [M$^+$]; MALDI-TOF (m/z, %) = 1365.2 [M$^+$]; (calcd for $C_{99}H_{132}N_2O$ = 1366.7).

2-(*N*-Formyl-L-alanyl-4-aminobutyl)-5,8,11,14,17-penta(3,7-dimethyloctanyl)-hexa-*peri*-hexabenzocoronene (4).

Under an argon atmosphere **3** (80 mg, 0.059 mmol) was dissolved in 2.0 ml of THF while stirring. Diisopropylethylamine (0.17 ml) was added to this solution and the flask was cooled to 0 ºC. Subsequently, *p*-nitrophenylformate (20 mg, 0.12 mmol) was added. After stirring for 4 h the mixture was evaporated to dryness and the residue redissolved in CH_2Cl_2. The product was purified using flash column chromatography (silica gel, eluent: first 100 % CH_2Cl_2, changed to 100 % THF after all compounds that run with CH_2Cl_2 were removed), yielding 29 mg (36 %) of **4** as a yellow solid. ^{1}H NMR (250 MHz, $C_2D_2Cl_4$) δ 8.28 (s, 12H, C*H* (HBC)), 8.07 (s,

1H, C(O)*H*), 6.66 (m, 1H, CH_2NH), 4.53 (m, 1H, N*H*C(O)), 3.63 (m, 1H, C*H*CH_3), 3.37 (m, 2H, CH_2NH), 2.97 (br, 12H, CCH_2), 1.91-1.13 (m, 57H), 0.87 (d, 45H, CH_3, J = 6.0 Hz) ppm; FT-IR (cm^{-1}, KBr) 3300 (NH), 2954, 2925 and 2855 (CH), 1655 and 1610 (C=O), 1558 and 1517 (N-H); MS (FD, 8 kV, m/z, %) = 1395.1 [M^+]; MALDI-TOF (m/z, %) = 1393.45 [M^+] (calcd for $C_{100}H_{132}N_2O_2$ = 1394.1).

2-(Isocyano-L-alanyl-4-aminobutyl)-5,8,11,14,17-penta(3,7-dimethyloctanyl)-hexa-*peri*-hexabenzocoronene (5).

A solution of **4** (24 mg, 17 µmol) and *N*-methylmorpholine (3.8 µl, 34 µmol) in 2.0 ml of CH_2Cl_2 was cooled to -30 ºC under an inert atmosphere of argon. Diphosgene (1.0 µl, 8.6 µmol) was added and the reaction was kept at -30 ºC. After 30 min the mixture was gently warmed up to room temperature. The solution was evaporated to dryness and the residue isolated. No further purification was performed before polymerization, see text for details. FT-IR (cm^{-1}, KBr) 3294 (NH), 2924 and 2854 (CH), 2123 (N≡C), 1633 (C=O), 1580 (N-H); MS (FD, 8 kV, m/z, %) = 1379.1 [M^+] (calcd for $C_{100}H_{130}N_2O$ = 1376.1).

Poly(2-(isocyano-L-alanyl-4-aminobutyl)-5,8,11,14,17-penta(3,7-dimethyloctanyl)-hexa-*peri*-hexabenzocoronene (6).

A solution of **5** (24 mg, 17 µmol) in 2.0 ml of CH_2Cl_2 was stirred and 1.0 ml of a $Ni(ClO_4)_2.6(H_2O)$ solution (0.58 mM) in EtOH/CH_2Cl_2 1:9 (v/v) was added. After 2 days of stirring the reaction mixture was precipitated in a stirred solution of MeOH/water 1:1 (v/v). The product was filtered off and washed two times with 2.0 ml MeOH/water 1:1 (v/v). Drying of the product *in vacuo* yielded 2.0 mg of **6** (8 %) as a yellow solid. FT-IR (cm^{-1}, KBr) 3291 (NH), 2952, 2925 and 2853 (CH), 1622 (C=O and N=C), 1572 (NH).

***N*-Formyl-L-alanyl- L-alanyl-2,3-bis-dodecylthio-6-methoxy-tetrathiafulvalene ester (8).**

Compound **7** (0.840 g, 1.32 mmol) was dissolved in 5.0 ml of CH_2Cl_2 and *N*-formyl-L-alanyl-L-alanine (0.426 g, 2.26 mmol), 1-hydroxybenzotriazole (HOBT, 0.237 g, 1.75 mmol), and 2.0 ml DMF were added. DCC (0.279 g, 1.35 mmol) was added to the suspension and the mixture was stirred overnight. The formed dicyclohexylurea was removed by filtration and the reaction mixture was evaporated to dryness. The product was purified by column chromatography (silica gel, eluent: 5 % (v/v) MeOH in CH_2Cl_2) to yield 0.39 g (86 %) of (**2**) as a yellow solid. $[\alpha]_D^{20}$ (CH_2Cl_2 c 0.3) = -4.9°.$cm^2.g^{-1}$; ^{1}H NMR (200 MHz, $CDCl_3$) δ 8.17 (s, 1H, C(O)*H*), 6.72 and 6.45 (br, 1H, N*H*C(O)), 6.37 (s, 1H, SC(*H*)=C), 4.84 (s, 2H, CH_2OC(O)), 4.62 and 4.57 (m, 1H, C(O)C*H*(CH_3)), 2.81 (m, 4H, SC$H_2$$CH_2$), 1.62 (m, 4H, SCH_2CH_2), 1.46–1.38 (m, 42H, CH_2 and CH_3), 0.88 (t, 6H, CH_2CH_3, J = 2.7 Hz) ppm; FT-IR (cm^{-1}, KBr) 3305 (NH), 3050, 2918 and 2850 (CH), 1735 and 1642 (C=O), 1542 and 1515 (N-H); MALDI-TOF (m/z, %) = 805.1 [M^+] (calcd for $C_{38}H_{64}N_2O_4S_6$ = 805.3).

L-Isocyanoalanyl- L-alanyl-2,3-bis-dodecylthio-6-methoxy-tetrathiafulvalene ester (9).

A solution of **8** (0.105 g, 0.130 mmol) and NEt_3 (0.036 ml, 0.26 mmol) in 4.0 ml of CH_2Cl_2 was cooled to -15°C with the help of an ice/NaCl bath. To the cooled solution 1.0 ml of a 0.065 M diphosgene solution in CH_2Cl_2 was added while stirring under a N_2 atmosphere. After 30 min. more NEt_3 (0.036 ml, 0.26 mmol) and diphosgene solution (1.0 ml) were added. After 1 h the reaction mixture was gradually brought to room temperature, after which 5.0 ml of an aqueous saturated $NaHCO_3$ solution was added and the mixture was stirred

for 5 min. The content of the flask was transferred to a separation funnel and the aqueous layer was removed. The organic layer was extracted two times with water, followed by drying on Na_2SO_4, filtration, and evaporation of the solution to dryness. The resulting product was purified by column chromatography (silica gel, eluent: 2.5 % (v/v) MeOH in CH_2Cl_2). Compound **9** was obtained in 51 mg (50 %) as a yellow solid. ^{1}H NMR (200 MHz, $CDCl_3$) δ 6.82 (br, 1H, N*H*C(O)), 6.40 (s, 1H, SC(*H*)=C), 4.90 (s, 2H, CH_2OC(O)), 4.61 and 4.30 (m, 1H, C(O)C*H*(CH_3)), 2.83 (m, 4H, SCH_2CH_2), 1.71–1.38 (m, 46H, CH_2 and CH_3), 0.92 (t, 6H, CH_2CH_3, J = 2.7 Hz) ppm; FT-IR (cm^{-1}, KBr) 3321 (NH), 3050, 2921 and 2851 (CH), 2140 (C≡N), 1743 and 1680 (C=O), 1542 (N-H); MALDI-TOF (m/z, %) = 786.5 [M^+] (calcd for $C_{38}H_{62}N_2O_3S_6$ = 787.3).

Poly(L-isocyanoalanyl-L-alanyl-2,3-bis-dodecylthio-6-methoxy-tetrathiafulvalene ester) (10).

To a solution of isocyanide **9** (28 mg, 0.036 mmol) dissolved in 7.0 ml of CH_2Cl_2, 1.0 ml of a $NiCl_2$ solution (1.1 mM) in EtOH/CH_2Cl_2 1:9 (v/v) was added while stirring under a N_2 atmosphere. The progress of the reaction was monitored by IR spectroscopy, which showed that after 2 days monomer still remained. The reaction was quenched by precipitation in a stirred solution of MeOH/water 1:1 (v/v). The product was filtered off and washed with 5.0 ml MeOH/water 1:1 (v/v). After drying *in vacuo* **10** was obtained as a yellow solid (yield 20 mg, 71 %). $[\alpha]_D^{20}$ (CH_2Cl_2 c 0.7) = -15°.$cm^2.g^{-1}$; ^{1}H NMR (200 MHz, $CDCl_3$) δ 6.5–6.3 (s, 1H, SC(*H*)=C), 5.1–4.1 (br, 3H, CH_2OC(O) and C(O)C*H*(CH_3)), 2.9–2.7 (br, 4H, SCH_2CH_2), 1.8–1.1 (br, 46H, CH_2 and CH_3), 1.0–0.8 (br, 6H, CH_2CH_3) ppm; FT-IR (cm^{-1}, KBr) 3293 (NH), 2961, 2925 and 2854 (CH), 1744 and 1651 (C=O), 1538 (N-H); M_w = 42.9 10^3 $g.mol^{-1}$ (GPC).

7.6 References and Notes

[1] R. J. M. Nolte, *Chem. Soc. Rev.* **1994**, *23*, 11.
[2] J. J. L. M. Cornelissen, J. J. J. M. Donners, R. de Gelder, W. S. Graswinckel, G. A. Metselaar, A. E. Rowan, N. A. J. M. Sommerdijk, R. J. M. Nolte, *Science* **2001**, *293*, 676.
[3] P. Samorí, C. Ecker, I. Gössl, P. A. J. de Witte, J. J. L. M. Cornelissen, G. A. Metselaar, M. B. J. Otten, A. E. Rowan, R. J. M. Nolte, J. P. Rabe, *Macromolecules* **2002**, *35*, 5290.
[4] P. A. J. de Witte, *Helical chromophoric nanowires*, Ph.D. thesis, University of Nijmegen, Nijmegen, **2004**.
[5] N. Kobayashi, A. B. P. Lever, *J. Am. Chem. Soc.* **1987**, *109*, 7433.
[6] C. F. van Nostrum, S. J. Picken, A.-J. Schouten, R. J. M. Nolte, *J. Am. Chem. Soc.* **1995**, *117*, 9957.
[7] H. Rengel, P. Gattinger, R. Silerova, D. Neher, *J. Phys. Chem. B* **1999**, *103*, 6858.
[8] A. Stabel, P. Herwig, K. Müllen, J. P. Rabe, *Angew. Chem. Int. Ed.* **1995**, *34*, 1609.
[9] S. P. Brown, I. Schnell, J. D. Brand, K. Müllen, H. W. Spiess, *J. Am. Chem. Soc.* **1999**, *121*, 6712.
[10] M. Keil, P. Samorí, D. A. Dos Santos, T. Kugler, S. Stafström, J. D. Brand, K. Müllen, J. L. Brédas, J. P. Rabe, W. R. Salaneck, *J. Phys. Chem. B* **2000**, *104*, 3967.
[11] S. Ito, M. Wehmeier, J. D. Brand, R. Epsch, J. P. Rabe, K. Müllen, *Chem. Eur. J.* **2000**, *6*, 4327.
[12] J. Piris, W. Pisula, A. Tracz, T. Pakula, K. Müllen, J. M. Warman, *Liq. Cryst.* **2004**, *31*, 993.
[13] A. M. van de Craats, J. M. Warman, A. Fechtenkötter, J. D. Brand, M. A. Harbison, K. Müllen, *Adv. Mater.* **1999**, *11*, 1469.
[14] C. Kübel, S.-L. Chen, K. Müllen, *Macromolecules* **1998**, *31*, 6014.
[15] A. F. Thünemann, D. Ruppelt, S. Ito, K. Müllen, *J. Mater. Chem.* **1999**, *9*, 1055.
[16] A. F. Thünemann, D. Ruppelt, C. Burger, K. Müllen, *J. Mater. Chem.* **2000**, *10*, 1325.
[17] A. F. Thünemann, S. Kubowicz, C. Burger, M. D. Watson, N. Tchebotareva, K. Müllen, *J. Am. Chem. Soc.* **2003**, *125*, 352.
[18] J. P. Hill, W. Jin, A. Kosaka, T. Fukushima, H. Ichihara, T. Shimimura, K. Ito, T. Hashizume, N. Ishii, T. Aida, *Science* **2004**, *304*, 1481.
[19] M. B. Nielsen, C. Lomholt, J. Becher, *Chem. Soc. Rev.* **2000**, *29*, 153.

[20] J. L. Segura, N. Martín, *Angew. Chem. Int. Ed.* **2001**, *40*, 1372.
[21] J. O. Jeppesen, J. Becher, *Eur. J. Org. Chem.* **2003**, 3245.
[22] T. Otsubo, K. Takimiya, *Bull. Chem. Soc. Jpn.* **2004**, *77*, 43.
[23] H. R. Tseng, S. A. Vignon, P. C. Celestre, J. Perkins, J. O. Jeppesen, A. Di Fabio, R. Ballardini, M. T. Gandolfi, M. Venturi, V. Balzani , J. F. Stoddart, *Chem. Eur. J.* **2004**, *10*, 155.
[24] C. Lampard, J. A. Murphy, N. Lewis, *J. Chem. Soc., Chem. Commun.* **1993**, 295.
[25] T. Jørgensen, T. K. Hansen, J. Becher, *Chem. Soc. Rev.* **1994**, *23*, 41.
[26] K. B. Simonsen, J. Becher, *Synlett* **1997**, 1211.
[27] M. R. Bryce, W. Davenport, L. M. Goldenberg, C. Wang, *Chem. Commun.* **1998**, 945.
[28] D. Philp, A. M. Z. Slawin, N. Spencer, J. F. Stoddart, D. J. Williams, *J. Chem. Soc., Chem. Commun.* **1991**, 1584.
[29] D. Amabilino, J. F. Stoddart, *Chem. Rev.* **1995**, *95*, 2725.
[30] P. Day, M. Kurmoo, T. Mallah, I. R. Marsden, R. H. Friend, F. L. Pratt, W. Hayes, D. Chasseau, L. Gaultier, G. Bravic, L. Ducasse, *J. Am. Chem. Soc.* **1992**, *114*, 10722.
[31] A. Aviram, M. Ratner, *Chem. Phys. Lett.* **1974**, *9*, 2271.
[32] R. Andreu, A. I. de Lucas, J. Garín, N. Martín, J. Orduna, L. Sánchez, C. Seoane, *Synth. Met.* **1997**, *86*, 1817.
[33] N. Martín, L. Sánchez, D. M. Guldi, *Chem. Commun.* **2000**, 113.
[34] S. Frenzel, S. Arndt, R. M. Gregorious, K. Müllen, *J. Mater. Chem.* **1995**, *5*, 1529.
[35] R. L. Meline, I. T. Kim, J. Chen, S. Basak, R. L. Elsenbaumer, *Polym. Prepr.* **1998**, *39*, 341.
[36] L. Huchet, S. Akoudad, E. Levilain, J. Roncali, A. Emge, P. Bäuerle, *J. Phys. Chem. B* **1998**, *102*, 7776.
[37] M. R. Bryce, A. D. Chissel, J. Gopal, P. Kathirgamanathan, D. Parker, *Synth. Met.* **1991**, *39*, 397.
[38] L. Huchet, S. Akoudad, J. Roncali, *Adv. Mater.* **1998**, *10*, 541.
[39] S. Booth, E. N. K. Wallace, K. Shingal, P. N. Bartlett, J. D. Kilburn, *J. Chem. Soc., Perkin Trans. I* **1998**, 1467.
[40] J. J. L. M. Cornelissen, *Polymers and block copolymers of isocyanopeptides*, Ph.D. thesis, University of Nijmegen, Nijmegen, **2001**.
[41] M. Bodansky, *Int. J. Peptide Protein Res.* **1985**, *25*, 449.
[42] A. J. M. van Beijnen, R. J. M. Nolte, W. Drenth, A. M. F. Hezemans, P. J. F. M. van de Coolwijk, *Macromolecules* **1980**, *13*, 1386.

Summary

In this thesis the synthesis and physical properties of polymers of isocyanides containing thiophene and other functional groups are described. Polyisocyanides are ideal frameworks for the incorporation of such groups, because they possess a high degree of structural regularity as a result of the helical arrangement of the polymer backbone. A new type of isocyanide, viz. L-isocyanoalanine(2-thiophen-3-yl-ethyl)amide (IAT), was synthesized and polymerized using Ni(II) catalysts to give the corresponding polymer PIAT. Spectroscopic studies showed that PIAT possesses a network of hydrogen bonds, i.e. between the amide groups of the side chains, which run parallel to the polymer helix axis. It was found that the degree of order in the polymer depended on the optical purity of the chiral monomer. When partly racemized IAT was used, both enantiomers became incorporated into the growing polyisocyanide chain. This led to a more flexible polymer, as a result of a less well defined network of hydrogen bonds between the polymer side chains. Introduction of a second L-alanine group in the monomer improved the regularity of the resulting thiophene containing polyisocyanide, because extra hydrogen bonds could be formed between the side groups. Changing the chirality of the second alanine group from L to D altered the physical properties of the resulting polymer significantly, probably as a result of a difference in packing of the side groups in the two polymers.

The use of an amino-terminated polystyrene as the initiator in the polymerization of IAT resulted in the formation of a diblock copolymer (PS-PIAT), which displayed amphiphilic character. On dispersal in THF/water, aggregates with morphologies that depended on the ratio between the PS and PIAT block lengths could be obtained. Interestingly, PS-PIAT diblock copolymers also formed well-defined aggregates in organic solvents. In aqueous solution typically polymersomes were obtained, which were found to fuse upon standing, thereby increasing their average diameter by a factor of 20 (Figure 1 a).

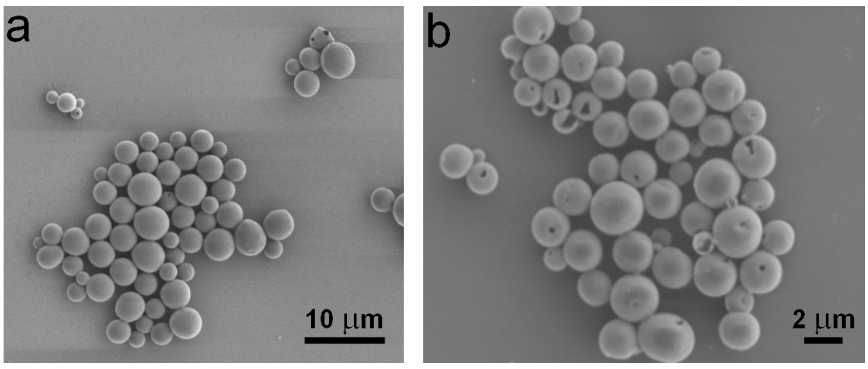

Figure 1. *Scanning electron micrographs of polymersomes of a) PS-PIAT and b) OD-PIAT.*

THF proved to be an essential component for this behavior, since no fusion was observed in its absence. The optical purity of PS-PIAT appeared to be of major importance to the aggregation behavior of this amphiphile. A mixture of 75 % L-IAT and 25 % D-IAT gave polymersomes with the highest degree of order, while PS-PIAT prepared with 100 % L-IAT formed very small and less well-defined polymersomes as well as films. Using the electroformation method, very large polymersomes could be prepared with diameters up to 100 μm. The membranes of the latter were still fluidic in nature. When brought in close proximity with the help of a micropipette, fusion between two large polymersomes could be induced.

The thiophene groups present in the polymersomes of PS-PIAT could be polymerized both electrochemically and chemically. Chemical polymerization proved to be the most suitable procedure, because it left the morphology of the polymersomes unaltered, in contrast to electrochemical polymerization, which led to destruction of the aggregates. It appeared that the electron conductivity of the polymerized (cross-linked) polymersomes was 3 orders of magnitude higher than the electron conductivity of the non-cross-linked polymersomes. Doping of the cross-linked material with I_2 resulted in a further improvement of the conductivity by a factor of 24.

Nanoreactors were constructed by encapsulating enzymes within the aqueous compartment of the PS-PIAT polymersomes. Three different enzymes, viz. lipase B from *Candida antarctica*, horseradish peroxidase, and glucose oxidase, were successfully compartmentalized. With the help of enzyme activity assays it was possible to prove that the enzymes inside the polymersomes remained active. Externally added substrates were found to diffuse through the polymersome membrane into the inner aqueous compartment of the nanoreactors where they were converted by the enzymes present. The resulting products were capable of diffusing out of the polymersomes, while the enzymes remained entrapped. Chemical cross-linking of the polymersome membranes was shown to reduce the rate of diffusion of substrates across the membranes, as was concluded from a decrease in the rate of substrate conversion. Increasing the cross-linking time or the concentration of the cross-linking agent led to a further decrease in the diffusion rate.

A procedure has been developed to selectively entrap lipase enzymes within the membrane of PS-PIAT polymersomes. It involved the lyophilization of a mixture of the enzyme and PS-PIAT prior to aggregate formation. When aggregates were made from a lyophilized lipase enzyme/PS-PIAT mixture in a solution containing another type of enzyme, polymersomes were obtained possessing lipase enzymes inside their membranes and the second enzyme in their inner aqueous compartment. Using fluorescence microscopy, the

presence of two different enzymes, i.e. in the membrane and in the water pool of the polymersomes, could be elegantly demonstrated.

The influence of the apolar block on the aggregation behavior of the thiophene-containing amphiphilic polyisocyanides was studied by preparing a series of diblock copolymers with an octadecene group instead of a polystyrene block as the apolar part, named OD-PIAT. These diblock copolymers were found to display significantly different aggregation behavior. Depending on the length of the polyisocyanide block, fibers, micelles, networks, and phase separated structures were observed by transmission electron microscopy. For one particular OD-PIAT polymer the formation of polymersomes was observed after standing for several hours. Initially, no defined structures were observed, but in time small spherical aggregates were formed, which fused, similar to PS-PIAT, into polymersomes with a much larger diameter (Figure 1 b). Although the OD-PIAT amphiphile is smaller than the PS-PIAT amphiphile, it appeared to be less dynamic during the fusion process: the time needed for complete fusion took 6 days compared to 2 days for the aggregates from PS-PIAT. Comparing the aggregation behavior of OD-PIAT and PS-PIAT indicates that it is mainly the head group of the diblock copolymer that controls the morphology of the resulting aggregates.

The possibility to prepare polyisocyanides with other types of functional groups was studied using isocyanide monomers that contained hexabenzocoronene and tetrathiafulvalene derivatives. From both types of monomers polyisocyanides could be prepared successfully. Although detailed physical studies still have to be performed, these experiments show that polyisocyanides are versatile frameworks for the incorporation of all kinds of functional groups.

Samenvatting

In dit proefschrift zijn de synthese en de fysische eigenschappen beschreven van isocyanidepolymeren die thiofenen en andere functionele groepen bevatten. Polyisocyaniden zijn ideale verbindingen om te worden gebruikt als raamwerk voor het bevestigen van dit soort groepen, omdat ze een hoge structurele regelmaat bezitten als gevolg van de schroefvormige ordening van de ruggengraat van het polymeer. Een nieuw type isocyanide, L-isocyanoalanine(2-thiophen-3-yl-ethyl)amide (IAT), werd gesynthetiseerd en gepolymeriseerd met Ni(II)-katalysatoren, hetgeen resulteerde in het overeenkomstige polymeer PIAT. Spectroscopische studies toonden aan dat PIAT een netwerk van waterstofbruggen bevat en wel tussen de amide-groepen van de zijketens, die evenwijdig lopen aan de ruggengraat van het polymeer. Het bleek dat de mate van regelmaat in het polymeer afhing van de optische zuiverheid van het chirale monomeer. Bij gebruik van gedeeltelijk geracemiseerd IAT werden beide enantiomeren ingebouwd in de groeiende polyisocyanide-keten. Dit leidde tot een flexibeler polymeer als gevolg van een minder goed gedefinieerd netwerk van waterstofbruggen tussen de zijketens van het polymeer. De introductie van een tweede L-alanine-groep in het monomeer verbeterde de regelmaat van het overeenkomstige, thiofeen-bevattende polyisocyanide, doordat additionele waterstofbruggen tussen de zijketens konden worden gevormd. Het wijzigen van de chiraliteit van de tweede alanine-groep van L naar D resulteerde in een aanzienlijke verandering van de fysische eigenschappen van het polymeer, hetgeen waarschijnlijk het gevolg is van een verschil in de organisatie van de zijgroepen in de twee polymeren.

Door gebruik te maken van polystyreen met een amine-eindgroep als initiator voor de polymerisatie van IAT kon een diblok-copolymeer (PS-PIAT) worden gemaakt, dat een amfifiel karakter vertoonde. Wanneer het werd gedispergeerd in THF/water vormde het aggregaten waarbij de morfologie afhankelijk was van de verhouding tussen de PS- en PIAT-bloklengtes. Het was opmerkelijk dat de PS-PIAT diblok-copolymeren ook goed gedefinieerde aggregaten vormden in organische oplosmiddelen. In waterige oplossingen werden over het algemeen “polymeersomen” gevormd, die bleken te fuseren in de tijd. Hierbij nam hun gemiddelde diameter met een factor 20 toe (Figuur 1 a).

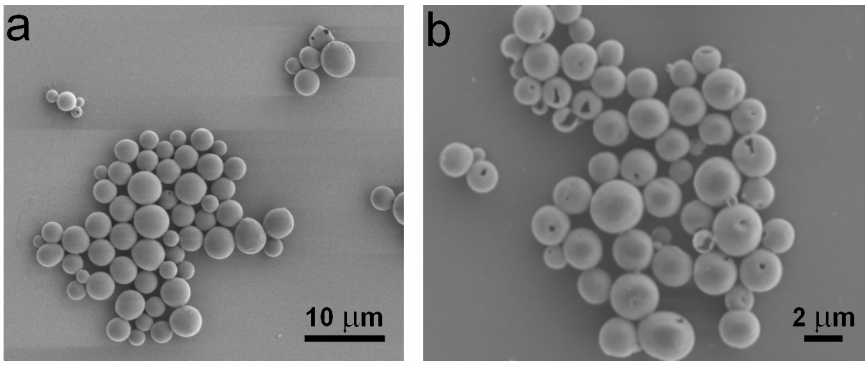

Figuur 1. *Raster-elektronenmicroscopie opnames van polymeersomen van a) PS-PIAT en b) OD-PIAT.*

THF bleek een wezenlijke bijdrage te leveren aan dit gedrag, want in de afwezigheid van deze verbinding werd er geen fusie waargenomen. De optische zuiverheid van PS-PIAT bleek van grote invloed te zijn op het aggregatiegedrag van dit amfifiel. Een mengsel van 75 % L-IAT en 25 % D-IAT vormde polymeersomen met de hoogste mate van regelmaat, terwijl PS-PIAT dat was gemaakt met 100 % L-IAT zeer kleine en minder goed gedefinieerde polymeersomen en films vormde. Met de elektroformatie-methode konden zeer grote polymeersomen gemaakt worden met diameters tot 100 μm. De membranen van deze aggregaten bleken nog steeds over een grote mate van fluïditeit te beschikken. Wanneer twee polymeersomen met behulp van een micropipet dicht bij elkaar werden gebracht, kon fusie worden geïnduceerd.

De aanwezige thiofeengroepen in de PS-PIAT polymeersomen konden worden gepolymeriseerd, zowel elektrochemisch als chemisch. Chemische polymerisatie verdiende de voorkeur, omdat het de morfologie van de polymeersomen ongewijzigd liet, in tegenstelling tot elektrochemische polymerisatie, dat de polymeersomen bleek af te breken. Geleidingsmetingen toonden aan dat de elektrische geleiding van de gepolymeriseerde (vernette) polymeersomen 1000 keer hoger was dan de elektrische geleiding van niet-vernette polymeersomen. Het introduceren van lading in het vernette materiaal met I_2 resulteerde in een verbetering van de geleidbaarheid met een factor 24.

Nanoreactoren konden worden geconstrueerd door enzymen in het watercompartiment van de PS-PIAT polymeersomen in te sluiten. Drie verschillende enzymen, lipase B van *Candida antarctica*, mierikswortel peroxidase en glucose oxidase, werden met succes ingesloten. Met behulp van enzymactiviteitstesten kon worden aangetoond dat de ingekapselde enzymen actief bleven. Verdere studies lieten zien dat substraat dat uitwendig werd toegevoegd door het polymeersoom-membraan heen kon diffunderen waar het in het watercompartiment werd omgezet door de aanwezige enzymen. Het gevormde product was in staat om de polymeersomen weer te verlaten, terwijl de enzymen opgesloten bleven. Uit een

afname van de omzettingssnelheid van substraat na het chemisch vernetten van de polymeersoom-membranen werd geconcludeerd dat deze vernetting leidde tot een afname van de diffusiesnelheid door het membraan. Een verhoging van de vernettingstijd of de concentratie van het vernettingsreagens resulteerde in een verdere afname van de diffusiesnelheid.

Er werd een procédé ontwikkeld om lipase-enzymen selectief op te sluiten in het membraan van PS-PIAT-polymeersomen. Om dit te bewerkstelligen werd een mengsel van lipase-enzym en PS-PIAT gevriesdroogd vóór de aggregaatvorming. Polymeersomen die vervolgens werden gemaakt van deze gevriesdroogde lipase-enzym/PS-PIAT mengsels in waterige oplossingen die tevens een ander soort enzym bevatten, bleken lipase-enzymen in het membraan te bezitten en het andere enzym in het waterige compartiment. Met fluorescentie-microscopie kon de aanwezigheid van de twee verschillende enzymen, in het membraan en in het watercompartiment van de polymeersomen, op elegante wijze worden aangetoond.

De invloed van het apolaire blok op het aggregatiegedrag van de thiofeenbevattende amfifiele polyisocyaniden werd bestudeerd door een reeks diblok-copolymeren te maken, die een octadeceengroep bevatten in plaats van een polystyreen-blok (genaamd OD-PIAT). Er werd vastgesteld dat deze diblok-copolymeren een zeer afwijkend aggregatiegedrag vertoonden. Afhankelijk van de lengte van het polyisocyanide-blok werden fibers, micellen, netwerken en fasen-gescheide structuren waargenomen met transmissie-elektronenmicroscopie. Voor een bepaald OD-PIAT-polymeer waren na enkele uren staan bij kamertemperatuur polymeersomen zichtbaar. In eerste instantie werden er geen goed gedefinieerde aggregaten gevormd, maar na verloop van tijd ontstonden er sferische aggregaten die, op dezelfde wijze als PS-PIAT, tot polymeersomen fuseerden en wel met een veel grotere diameter (Figuur 1 b). Alhoewel het OD-PIAT-amfifiel veel kleiner is dan het PS-PIAT-amfifiel, bleek het toch minder dynamisch te zijn tijdens het fusieproces, aangezien de benodigde tijd voor fusie 6 dagen bedroeg, terwijl PS-PIAT-polymeersomen 2 dagen nodig hadden. Een vergelijking van het aggregatiegedrag van OD-PIAT met PS-PIAT gaf aan, dat het voornamelijk de kopgroep van het diblok-copolymeer is die de morfologie van het uiteindelijke aggregaat bepaalt.

De mogelijkheid om polyisocyaniden te synthetiseren met andere functionele groepen dan thiofeen werd onderzocht door gebruik te maken van isocyaniden afgeleid van hexabenzocoroneen en tetrathiafulvaleen. Van beide soorten monomeren konden met succes polymeren worden gemaakt. Alhoewel gedetailleerde fysische studies nog moeten worden uitgevoerd, geven deze experimenten aan dat polyisocyaniden uitermate geschikt zijn als dragermateriaal voor een verscheidenheid aan functionele groepen.

Dankwoord

Een proefschrift is niet compleet zonder een dankwoord en dat gaat zeker in mijn geval op. Door het multidisciplinaire karakter van mijn onderzoek heb ik het geluk gehad met veel verschillende mensen te mogen samenwerken.

Ten eerste wil ik Prof. Roeland Nolte hartelijk danken voor het in mij gestelde vertrouwen. Voordat ik begon aan mijn promotieonderzoek had ik twijfel of ik de capaciteiten had om het met succes af te ronden. We hadden afgesproken om na een jaar te kijken of ik door zou gaan, maar gelukkig was u dat toen al weer vergeten. Blijkbaar vond u het dus goed gaan. De interesse waarmee u mijn werk volgde, heb ik als zeer motiverend beschouwd. Ik ben u ook erkentelijk voor de mogelijkheid om verscheidene internationale conferenties te bezoeken en dat ik talloze lezingen heb kunnen geven. De gelegenheid die u mij nu biedt, om een spin-off op te zetten, is zeer genereus en ik hoop dat ik het vertrouwen dat u in mij stelt, kan waarmaken.

Alan, jou wil ik heel erg danken voor de inspirerende manier van begeleiden. Jouw tomeloze enthousiasme en constante stroom aan nieuwe ideeën zorgden er altijd voor dat ik met goede moed jouw kantoor verliet. Dankzij de contacten die jij had in het buitenland heb ik een gedeelte van mijn onderzoek buiten Nederland kunnen doen. Een unieke kans om mee te maken hoe andere onderzoeksgroepen werken. Ook na mijn promotietijd heb je geweldig geholpen door mij een post-doc contract te geven en door het steunen van het bedrijfje Encapson.

Het was plezierig om Irene als hoofdvakstudent te mogen begeleiden. Jouw frustraties van de vorige stageplaats maakten al snel plaats voor enthousiasme voor het polyisocyanide-werk. Je hebt zeer hard en zelfstandig gewerkt en dat heeft geresulteerd in hoofdstuk 6 en een groot deel van hoofdstuk 2 in dit proefschrift. Goed om te zien dat je bent gaan promoveren. Wat later kwam Eva als Erasmusstudent stage lopen. Eva, your project proved to be more difficult than expected, but that didn't stop you. The compounds you prepared at the end of your stay were very useful for the studies in chapter 2. Good luck with your Ph.D. work in Barcelona. Ik wil Jeroen bedanken voor al zijn tips en goede adviezen. Als zeer ervaren polyisocyanide-syntheticus was jij een grote bron van informatie. Mijn dank gaat ook naar jou uit voor het nakijken van het manuscript.

Een belangrijke factor voor het hebben van plezier in je werk zijn de collega's waarmee je dagelijks omgaat. Degene naast wie ik de meeste tijd heb gewerkt was Pieter. Ongelofelijk dat iemand met kleurenblindheid met porfyrines gaat werken. De tijd die wij samen zowel in het lab als daarbuiten hebben doorgebracht, was erg tof. Een aantal van de mooie resultaten die in dit boekje staan beschreven, heb ik te danken aan Kelly. Kelly, thanks for our good collaboration and the interesting conversations about other countries, cultures, holidays, etc. I am happy to have you as a friend. It was also very nice that you were the first

customer of Encapson. Twee mensen die zeer bepalend waren voor de sfeer in het lab, waren Matthijs en Aurélie. Het was gelijk een stuk stiller wanneer jullie er een dag niet waren. Vermakelijk waren de vaak lange discussies over polyisocyanides die Matthijs en ik soms hadden. Matthijs, ook bedankt voor de AFM plaat in hoofdstuk 2. Aurélie was vaak een gewillig slachtoffer voor mijn flauwe grappen. Volgens mij heb je veel bijgeleerd, want het wordt steeds moeilijker je te foppen. Ook de andere mensen die lab U004 hebben bevolkt, zoals Henar, Iris, Joost (medekakkerlakverdelger), Jurry (bedankt voor de POVray plaatjes), Marta, Pedro, Peter, Pili, Raquel, Ton en de verschillende Erasmusstudenten wil ik danken voor de goede sfeer. Uiteraard kan ik hierbij Paula niet onvermeld laten. My sweet, I would like to thank you for the time we worked together. I have a lot of respect for your way of working and you taught me quite a number of things. It is nice to see that a part of your work is taken up in this thesis.

Ook de mensen van de andere Noltelabs hebben eraan bijgedragen dat ik met veel plezier op mijn promotietijd kan terugkijken. Johan Hoogboom verdient zeer zeker een eervolle vermelding. Johan, dankzij jouw geweldige inzet, zoals onder andere het synthetiseren van het rutheen complex en het uitvoeren van elektrochemische experimenten, hebben we een goed artikel en veel mooie resultaten behaald. Alhoewel we twee totaal verschillende karakters hebben, kunnen we het toch goed met elkaar vinden. Tijdens allerlei conferenties hebben we dan ook veel lol gehad. Onze voormalige begeleider, Alexander, heeft de elektroformatie-experimenten uit hoofdstuk 3 uitgevoerd. Grappig om te zien dat juist Alexander, die een kei is in het laten werken van andere mensen voor hemzelf, voor mij metingen heeft gedaan. De gesprekken met Hans Elemans en Martin tijdens koffiepauzes of op tijden dat iedereen al naar huis was, hielpen uitstekend om frustraties over allerlei zaken kwijt te raken. Hans en Sandra, bedankt voor jullie bijdrage. De gesprekken met Femke en Gerald tijdens de autoritten naar de polymeercursus waren vaak erg boeiend. Ook alle andere mensen uit de Noltegroep, die ik niet heb genoemd, wil ik danken voor de leuke sfeer in de groep. De mensen van de Van Hest- en Rutjesgroepen die op welke wijze dan ook hebben geholpen met de inhoud van dit boekje wil ik hierbij bedanken. Hans Adams mag niets onvermeld blijven voor zijn goede adviezen op het vlak van de peptidekoppelingen. Mijn dank gaat uit naar Prof. Jan van Hest voor zijn deelname in de manuscriptcommissie en zijn steun aan Encapson.

I would like to thank Dr. Elba Gomar and Dr. David Amabilino from the ICMAB in Barcelona for the great collaboration. Although our approach to combine TTF's with polyisocyanides turned out to be very difficult, we still had a good time together. And thank you David for being a member of my manuscript committee. Een woord van dank gaat uit naar Steven De Feyter en Atsushi Miura van de Katholieke Universiteit Leuven voor het uitvoeren van microscopiestudies. I would like to thank the following people from the Max Planck Institut für Polymerforschung in Mainz for having me for one week to synthesize a

polyisocyanide with HBC side groups: Dr. Natalia Tchebotareva, Dr. Mark Watson, and Prof. Klaus Müllen.

De mensen van het magnetenlab, Peter Christianen, Ken Takazawa en Igor O'Shklyarevskiy hebben ervoor gezorgd dat er gedegen studies aan de polymeersomen konden worden gedaan. Hartelijk dank daarvoor. De volgende mensen zou ik willen bedanken voor het uitvoeren van verschillende metingen: Ad (NMR), Christien (chirale HPLC), Hans Engelkamp (confocale microscopie), Hélène (element analyse), Peter (massa), René (kristallografie) en Wim Scheenen (Patch Clamp). Een speciaal woord van dank gaat uit naar Huub en Liesbeth van het Gemeenschappelijk Instrumentarium. Dankzij jullie enorme inzet heb ik veel geleerd over microscopie en kon ik mooie plaatjes in mijn proefschrift zetten. Jullie zijn geweldig. Ook het ondersteunende personeel heeft er voor gezorgd dat ik een goede tijd heb gehad, zoals Désirée, jij bent zeer belangrijk voor de groep, Chris, Jacky, Peter, Pieter en Wim.

De activiteiten na werktijd zorgden voor de broodnodige afleiding, daarom wil ik de bezoekers van de foutefilmavonden, de voetbalploeg, oud studiegenoot Arno en mijn trainingsmaten Aurélie en Edward, tevens gelegenheidskoks, bedanken. Jullie hebben voor veel plezier gezorgd. Vera, jou wil ik bedanken voor het samen delen van een huis en het zijn van een prima vriendin. Veel succes met het afronden van je opleiding als octrooigemachtigde. Lee, partner in crime, thanks for being in Encapson with me. Let's make it a huge success.

Tenslotte ook een woord van dank aan het thuisfront. Zonder de goede zorg van mijn ouders zou ik nooit zover gekomen zijn. Ik ben jullie ontzettend dankbaar voor de onvoorwaardelijke steun en zorg al die jaren. Ik zou me niets beters kunnen wensen. Mijn zus Danielle en haar vriend Bas wil danken voor de getoonde interesse. De overige leden van mijn familie hebben er altijd voor gezorgd dat ik alles goed kon blijven relativeren. Ik hoop dat jullie een klein idee hebben van waar ik me mee bezig heb gehouden. Last, but not least, I would like to thank my fiancée Paula. You have been the prefect partner for me, not only for the unconditional love and support you gave me, but also for increasing my view, being a good friend, and a great colleague. Thank you.

Dennis

Curriculum Vitae

In 1992 behaalde Dennis Vriezema het HAVO diploma op de Andreas Scholengemeenschap te Zevenaar. Vervolgens werd van september 1992 tot juni 1996 met succes het HLO doorlopen op de Hogeschool Gelderland in Arnhem. In september van dat jaar werd begonnen met het scheikunde-doorstroomprogramma aan de toenmalige Katholieke Universiteit Nijmegen. Een jaar later werd de hoofdvakstage uitgevoerd in de groep van Prof. Nolte. Aansluitend werd hij in december 1998 voor een jaar aangesteld als onderzoeksmedewerker op het STW-project NGN.3611 met als titel “Ontwikkeling van een percutane glucose monitor ten behoeve van diabetes-mellitus patiënten” in de groep van Prof. Nolte. In juni 1999 werd het doctoraal diploma scheikunde behaald. Met het promotieonderzoek, zoals beschreven in dit proefschrift, werd aangevangen in maart 2000. Sinds juli 2004 is hij werkzaam in de groep van Prof. Nolte in samenwerking met Dr. Alan Rowan als post-doctoraal onderzoeker. Daarnaast is hij samen met Lee Ayres als ondernemer bezig met het opzetten van Encapson, een spin-off-bedrijf van het hier beschreven werk.

List of Publications

M. Gerritsen, J. A. Jansen, A. Kros, D. M. Vriezema, N. A. J. M. Sommerdijk, R. J. M. Nolte, J. A. Lutterman, S. W. F. M. van Hövell, A. van der Gaag, *J. Biomed. Mater. Res.* **2001**, *54*, 69. "*Influence of Inflammatory Cells and Serum on the Performance of Implantable Glucose Sensors*"

J. Foekema, A.P.H.J. Schenning, D.M. Vriezema, F.B.G. Benneker, K. Norgaard, J.K.M. Kroon, T. Bjornholm, M.C. Feiters, A.E. Rowan, R.J.M. Nolte, *J. Phys. Org. Chem.* **2001**, *14*, 501. "*Synthesis of Multi-Porphyrin Arrays and Study of their Self-Assembly Behaviour at the Air-Water Interface*"

D.M. Vriezema, A.E. Rowan, R.J.M. Nolte, *Polym. Prepr.* **2002**, *45*, 749. "*Functional Materials by Self-Assembly of Thiophene-Containing Block Copolymers*"

D. M. Vriezema, J. Hoogboom, K. Velonia, K. Takazawa, P. C. M. Christianen, J. C. Maan, A. E. Rowan, R. J. M. Nolte, *Angew. Chem. Int. Ed.* **2003**, *42*, 772. "*Vesicles and Polymerized Vesicles from Thiophene-Containing Rod-Coil Block Copolymers*"

D. M. Vriezema, A. Kros, J. Hoogboom, A. E. Rowan, R. J. M. Nolte, *Polym. Prepr.* **2004**, *45*, 749. "*Functional Aggregates by Self-Assembly of Thiophene Containing Diblock Copolymers*"

D. M. Vriezema, A. Kros, R. de Gelder, J. J. L. M. Cornelissen, A. E. Rowan, R. J. M. Nolte, *Macromolecules* **2004**, *37*, 4736. "*Electroformed giant vesicles from thiophene-containing rod-coil diblock copolymers*"

D.M. Vriezema, M. Comellas Aragones, J.A.A.W. Elemans, J.J.L.M. Cornelissen, A.E. Rowan, R.J.M. Nolte, *Chem. Rev.*, accepted. "*Self-Assembled Nanoreactors*"

D.M. Vriezema, A.E. Rowan, R.J.M. Nolte, patent application submitted. "*Permeabele Capsules, Werkwijze voor de Vervaardiging evenals Toepassing daarvan*"